



NÚMERO: 441/2011

UNIVERSIDADE ESTADUAL DE CAMPINAS

INSTITUTO DE GEOCIÊNCIAS

**PATRICK FRANCISCO FÜHR DAL' BÓ**

**MECANISMOS DEPOSIONAIS E PROCESSOS PEDOGENÉTICOS EM  
LENÇÓIS DE AREIA EÓLICA: A FORMAÇÃO MARÍLIA,  
NEOCRETÁCEO DA BACIA BAURU, BRASIL, E LA SALINA,  
HOLOCENO DA BACIA TULUM, ARGENTINA.**

TESE DE DOUTORADO APRESENTADA AO  
INSTITUTO DE GEOCIÊNCIAS DA UNICAMP  
PARA OBTENÇÃO DO TÍTULO DE DOUTOR EM  
CIÊNCIAS, ÁREA DE GEOLOGIA E RECURSOS  
NATURAIS.

**ORIENTADOR: PROF. DR. GIORGIO BASILICI**

ESTE EXEMPLAR CORRESPONDE À VERSÃO FINAL DA TESE DE DOUTORADO  
DEFENDIDA PELO ALUNO E ORIENTADA PELO PROF. DR. GIORGIO BASILICI

---

Giorgio Basilici

Campinas, 2011

FICHA CATALOGRÁFICA ELABORADA POR  
HELENA FLIPSEN - CRB8/5283 - BIBLIOTECA CENTRAL “CESAR LATTES” DA UNICAMP

D15m	<p>Dal Bó, Patrick Francisco Führ. Mecanismos deposicionais e processos pedogenéticos em lençóis de areia eólica: a Formação Marília, Neocretáceo da Bacia Bauru, Brasil, e La Salina, Holocene da Bacia Tulum, Argentina / Patrick Francisco Führ Dal Bó. -- Campinas, SP : [s.n.], 2011.</p> <p>Orientador: Giorgio Basilici. Tese (doutorado) - Universidade Estadual de Campinas, Instituto de Geociências.</p> <p>1. Paleopedologia. 2. Geologia estratigráfica. 3. Sedimentação eólica. I. Basilici, Giorgio, 1959- II. Universidade Estadual de Campinas. Instituto de Geociências. III. Título.</p>
------	---

Informações para Biblioteca Digital

**Título em Inglês:** Depositional mechanisms and pedogenetic processes in eolian sand sheets: The Marília Formation (Late Cretaceous of the Bauru Basin, Brazil) and La Salina (Holocene of the Tulum Basin, Argentina)

**Palavras-chave em Inglês:**

Paleopedology  
Stratigraphic geology  
Eolian sedimentation

**Área de concentração:** Geologia e Recursos Naturais

**Titulação:** Doutor em Ciências

**Banca examinadora:**

Giorgio Basilici [Orientador]  
Alexandre Campane Vidal  
Celso Dal Ré Carneiro  
Geraldo Norberto Sgarbi  
Ismar de Souza Carvalho

**Data da defesa:** 14-12-2011

**Programa de Pós-Graduação:** Geociências



UNIVERSIDADE ESTADUAL DE CAMPINAS  
INSTITUTO DE GEOCIÊNCIAS  
PÓS-GRADUAÇÃO EM GEOCIÊNCIAS NA  
ÁREA DE GEOLOGIA E RECURSOS NATURAIS

**AUTOR:** Patrick Francisco Führ Dal Bó

"Mecanismos Depositionais e Processos Pedogenéticos em Lençóis de Areia Eólica: a formação Marilia, Neocretáceo da Bacia Bauru, Brasil, e La Salina, Holoceno da Bacia Tulum, Argentina".

**ORIENTADOR:** Prof. Dr. Giorgio Basilici

Aprovada em: 14 / 12 / 2011

**EXAMINADORES:**

Prof. Dr. Giorgio Basilici

A handwritten signature in blue ink, appearing to read "Basilici", followed by a horizontal line and the title "- Presidente".

Prof. Dr. Alexandre Campane Vidal

A handwritten signature in blue ink, appearing to read "Campane Vidal", followed by a horizontal line and the name "Carneiro".

Prof. Dr. Celso Dal Ré Carneiro

A handwritten signature in blue ink, appearing to read "Carneiro", followed by a horizontal line.

Prof. Dr. Geraldo Norberto Sgarbi

A handwritten signature in blue ink, appearing to read "Geraldo Sgarbi", followed by a horizontal line.

Prof. Dr. Ismar de Souza Carvalho

A handwritten signature in blue ink, appearing to read "Ismar de S. Carvalho", followed by a horizontal line.

Campinas, 14 de dezembro de 2011



**Lenir Führ Faria,  
pelos anos de irrevogável renúncia, amor e afeto doados à mim,  
a ti, Mãe, dedico.**



*“There is no comparison between that which is lost by not succeeding and that which is lost by not trying.”*

Sir Francis Bacon



## **AGRADECIMENTOS**

Gostaria de manifestar meus profundos e sinceros agradecimentos a todos que - de forma direta ou indireta -, contribuíram de alguma maneira à realização deste trabalho.

Ao Prof. Dr. Giorgio Basilici, amigo e orientador, que ao longo destes últimos anos esteve sempre presente e disposto a me incentivar e auxiliar em todas as etapas deste trabalho e que, através de críticas, sugestões e esclarecimentos, muito tem me ajudado na formação de meu perfil profissional como pesquisador e professor.

Aos professores doutores do DGRN Alessandro Batezelli, Emilson Pereira Leite, Ricardo Perobelli Borba, do DGEO Francisco Sérgio Bernardes Ladeira, da UNESP – RC Antenor Zanardo, da EMBRAPA Luiz Eduardo Vicente, da UFPA Rômulo Simões Angélica, pela amizade e incentivo.

Às secretárias Valdirene Pinotti (SPG) e Maria Helena Sabino Ricardo (DGRN), pela prontidão, capacidade e irrevogável anseio em ajudar com prestimosidade em todas as dúvidas e eventuais contratemplos.

Aos amigos de Universidade, geólogos Pedro Henrique Vieira de Luca, Pedro Lifter Rodrigues Prandi, Fábio Simplício e Danilo Barbuena, biólogo Rafael de Souza Faria, geógrafa Melina Mara de Souza, geólogas Lenita de Souza Fioriti e Patrícia Piaia e aos outros tantos companheiros de PG e estudantes de graduação, pelo suporte e estima.

Aos amigos extracampus, Fábio Kendi Tamaki e Oliver Raposo, pelos valiosos momentos juntos.

À Paula Amato, por seu amor.

À minha família, pelo infindável respaldo, apoio e respeito.

Aos professores doutores Alexandre Campane Vidal e Fresia Soledad Ricardi Torres Branco, pela solicitude em meu acompanhamento desde o mestrado e pelas valiosas críticas e sugestões ao decorrer desta tese.

Aos órgãos de fomento ao ensino, pesquisa e extensão ligados à Universidade, PROAP, FAEPEX, FUNCAMP (administração de convênios) e PRPG, pelos auxílios financeiros em viagens nacionais e internacionais e concessões de bolsas do Programa de Estágio Docente.

À *International Association of Sedimentologists* (IAS), pelos auxílios financeiros através do *IAS PhD Grant* (2009) e *IAS Field Trip Grant* (2010).

À Fundação de Amparo à Pesquisa do Estado de São Paulo – FAPESP, pelo Auxílio à Pesquisa (Processo 2007/00140-6).

Ao Conselho Nacional de Desenvolvimento Científico e Tecnológico (CNPq), pela concessão da bolsa de Doutorado (Processo 142651/2008-7).

## **BIOGRAFIA**

### **Patrick Francisco Führ Dal' Bó**

Bacharel e licenciado em Geografia pela Universidade Estadual Paulista Júlio de Mesquita Filho, Campus Rio Claro (2005), Mestre (2008) e Doutor (2011) em Geociências, Área de Geologia e Recursos Naturais, pela Universidade Estadual de Campinas.

Tem experiência na área de Geociências, atuando principalmente em temas relacionados com a inter-relação entre sedimentação e pedogênese em sistemas deposicionais siliciclásticos modernos e antigos.

Atualmente, é pesquisador do Centro de Estudos de Petróleo da Universidade Estadual de Campinas, atuando na Caracterização e Modelagem Geológica de Reservatórios e em Sedimentologia de Depósitos Carbonáticos.



## SUMÁRIO

<b>AGRADECIMENTOS .....</b>	<b>xi</b>
<b>LISTA DE FIGURAS .....</b>	<b>xv</b>
<b>LISTA DE ANEXOS .....</b>	<b>xvii</b>
<b>RESUMO .....</b>	<b>xix</b>
<b>ABSTRACT .....</b>	<b>xxi</b>
<b>1. INTRODUÇÃO .....</b>	<b>1</b>
<b>2. ORGANIZAÇÃO DA TESE .....</b>	<b>5</b>
<b>3. DISCUSSÃO E REVISÃO DOS ARTIGOS ELABORADOS .....</b>	<b>9</b>
<b>4. CONCLUSÕES .....</b>	<b>11</b>
<b>5. REFERÊNCIAS BIBLIOGRÁFICAS .....</b>	<b>15</b>



## LISTA DE FIGURAS

**Figura 1.** Localização das áreas de estudo. A) La Salina, localizada na província de San Juan, centro-oeste da Argentina. B) Área de ocorrência da Formação Marília e áreas de estudo na Bacia Bauru

3



## LISTA DE ANEXOS

<b>ANEXO I.</b> “Dal’ Bo, P.F.F., Basilici, G., Angélica, R.S., 2010. <i>Factors of paleosol formation in a Late Cretaceous eolian sand sheet paleoenvironment, Marília Formation, southeastern Brazil. Palaeogeography, Palaeoclimatology, Palaeoecology</i> 292, 349-365.”	<b>19</b>
<b>ANEXO II.</b> “Dal’ Bo, P.F.F., Basilici, G., Angélica, R.S., Ladeira, F.S.B., 2009. <i>Paleoclimatic interpretations from pedogenic calcretes in a Maastrichtian semi-arid eolian sand sheet paleoenvironment: Marília Formation (Bauru Basin, southeastern Brazil). Cretaceous Research</i> 30, 659-675.”	<b>65</b>
<b>ANEXO III.</b> “Dal’ Bo, P.F.F. & Basilici, G., 2010. <i>Estimativas de paleoprecipitação e gênese de feições cárnicas e argílicas em paleossolos da Formação Marília (Neocretáceo da Bacia Bauru). Geociências</i> 29(1): 33-47.”	<b>111</b>
<b>ANEXO IV.</b> “Dal’ Bo, P.F.F. & Basilici, G., 2010. <i>Interpretação paleoambiental da Formação Marília na porção noroeste da Bacia Bauru: relações entre sedimentação e paleopedogênese em um antigo lençol de areia eólica. Geociências, no prelo.</i> ”	<b>147</b>
<b>ANEXO V.</b> “Basilici, G. & Dal’ Bo, P.F.F., 2010. <i>Anatomy and controlling factors of a Late Cretaceous aeolian sand sheet: The Marília and the Adamantina formations, NW Bauru Basin, Brazil. Sedimentary Geology</i> 226, 71-93.”	<b>191</b>
<b>ANEXO VI.</b> “Dal’ Bo, P.F.F. & Basilici, G., 2011. <i>Interactions of eolian and subaqueous processes in the development of the La Salina eolian sand sheet, central-western Argentina. Sedimentary Geology, em submissão.</i> ”	<b>251</b>
<b>ANEXO VII. GLOSSÁRIO</b>	<b>293</b>





UNIVERSIDADE ESTADUAL DE CAMPINAS  
INSTITUTO DE GEOCIÊNCIAS  
PÓS-GRADUAÇÃO EM GEOCIÊNCIAS  
ÁREA DE GEOLOGIA E RECURSOS NATURAIS

**MECANISMOS DEPOSIONAIS E PROCESSOS PEDOGENÉTICOS EM LENÇÓIS  
DE AREIA EÓLICA: A FORMAÇÃO MARÍLIA, NEOCRETÁCEO DA BACIA BAURU,  
BRASIL, E LA SALINA, HOLOCENO DA BACIA TULUM, ARGENTINA**

**RESUMO**

*Tese de Doutorado*

**Patrick Francisco Führ Dal' Bó**

Lençóis de areia eólica são áreas morfodeposicionais caracterizadas por morfologias planas e ausência de dunas com faces de avalanche. Exemplos atuais e antigos de lençóis de areia eólica são conhecidos em todos os continentes e descritos na literatura desde o Paleoproterozóico. Em áreas em sedimentação, areias com marcas onduladas eólicas formam a feição sedimentar mais conspícuia e a identificação de arenitos com estratificação cavalgante transladante permite o reconhecimento de sucessões sedimentares de lençóis de areia eólica. Apesar de inúmeros estudos centrados na organização faciológica e caracterização de fatores de controle à gênese e distribuição de depósitos eólicos nessas áreas, a inter-relação entre depósitos eólicos e solos foi pouco abordada na literatura. O estudo de dois exemplos de lençóis de areia eólica nesta tese, a Formação Marília, Neocretáceo da Bacia Bauru, Brasil, e La Salina, uma área em sedimentação na Bacia Tulum, Argentina, permitiu a elucidação dos principais processos e fatores ambientais que influenciam a sedimentação eólica e a pedogênese nessas áreas. Os processos eólicos e pedogênicos parecem ocorrer em intervalos temporais distintos e respondem a mudanças ambientais alogênicas ao sistema, principalmente climáticas, que governam diferentes fases de estabilidade e instabilidade da superfície morfodeposicional e podem conduzir à criação de um registro sedimentar marcado por alternâncias cíclicas verticais entre depósitos eólicos e paleossolos. O modelo de construção, acumulação e preservação do sistema eólico também é condicionado a diversas variáveis autogênicas e alogênicas ao sistema e é distinto nos dois casos estudados. A construção do sistema eólico na Formação Marília foi diferenciada em duas fases paleoclimáticas, caracterizadas por maiores ou menores índices pluviométricos, que controlaram o suprimento e a disponibilidade sedimentar, enquanto em La Salina, o processo de construção não parece ter sido determinado por variações climáticas. A acumulação dos corpos geológicos foi favorecida nos dois sistemas eólicos devido à presença de cobertura vegetal e outros fatores estabilizadores à superfície dos lençóis. A preservação em ambos os sistemas foi controlada por subsidência tectônica seguida de progressivo soterramento dos corpos geológicos.

**Palavras-Chave:** Lençóis de areia eólica; depósitos eólicos; paleossolos; Formação Marília; La Salina.





UNIVERSIDADE ESTADUAL DE CAMPINAS  
INSTITUTO DE GEOCIÊNCIAS  
PÓS-GRADUAÇÃO EM GEOCIÊNCIAS  
ÁREA DE GEOLOGIA E RECURSOS NATURAIS

**DEPOSITIONAL MECHANISMS AND PEDOGENETIC PROCESSES IN EOLIAN SAND SHEETS: THE MARÍLIA FORMATION (LATE CRETACEOUS OF THE BAURU BASIN, BRAZIL) AND LA SALINA (HOLOCENE OF THE TULUM BASIN, ARGENTINA)**

**ABSTRACT**

*PhD Thesis*

**Patrick Francisco Führ Dal' Bó**

Eolian sand sheets are morpho-depositional areas characterized by flat or gently undulated sandy surfaces covered predominantly with wind ripples and slipfaceless dunes. Ancient and modern eolian sand sheets are known to occur in all continents and ancient examples are described in the literature since the Paleoproterozoic, being largely recognized in the sedimentary record by inversely graded climbing translatent strata. Although many sedimentological studies have focused on characterization of eolian facies and environmental factors favorable for sand sheet development, studies on dynamic interactions between eolian deposits and soils in sand sheet areas are still lacking. The study of the Late Cretaceous Marília Formation and the modern La Salina eolian sand sheet has contributed to understand which environmental factors act to promote soil development and principally those that operate to withhold its development and favors eolian sedimentation in eolian sand sheets. The eolian sedimentation and pedogenesis seem to occur in different environmental phases, mainly controlled by climate, which are responsible for the stability and instability of the morpho-depositional surface. Eolian sedimentation prevails during the phase of instability and construction of the eolian sand sheet, whereas soil formation are dominant during the stable phase, when unavailability or bypassing of sediments, allied with the development of a vegetation covering, led to the absence of sedimentation and erosional processes. The constructional phase of the eolian system in the Marília Formation was subjected to paleoclimate variations, which controlled sediment supply and availability, whereas in the La Salina area, the construction has not been directly affected by climate. Accumulations of geological bodies were favored by vegetation covering and soil development in the Marília Formation and have been occurring through stabilization of the accumulation surface by vegetation, thin mud veneers, and surface cementation in the La Salina. The preservation of both eolian systems was controlled by tectonically induced subsidence and burial.

**Keywords:** Eolian sand sheets; eolian deposits; paleosols; Marília Formation; La Salina.



## 1. INTRODUÇÃO

Lençóis de areia eólica ocorrem em sistemas deposicionais desérticos caracterizados por morfologias planas a levemente onduladas e ausência de dunas com faces de avalanche (Bagnold, 1941). Exemplos atuais de áreas em desenvolvimento de lençóis de areia eólica são comuns em áreas marginais a sistemas deposicionais de *erg* (Fryberger *et al.*, 1979; Kocurek e Nielson, 1986; Lancaster, 1994), de leques aluviais (Nielson e Kocurek, 1986), de *playa* (Breed *et al.*, 1987), em áreas costeiras (Hummel e Kocurek, 1984; El-Baz *et al.*, 2000) e regiões periglaciais (Koster, 1988; Mountney e Russell, 2004). Em sucessões sedimentares são documentados desde o Paleoproterozóico (Patterson e Heaman, 1991). Os lençóis de areia ocorrem restritos a pequenas extensões ( $<1 \text{ km}^2$ ) (Mountney, 2006), ou podem ocupar grandes áreas ( $>100.000 \text{ km}^2$ ) e, praticamente constituir toda a extensão do sistema desértico, como no caso do *Gran Desierto* (México) (Lancaster *et al.*, 1987) ou do *Selima Sand Sheet* (Egito) (Breed *et al.*, 1987).

O desenvolvimento de lençóis de areia eólica é controlado por diversos fatores, sendo considerado como primordiais a disponibilidade de areia para o transporte e deposição eólica de granulação superior a areia grossa e a presença de cobertura vegetal (Bagnold, 1941; Kocurek e Nielson, 1986; Breed *et al.*, 1987). Outros fatores que podem contribuir para a sedimentação em lençol em detrimento da formação de dunas com faces de avalanche nessas áreas são: nível do lençol freático próximo à superfície (Fryberger *et al.*, 1988), cimentação superficial (Nickling, 1984; Talbot, 1985) e inundações periódicas (Pye, 1983).

A principal feição sedimentar que ocorre nessas áreas é a presença de marcas onduladas eólicas que ao migrarem formam estratos suborizontais compostos por laminações transladantes cavalgantes (Bagnold, 1941; Hunter, 1977; Fryberger *et al.*, 1979). Em alguns casos, a superfície de lençóis de areia pode apresentar cordões arenosos de granulação grossa, orientados de forma transversal a oblíqua a direção predominante dos ventos, formando pequenos montículos por rolamento de grãos sem face de avalanche nominados de *zibars* (Nielson e Kocurek, 1986) e também podem apresentar laminações plano-paralelas produzidas por transporte tracional eólico de alta energia (*planebed lamination* de Hunter, 1977) ou megaondulações eólicas (Fryberger *et al.*, 1992). A atuação de processos pedogenéticos responsáveis pela formação de solos nessas áreas é condicionada a disponibilidade limitada de sedimentos por estabilização da superfície morfológica (Lancaster, 1993; Kocurek e Lancaster, 1999), em última instância ligada a

mudanças climáticas que conduziram a uma maior disponibilidade hídrica do sistema (Lancaster, 1997). Como consequência da estabilização da superfície morfológica é comum a ocorrência de feições pedogênicas intercaladas com estruturas sedimentares biogênicas como pistas, pegadas, escavações animais e rizólitos, em sucessões sedimentares continentais formadas por alternâncias entre depósitos eólicos e paleossolos (Loope, 1988).

Os processos sedimentares e erosivos que ocorrem em áreas de lençóis de areia eólica são bem documentados na literatura, seja em áreas modernas ou antigas, porém estudos sobre a inter-relação entre os processos sedimentares e erosivos, característicos de fases de instabilidade da superfície morfodeposicional e processos pedogenéticos, que ocorrem em fases de estabilidade morfodeposicional ainda são raros na literatura, se destacando os estudos de Gustavson e Winkler (1988) e Gustavson e Holliday (1999), que conduziram a reinterpretações de formações geológicas neogênicas nos altiplanos norte-americanos do Texas e Novo México.

O objetivo geral desta tese é a definição de processos e fatores genéticos que controlam a sedimentação e a pedogênese em áreas modernas e antigas de lençóis de areia eólica. Os objetivos específicos compreendem: a) determinação de características genéticas de sedimentos e paleossolos, b) estabelecimento de fatores de controle a instabilidade e estabilidade da superfície morfodeposicional, c) definição da arquitetura deposicional e organização sequencial de sucessões sedimentares em lençóis de areia eólica.

Para a realização dos objetivos propostos foram selecionadas duas áreas de lençóis de areia eólica: La Salina (província de San Juan, centro-oeste da Argentina) (Figura 1A) e áreas de afloramento da Formação Marília (centro-oeste e centro-norte de São Paulo, nordeste de Mato Grosso do Sul e sul de Goiás) (Figura 1B). A primeira é uma área em sedimentação e a segunda representa um exemplo antigo de sedimentação e pedogênese em lençol de areia eólica que data do Neocretáceo.

A interpretação dos resultados obtidos tem contribuído à visualização dos fatores de controle e processos responsáveis pela sedimentação e pedogênese no espaço e tempo em lençóis de areia eólica, auxiliando na melhor definição de fatores (exógenos e endógenos) que controlam as fases de construção, acumulação e preservação de depósitos e paleossolos em ambientes desérticos de lençóis de areia eólica.

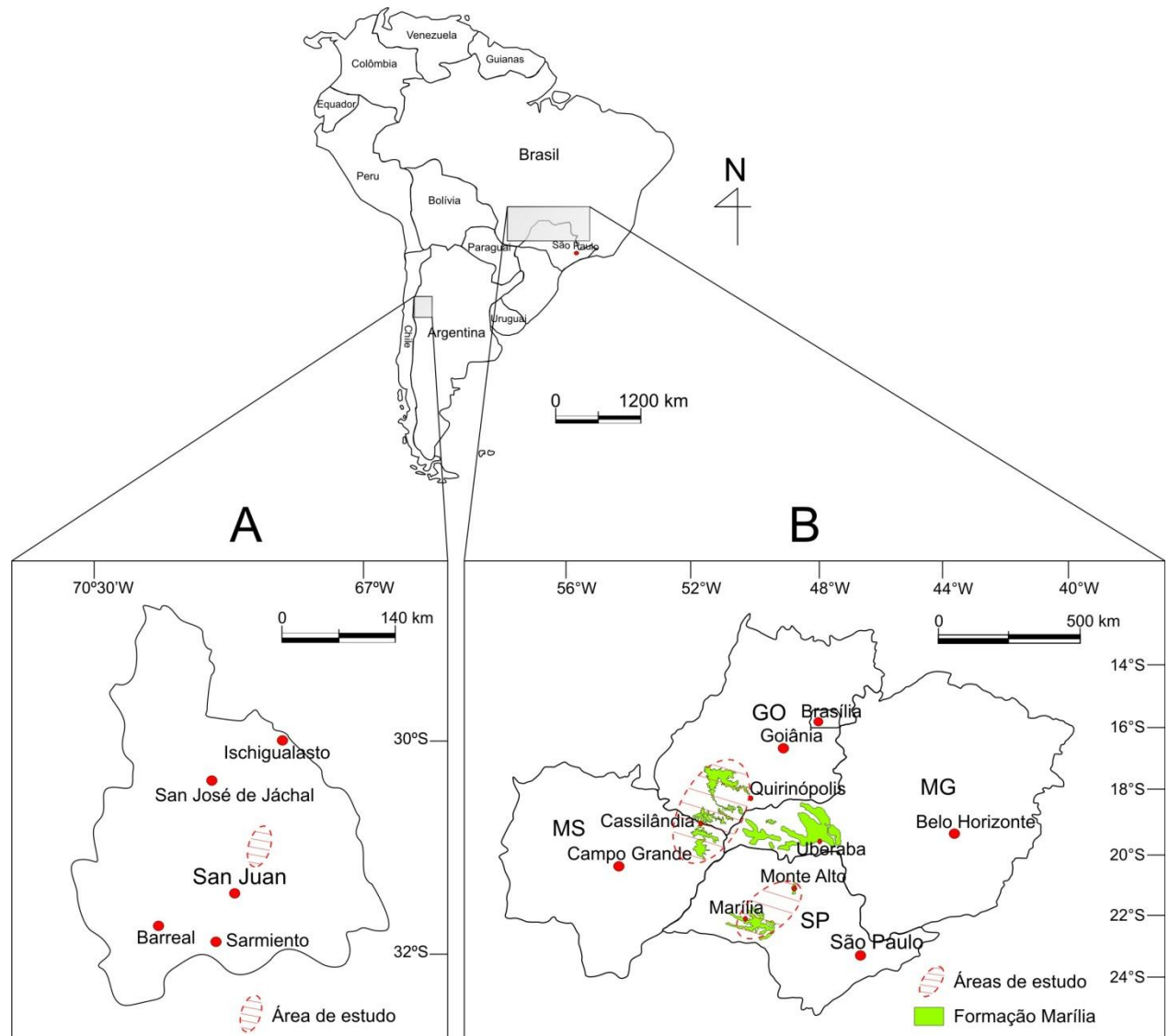


**Figura 1.** Localização das áreas de estudo. A) La Salina, localizada na província de San Juan, centro-oeste da Argentina. B) Área de ocorrência da Formação Marília e áreas de estudo na Bacia Bauru.



## 2. ORGANIZAÇÃO DA TESE

Os objetivos propostos para o desenvolvimento deste trabalho foram alcançados e serão apresentados na forma de seis artigos científicos originais que foram submetidos ao corpo editorial de periódicos científicos arbitrados e inclusos neste documento como anexos.

A apresentação dos artigos segue a seguinte ordenação: a) fatores de formação de paleossolos na Formação Marília, b) calcretes pedogênicos da Formação Marília e sua importância para a interpretação paleoambiental, c) gênese de feições paleopedogênicas particulares (cálcicas e argílicas) nos paleossolos analisados, d) relações entre sedimentação e pedogênese em áreas de lençóis de areia eólica da Formação Marília, e) fatores de controle à construção, acumulação e preservação de paleossolos e depósitos no registro sedimentar da Formação Marília, f) interações entre processos eólicos e subaquosos no desenvolvimento do lençol de areia eólica La Salina.

No Anexo I (página 15) está contida a seguinte referência: “Dal’ Bo, P.F.F., Basilici, G., Angélica, R.S., 2010. *Factors of paleosol formation in a Late Cretaceous eolian sand sheet paleoenvironment, Marília Formation, southeastern Brazil. Palaeogeography, Palaeoclimatology, Palaeoecology* 292, 349-365.” Neste artigo são discutidos os principais fatores de formação de solos (clima, organismos, material de origem, topografia e tempo de formação) e como tais influenciaram a formação e o desenvolvimento de paleossolos na Formação Marília. Este artigo mostra em detalhe como se formaram e evoluíram as duas principais ordens de paleossolos que ocorrem na Formação Marília: *Aridisols* e *Alfisols*.

No Anexo II (página 59) está contida a seguinte referência: “Dal’ Bo, P.F.F., Basilici, G., Angélica, R.S., Ladeira, F.S.B., 2009. *Paleoclimatic interpretations from pedogenic calcretes in a Maastrichtian semi-arid eolian sand sheet paleoenvironment: Marília Formation (Bauru Basin, southeastern Brazil). Cretaceous Research* 30, 659-675.” Este artigo discute a ocorrência de calcretes pedogênicos na Formação Marília e apresenta uma distinção entre os calcretes pedogênicos e outras formas de concentração de carbonato de cálcio em rochas sedimentares. No artigo é apresentada uma descrição micro- e macroscópica de horizontes de calcrete da Formação Marília e discutida a importância que estes horizontes possuem na interpretação paleoambiental da unidade rochosa.

No Anexo III (página 103) está contida a seguinte referência: “Dal’ Bo, P.F.F. & Basilici, G., 2010. *Estimativas de paleoprecipitação e gênese de feições cárnicas e argílicas em paleossolos da Formação Marília (Neocretáceo da Bacia Bauru)*. *Geociências* 29(1): 33-47.” Neste artigo são investigadas as condições paleoclimáticas e paleoambientais relacionadas à gênese de feições paleopedogênicas que indicam a concentração de carbonato de cálcio e outras que indicam a concentração de feições iluviais de ferro e argila em horizontes Bk de *Aridisols* e Bt de *Aridisols* e *Alfisols* da Formação Marília, respectivamente. Este artigo é complementar ao anterior e dá particular importância à relação entre índices de paleoprecipitação e a gênese das feições paleopedogênicas mais conspícuas (cárnicas e argílicas) que ocorrem nos paleossolos analisados.

No Anexo IV (página 135) está contida a seguinte referência: “Dal’ Bo, P.F.F. & Basilici, G., 2010. *Interpretação paleoambiental da Formação Marília na porção noroeste da Bacia Bauru: relações entre sedimentação e paleopedogênese em um antigo lençol de areia eólica*. *Geociências, no prelo*.” Neste artigo são discutidas as relações espaço-temporais entre as fases de sedimentação e as fases de pedogênese que ocorreram na Formação Marília. Este artigo difere dos anteriores, pois introduz duas novas ordens de paleossolos, os *Vertisols* e *Entisols*, e apresenta uma descrição de detalhe dos depósitos que ocorrem na porção noroeste da Bacia Bauru, destacando as inter-relações entre sedimentação e pedogênese nesta porção da bacia.

No Anexo V (página 177) está contida a seguinte referência: “Basilici, G. & Dal’ Bo, P.F.F., 2010. *Anatomy and controlling factors of a Late Cretaceous aeolian sand sheet: The Marília and the Adamantina formations, NW Bauru Basin, Brazil*. *Sedimentary Geology* 226, 71-93.” Neste artigo é apresentado um modelo de organização anatômica e evolução sequencial da Formação Marília, considerando os fatores paleoambientais e tectônicos que atuaram na construção, acumulação e preservação de paleossolos e depósitos no registro sedimentar da Formação Marília. Este artigo discute as diferentes fases temporais de evolução dos lençóis de areia eólica da Formação Marília e introduz os principais elementos físicos para a análise estratigráfica da formação.

No Anexo VI (página 233) está contida a seguinte referência: “Dal’ Bo, P.F.F. & Basilici, G., 2011. *Interactions of eolian and subaqueous processes in the development of the La Salina eolian sand sheet, central-western Argentina*. *Sedimentary Geology, em submissão*.” Neste artigo são discutidos os dados referentes à área de La Salina, com ênfase nas interações entre processos eólicos e processos subaquosos atuais e subatuais que atuaram no desenvolvimento do lençol de areia eólica La Salina.

### **3. DISCUSSÃO E REVISÃO DOS ARTIGOS ELABORADOS**

A primeira fase de pesquisa em campo foi realizada nas áreas de ocorrência da Formação Marília, nos estados de São Paulo, Mato Grosso do Sul e Goiás. Desta fase resultou a preparação dos cinco primeiros artigos aqui apresentados. A maior ênfase dada ao estudo da sucessão neocretácea se justifica pela maior área de ocorrência, pela grande diversidade e complexidade dos elementos analisados e devido às dificuldades logísticas presentes na área de La Salina.

A análise de fácies e a análise paleopedológica de detalhe da sucessão sedimentar da Formação Marília permitiram a identificação de diferentes fácies e tipos de paleossolos, que foram agrupados em três elementos arquiteturais: Paleossolos, Depósitos eólicos de lençóis de areia e Depósitos de canais fluviais efêmeros. A distribuição por espessura dos elementos arquiteturais revelou a preponderância do elemento Paleossolos no registro sedimentar, respondendo por 66% do total da espessura da Formação Marília. O elemento Depósitos eólicos de lençóis de areia apresenta distribuição subordinada, representando 23% da espessura, e o elemento Depósitos de canais fluviais efêmeros equivale a outros 11%. A maior frequência por espessura do elemento Paleossolos foi fator determinante ao estudo mais aprofundado deste elemento e sua caracterização micro- e macromorfológica em detalhe como constante do artigo apresentado no Anexo I (Dal' Bo *et al.*, 2010. *Palaeogeog., Palaeoclim., Palaeoecol.* 292, 349-365).

O Anexo II (Dal' Bo *et al.*, 2009. *Cret. Res.* 30, 659-675) apresenta também um estudo sobre a caracterização do elemento Paleossolos, porém com ênfase na discriminação e no detalhamento de horizontes de calcretes pedogênicos, os quais têm sido objeto de diversos estudos na Formação Marília (Suguió, 1973; Suguió e Barcelos, 1983; Fernandes, 1998) e matéria controversa quanto à sua origem e significado paleoambiental (Etchebehere *et al.*, 1993; Silva *et al.*, 1994; Goldberg e Garcia, 2000; Fernandes, 2010). O artigo exposto no Anexo III (Dal' Bo & Basilici, 2010. *Geoc.* 29(1): 33-47) aprofunda a discussão da gênese das concentrações de carbonato de cálcio em perfis de paleossolos, e apresenta um modelo de evolução genética no qual as concentrações de carbonato estariam ligadas a períodos paleoclimáticos caracterizados por baixos índices de paleoprecipitações aos quais se seguiram momentos com marcada lixiviação do conteúdo de carbonato, indicativos de períodos com maior umidade atmosférica.

A interpretação paleoambiental da Formação Marília é discutida no Anexo IV (Dal' Bo & Basilici, 2010. *Geoc., no prelo*), no qual é apresentado um modelo de relação espaço-temporal entre sedimentação e pedogênese para explicar as alternâncias cíclicas verticais entre depósitos eólicos e paleossolos verificadas na sucessão sedimentar. O estudo dessas alternâncias fomentou a proposição de um modelo de organização anatômica e evolução sequencial da Formação Marília, que é apresentado no Anexo V (Basilici & Dal' Bo, 2010. *Sed. Geol.* 226, 71-93) e considera as diferentes fases de construção, acumulação e preservação de depósitos e paleossolos no registro geológico.

A segunda etapa da pesquisa buscou a caracterização de mecanismos deposicionais e a compreensão da inter-relação entre processos atuais e subatuais que influenciaram na gênese e desenvolvimento do lençol de areia eólica La Salina. Por se tratar de uma área em sedimentação, foi dada ênfase maior à observação e quantificação de elementos morfológicos e à descrição de estruturas sedimentares em formação. A ausência de evidências de desenvolvimento de solos e/ou paleossolos impossibilitou o emprego de métodos pedológicos e a análise direta de perfis de solos em formação sob a influência de fatores ambientais quantificáveis. A análise faciológica do registro sedimentar foi complementada pela datação de sedimentos por luminescência opticamente estimulada (LOE), que permitiu a quantificação de taxas de sedimentação e a verificação da evolução sedimentar da área durante o Holoceno. Os dados e interpretações disponíveis são apresentados no Anexo VI (Dal' Bo & Basilici, 2011. *Sed. Geol., em submissão*).

## **4. CONCLUSÕES**

As conclusões principais sobre a dinâmica sedimentar e pedogênica das áreas de lençóis de areia eólica estudadas nesta tese são:

a) Dentre os principais fatores que governam a sedimentação em lençóis de areia eólica em detrimento da formação de dunas com faces de avalanche, destacados por Kocurek e Nielson (1986), na Formação Marília assumem especial importância a presença de cobertura vegetal e a disponibilidade de clastos de granulação superior a areia grossa para a sedimentação eólica. Na área de La Salina, a vegetação somada a filmes de lama e cimentação superficial oriundos de inundações periódicas do lençol freático preponderam sobre os demais fatores;

b) A pedogênese em lençóis de areia eólica é restrita a momentos nos quais a superfície morfodeposicional encontra-se estabilizada. As condições ideais para a estabilização da superfície ocorrem em momentos de diminuição do aporte e regulação sedimentar (efluxo equivalente ao influxo) e em situações de aumento da densidade vegetacional. Na Formação Marília, as duas condições se manifestaram em períodos de maior umidade atmosférica e permitiram o desenvolvimento de perfis espessos de solos. Em La Salina, apesar de parte da superfície do lençol ser coberta por vegetação, esta não é suficientemente extensa para criar uma condição de estabilidade da superfície. As altas taxas de sedimentação que caracterizam a área são responsáveis pela não interrupção dos processos sedimentares e assim não geração de condições favoráveis ao desenvolvimento de solos. Provavelmente, durante a deposição da Formação Marília, houve concomitância entre a diminuição do aporte sedimentar e o aumento da cobertura vegetal, pois não há registros que assegurem a existência de um paleoclima mais úmido na formação estudada que o vigente em La Salina;

c) A construção do sistema eólico foi diferenciada nas duas áreas. Na Formação Marília, o suprimento primário de sedimentos foi alogênico, proveniente de rios que fluíram durante fases paleoclimáticas mais úmidas, e secundariamente houve significativa contribuição autogênica, derivada de erosão de porções superficiais de perfis de solos durante as fases mais secas. Em La Salina, o suprimento sedimentar é originado por deflação de morros conglomeráticos neogênicos que afloram a oeste da área. A deflação gera significativa quantidade de areia que alimenta o sistema eólico, deixando os morros compostos por pavimentos de deflação de granulação superior a areia muito grossa.

A disponibilidade de sedimentos para o transporte e deposição eólica foi controlada na Formação Marília pela extensa cobertura vegetal e elevação temporária do nível do lençol freático nos canais fluviais, durante as fases paleoclimáticas mais úmidas e por cimentação de horizontes de solos, nas fases mais secas, que limitaram a atividade de deflação às porções superficiais dos solos. Em La Salina, a disponibilidade não deve ter sido um fator limitante à construção do sistema eólico, tendo em vista que a deflação dos morros neogênicos depende da capacidade de transporte dos ventos, que não representa um fator limitante. A distribuição desigual das precipitações, com grandes volumes de chuva concentrados em períodos curtos, favorece também a rápida infiltração e o escoamento superficial da água num substrato predominantemente arenoso, não possibilitando o encharcamento da superfície e diminuindo, assim, o tempo de adesão capilar das areias.

A capacidade de transporte pelo vento é função de sua força e independe da disponibilidade sedimentar. Na Formação Marília, a capacidade de transporte foi considerada como um fator limitante à construção do sistema eólico apenas em circunstâncias nas quais o potencial de transporte eólico se equivaleu a capacidade realizada de transporte, situação que ocorreu em momentos nos quais o suprimento de sedimentos foi gerado a uma taxa maior que a capacidade de transporte dos ventos (cf. Fig. 21, Basilici e Dal' Bo, 2009, *Sed. Geol.*). A ausência de dados sobre a capacidade de transporte e o regime dos paleoeventos impossibilitou uma análise mais refinada dessa variável. Em La Salina, a análise de dados climáticos dos últimos 37 anos revelou que a capacidade de transporte pelo vento não tem sido um fator limitante à construção do sistema eólico, tendo em vista que a velocidade limiar para o transporte tem sido alcançada periodicamente, principalmente nos meses de verão (cf. Fig. 3F, Dal' Bo e Basilici, 2011, *Sed. Geol.*, em submissão);

d) Os mecanismos de acumulação, responsáveis pela formação de corpos geológicos tridimensionais, também foram diferenciados nas duas áreas. Na Formação Marília, ao decorrer de fases paleoclimáticas mais úmidas, a superfície de acumulação foi controlada pelo aumento da cobertura vegetal e consequente formação de perfis de solo que estabilizaram a superfície. Durante as fases mais secas, a superfície de acumulação foi erodida por deflação e decaiu até o nível de desenvolvimento de horizontes cimentados nos solos (Bk e Bkm) mais resistentes à deflação ou foi controlada pela regulação sedimentar eólica nas áreas caracterizadas por depósitos ou por solos que não desenvolveram horizontes cimentados. Em La Salina, a

acumulação de estratos sedimentares está ligada a fatores localizados e intermitentes de estabilização da superfície de acumulação. A vegetação é o principal agente estabilizante e atua como um obstáculo natural à livre circulação de ventos saturados ou subsaturados em sedimentos, permitindo a acumulação localizada de sedimentos em suas zonas de sombra. O desenvolvimento de estruturas radiculares atua também na fixação e manutenção desse sedimento preso ao substrato e assim possibilita a elevação da superfície de acumulação no tempo. Corpos lamíticos e cimentação superficial por sulfato de cálcio são outros agentes estabilizantes, que estão relacionados às inundações periódicas ocasionadas por elevação temporária do nível do lençol freático em períodos de maior precipitação atmosférica. A atuação dos agentes estabilizadores aumenta o potencial de preservação dos depósitos, porém, como a atuação desses agentes na natureza é transitória, uma vez eliminadas as condições que permitem a estabilização, a acumulação estará sujeita à erosão e até à sua completa destruição, não deixando vestígios no registro sedimentar;

e) A incorporação da acumulação e consequente preservação do sistema eólico no registro sedimentar da Formação Marília ocorreu por subsidência tectônica, que criou o espaço de acomodação, e por progressivo soterramento dos corpos geológicos, que foram sujeitos a diversas fases de construção, destruição e estabilidade do sistema deposicional. Em La Salina, a porção preservada do sistema eólico possui espessura mínima de 4 m, e sua incorporação no registro sedimentar tem sido favorecida por altas taxas de criação de espaço de acomodação, em uma região tectonicamente ativa, e por altas taxas de sedimentação, que propiciam o contínuo soterramento dos corpos geológicos.



## 5. REFERÊNCIAS BIBLIOGRÁFICAS

- Bagnold, R.A., 1941. The physics of blow sand and desert dunes. Methuen, London, 265 pp.
- Breed, C.S., McCauley, J.F., Davis, P.A., 1987. Sand sheet of the eastern Sahara and ripples blankets on Mars. In: Frostick, L., Reid, I. (Eds.), Desert sediments: ancient and modern. Geological Society of America Special Publication, 35, pp. 337-359.
- El-Baz, F., Maingue, M., Robinson, C., 2000. Fluvio-aeolian dynamics in the northeastern Sahara: the relationship between fluvial/aeolian systems and groundwater concentration. *Journal of Arid Environments* 44, 173-183.
- Etchebehere, M.L.C., Silva, R.B., Saad, A.R., Resende, A.C., 1993. Reavaliação do potencial do Grupo Bauru para evaporitos e salmouras continentais. *Geociências* 12, 333-352.
- Fernandes, L.A., 1998. Estratigrafia e evolução geológica da parte oriental da Bacia Bauru (Ks, Brasil). Tese de Doutorado, Instituto de Geociências, Universidade de São Paulo, 216 p.
- Fernandes, L.A., 2010. Calcretes e registros de paleossolos em depósitos continentais neocretáceos (Bacia Bauru, Formação Marília). *Revista Brasileira de Geociências* 40, 19-35.
- Fryberger, S.G., Ahlbrandt, T.S., Andrews, S., 1979. Origin, sedimentary features and significance of low-angle aeolian ‘sand sheet’ deposits, Great Sand Dunes National Monument and vicinity, Colorado. *Journal of Sedimentary Petrology* 49, 733-746.
- Fryberger, S.G., Schenk, C.J., Krystinik, L.K., 1988. Stokes surfaces and the effects of near-surface groundwater-table on aeolian deposition. *Sedimentology* 35, 21-41.
- Fryberger, S.G., Hesp, P., Hastings, K., 1992. Aeolian granule ripple deposits. Namibia. *Sedimentology* 39, 319-331.
- Goldberg, K., Garcia, A.J.V., 2000. Palaeobiogeography of the Bauru Group, a dinosaur-bearing Cretaceous unit, northeastern Paraná Basin, Brazil. *Cretaceous Research* 21, 241-254.
- Gustavson, T.C., Holliday, V.T., 1999. Eolian sedimentation and soil development on a semi-arid to subhumid grassland, Tertiary Ogallala and Quaternary Blackwater Draw formations, Texas and New Mexico High Plains. *Journal of Sedimentary Research* 69, 622-634.
- Gustavson, T.C., Wrinkler, D.A., 1988. Depositional facies of the Miocene-Pliocene Ogallala Formation, northwestern Texas and eastern New Mexico. *Geology* 16, 203-206.
- Hummel, G., Kocurek, G., 1984. Interdune areas of the Back Island dune field, North Padre Island, Texas. *Sedimentary Geology* 39, 1-26.

- Hunter, R.E., 1977. Basic types of stratification in small eolian dunes. *Sedimentology* 24, 361-387.
- Kocurek, G., Lancaster, N., 1999. Aeolian system sediment state: theory and Mojave Desert Kelso dune field example. *Sedimentology* 46, 505-515.
- Kocurek, G., Nielson, J., 1986. Conditions favourable to the formation of warm-climate aeolian sand sheets. *Sedimentology* 33, 795-816.
- Koster, E.A., 1988. Ancient and modern cold-climate aeolian sand deposition: a review. *Journal of Quaternary Science* 3, 69-83.
- Lancaster, N., 1993. Origins and sedimentary features of supersurfaces in the northwestern Gran Desierto sand sea. In: Pye, K., Lancaster, N. (Eds.), *Aeolian sedimentation, ancient and modern: International Association of Sedimentologists Special Publication*, 16, pp. 71-83.
- Lancaster, N., 1994. Dune morphology and dynamics. In: Abrahams, A.D., Parson, A.J. (Eds.), *Geomorphology of desert environments*. Chapman & Hall, London, pp. 474-505.
- Lancaster, N., 1997. Response of eolian geomorphic systems to minor climate change: examples from the southern Californian deserts. *Geomorphology* 19, 333-347.
- Lancaster, N., Greeley, R., Christensen, P.R., 1987. Dunes of the Gran Desierto sand sea, Sonora, Mexico. *Earth Surface Processes and Landforms* 12, 277-288.
- Loope, D.B., 1988. Rhizoliths in ancient aeolianites. *Sedimentary Geology* 56, 301-314.
- Mountney, N.P., 2006. Eolian facies models. In: Posamentier, H.W., Walker, R.G. (Eds.), *Facies models revisited*. Society for Sedimentary Geology Special Publication, 84, pp. 19-83.
- Mountney, N.P., Russell, A.J., 2004. Sedimentology of aeolian sand sheet deposits in the Askja region of northeast Iceland. *Sedimentary Geology* 166, 223-244.
- Nickling, W.G., 1984. The stabilizing role of bonding agents on the entrainment of sediments by wind. *Sedimentology* 31, 111-117.
- Nielson, J., Kocurek, G., 1986. Climbing zibars of the Algodones. *Sedimentary Geology* 48, 1-15.
- Patterson, J.G., Heaman, L.M., 1991. New geochronologic limits on the depositional age of the Hurwitz Group, Trans-Hudson hinterland, Canada. *Geology* 19, 1137-1140.
- Pye, K., 1983. Coastal dunes. *Progress in Physical Geography* 7, 531-546.
- Silva, R.B., Etchebehere, M.L.C., Saad, A.R., 1994. Groundwater calcrites: uma interpretação alternativa para os calcários da Formação Marília no Triângulo Mineiro. In: Simpósio sobre o Cretáceo do Brasil, 3, Rio Claro, Boletim, pp. 81-84.

Suguio, K., 1973. Formação Bauru: calcários e sedimentos detriticos associados. Tese de Livre Docência, Instituto de Geociências, Universidade de São Paulo. 2v.

Suguio, K., Barcelos, J.H., 1983. Calcretes of the Bauru Group (Cretaceous), Brazil: petrology and geological significance. Boletim do Instituto de Geociências da Universidade de São Paulo 14, 31-47.

Talbot, M.R., 1985. Major bounding surfaces in aeolian sandstones - a climatic model. Sedimentology 32, 257-265.



## ANEXO I

“Dal’ Bo, P.F.F., Basilici, G., Angélica, R.S., 2010. *Factors of paleosol formation in a Late Cretaceous eolian sand sheet paleoenvironment, Marília Formation, southeastern Brazil. Palaeogeography, Palaeoclimatology, Palaeoecology* 292, 349-365.”



*“Each soil has had its own history. Like a river, a mountain, a forest, or any natural thing, its present condition is due to the influences of many things and events of the past.”*

*Charles Kellogg*



# **FACTORS OF PALEOSOL FORMATION IN A LATE CRETACEOUS EOLIAN SAND SHEET PALEOENVIRONMENT, MARÍLIA FORMATION, SOUTHEASTERN BRAZIL**

Patrick Francisco Führ Dal' Bó<sup>a\*</sup>, Giorgio Basilici<sup>a</sup>, Rômulo Simões Angélica<sup>b</sup>

<sup>a</sup>DGRN/IG – Universidade Estadual de Campinas, Cidade Universitária, 13083-870, Campinas (SP), Brazil (patrickdalbo@ige.unicamp.br, basilici@ige.unicamp.br)

<sup>b</sup> IG – Universidade Federal do Pará, 66075-110, Belém (PA), Brazil (angelica@ufpa.br)

\* Corresponding author (Tel.: 55 19 35215944)

## **Abstract**

The Marília Formation, which crops out in southeastern Brazil, is interpreted as a Late Cretaceous eolian sand sheet area. The sedimentary succession, *ca* 110 m thick, is characterized by alternating strata of eolian deposits and paleosols. The paleosols constitute more than 66% of the thickness, and are an important element in the interpretation of the paleoenvironmental controlling factors which affected the soil formation in this eolian sand sheet. In this paper six paleosol profiles are described and assigned to two pedotypes: Itaja and Apore. The Itaja pedotype is constituted of a sequence of five superimposed polygenetic profiles which show different phases of clay illuviation and carbonate precipitation, and it has been classified as Aridisol. The Apore pedotype overlies the Itaja pedotype. This pedotype shows an increase in leaching, CIA-K ratios, reddening, and illuvial clay features in respect to Itaja, and has been classified as Alfisol. The analysis of the factors which controlled the soil formation revealed that both pedotypes formed on a stable landscape probably covered by a community of low stature plants, in which the soils had sufficient time to develop very mature profiles. The changes in soil-forming processes were driven principally by variations in available soil moisture from precipitation. Using depth-to-carbonate functions from Bk and CIA-K proxy from Bt horizons of the Itaja pedotype, mean annual precipitation (MAP) estimates range from 240 to 1078 mm/year, respectively. These contrasting climatic conditions resulted in the superimposition of arid or semi-arid with more humid climates and determined the considerable change in the pedogenic features, with many horizons showing the interlacing of calcite and clay features. In the Apore pedotype CIA-K proxy from Bt horizons estimates that averaged MAP was around 900 mm/year,

and the prevalent humid conditions can be attested by soil properties and abundance and depth of root traces. Our results show that the diversity in pedotypes is mainly attributed to differences in paleoclimatic conditions during Maastrichtian time, and that eolian sedimentation was restricted to periods of harsh arid conditions, as in semi-arid climates, with MAP estimates around 240 mm/year, the formation of soils with well developed calcic horizons was possible.

Keywords: Paleosols; Paleoclimate; Eolian Sand Sheet; Bauru Basin; Late Cretaceous.

## **1. Introduction**

The development of soils in modern eolian sand sheet environments is controlled by low sedimentation rates and humid climatic conditions (Gustavson and Holliday, 1999). Ancient sand sheet areas are widespread in all continents and occupy a significant part of the geological record in desertic successions (Kocurek and Nielson, 1986). Although paleosols are an important element in interpreting eolian sand sheet successions, few studies have focused on the genesis of paleosol profiles in such successions and in the paleoenvironmental and paleoclimatic proxies which they represent. The use of pedogenic features that can be quantitatively related to the factors that control soil formation have proven to be a worthy tool in interpreting paleoenvironments from Paleozoic to Cenozoic paleosols (Retallack, 2001, 2007; Sheldon et al., 2002; Sheldon, 2003, 2005; Therrien, 2005; Hamer et al., 2007a, b; Kraus and Riggins, 2007; Cleveland et al., 2008; Kahmann and Driese, 2008; Sheldon and Tabor, 2009).

The Marília Formation was deposited during Maastrichtian in the intracratonic Bauru Basin and it is interpreted as a desertic sand sheet area. The sedimentary succession is mainly characterized by alternating eolian sand sheet deposits and paleosols (Basilici et al., 2009). Previous studies of Late Cretaceous climate of the Bauru Basin indicate that it was in general arid (Suguió and Barcelos, 1983) with well-defined seasons distinguished by alternating dry and rainy periods (Goldberg and Garcia, 2000). According to Goldberg and Garcia (2000) and Garcia et al. (2005) an increase in aridity marked the transition Coniacian-Campanian to Maastrichtian times in the Bauru Basin. This increasingly aridity is believed to be caused not only by shifts in global paleoclimate but also to the uplifting of surrounding hills which acted as topographic barriers and inhibited the entrance of humid Atlantic winds favoring the development of conifer forests in the marginal highlands (Lima, 1983) and increased drought conditions basinwards. However, detailed studies which focus on the influence of the paleoclimate conditions on sedimentation and paleosol formation in the Bauru Basin are not common.

The purpose of this study is to discuss the paleoenvironmental factors which controlled soil formation and evolution in the Late Cretaceous eolian sand sheet paleoenvironment of the Marília Formation. To achieve this goal, six paleosol profiles that crop out in the same vertical succession were described, and the following factors that control soil formation were evaluated: climate, organisms, parent material, topographic relief, and time.

## **2. Geological and stratigraphical setting**

The paleosol succession analyzed in this paper is part of the Late Cretaceous Marília Formation which crops out near the town of Itajá, in the northwestern portion of the Bauru Basin, southeastern Brazil (Fig. 1A). The Bauru Basin, Santonian-Maastrichtian in age (Fernandes and Coimbra, 1996), is an intracratonic basin developed in the interior of South-American Platform. Its genesis is considered as a response to thermal and isostatic subsidence after the accumulation of Early Cretaceous basaltic lavas of the Serra Geral Formation which is almost 2000 m thick (Riccomini, 1997). The sedimentary record of this basin occupies approximately 370.000 km<sup>2</sup> in the southeast of Brazil and has a maximum thickness of 300 m. The Bauru Basin has been divided into two lithostratigraphic units: Caiuá and Bauru groups (Fernandes and Coimbra, 1996). In the study area, only the Adamantina and Marília formations (Bauru Group) crop out. Towards the southwest, the transition to Caiuá Group (an eolian sand sea) is poorly defined (Fig. 1B).

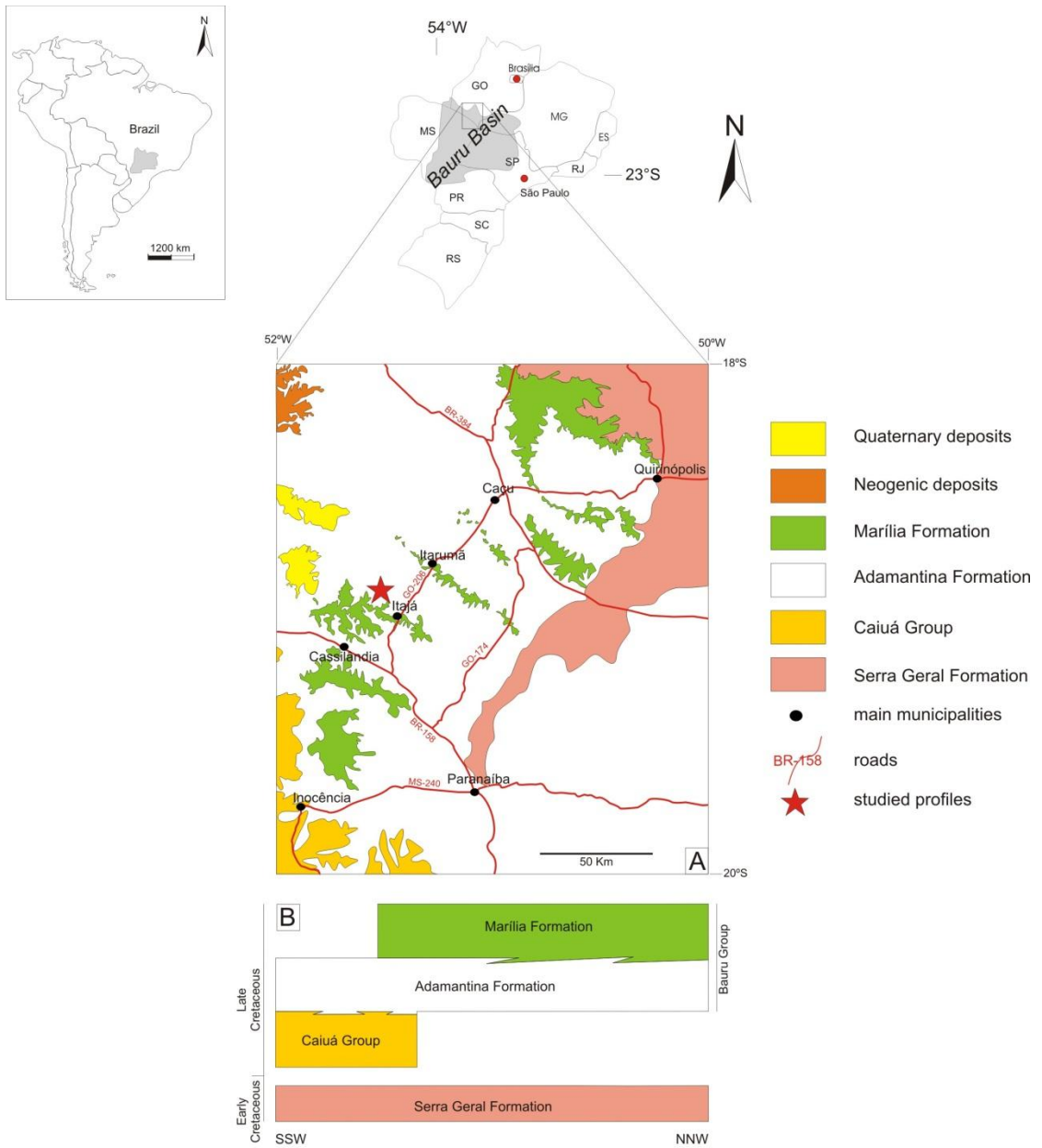


**Figure 1.** (A) Map showing the location of the study area in the southeastern Brazil and the geology of the northwest portion of the Bauru Basin. Star indicates the location of the profiles site. Geological units were modified from CPRM – Serviço Geológico do Brasil (2004). (B) Stratigraphic synthesis of the Bauru Basin. Modified from CPRM - Serviço Geológico do Brasil (2004) and Zaher et al. (2006).

The Adamantina Formation is the older unit and is mainly composed of very fine to fine-grained, moderate to well sorted sandstone, with local interbedding of siltstone and mudstone (Soares et al., 1980). This formation is interpreted as having been deposited in a wide alluvial plain with braided rivers and small ponds (Goldberg and Garcia, 2000). The transition to Marília

Formation is gradational. The Marília Formation is made up of very fine to medium-grained sandstone with rare beds of sandstone conglomerate and mudstone (Soares et al., 1980). Based on biostratigraphic data obtained from carophytes and ostracods recovered from a quarry *ca* 200 km east of the study area, this last unit is considered Maastrichtian in age (Dias-Brito et al., 2001).

The depositional paleoenvironment is interpreted as an eolian sand sheet area, dominated by eolian ripples, pedogenesis, and few ephemeral channels (Basilici et al., 2009). Although the paleosols constitute around 66% of the thickness of the Marília Formation, only few recent works have given attention to them and to the paleoclimatic and paleoenvironmental proxy which they represent (Basilici et al., 2009; Dal' Bo et al., 2009).

### **3. Methods**

In this paper we present a detailed study on the factors of soil formation of a stratigraphic succession located near the town of Itajá. This succession contains six paleosol profiles that are grouped in two pedotypes (Itaja and Apore) (Fig. 2) following the methodology of Retallack (1994a). The name of the pedotypes is merely descriptive, and refers to the city of Itajá and the regional Aporé River.

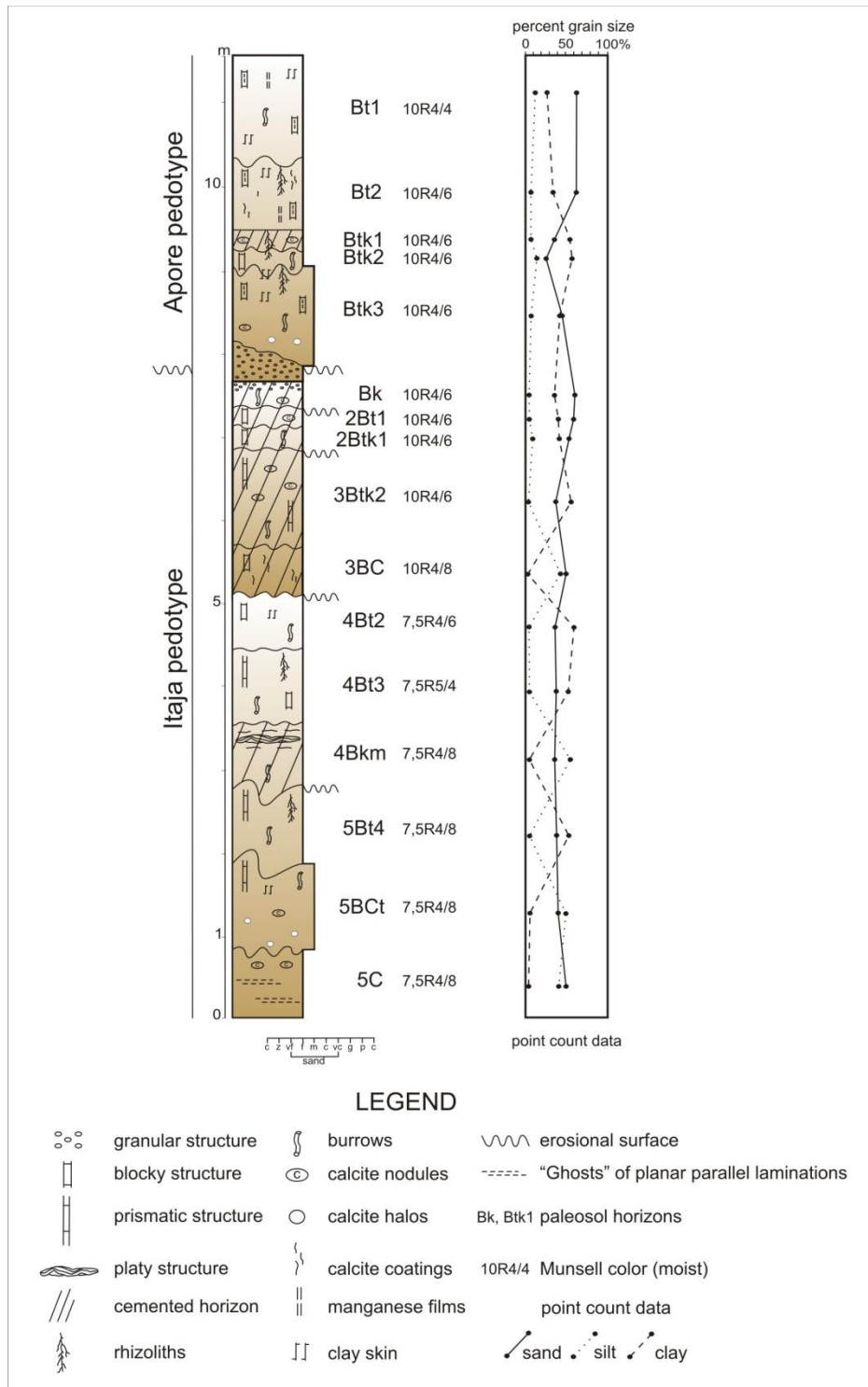


**Figure 2.** Measured section located near the town of Itajá (19°03'40"S and 51°33'78"W). Star in Figure 1 indicates the location of the section.

The paleosols were recognized in the field on the basis of soil structures, horizonation, root traces, and textural variations (Catt, 1990; Retallack, 2001). All paleosols were described

following the procedures of the Soil Survey Manual (Soil Survey Staff, 1993) and classified according to US Soil Taxonomy (Soil Survey Staff, 1999). Grain size variations were noted from point counting of thin sections (250 counts per section). Twenty-four oriented samples were collected for micromorphologic analysis. They were prepared from air-dried samples using standard techniques (Murphy, 1986). Micromorphological features were described following Bullock et al. (1985) guideline.

The mineralogy of horizons was determined by X-ray powder diffraction (XRD), for whole and oriented samples. The XRD patterns were recorded using a PANalytical X'Pert Pro MPD (PW3040/60) theta-theta diffractometer with FeK $\beta$ -filtered CoK $\alpha$  radiation at an operating setting of 40 kV/35 mA. The patterns were recorded from 3 to 40° 2 $\theta$ , with a step scan of 0.02° 2 $\theta$  and time per step of 10s. Oriented samples of <2  $\mu$ m fraction were carried out to identify clay minerals. For each sample (glass mounting), three x-ray diffractograms were obtained, following the sequence: 1) Air-dried, 2) ethylene glycol-solvated, and 3) heating at 550°C.

The major oxides and trace elements were determined on fused beads and pressed pellets, respectively by X-ray fluorescence spectrometer (Philips, PW2404). The XRF analytical procedure employed reports major oxides in weight percent and trace elements in ppm. Loss on ignition (LOI) was determined after solids were heated for 2 h at 1000°C. The sample taken for parent material characterization is located below the stratigraphic level of Itaja pedotype.

Calcite nodules, clay coatings, surface oxides, mineral forms, and surface grain textures were also studied using a LEO 430 scanning electron microscope (SEM) equipped with an energy dispersive X-ray spectrometer (EDS). Undisturbed dried samples were coated with Au film.

## 4. Results

### 4.1. Field observations of paleosols

In the studied stratigraphic succession, the Apore pedotype overlies the Itaja pedotype (Fig. 2). The base of the Apore pedotype corresponds to the lower boundary with the Itaja pedotype. It is characterized by an undulating erosional surface probably associated to wind

deflation which was responsible for the truncation of the uppermost A horizon of the Itaja pedotype.

The pedotypes are developed on eolian sandstone deposits. These deposits are constituted of very-fine to medium-grained sandstone with planar horizontal or low-angle laminations. The sandstone is well-sorted and consists of well-rounded quartz grains, lithic fragments, and rare feldspars. Where the parent material is not altered by paleopedogenesis, sandstone beds show planar horizontal or low-angle laminas with limited lateral continuity, commonly pinching out. Internally, each lamina can be differentiated by a rough inverse gradation, and by a thin lamina of very fine sandstone. These beds are formed by deposition of translatent wind-ripples strata (Hunter, 1977).

#### **4.1.1. Apore pedotype**

This pedotype is 3.57 m thick and consists of the following sequence of horizons: Bt1-Bt2-Btk1-Btk2-Btk3 (Fig. 3). The sandy texture predominates, and ranges from fine-grained in upper Bt horizons to medium-grained sand in lower Btk horizons. The Bt horizons (Bt1, Bt2) are 2.15 m thick and red (10R4/6, 10R4/8) to reddish brown (10R4/4) in color. The structure is strong very coarse subangular blocky parting to strong coarse angular blocky with common prominent dark gray (N3/0) films of manganese oxyhydroxides on ped faces. Signs of clay translocation are indicated by few to common distinct clay skins that occur on ped faces, inside pores, and coating and bridging sand grains. The calcium carbonate cementation is weakly developed, with no evidence of calcite nodules. Two kinds of bioturbation traces were observed in Bt horizons. They are sand filled vertically oriented cylindrical tubes, 5-10 mm in diameter, 24-80 mm long, and common vertically elongated sand filled structures, with downward and lateral tapering, 10-12 mm in diameter (main axis), 4-6 mm (secondary axis), and more than 180 mm long. The transition to the Btk horizons is abrupt and smooth. The Btk horizons are 1.42 m thick and red (10R4/6, 10R4/8) in color with common medium faint red (10R4/8) mottles in Btk1. The structure is strong very coarse sub- and angular blocky parting to strong coarse angular blocky with few faint clay skins, and few distinct calcite coatings on ped faces. The calcium carbonate cementation is strongly developed. The nodules vary from few white hard calcite nodules, medium to coarse in size (5-13 mm across), and spherical to irregular in shape in Btk1

and Btk2 to few white hard calcite nodules, coarse to very coarse in size (15-35 mm across), and ellipsoidal in shape in Btk3. In the last Btk3 horizon, few white soft calcite nodules with diffuse outer boundaries also occur. They are fine to medium in size (4-7 mm across), and irregular in shape. The bioturbation traces are conspicuous in the Btk3 horizon. They are vertically elongated tubular structures that taper and branch downwards, 7-9 mm in diameter (main axis), 4-2 mm (secondary axis), and more than 200 mm long. These structures are sand filled and show an impregnated outer boundary of manganese oxyhydroxides.

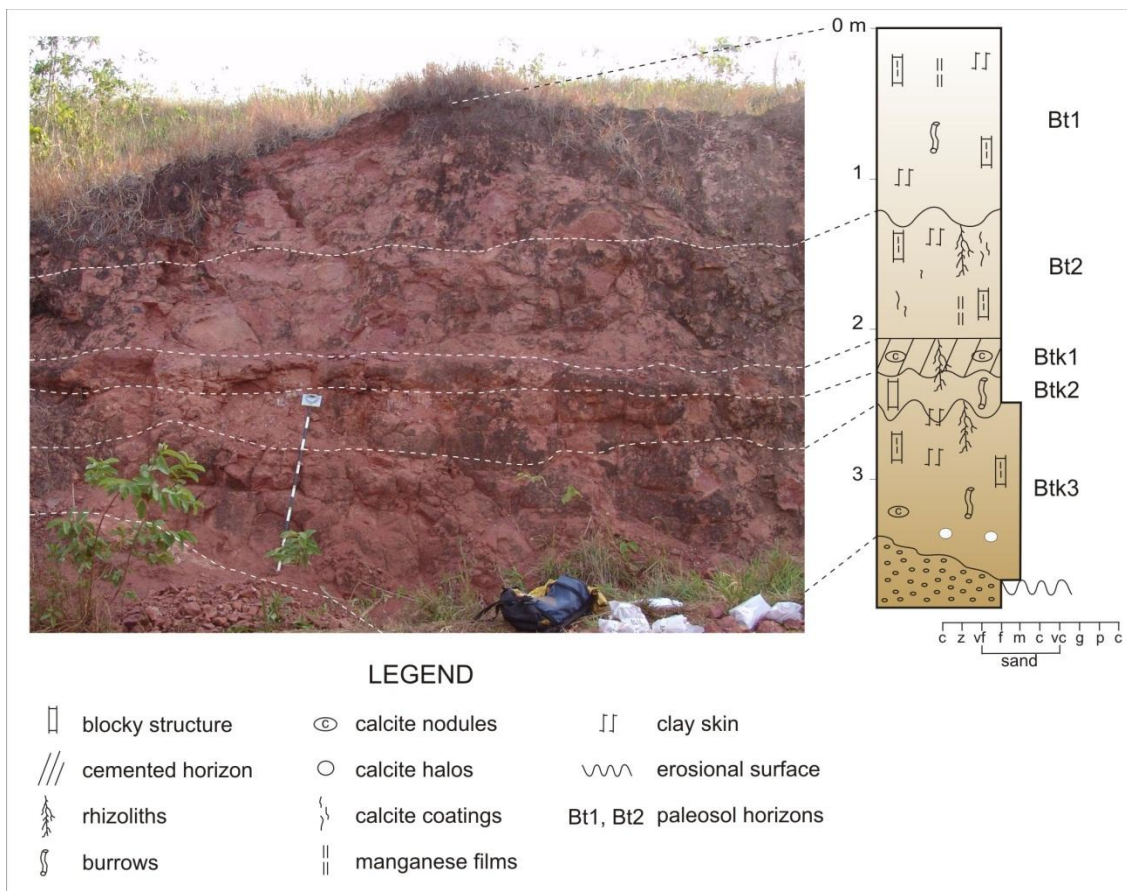


**Figure 3.** Apore pedotype of Marília Formation. Apore pedotype is an Alfisol-like paleosol.

#### 4.1.2. Itaja pedotype

This pedotype is constituted of a sequence of five vertically stacked cumulative profiles with 7.84 m of total thickness (Fig. 4). The texture is sandy, from fine to medium-grained sand, in all paleosol horizons.

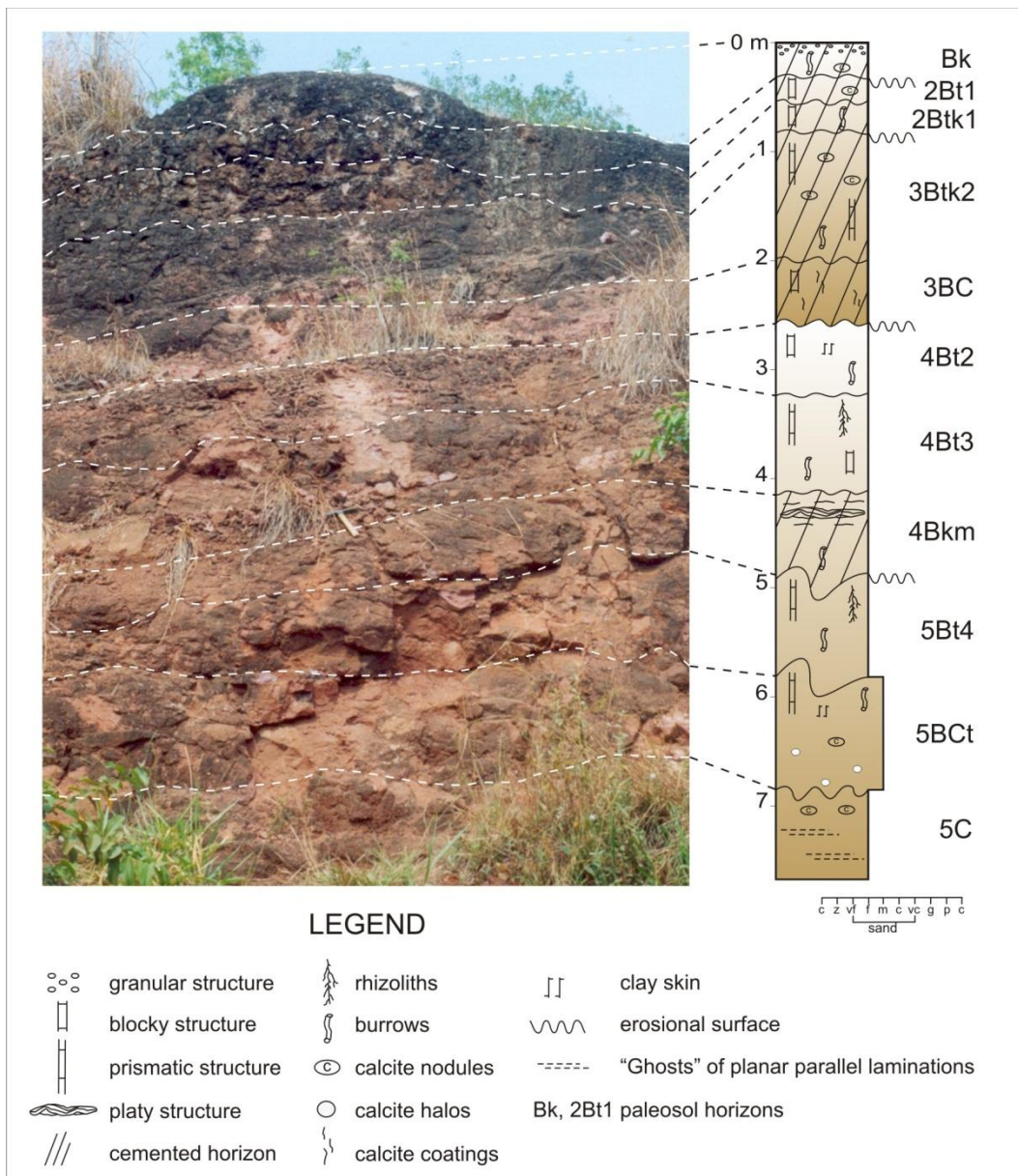


**Figure 4.** Itaja pedotype of Marília Formation. Itaja pedotype is an Aridisol-like paleosol.

The first profile is 0.30 m thick and shows only Bk horizon. The top of this thin profile is marked by an undulating erosional surface, probably associated to wind deflation which caused the erosion of the soft A horizon soil up to hardened Bk horizon. The Bk is reddish orange (10R6/6) to red (10R4/6) in color. The structure is strong very coarse granular, and is indurated cemented by calcium carbonate. Calcite nodules are the most conspicuous feature of this horizon. They are hard, white, from medium to very coarse in size (5-30 mm across), subspherical to irregular in shape, and may occupy more than 20% of the horizon surface. Few bioturbation

traces were noticed. They consist of vertical tubes filled by microcrystalline and sparry calcite, 3-5 mm in diameter, up to 15 mm long. The transition to the second paleosol profile is abrupt and wavy.

The second profile is 0.63 m thick and displays two 2Bt1 and 2Btk1 horizons. The 2Bt1 horizon is 0.35 m thick and reddish orange (10R6/6) to red (10R4/6) in color. The structure is strong medium subangular blocky strongly cemented by calcium carbonate, with few faint clay skins on ped faces. The bioturbation traces are constituted of few cylindrical tubes filled by sand, 6-8 mm in diameter, and more than 15 mm long. The transition to the 2Btk1 is clear and wavy. The 2Btk1 is 0.28 m thick and red (10R5/6, 10R4/6) in color. The structure is moderate very coarse subangular blocky parting to moderate medium angular blocky. The structure surface is strongly cemented by calcium carbonate with few faint clay skins and calcite coatings. The transition to the underlying profile is clear and wavy.

The third profile is 1.72 m thick, and is subdivided in 3Btk2 and 3BC horizons. The 3Btk2 is 1.20 m thick and reddish orange (10R6/6) to red (10R4/6) in color. This horizon presents a primary strong very coarse prismatic structure parting to strong very coarse angular blocky structure. The structures are strongly cemented by calcium carbonate and exhibit few faint clay skins on ped faces. Many hard white calcite nodules are very coarse in size (10-40 mm across), and subspherical to irregular in shape. The bioturbation traces are constituted of tubular structures filled by sparry calcite, 6-8 mm in diameter, 10-15 mm long. The transition to the 3BC is clear and wavy. The 3BC is 0.52 m thick and reddish orange (10R6/8) to red (10R4/8) in color. The structure varies from strong coarse angular blocky in the upper horizon portions to structureless in the lower parts. The calcium carbonate cementation is strong, and very few faint clay and calcite coatings appear on sand grains. The transition to underlying profile is clear and wavy.

The fourth profile has a thickness of 2.45 m and is constituted of a sequence of 4Bt2, 4Bt3, and 4Bkm horizons. The Bt horizons are 1.65 m thick and red (7,5R5/6, 7,5R4/6, 7,5R6/4) to dusky red (7,5R5/4) in color. The structure is strong very coarse angular blocky in 4Bt2 and strong very coarse prismatic parting to strong very coarse angular blocky in 4Bt3. Few faint clay skins are visible on ped faces and lining pores. The bioturbation traces are many sand filled vertically elongated tubes, 6-18 mm in diameter and more than 50 mm long, with downward tapering and lateral branching. The tubes show an encrusting cap of calcite. The transition to the

4Bkm is clear and smooth. The 4Bkm is 0.8 m thick and red (7,5R6/4, 7,5R4/8) in color. The structure is strong very thick platy and is indurated cemented by calcium carbonate. The transition to the undermost profile is diffuse and irregular.

The fifth profile is 2.74 m thick and composed of three 5Bt4, 5BCt, and 5C horizons. The 5Bt4 is 0.85 m thick and red (7,5R5/8, 7,5R4/8) in color. The structure is strong very coarse prismatic with few faint clay skins on ped faces. The bioturbation traces consist in vertically elongated tubes, with downward tapering and lateral branching, 10-15 mm in diameter (main axis), 4-6 mm in the bifurcating branching, and more than 60 mm long. The tubes are filled with sand and exhibit an outer encrusting cap of calcite. The transition to the 5BCt is diffuse and irregular. The 5BCt is 1.05 m thick and red (7,5R5/8, 7,5R4/8). The structure ranges from strong very coarse prismatic at the horizon depth 5.95-6.30 m to structureless up to the contact with the lower 5C horizon. Few white hard calcite nodules are fine in size (<2 mm across), and subspherical in shape. Other forms are few white soft calcite nodules with diffuse outer boundaries, fine to medium in size (1.5-5 mm across), and irregular in shape. The bioturbation traces are cylindrical tubes, 4-6 mm in diameter, 70-80 mm long. They are filled by sand with the outer boundary impregnated with manganese oxyhydroxides. The transition to the 5C is diffuse and wavy. The 5C is 0.84 m thick and red (7,5R5/8, 7,5R4/8) in color with few medium prominent orange (5YR6/6) mottles. The horizon is structureless with “ghosts” of planar parallel laminations. The calcium carbonate cementation is weakly developed and only few white hard calcite nodules, medium to coarse in size (2-15 mm across), and irregular in shape occur.

## 4.2. Micromorphology

The micromorphological observations are summarized in Table 1, and only the key pedological features of the pedotypes will be discussed in the text.

**Table 1.** Summary of micromorphological observations

Horizon	Depth (cm)	C/f rel. dist.	Microstructure	B-fabric	Pedofeatures
<i>Apore pedotype</i>					
<b>Bt1</b>	0-125	chito-gefuric	moderately developed subangular blocky with intrapedal fissures and many vughs	granostriated (90%), monostriated (10%)	microlaminated clay coatings on sand grains (5%), fragments of clay coatings (papules) (1%), laminated crescent clay coatings on channels and vughs (5%), loose continuous grain infillings (1-4 mm, 3%), calcite depletion zones (10%), FeMn impregnative amorphous pedofeatures (2%)
<b>Bt2</b>	125-215	chitonic	moderately developed subangular blocky with intrapedal fissures and many vughs	granostriated (90%), monostriated (10%)	microlaminated clay coatings on sand grains (2%), laminated crescent clay coatings on channels and vughs (5%), dense incomplete clay and grain infilling (2-4 mm, 2%), calcite depletion zones (10%), FeMn impregnative amorphous pedofeatures (5%)
<b>Btk1</b>	215-237	close porphyric (60%), open porphyric (20%), chitonic (20%)	massive (70%), pellicular grain (30%)	crystallitic (70%), granostriated (30%)	external grain calcite hypocoatings (1%), typic calcite nodules (0,5-2 mm, 3%), typic crystalline calcite pedofeatures (50-120 mm, 10%), FeMn impregnative amorphous pedofeatures (2%)
<b>Btk2</b>	237-260	close porphyric (40%), open porphyric (30%), chito-gefuric (30%)	bridged grain	granostriated (70%), crystallitic (30%)	calcite coatings on sand grains covered with clay coatings (2%), typic calcite nodules (1-2 mm, 2%), typic crystalline calcite pedofeatures (5-10 mm, 2%), FeMn impregnative amorphous pedofeatures (5%)
<b>Btk3</b>	260-357	close porphyric (50%), open porphyric (30%), chitonic (20%)	pellicular grain	granostriated (70%), crystallitic (30%)	clay coatings on sand grains (10%), calcite coatings on sand grains covered with clay coatings (2%), dense incomplete clay and grain infilling (1-3 mm, 5%), typic calcite nodules (0,5-1 mm, 2%), calcite halos (1-3 mm, 2%), FeMn impregnative amorphous pedofeatures (5%)
<i>Itaja pedotype</i>					
<b>Bk</b>	0-30	close porphyric (80%), open porphyric (20%)	massive	crystallitic	calcite coatings on sand grains (2%), typic calcite nodules (0,5-4 mm, 15%), dense complete calcite infillings (5%)
<b>2Bt1</b>	30-65	open porphyric (20%), chitonic (80%)	pellicular grain	granostriated (90%), crystallitic (10%)	clay coatings on sand grains (2%), calcite hypocoatings on voids (2%), typic calcite nodules (0,5-2 mm, 2%), geodic nodules filled with sparry calcite (1-3 mm, 3%), dense complete calcite infillings (4%), typic crystalline calcite pedofeatures (5-10 mm, 3%)

<b>2Btk</b>	65-93	chito- gefuric (90%), open porphyric (10%)	bridged grain	granostriated	microlaminated clay coatings on sand grains (2%), calcite hypocoatings on voids (2%), calcite coatings on sand grains covered with clay coatings (1%)
<b>3Btk2</b>	93-213	chitonic (80%), monic (20%)	pellicular grain	crystallitic (80%), speckled (20%)	clay coatings on sand grains (2%), external grain and void calcite hypocoatings, typic calcite nodules (2- 4 mm, 10%), loose continuous grain infillings (0,5- 2 mm, 4%), dense incomplete calcite infillings (5%), typic crystalline calcite pedofeatures (2-4 mm, 2%)
<b>3BC</b>	213-265	monic (90%), chitonic (10%)	single grain	mosaic- speckled (30%)	clay and calcite coatings on sand grains (3%), FeMn impregnative amorphous pedofeatures (3%)
<b>4Bt2</b>	265-335	chito- gefuric	bridged grain	granostriated	microlaminated clay coatings on sand grains (5%), laminated crescent clay coatings on channels and vughs (5%), dense incomplete clay and grain infilling (5%), calcite depletion zones (10%), FeMn impregnative amorphous pedofeatures (10%)
<b>4Bt3</b>	335-430	chito- gefuric	bridged grain	granostriated	microlaminated clay coatings on sand grains (5%), laminated crescent clay coatings on channels and vughs (3%), calcite hypocoatings on voids (2%), calcite depletion zones (10%), FeMn impregnative amorphous pedofeatures (3%)
<b>4Bkm</b>	430-510	close porphyric	strongly developed platy with many parallel interaggregate voids	crystallitic	laminar calcite pendants underneath clastic grains (0,1-0,3 mm, 3%), calcite micropans on channels and vughs (>0,5 mm, 5%), dense complete calcite infillings (10%), typic crystalline calcite pedofeatures (8-12 mm, 5%), FeMn impregnative amorphous pedofeatures (2%)
<b>5Bt4</b>	510-595	chitonic (90%), monic (10%)	pellicular grain	granostriated (70%), speckled (30%)	clay coatings on sand grains (3%), calcite hypocoatings on voids (2%), dense incomplete clay and grain infilling (1-4 mm, 5%), calcite depletion zones (5%)
<b>5BCt</b>	595-700	monic (80%), chitonic (20%)	single grain (80%), pellicular grain (20%)	mosaic- speckled (20%)	clay coatings on sand grains (2%), loose continuous grain infillings (1-3 mm, 3%), typic calcite nodules (1-4 mm, 3%), calcite halos (2-6 mm, 5%)
<b>5C</b>	700-784+	monic	single grain	stipple-speckled (5%)	loose continuous grain infillings (1-3 mm, 2%), typic calcite nodules (4-6 mm, 5%)

#### 4.2.1. Apore pedotype

The microfabric is mainly clay nanocrystals with calcite crystals ranging in size from 2-5 µm. It has reddish brown-speckled (10R5/4) colors and yellowish-speckled (2,5Y8/8) colors in plasma separations. Striated b-fabric is common in Bt and Btk horizons, principally granostriated (Fig. 5A). The related distribution varies from chitonic to chito-gefuric in Bt (Fig. 5B), and chitonic, chito-gefuric, open and close porphyric in Btk.

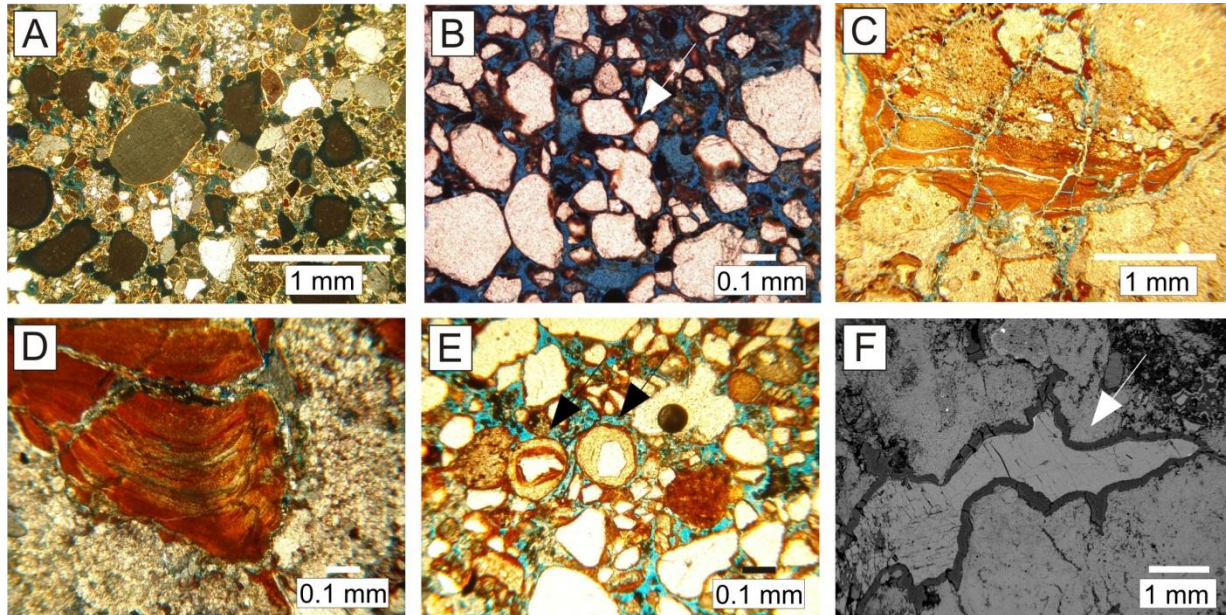


**Figure 5.** Apore pedotype micromorphology. (A) Granostriated b-fabric in Bt1 horizon. Photomicrograph in crossed-polarized light (XPL). (B) Chito-gefuric related distribution in Bt2 horizon. Photomicrograph in plane-polarized light (PPL). (C) Clay coating in Bt2 horizon, PPL. (D) Typic laminated iron stained clay coating in Bt2 horizon showing post-depositional iron segregation, XPL. (E) Compound coatings in Btk3 horizon showing alternations between calcite and clay coatings on sand grains, PPL. (F) Scanning electron microscope (SEM) image of a compound coating in Btk3 horizon showing the internal coating wall filled with sparry calcite and the external wall filled with clay.

The microstructures are principally apedal pellicular and bridged grain. The Bt1 shows moderately developed subangular blocky microstructure with a variable size of 200-1000 µm, and fissural intrapedal microvoids (5-30 µm), which are partly separated from the adjacent units by a system of unaccommodated macrovoids and vughs.

The nodules are composed entirely of microcrystalline calcite. They appear in Btk horizons, and the principal forms are typic and halos.

The key pedofeature is clay coatings. They are best developed in Bt1 and Bt2 horizons (Fig. 5C). The principal form is typic laminated iron stained clay coating, which internally shows microfissures and post-depositional iron segregation (Fig. 5D). In Btk horizons, the occurrence of compound coatings which show two or three different layers of calcite alternating with clay coatings are common (Fig. 5E, F). These coatings are reported in soils submitted to contrasting climatic situations, where periods of more humid and arid conditions alternate periodically in time (Khormali et al., 2003), and are responsible for decalcification and recalcification processes in polygenetic horizons (Nettleton and Peterson, 1983; Reheis, 1987; Eghbal and Southard, 1993).

#### **4.2.2. Itaja pedotype**

The microfabric is mainly clay nanocrystals with calcite crystals ranging in size from 2-10  $\mu\text{m}$ . The prevalent micromass color is reddish brown-speckled (10R5/4). Crystallitic b-fabric is dominant in Bk, Bkm, and part of Btk horizons (Fig. 6A). The speckled b-fabric occurs in C horizons, principally at the transitions B/C. The related distribution is chito-gefuric in Bt and Btk, open and close porphyric in Bk, close porphyric in Bkm, and monic in C horizons. At the transition B/C some residual chitonic pattern can be observed.

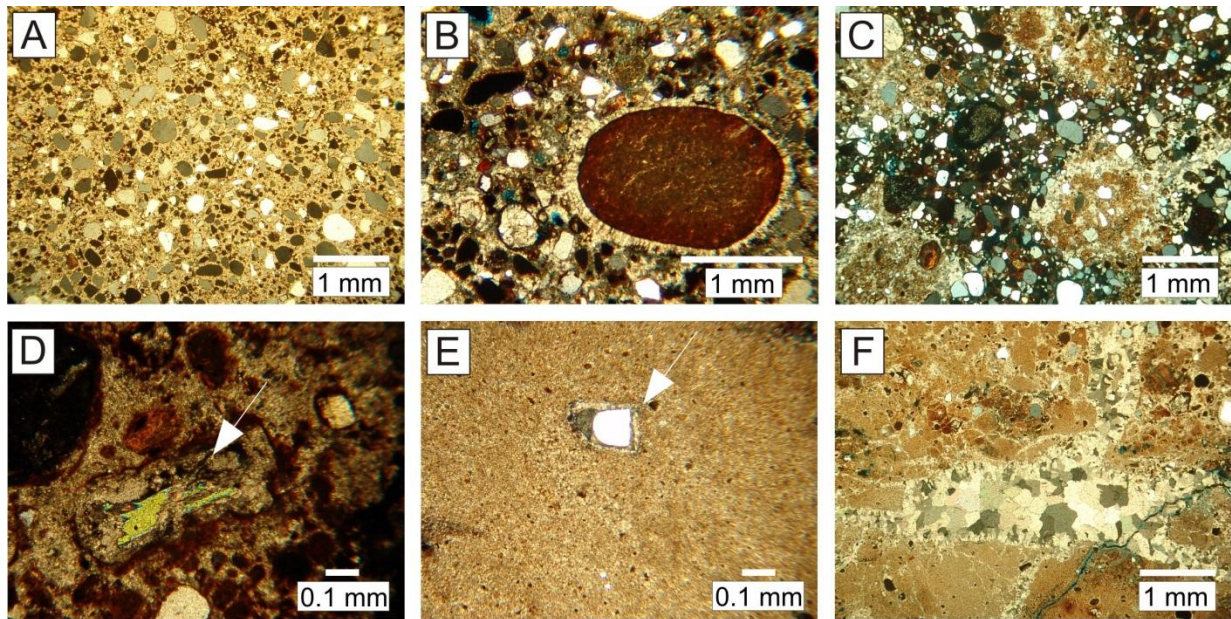


**Figure 6.** Itaja pedotype micromorphology. (A) Crystallitic b-fabric in Bk horizon, XPL. (B) Typic microcrystalline calcite nodule in Bk horizon, XPL. (C) Calcite halos in 5BCt horizon, XPL. (D) Mica crystal partially replaced by calcite in 4Bkm horizon, XPL. (E) Floating quartz grain in microcrystalline calcite matrix found in Bk horizon, PPL. (F) Void filled with sparry calcite in 4Bkm horizon, XPL.

The microstructures are apedal pellicular and bridged grain, and only 4Bkm horizon presents pedal laminar microstructure (10-100  $\mu\text{m}$ ), that is characterized by skeletal grains aligned in a parallel arrangement following the subhorizontal development of microcrystalline and sparry calcite. The laminations are separated by a partially accommodated system of parallel voids.

The nodules are composed of microcrystalline and rare sparry calcite. Typic forms are fine to medium in size (0.5-4 mm across), subspherical to amygdaloidal in shape, and occur in Bk and Btk horizons (Fig. 6B). The halos are fine to coarse in size (1-6 mm across), subspherical to amygdaloidal in shape, and only occur in 5BCt horizon (Fig. 6C). Geodic forms are rare; only 1% of the nodules. These nodules have a hollow internal fabric, incompletely filled with sparry calcite. They are fine to medium in size (1-3 mm across), subspherical in shape, and only occur in 2Btk1 horizon.

Calcitic pedofeatures are the most striking feature of the Btk, Bk, and Bkm horizons. The high concentration of the calcite in Bk and 4Bkm was responsible for the replacement of silicate grains by calcite. In these calcic horizons, the process of replacement is quite generalized,

because the replacement does not only affect the coatings of illuvial clay as is commonly observed in Btk horizons, but also the hard detrital quartz, feldspars, and mica grains. The mica grains display the replacing of the silicate material by calcite along the cleavage planes (Fig. 6D), and quartz, feldspars and lithic fragments may show brecciation of the grains. This is a highly characteristic result of the replacement process in hard detrital grains (Wright, 1990). According to Gile et al. (1966), Watts (1980), and Goudie (1983), the replacement of siliciclastic material is indicated by the presence of floating quartz and feldspars grains in calcite matrix (Fig. 6E). In arid paleoclimates, even locally high pH conditions can increase the solubility of silica and consequently favor oversaturation for carbonates (Alonso et al., 2004).

Most of the calcite crystals identified are made up of microcrystalline calcite ( $<2\text{ }\mu\text{m}$ ), which indicates very rapid crystallization processes (Gile et al., 1965; Wielder and Yaalon, 1974). Euhedral sparry calcite crystals,  $>4$  mm across, are observed in the petrocalcic 4Bkm horizon (Fig. 6F). The presence of sparry calcite in paleosols is associated with supersaturated calcium carbonate solutions or microcrystalline calcite recrystallization caused by diagenetic modifications (Bathurst, 1971). The action of supersaturated calcium carbonate solution is considered as the main factor for sparry calcite precipitation, which is clearly shown in the following: (1) the size of sparry calcite crystals increases away from the initial void walls, (2) the voids present incompletely calcite infillings, (3) different phases of sparry calcite formation are recognized and sparry calcite with fibroradiated aspect does not exist, (4) the surface of contact between crystals is not undulating or rounded, and abrupt limits between microcrystalline and sparry calcite crystals do not occur as described by Alonso et al. (2004).

#### **4.3. Clay mineralogy**

The clay mineralogy of the Itaja pedotype is dominated by palygorskite and the Apore pedotype by smectite (Fig. 7). The Itaja pedotype shows large amounts of palygorskite in all horizons, principally in Bk horizon, where semi-quantitative estimates revealed that more than 80% of the clay content is composed of palygorskite (Fig. 7A).

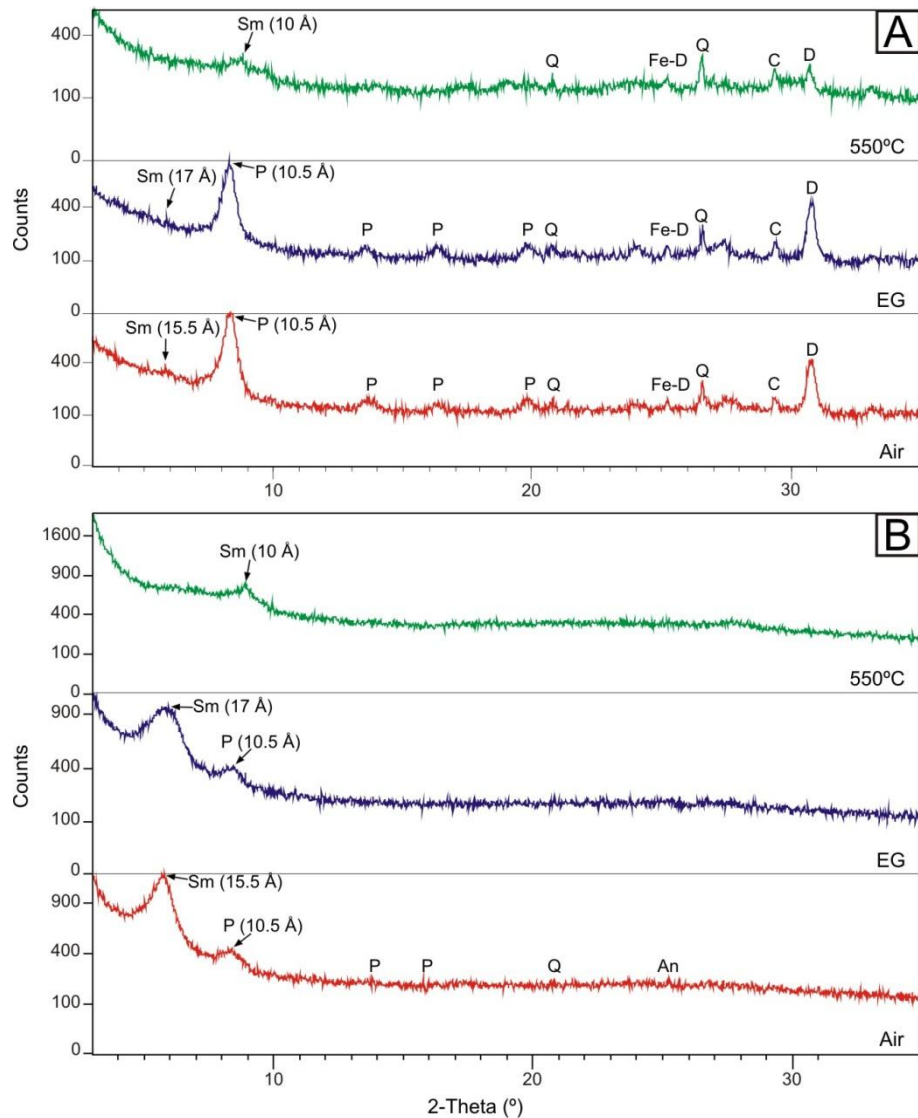


**Figure 7.** X-ray diffraction pattern for air-dried (Air), ethylene glycol-solvated (EG), and heat-treated ( $550^{\circ}\text{C}$ ) samples showing  $d$ -spacing for clay mineral interpretation. (A) Itaja pedotype. (B) Apore pedotype. Sm, smectite; P, palygorskite; Q, quartz; An, anatase; Fe-D, Fe-dolomite; C, calcite; D, dolomite.

Whole-rock X-ray patterns indicated the presence of palygorskite, smectite, quartz, calcite, Fe-dolomite, and dolomite in Bk horizon of the Itaja pedotype, and smectite, palygorskite, quartz, and anatase in Bt1 horizon of the Apore pedotype (Fig. 7B). The presence of palygorskite in air-dried samples produced a  $d$ -spacing peak of  $10.5\text{ \AA}$ , and this peak remains under ethylene glycol-solvated (EG) treatment. After heating at  $550^{\circ}\text{C}$ , the palygorskite structure was destroyed, and the peak disappeared. There is a considerable increase in the amount of

smectite in Apore pedotype. In air-dried samples it produces a *d*-spacing peak of 15.5 Å that shifts to 17 Å under EG treatment, and collapses to 10 Å after a heat treatment at 550°C.

## 4.4. Geochemistry

### 4.4.1. Loss on ignition

Geochemical analysis of the major oxides of the paleosols shows that both pedotypes have high loss on ignition (LOI) values in specific horizons which are consistent with high CaO ratios (Table 2). High percentage of LOI values in these horizons can be explained by the intense liberation of volatile CO<sub>2</sub> during ignition of samples at 1000°C, principally due to high carbonate and water content in these horizons.

**Table 2.** Major and trace elements for each paleosol horizon and parent material reported as oxide percentages or in ppm.

Horizon	SiO <sub>2</sub>	TiO <sub>2</sub>	Al <sub>2</sub> O <sub>3</sub>	Fe <sub>2</sub> O <sub>3</sub>	MnO	MgO	CaO	Na <sub>2</sub> O	K <sub>2</sub> O	P <sub>2</sub> O <sub>5</sub>	Ba	Sr	LOI	Total
<i>Apore pedotype</i>														
<b>Bt1</b>	83.08	1.02	3.87	3.51	0.042	2.64	0.92	0.09	1.27	0.058	321	95	3.80	100.3
<b>Bt2</b>	82.44	1.31	4.75	4.34	0.046	1.83	0.74	0.16	1.66	0.051	359	138	3.08	100.4
<b>Btk1</b>	61.18	1.03	4.11	3.56	0.058	4.50	10.31	0.09	1.23	0.054	314	503	13.6	99.7
<b>Btk2</b>	75.56	1.36	5.25	4.41	0.082	3.40	2.21	0.10	1.49	0.055	395	155	6.04	100.0
<b>Btk3</b>	74.47	1.36	5.05	4.48	0.069	3.15	3.36	0.14	1.62	0.072	407	241	6.38	100.2
<i>Itaja pedotype</i>														
<b>Bk</b>	32.06	0.39	1.78	1.59	0.041	12.47	20.93	0.03	0.37	0.056	186	1677	29.8	99.5
<b>2Bt1</b>	82.29	1.26	5.12	4.52	0.069	1.68	0.53	0.17	1.78	0.080	423	101	2.81	100.3
<b>2Btk1</b>	65.95	1.01	3.35	3.23	0.052	4.05	9.62	0.04	0.76	0.079	245	307	12.0	99.8
<b>3Btk2</b>	78.14	1.35	5.28	4.55	0.038	2.81	1.53	0.15	1.93	0.084	351	158	4.59	100.4
<b>3BC</b>	76.46	1.37	5.15	4.52	0.060	2.31	2.62	0.19	1.89	0.085	423	147	4.93	99.6
<b>4Bt2</b>	72.70	1.35	5.36	4.46	0.040	3.02	3.71	0.17	2.01	0.074	373	217	6.72	99.6
<b>4Bt3</b>	74.45	1.66	5.95	5.28	0.103	2.89	2.19	0.21	2.11	0.096	502	173	5.40	100.3
<b>4Bkm</b>	73.30	1.59	5.81	5.21	0.049	2.75	3.33	0.20	2.09	0.173	381	186	5.81	100.3
<b>5Bt4</b>	75.37	1.25	6.55	4.42	0.069	3.05	1.87	0.20	2.34	0.094	495	164	5.10	100.3
<b>5BCt</b>	73.19	1.62	6.21	5.51	0.068	2.23	3.18	0.21	2.24	0.122	453	141	5.27	99.8
<b>5C</b>	63.48	1.49	5.00	5.19	0.065	1.86	10.01	0.21	1.81	0.131	419	264	10.4	99.6
<i>Parent Material</i>														
<b>BA1</b>	52.35	0.79	3.32	3.04	0.037	7.68	12.46	0.21	1.49	0.178	298	757	17.7	99.2

#### **4.4.2. Molecular weathering ratios**

Eight molecular weathering ratios were calculated to evaluate the degree of chemical weathering of paleosols and to evaluate which pedogenic processes were most important (Retallack, 2001; Sheldon and Tabor, 2009). Additionally these indices were used to separate paleosol orders (Sheldon et al., 2002).

The chemical index of alteration without potassium (CIA-K) measures the extent of rock weathering in different horizons. It was firstly proposed by Nesbitt and Young (1982) as taking the molar ratio of  $\text{Al}_2\text{O}_3$  to  $\text{Al}_2\text{O}_3 + \text{CaO} + \text{Na}_2\text{O} + \text{K}_2\text{O}$  and multiplying it by 100. The application of this index without potash was suggested by Maynard (1992) for controlling diagenetic potassium metasomatism. Other studies (e.g., Driese et al., 2000; Sheldon et al., 2002) have stressed the importance of calculating CIA without potassium as proposed by Maynard.

CIA-K index (Fig. 8, Table 3) shows considerably trends to increase in Bt horizons of both pedotypes, which can be directly related to an increase in chemical weathering in these horizons. Therefore, as the CIA-K increases, it is accompanied by an increase in leaching ( $\text{Ba/Sr}$ ) and consequently lessens in base loss ( $m\sum\text{bases}/m\text{Al}_2\text{O}_3$ ) values. The CIA-K values in Bt horizons show two classes of leaching, one from 43 to 63, which indicates moderate weathering conditions, and other from 68 to 80, which indicates moderate to intense weathering conditions (White and Schiebout, 2008). These horizons are characterized by high values of leaching and very low concentration of bases. These values are similar to those described by Sheldon (2003) for Bt Alfisol horizons developed upon basalts of the Picture Gorge subgroup in Oregon.

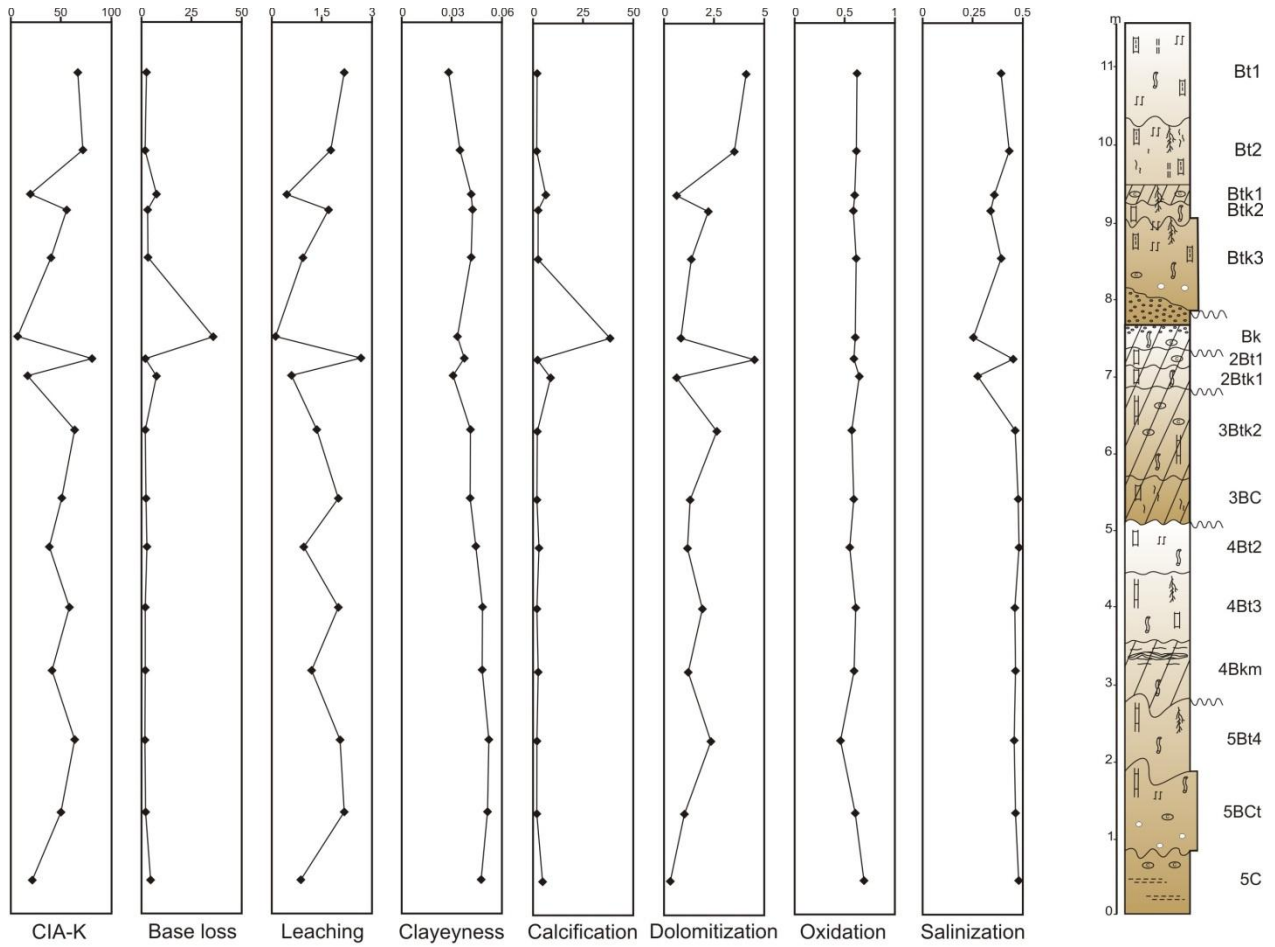


**Figure 8.** Molecular weathering ratios from Apore and Itaja pedotypes.

The ratio bases/alumina, can be used to quantify the extent of hydrolysis (Retallack, 1997). Plotting this ratio with CIA-K ratio it is observed that these ratios co-vary in inverse relation. The Bk horizon of the Itaja pedotype shows the minimal CIA-K value around 4 and higher 39 value of base loss, thus indicating the minimal chemical weathering in this horizon. The value of leaching in this horizon is very low 0.07.

Leaching was quantified using Ba/Sr ratio. It is known that strontium is significantly more soluble than barium, so higher values are expected in more leached horizons (Retallack, 2001). Trends in leaching co-vary in inverse relation with base loss; consequently higher values of leaching are expected with decreased ratios of base loss. When comparing Bt and Bk horizons of both pedotypes it is possible to observe that Bt presents the maximal leaching and minimal values of base loss, whereas Bk shows very low values of leaching 0.07 and the maximum conservation of bases of 39.

**Table 3.** Geochemical data

Horizon	CIA-K <sup>a</sup>	(Σbases/Al) <sup>a</sup>	Leach. <sup>a</sup>	Clay. <sup>a</sup>	Calcific. <sup>a</sup>	Dolomit. <sup>a</sup>	Oxid. <sup>a</sup>	Salin. <sup>a</sup>	Prov. <sup>a</sup>	MAP (mm)
<i>Apore pedotype</i>										
<b>Bt1</b>	68.00	2.55	2.16	0.027	2.15	3.99	0.59	0.39	0.33	843
<b>Bt2</b>	74.70	1.69	1.66	0.033	1.25	3.43	0.59	0.43	0.35	962
<b>Btk1</b>	17.86	7.68	0.39	0.039	7.32	0.60	0.57	0.35	0.31	-
<b>Btk2</b>	55.65	2.74	1.62	0.040	2.40	2.13	0.55	0.33	0.33	-
<b>Btk3</b>	44.34	3.17	1.07	0.039	2.78	1.30	0.58	0.39	0.34	-
<i>Itaja pedotype</i>										
<b>Bk</b>	4.46	39.34	0.07	0.032	39.09	0.82	0.60	0.25	0.27	240
<b>2Bt1</b>	80.46	1.44	2.67	0.036	1.01	4.40	0.58	0.43	0.31	1078
<b>2Btk1</b>	16.02	8.54	0.51	0.029	8.27	0.58	0.63	0.26	0.38	-
<b>3Btk2</b>	63.54	2.31	1.42	0.039	1.87	2.55	0.56	0.44	0.32	-
<b>3BC</b>	50.36	2.51	1.83	0.039	2.05	1.22	0.57	0.45	0.33	-
<b>4Bt2</b>	43.27	3.14	1.09	0.043	2.68	1.13	0.54	0.45	0.32	518
<b>4Bt3</b>	57.89	2.33	1.85	0.047	1.89	1.83	0.59	0.44	0.35	691
<b>4Bkm</b>	47.64	2.68	1.30	0.046	2.23	1.14	0.58	0.44	0.34	-
<b>5Bt4</b>	63.72	2.13	1.92	0.051	1.69	2.26	0.44	0.43	0.24	775
<b>5Bct</b>	50.33	2.28	2.05	0.050	1.83	0.97	0.58	0.44	0.33	-
<b>5C</b>	21.23	5.04	1.01	0.046	4.58	0.25	0.68	0.46	0.38	-
<i>Parent Material</i>										
<b>BA1</b>	-	-	-	-	-	-	-	-	0.30	-

<sup>a</sup> Molar ratios: CIA-K = 100 x ((Al<sub>2</sub>O<sub>3</sub>/(Al<sub>2</sub>O<sub>3</sub>+CaO+Na<sub>2</sub>O)); Σbases/Al = ((CaO+MgO+Na<sub>2</sub>O+K<sub>2</sub>O)/Al<sub>2</sub>O<sub>3</sub>); Leaching = (Ba/Sr); Clayeyness = (Al<sub>2</sub>O<sub>3</sub>/SiO<sub>2</sub>); Calcification = ((CaO+MgO)/Al<sub>2</sub>O<sub>3</sub>); Dolomitization = (MgO/CaO); Oxidation = ((Fe<sub>2</sub>O<sub>3</sub>+MnO)/Al<sub>2</sub>O<sub>3</sub>); Salinization = ((Na<sub>2</sub>O+K<sub>2</sub>O)/Al<sub>2</sub>O<sub>3</sub>); Provenance = (Ti/Al).

One of the most diffused applications of the clayeyness ( $m\text{Al}_2\text{O}_3/m\text{SiO}_2$ ) ratio in paleosol analyses is the field confirmation of Bt horizons (Hamer et al., 2007b). In the analyzed profiles, Bt horizons do not show an increase in clayeyness ratio, which shows an irregular pattern when compared with point-counting sections, that presented a considerable textural fining enrichment in these horizons (Fig. 2). This dissimilar trend can be explained by syn-formational additions of Si due to eolian additions (Sheldon and Tabor, 2009).

The calcification ( $(m\text{CaO}+m\text{MgO})/ m\text{Al}_2\text{O}_3$ ) ratio displays very irregular distribution of values through horizons in both pedotypes. This irregular pattern is a characteristic of pedogenic horizons enriched in calcium carbonate which occur in areas where the main source of ions is wind blown dust (Goudie, 1983; Machette, 1985).

The minimum and maximum index of dolomitization ( $m\text{MgO}/m\text{CaO}$ ) occurs in Itaja pedotype. It ranges from 0.25 in 5C to more than 4.40 in 2Bt1 horizon. Although low-Mg calcite is by far the dominant mineral of soil carbonate in arid areas (Watts, 1980; Monger et al., 1991), infiltration of soil solutions with elevated MgO/CaO (>1) ratios may have led to dolomitization

of early-precipitated soil calcite and/or to direct dolomite precipitation in the pedogenic horizons (Capo et al., 2000). Most of the dolomite observed in both pedotypes is very poorly crystallized and the rhombohedric crystals are not clearly visible under optical microscope, but the rhombs and XRD width peaks are very characteristic in SEM images and diffratograms (Fig. 9A, B).

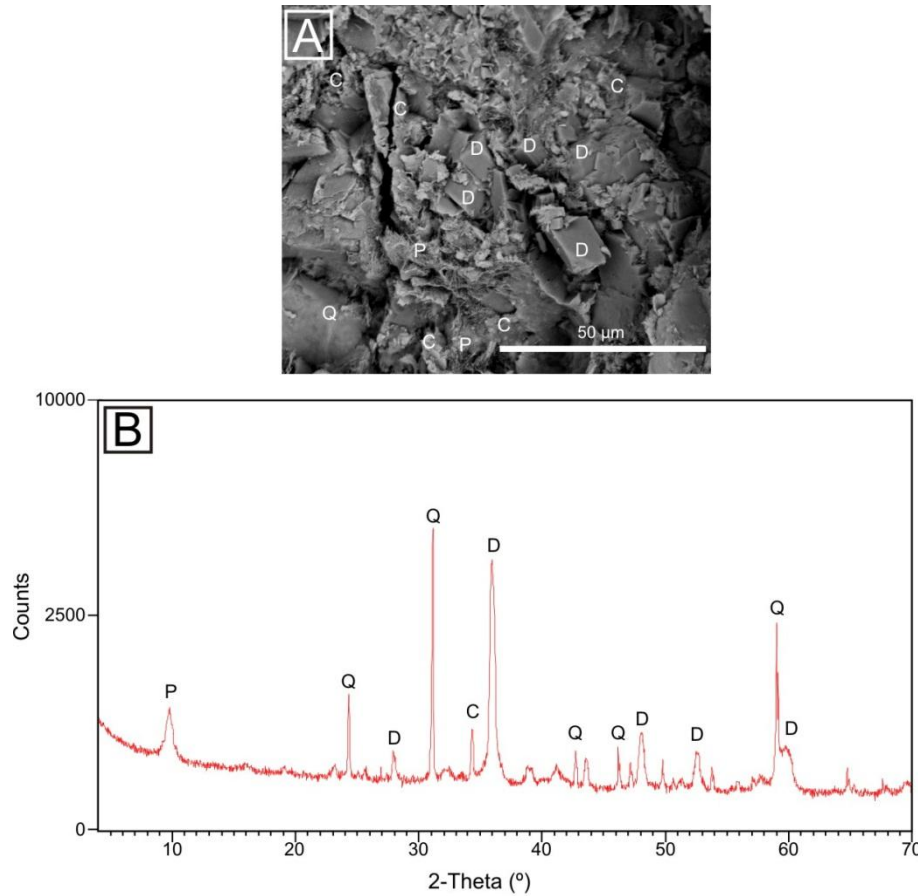


**Figure 9.** SEM image and diffratogram from 4Bkm horizon of the Itaja pedotype. (A) SEM image showing mixed mineralogy. (B) Whole-rock X-ray pattern showing d-spacing used for the identification of main minerals. P, palygorskite; Q, quartz; D, dolomite; C, calcite.

The oxidation  $((m\text{Fe}_2\text{O}_3+m\text{MnO})/m\text{Al}_2\text{O}_3)$  ratio has a uniform behavior throughout the horizons of the Itaja and Apore pedotypes, revealing very low influence of the reduction processes. Soil horizons have nearly uniform red colors, which are produced by the abundance of iron oxides, principally hematite. The blend of red and brown colors is formed under oxidizing conditions in well-drained environments (PiPujol and Buurman, 1994).

The salinization  $((m\text{Na}_2\text{O}+m\text{K}_2\text{O})/m\text{Al}_2\text{O}_3)$  ratio is generally low; the values vary from 0.25 to 0.46 in the Itaja pedotype and from 0.33 to 0.43 in the Apore. According to Retallack

(2001), the process of salinization in paleosols can be indicated by the molar ratio of soda plus potash to alumina greater than 1 or by an increase in this ratio up-profile. The lack of evaporite minerals or their pseudomorphs also seems to be an indicative of limits to this process during soil formation.

## 5. Discussion

### 5.1. Paleosol classification

The main drawback in using modern soil classification to lithified paleosols is their dependence on certain soil properties (i.e., cation exchange capacity, soil moisture regime, the amount of organic matter, etc.) that are not preserved in paleosols. Despite these drawbacks, many other modern soil equivalents such as diagnostic horizons, morphological properties, and bulk chemical composition are sufficiently preserved in paleosols (Kraus, 1999; Retallack, 2001; Driese and Ober, 2005). Therefore the classification of pedotypes as modern analogs of Alfisol and Aridisols (Soil Survey Staff, 1999) (Table 4) is based on the recognition of physical properties, diagnostic horizons, and geochemical trends.

**Table 4.** Classification of pedotypes

Pedotypes	Mack et al., 1993	Nettleton et al., 2000	Soil Survey Staff, 1999
Apore	Argillisol	Paleoevolvisols	Alfisol
Itaja	Calcisol	Paleoaridisols	Aridisol

The Apore pedotype was classified as Alfisol. The most prominent feature that enables this classification is the presence of argillic horizons containing illuvial clay features. The differentiation between modern Alfisols and Ultisols, which both have a subsurface Bt horizon characterized by an enrichment in illuvial clay content, is defined by a base saturation of 35% or more for Alfisols and less for Ultisols (Soil Survey Staff, 1999). In paleosol analysis such base saturation can be assumed for paleosols which contain calcite nodules in a horizon deeper than 1 m from the uppermost horizon (Retallack, 2001) or by calculating the molar ratio of bases/alumina in B horizons (Sheldon et al., 2002). According to Sheldon et al. (2002) the B

horizons of Alfisols have molar ratio of bases/alumina greater than 0.5, whereas the B horizons of Ultisols have bases/alumina ratio typically lesser than 0.5. The B horizons of the Apore pedotype are characterized by the ratio bases/alumina greater than 0.5, and the calcite nodules are concentrated in a horizon deeper than 1 m from the surface of Bt1 horizon. Simonson (1949) also suggested the use of smectite in argillic horizons as an element of distinction between Alfisols and Ultisols. The soils containing kaolinitic clay minerals are mainly Ultisols, whereas soils with smectite in their clay fraction should be called Alfisols.

The Itaja pedotype was classified as Aridisol. From modern soil examples, the principal condition required for Aridisol formation is a soil moisture regime in that potential evapotranspiration greatly exceeds precipitation during most of the year (Soil Survey Staff, 1999), which favors the development of a sequence of horizons enriched in secondary minerals (i.e., calcium carbonate, calcium sulfate, etc.). Because only approximations can be made of rainfall and it is impossible to quantify the potential evapotranspiration or water loss by surface runoff, our comparison relies upon morphologic properties of diagnostic horizons.

The Itaja pedotype has calcic, petrocalcic, and argillic horizons. All of these subsurface horizons are diagnostic of Aridisols (Soil Survey Staff, 1999). This pedotype constitutes a succession of five superimposed polygenetic paleosols. Thick, cumulative paleosols indicate that pedogenesis exceeds erosion rates, and that sedimentation rate was relatively steady and low (Kraus, 1999). Evidence of the sedimentation (i.e., traces of relict bedding) or erosional surfaces between different stacked Aridisol profiles is minimal; the successive intense phases of paleosol development attested for abundant root traces, well developed soil structures, and soil horizonation obliterated this register. The great degree of maturity of this pedotype can also be attested by to the well developed petrocalcic 4Bkm horizon, which contains layers of coalescent calcite nodules and indurated laminas of calcite that require long periods of exposure in order to develop (Gile et al., 1966; Goudie, 1983; Machette, 1985; Birkeland, 1999).

The development of carbonate-free argillic Bt horizons in a sequence of calcic horizons has been largely interpreted as evidence of wet pluvial periods during Aridisol formation (Nettleton and Peterson, 1983; Reheis, 1987; Eghbal and Southard, 1993; Khormali et al., 2003), and is described in polygenetic Aridisols of California as a result of more humid conditions in a general arid climate (Eghbal and Southard, 1993). The coexistence of palygorskite, calcite nodules, and clay coatings in argillic horizons was described by Khademi and Mermut (1999) in

Aridisols of central Iran. The authors suggested that clay coatings are formed firstly in wetter situations and are followed by the authigenic formation of palygorskite which is trapped by pedogenic carbonate during calcite nodules growth in subsequent drier periods.

## 5.2. Factors of soil formation

### 5.2.1. Climate

The remarkable influence of the climatic conditions on chemical properties of the soils allows the use of chemical parameters of the paleosols to estimate paleoprecipitation and paleotemperature. The measurement of the degree of chemical weathering of Bt paleosol horizons can be related to mean annual precipitation (MAP) and mean annual temperature (MAT) using climofunctions derived from the Bt and Bw horizons of modern North American soils (Sheldon et al., 2002). The CIA-K can be related to MAP as follows:

$$\text{MAP (mm)} = 221e^{0.0197(\text{CIA-K})},$$

which has a reasonable accuracy of  $R^2 = 0.72$ , and a standard error of  $\pm 182$  mm.

High CIA-K values reflect high precipitation values and consequently soils are submitted to intense chemical weathering that leads alkalis and alkaline earth elements to be removed while less mobile elements like aluminum remain in place. Low CIA-K values evidence low precipitation values which are favorable to accumulation of Ca and Mg in Bk horizons and Na in evaporite minerals. A CIA-K value of 100 (CIA-K = 100) points out a precipitation estimate of approximately 1585 mm/year and represents a soil that is composed largely of kaolinite clay minerals (Sheldon et al., 2002).

As shown in Fig. 10 the mean annual precipitation calculated from Bt horizons of the Itaja and Apore pedotypes varies greatly from 518 mm/year (4Bt2) to 1078 mm/year (2Bt1). The Itaja pedotype exhibits the superimposition of several phases of calcification and lixiviation. During the main episodes of rainfall, all the carbonate was removed from the profile and water illuviation favored the formation of clay and ferruginous coatings. In Btk horizons calcite coatings are observed which may have accumulated under alkaline dry conditions corroded by ferruginous clay coatings, which are typical of well-drained soils in wet climates (Bullock et al., 1985). This

polygenetic sequence shows vertical changes in soil properties that are related to changes in soil moisture. According to Kraus and Riggins (2007) the similar vertical trends in changing soil properties (i.e., alternating clay and calcite features) are most probably caused by regional climatic variations rather than by local controls, such as soil permeability or surface topography.

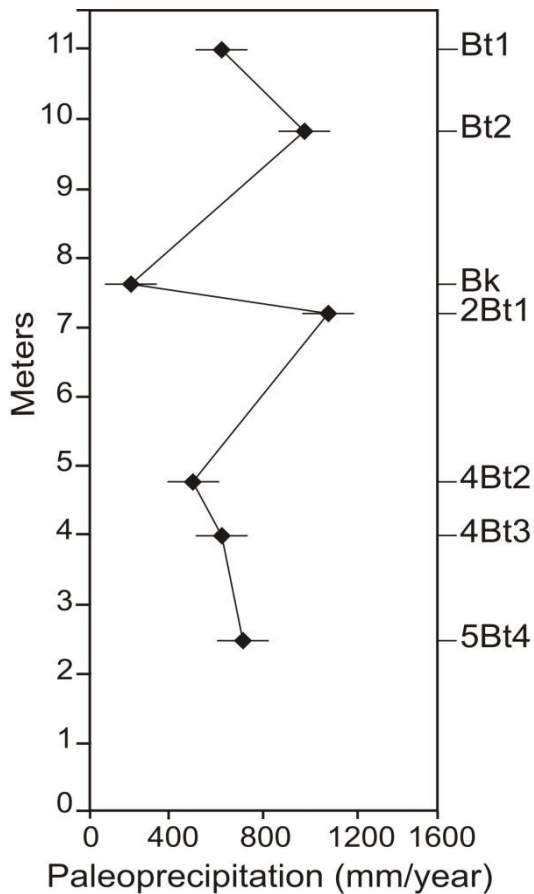


**Figure 10.** Paleoprecipitation estimates from Bk and Bt horizons of the Apore and Itaja pedotypes. The standard error on Bk depth paleoprecipitation is  $\pm 147$  mm, and the standard error on CIA-K paleoprecipitation estimates is  $\pm 182$  mm.

The MAP calculated for Apore pedotype shows a slight increase in the averaged paleoprecipitation values. The values around 900 mm/year are consistent with the general lack of calcite features and the increased amount of smectite and illuvial clay and ferruginous features in these horizons.

The paleoprecipitation estimated for Bk horizon of the Itaja pedotype around 240 mm/year, with a standard error of  $\pm 147$  mm, is based on the calcic-precipitation equation MAP (mm) = 137.24 + 6.45D + 0.013D (Retallack, 1994b, 2005), and it was previously calculated

from other Bk Aridisols horizons of the Marília Formation (Dal' Bo et al., 2009). The interval of paleoprecipitation assumed falls between arid to semi-arid climates of Köeppen's classification (1948), and presents a positive correlation with very low CIA-K values and high concentration of bases in this horizon (Retallack, 2001). This low MAP is consistent with low precipitation values admitted for pedogenic calcite nodules formation of <500 mm/year in semi-arid climates (Goudie, 1973). Although these values may be higher than expected (Mack and James, 1994; Retallack, 2001), especially in monsoonal climates characterized by highly seasonality, the abundance of palygorskite in this horizon seems to corroborate arid or semi-arid conditions (Paquet and Millot, 1972; Khormali and Abtahi, 2003).

The most important paleoclimatic shift recorded in the section is from a humid climate with MAP estimates of 1078 during 2Bt1 formation, followed by a sharp decrease to ~240 mm, attested for Bk development, and a return to general wetter conditions of ~900 mm during Bt2 and Bt1 Apore pedotype evolution. These spikes in MAP values are coeval with general changes in paleosol properties such as the formation of clayey, red, and decalcified horizons characterized by elevated base depletion. Retallack et al. (2006), Sheldon (2006), and Retallack (2009) have assigned these paleosol properties to high precipitation, temperatures, and seasonality events over geological times.

The moisture availability from precipitation varied considerably through time, as indicated for MAP reconstructions, although these variations in rainfall did not significantly affect the water table level. The water table was deep and fluctuations in its level did not influence the hydrologic conditions within pedotypes. The calcic horizons, calcite nodules, clay coatings, and oxidized red colors are field indicators that both pedotypes were formed under well-drained conditions. Micromorphological evidence also supports well-drained conditions, as exemplified by well developed microcrystalline calcite nodules, clay and calcite coatings, and the absence of redoximorphic features, such as FeMn nodules or concretions.

Mean annual temperature (MAT) can be estimated using salinization from Bt horizons (Sheldon et al., 2002) as follows:

$$\text{MAT } (\text{°C}) = -18.516(\text{S}) + 17.298,$$

where S = ((mNa<sub>2</sub>O+mK<sub>2</sub>O)/mAl<sub>2</sub>O<sub>3</sub>), with a R<sup>2</sup> = 0.37 and standard error of ± 4.4°C.

The results of mean annual temperature suggest that temperatures were around 9-10°C. These values are lower than expected for continental Maastrichtian paleosols developed in latitudes between 20°N and 20°S (Nordt et al., 2002). These areas are thought to have been considerably warmer in that time (Barron and Washington, 1982), and isotopic analysis indicates that temperatures were higher than those estimated (Nordt et al., 2003).

Probably, these anomalously low MAT estimates recorded from paleosol salinization are an artifact of seasonal precipitation. In a warm seasonal climate, K-rich minerals are less easily weathered than Na-rich evaporites (Birkeland, 1999). Low values of sodium contrasting with greater values of potassium indicate that there was enough water to remove most of sodium from paleosols, but it was not sufficient to remove potassium which is a less mobile cation. Therefore, the anomalously low temperature estimates obtained from analyzed pedotypes probably do not indicate a cold Maastrichtian climate but rather one characterized by strong seasonality of precipitation (Retallack, 2001; Therrien, 2005).

### **5.2.2. Organisms**

The Itaja and Apore pedotypes exhibit traces of bioturbation by both flora and fauna. The root traces or rhizoliths are the most evident ichnofossil in these pedotypes. Rhizoliths described include root molds and root casts (Klappa, 1980), where the mold is the void left behind by a decayed root and the cast is the sediment or cement that fills the mold. A highly oxidizing environment may explain the absence of organic matter within bioturbation structures.

The rhizoliths are better preserved in Apore pedotype. They show mineral replacements and impregnations that preserve anatomical features of the roots (Fig. 11A). These rhizoliths are morphologically similar to the taproots of small plants described by Hembree and Hasiotis (2007). Modern plants with taproot systems habitually occur in well-drained soils (Retallack, 2001). The absence of large rooting systems suggests that the vegetation was of low stature but the density of the rooting systems indicates that they were abundant. Another ichnofossil identified in the Apore pedotype is related to terrestrial invertebrate burrows. These burrows are vertically oriented subcylindrical structures filled with fine sand and have as the principal characteristic the unbranched nature and the hemispherical hollow extremity. This ichnofossil

may be interpreted as *Macanopsis* *isp.* Macanopsis burrows are attributed to a variety of invertebrates including insects, beetles, and spiders (Hasiotis, 2002).

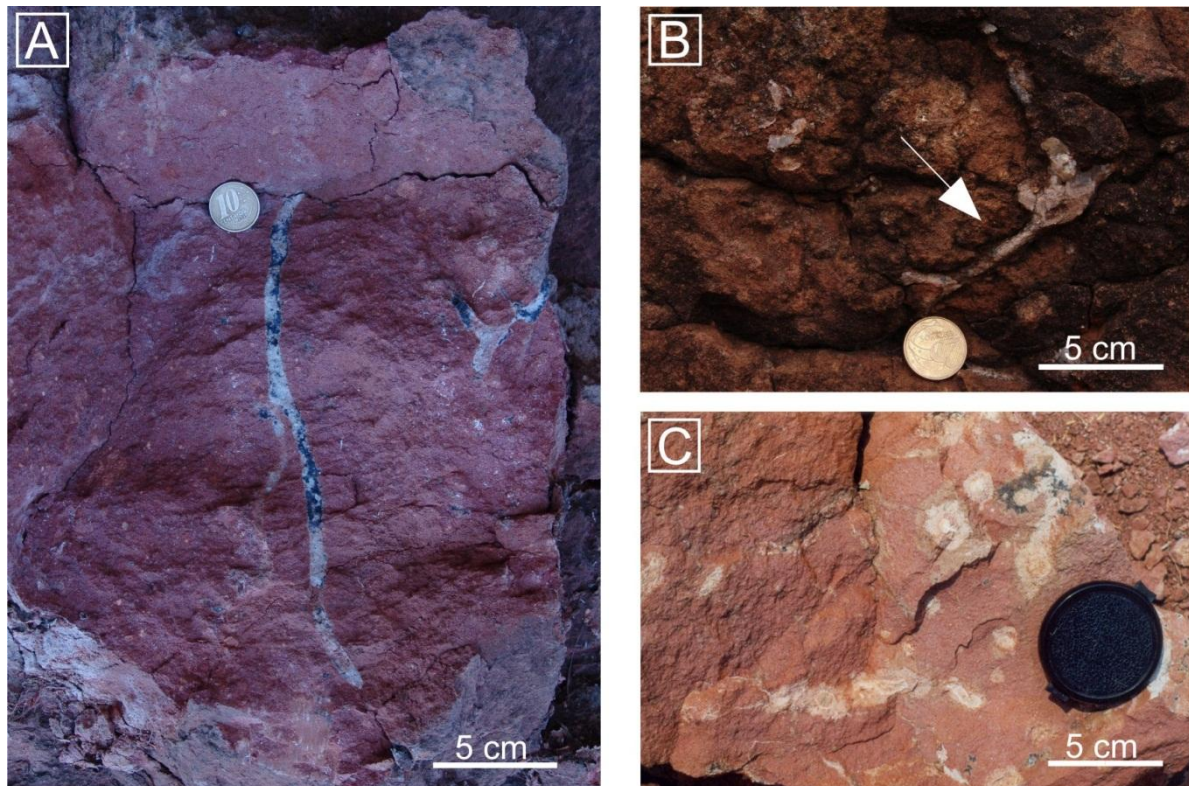


**Figure 11.** Ichnofossils. (A) Rhizolith preserved in Btk3 horizon of the Apore pedotype. (B) Rhizolith filled with sparry calcite in 3Btk2 horizon of the Itaja pedotype. (C) Rhizohaloes showing white bleached zones developed around a rhizotubules in 5Bt4 horizon of the Itaja pedotype.

Within the Itaja pedotype, the principal ichnofossil described is sand filled ramified structures. These structures exhibit downward tapering and lateral branching which are encrusted with a fine cap of calcite and are interpreted as rhizocretions (Klappa, 1980). Other root casts observed in 3Btk2 horizon are completely filled with sparry calcite (Fig. 11B). In some horizons, the root traces are not preserved as mold or cast, but they are identified by means of bleached zones, which may be interpreted as rhizohaloes (Kraus and Hasiotis, 2006) (Fig. 11C). The elongate and branch nature of these traces as well as their circular cross section indicate that these bleached zones were produced by roots.

### 5.2.3. Parent material

The parent material for the Itaja and Apore pedotypes is eolian sand sheet deposits. The molar ratio of less mobile elements titanium and aluminum ( $Ti/Al$ ) is useful for indicating differences in composition between pedotypes and within superimposed profiles (Hamer et al., 2007b; Sheldon and Tabor, 2009).

Fig. 12 shows the behavior of the  $Ti/Al$  ratio in relation to the constant curve of parent material. The low values of departure (<50%) from the constant curve of the parent material indicate that the source material is the same for both pedotypes (Maynard, 1992).

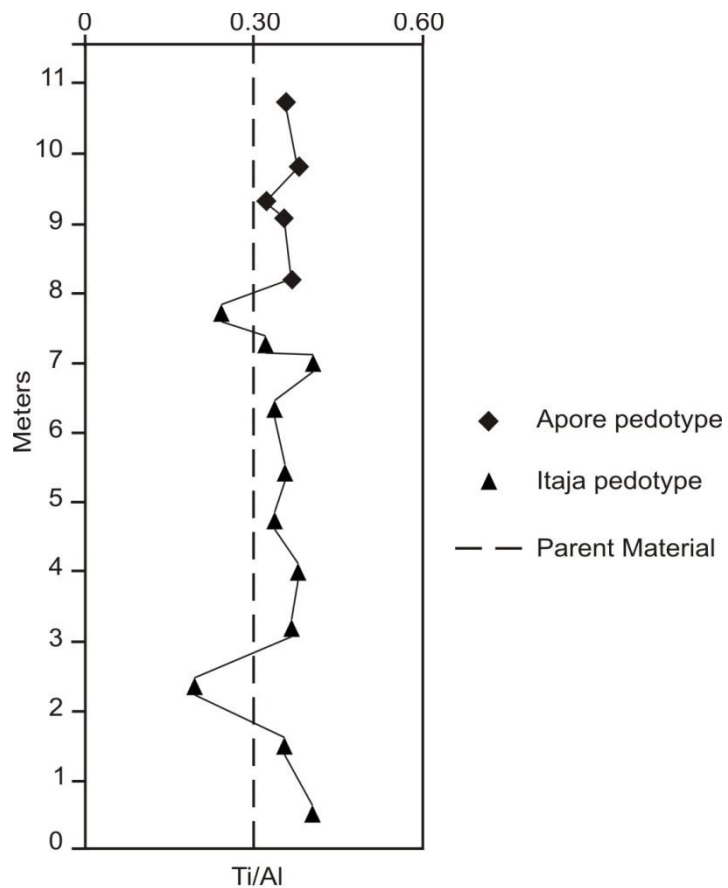


**Figure 12.** Graph showing the provenance as determined from the ratio of  $Ti/Al$ . The low values of departure (<50%) from the parent material curve indicate that the source material is the same for both pedotypes.

The enrichment in calcium carbonate content observed in some horizons is probably originated from dust input rather than from geological origin (i.e., phreatic activity) or pedogenic

weathering in that (1) soil horizons display highly irregular and heterogeneous distribution of calcite features (e.g., calcite laminas on sand grains overlaid by clay coatings and then covered by calcite), (2) irregular pattern of distribution of molar calcification ratio through horizons, (3) the amount of CaO in the pedotypes is by far in excess of what could be released by weathering from the analyzed parent material, and (4) there is minimal evidence for weathering of Ca-bearing minerals in the analyzed thin sections of the parent material.

#### **5.2.4. Topographic relief**

Present-day eolian sand sheet areas are characterized by flat to gently undulating surfaces (Kocurek and Nielson, 1986). The paleotopography of the study area was relatively flat and uniform, without expressive geomorphic forms such as mountains or valleys. There were only few rivers. The register of these rivers are similar to ephemeral desertic rivers, with wide and shallow channels that only excavated small sand and conglomerate channels (Basilici et al., 2009). The influence of tectonics is not thought to be determinant to the development of very mature paleosols. The low thermal and lithostatic subsidence of the Bauru Basin was favorable to the continuous modification of the eolian deposits by pedogenesis. Basilici and Dal' Bo (2010) show that the low rate of subsidence negatively controlled the preservation of eolian deposits in the Marília Formation, since it fostered intense pedogenesis during periods of topographic stability and the consequently thicker paleosol profiles recorded in the sedimentary succession.

#### **5.2.5. Time**

The time of subaerial exposure is directly related to the degree of paleosol development. In general, for the same paleosol order, it takes more time to develop in dry settings than in wetter ones (Birkeland, 1999). For quantifying the relative time that paleosols were subjected to subaerial exposure and thus to pedogenesis, the chronofunction based on the thickness of Bt horizons proposed by Markewich et al. (1990) is applied:

Formation time (yr) =  $17.7(\text{Bt thickness})^2 + 645.8(\text{Bt thickness})$ ,

where  $R^2 = 0.87$  (e.g., Sheldon, 2003; Hamer et al., 2007a).

On average, the calculated time for Bt horizons of the Itaja and Apore pedotypes to develop is ~175 ky. This assessed time is in agreement with the ideas of Crocker and Major (1955) and Birkeland (1999) about the minimum time required for the formation of well developed argillic horizons. The high degree of chemical weathering, the enrichment in clay content as well as the strongly developed soil structures is other evidences that taken as a whole point to minimum formation times of thousands of years for both pedotypes.

## 6. Conclusions

In this paper a succession with six paleosol profiles was studied to define the main paleoenvironmental controlling factors on soil formation and verify their variation on time. The main findings are indicated as follows:

(1) The paleosols developed on eolian sand sheet deposits of the Late Cretaceous Marília Formation are comparable to modern Alfisols and Aridisols (Apore and Itaja pedotypes, respectively). The analysis of the factors which controlled the soil formation revealed that soil profiles formed on a stable landscape probably covered by a community of low stature plants, in which the soils had sufficient time to develop very mature profiles. The changes in soil-forming processes were driven principally by variations in available soil moisture from precipitation.

(2) The Apore pedotype was classified as Alfisol, and was formed during a period with prevalent humid conditions. MAP estimates around 900 mm/year are coincident with the well developed argillic horizons, the absence of calcitic features, and the increased abundance and depth of rooting. The Itaja pedotype was classified as Aridisol. This pedotype clearly shows the influence of different precipitation regimes on the genesis of polygenetic profiles with soil horizons characterized by compound calcic and argillic properties. CIA-K proxy and depth-to-carbonate functions show that precipitation estimates varied from 240 mm/year during the formation of calcic Bk horizon up to 1078 mm/year at the time of Bt horizon formation.

(3) The polygenetic character of the paleosols, the variation in soil process through time, and the eolian deposition seem to have been controlled by climatic changes as forcing mechanism. The formation of Itaja pedotype takes place in a general arid or semi-arid climate

with seasonal humid periods, whereas the formation of Apore pedotype occurs in considerably more humid conditions. In this scenario, the eolian deposition was probably restricted to periods characterized by intense arid conditions, because semi-arid climates favored the leaching and precipitation of calcium carbonate in pedogenic calcic horizons.

## Acknowledgements

This research was supported by FAPESP (project numbers 07/00140-6 and 07/02079-2), CNPq (PhD scholarship to the first author), and International Association of Sedimentologists (IAS PhD grant to the first author). The manuscript has benefited greatly from the constructive review of an anonymous reviewer and Claudio Riccomini.

## 7. References

- Alonso, P., Dorronsoro, C., Egido, J.A., 2004. Carbonatation in palaeosols formed on terraces of the Tormes river basin (Salamanca, Spain). *Geoderma* 118, 261-276.
- Barron, E.J., Washington, W.M., 1982. Cretaceous climate: a comparison of atmospheric simulations with the geologic record. *Palaeogeography, Palaeoclimatology, Palaeoecology* 40, 103-133.
- Basilici, G., Dal' Bo, P.F.F., 2010. Anatomy and controlling factors of a Late Cretaceous aeolian sand sheet: The Marília and the Adamantina formations, NW Bauru Basin, Brazil. *Sedimentary Geology* 226, 71-93.
- Basilici, G., Dal' Bo, P.F.F., Ladeira, F.S.B., 2009. Climate-induced sediment-palaeosol cycles in a Late Cretaceous dry aeolian sand sheet: Marília Formation (North-West Bauru Basin, Brazil). *Sedimentology* 56, 1876-1904.
- Bathurst, R.G.C., 1971. *Carbonate Sediments and Their Diagenesis*. Elsevier, Amsterdam.
- Birkeland, P.W., 1999. *Soils and Geomorphology*, 3rd edition. Oxford University Press, New York.
- Bullock, P., Fedoroff, N., Jongerius, A., Stoops, G., Tursina, T., 1985. *Handbook for Soil Thin Section Description*. Waine Research Publications, Wolverhampton.
- Capo, R.C., Whipkey, C.E., Blachère, J.R., Chadwick, O.A., 2000. Pedogenic origin of dolomite in a basaltic weathering profile, Kohala peninsula, Hawaii. *Geology* 28, 271-274.
- Catt, J.A., 1990. Paleopedology manual. *Quaternary International* 6, 1-95.

Cleveland, D.M., Nordt, L.C., Atchley, S.C., 2008. Paleosols, trace fossils, and precipitation estimates of the uppermost Triassic strata in northern New Mexico. *Palaeogeography, Palaeoclimatology, Palaeoecology* 257, 421-444.

CPRM - Serviço Geológico do Brasil, 2004. Carta Geológica do Brasil ao Milionésimo, Folha SE22, Goiânia, Secretaria de Minas e Metalurgia e Ministério de Minas e Energia, Brasília.

Crocker, R.L., Major, L., 1955. Soil development in relation to vegetation and surface age at Glacier Bay, Alaska. *Journal of Ecology* 43, 427-448.

Dal' Bo, P.F.F., Basilici, G., Angelica, R.S., Ladeira, F.S.B., 2009. Paleoclimatic interpretations from pedogenic calcretes in a Maastrichtian semi-arid eolian sand-sheet palaeoenvironment: Marília Formation (Bauru Basin, southeastern Brazil). *Cretaceous Research* 30, 659-675.

Dias-Brito, D., Musacchio, E.A., Castro, J.C. de., Maranhão, M.da.S., Suarez, J.M., Rodrigues, R., 2001. Grupo Bauru: uma unidade continental do Cretáceo no Brasil – concepções baseadas em dados micropaleontológicos, isotópicos e estratigráficos. *Revue de Paléobiologie* 20 (1), 245-304.

Driese, S.G., Ober, E.G., 2005. Paleopedologic and paleohydrologic records of precipitation seasonality from Early Pennsylvanian “Underclay” paleosols, U.S.A. *Journal of Sedimentary Research* 75, 997-1010.

Driese, S.G., Mora, C.I., Stiles, C.A., Joeckel, R.M., Nordt, L.C., 2000. Mass-balance reconstruction of a modern Vertisol: implications for interpreting the geochemistry and burial alteration of paleo-Vertisols. *Geoderma* 95, 179-204.

Eghbal, M.K., Southard, R.J., 1993. Micromorphological evidence of polygenesis of three Aridisols, western Mojave Desert, California. *Soil Science Society of America Journal* 57, 1041-1050.

Fernandes, L.A., Coimbra, A.M., 1996. A Bacia Bauru (Cretáceo Superior, Brasil). *Anais da Academia Brasileira de Ciências* 68 (2), 195-205.

Garcia, A.J.V., da Rosa, A.A.S., Goldberg, K., 2005. Paleoenvironmental and paleoclimatic control on early diagenetic processes and fossil record in Cretaceous continental sandstones of Brazil. *Journal of South American Earth Sciences* 19 (3), 243-258.

Gile, L.H., Peterson, F.F., Grossman, R.B., 1965. The K horizon: a master soil horizon of carbonate accumulation. *Soil Science* 99, 74-82.

Gile, L.H., Peterson, F.F., Grossman, R.B., 1966. Morphological and genetic sequences of carbonate accumulation in desert soils. *Soil Science* 101, 347-354.

- Goldberg, K., Garcia, A.J.V., 2000. Palaeobiogeography of the Bauru Group, a dinosaur-bearing Cretaceous unit, northeastern Paraná Basin, Brazil. *Cretaceous Research* 21, 241-254.
- Goudie, A.S., 1973. Duricrusts in Tropical and Subtropical Landscapes. Clarendon, Oxford.
- Goudie, A.S., 1983. Calcrete. In: Goudie, A.S., Pye, K. (Eds.), *Chemical Sediments and Geomorphology: Precipitates and Residual in Near-Surface Environment*. Academic Press, London, pp. 93-131.
- Gustavson, T.C., Holliday, V.T., 1999. Eolian sedimentation and soil development on a semiarid to subhumid grassland, Tertiary Ogallala and Quaternary Blackwater Draw formations, Texas and New Mexico High Plains. *Journal of Sedimentary Research* 69, 622-634.
- Hamer, J.M.M., Sheldon, N.D., Nichols, G.J., 2007a. Global aridity during the Early Miocene? A terrestrial paleoclimate record from the Ebro Basin, Spain. *Journal of Geology* 115, 601-608.
- Hamer, J.M.M., Sheldon, N.D., Nichols, G.J., Collinson, M.E., 2007b. Late Oligocene-Early Miocene paleosols of distal fluvial systems, Ebro Basin, Spain. *Palaeogeography, Palaeoclimatology, Palaeoecology* 247, 220-235.
- Hasiotis, S.T., 2002. Continental Trace Fossils. Society for Sedimentary Geology Short Course 51.
- Hembree, D.I., Hasiotis, S.T., 2007. Paleosols and ichnofossils of the White River Formation of Colorado: insight into soil ecosystems of the North American Midcontinent during the Eocene-Oligocene transition. *Palaios* 22, 123-142.
- Hunter, R.E., 1977. Basic types of stratification in small eolian dunes. *Sedimentology* 24, 361-387.
- Kahmann, J.A., Driese, S.G., 2008. Paleopedology and geochemistry of Late Mississippian (Chesterian) Pennington Formation paleosols at Pound Gap, Kentucky, USA: Implications for high-frequency climate variations. *Palaeogeography, Palaeoclimatology, Palaeoecology* 259, 357-381.
- Khademi, H., Mermut, A.R., 1999. Submicroscopy and stable isotope geochemistry of carbonates and associated palygorskite in Iranian Aridisols. *European Journal of Soil Science* 50, 207-216.
- Khormali, F., Abtahi, A., 2003. Origin and distribution of clay minerals in calcareous arid and semi-arid soils of Fars Province, southern Iran. *Clay Minerals* 38, 511-527.
- Khormali, F., Abtahi, A., Mahmoodi, S., Stoops, G., 2003. Argillic horizon development in calcareous soils of arid and semiarid regions of southern Iran. *Catena* 53, 273-301.

- Klappa, C.F., 1980. Rhizoliths in terrestrial carbonates: classification, recognition, genesis and significance. *Sedimentology* 27, 613-629.
- Kocurek, G., Nielson, J., 1986. Conditions favourable to the formation of warm-climate aeolian sand sheets. *Sedimentology* 33, 795-816.
- Köeppen, W., 1948. *Climatología: con un estudio de los climas de la tierra*. Fondo de Cultura Económica, Pánuco.
- Kraus, M.J., 1999. Paleosols in clastic sedimentary rocks: their geologic applications. *Earth-Science Reviews* 47, 41-70.
- Kraus, M.J., Hasiotis, S.T., 2006. Significance of different modes of rhizolith preservation to interpreting paleoenvironmental and paleohydrologic settings: examples from Paleogene paleosols, Bighorn Basin, Wyoming. *Journal of Sedimentary Research* 76, 633-646.
- Kraus, M.J., Riggins, S., 2007. Transient drying during the Paleocene-Eocene Thermal Maximum (PETM): analysis of paleosols in the Bighorn Basin, Wyoming. *Palaeogeography, Palaeoclimatology, Palaeoecology* 245, 444-461.
- Lima, M.R., 1983. Paleoclimatic reconstruction of the Brazilian Cretaceous based on palynological data. *Revista Brasileira de Geociências* 13, 223-228.
- Machette, M.N., 1985. Calcic soils of the southwestern United States. In: Weide, D.L. (Ed.), *Soils and Quaternary Geology of the Southwestern United States*. Geological Society of America Special Paper 203, pp. 1-21.
- Mack, G.H., James, W.C., 1994. Paleoclimate and the global distribution of paleosols. *Journal of Geology* 102, 360-366.
- Mack, G.H., James, W.C., Monger, H.C., 1993. Classification of paleosols. *Geological Society of America Bulletin* 105, 129-136.
- Markewich, H.W., Pavich, M.J., Buell, G.R., 1990. Contrasting soils and landscapes of the Piedmont and Coastal Plain, eastern United States. *Geomorphology* 3, 417-447.
- Maynard, J.B., 1992. Chemistry of modern soils as a guide to interpreting Precambrian paleosols. *Journal of Geology* 100, 279-289.
- Monger, H.C., Daughert, A., Gile, L.H., 1991. A microscopic examination of pedogenic calcite in an Aridisol of southern New Mexico. In: Nettleton, W.D. (Ed.), *Occurrence, Characteristics, and Genesis of Carbonate, Gypsum, and Silica Accumulations in Soils*. Soil Science Society of America Special Publication 26, pp. 37-60.
- Murphy, C.P., 1986. *Thin Section Preparation of Soils and Sediments*. AB Academic Publishers, Berkhamsted.

- Nesbitt, H.W., Young, G.M., 1982. Early Proterozoic climates and plate motions inferred from major element chemistry of lutites. *Nature* 299, 715-717.
- Nettleton, W.D., Peterson, P.F., 1983. Aridisols. In: Wilding, L.P., Smeck, N.E., Hall, G.F. (Eds.), *Pedogenesis and Soil Taxonomy II. The Soil Orders. Developments in Soil Science 11B*. Elsevier, Amsterdam, pp. 165-215.
- Nettleton, W.D., Olson, C.G., Wysocki, D.A., 2000. Paleosol classification: problems and solutions. *Catena* 41, 61-92.
- Nordt, L., Atchley, S., Dworkin, S.I., 2002. Paleosol barometer indicates extreme fluctuations in atmospheric CO<sub>2</sub> across the Cretaceous-Tertiary boundary. *Geology* 30, 703-706.
- Nordt, L., Atchley, S., Dworkin, S.I., 2003. Terrestrial evidence for two greenhouse events in the latest Cretaceous. *Geological Society of America Today* 13 (12), 4-9.
- Paquet, H., Millot, C., 1972. Geochemical evolution of clay minerals in the weathered products and soils of Mediterranean climates. *Proceedings of the International Clay Conference*, Madrid, Spain, pp. 199-202.
- PiPujol, M.D., Buurman, P., 1994. The distinction between ground-water gley and surface-water gley phenomena in Tertiary paleosols of the Ebro Basin, NE Spain. *Palaeogeography, Palaeoclimatology, Palaeoecology* 110, 103-113.
- Reheis, M.C., 1987. Climatic implications of alternating clay and carbonate formation in semiarid soils of south-central Montana. *Quaternary Research* 27, 270-282.
- Retallack, G.J., 1994a. A pedotype approach to latest Cretaceous and earliest Tertiary paleosols in eastern Montana. *Geological Society of America Bulletin* 106, 1377-1397.
- Retallack, G.J., 1994b. The environmental factor approach to the interpretation of paleosols. In: Amundson, R., Harden, J., Singer, M. (Eds.), *Factors in Soil Formation: a Fiftieth Anniversary Retrospective*. Soil Science Society of America Special Publication 33, pp. 31-64.
- Retallack, G.J., 1997. *A Colour Guide to Paleosols*. John Wiley and Sons, Chichester.
- Retallack, G.J., 2001. *Soils of the Past*, 2nd edition. Blackwell, Oxford.
- Retallack, G.J., 2005. Pedogenic carbonate proxies for amount and seasonality of precipitation in paleosols. *Geology* 33, 333-336.
- Retallack, G.J., 2007. Cenozoic paleoclimate on land in North America. *Journal of Geology* 115, 271-294.
- Retallack, G.J., 2009. Greenhouse crises of the past 300 million years. *Geological Society of America Bulletin* 121, 1441-1455.

- Retallack, G.J., Metzger, C.A., Greaver, T., Jahren, A.H., Sheldon, N.D., Smith, R.M.H., 2006. Middle-Late Permian mass extinction on land. *Geological Society of America Bulletin* 118, 1398-1411.
- Riccomini, C., 1997. Arcabouço estrutural e aspectos do tectonismo gerador e deformador da Bacia Bauru no estado de São Paulo. *Revista Brasileira de Geociências* 27 (2), 153-162.
- Sheldon, N.D., 2003. Pedogenesis and geochemical alteration of the Picture Gorge subgroup, Columbia River Basalt, Oregon. *Geological Society of America Bulletin* 115, 1377-1387.
- Sheldon, N.D., 2005. Do red beds indicate paleoclimatic conditions?: a Permian case study. *Palaeogeography, Palaeoclimatology, Palaeoecology* 228, 305-319.
- Sheldon, N.D., 2006. Abrupt chemical weathering increase across the Permian-Triassic boundary. *Palaeogeography, Palaeoclimatology, Palaeoecology* 231, 315-321.
- Sheldon, N.D., Tabor, N.J., 2009. Quantitative paleoenvironmental and paleoclimatic reconstruction using paleosols. *Earth-Science Reviews* 95, 1-52.
- Sheldon, N.D., Retallack, G.J., Tanaka, S., 2002. Geochemical climofunctions from North American soils and application to paleosols across the Eocene–Oligocene boundary in Oregon. *Journal of Geology* 110, 687-696.
- Simonson, R.W., 1949. Genesis and classification of red-yellow podzolic soils. *Soil Science Society of America Proceedings* 14, 316-319.
- Soares, P.C., Landim, P.M.B., Fúlfaro, V.J., Sobreiro Neto, A.F., 1980. Ensaio de caracterização estratigráfica do Cretáceo no estado de São Paulo: Grupo Bauru. *Revista Brasileira de Geociências* 10, 177-185.
- Soil Survey Staff, 1993. *Soil Survey Manual*. Soil Conservation Service. U.S. Department of Agriculture Handbook 18, Washington, DC.
- Soil Survey Staff, 1999. *Soil Taxonomy*, 2nd edition. U.S Department of Agriculture, Natural Resource Conservation Service 436, Washington, DC.
- Suguio, K., Barcelos, J.H., 1983. Calcretes of the Bauru Group (Cretaceous), Brazil: petrology and geological significance. *Boletim do Instituto de Geociências da Universidade de São Paulo* 14, 31-47.
- Therrien, F., 2005. Palaeoenvironments of the latest Cretaceous (Maastrichtian) dinosaurs of Romania: insights from fluvial deposits and paleosols of the Transylvanian and Hațeg basins. *Palaeogeography, Palaeoclimatology, Palaeoecology* 218, 15-56.
- Watts, N.L., 1980. Quaternary pedogenetic calcretes from Kalahari (southern Africa): mineralogy, genesis and diagenesis. *Sedimentology* 27, 661-686.

White, P.D., Schiebout, J., 2008. Paleogene paleosols and changes in pedogenesis during the initial Eocene thermal maximum: Big Bend National Park, Texas, USA. Geological Society of America Bulletin 120 (11/12), 1347-1361.

Wieder, M., Yaalon, D.H., 1974. Effects of matrix composition on carbonate nodule crystallisation. Geoderma 11, 95-121.

Wright, V.P., 1990. A micromorphological classification of fossil and recent calcic and petrocalcic microstructures. In: Douglas, L.A. (Ed.), Soil Micromorphology: a Basic and Applied Science. Developments in Soil Science 19. Elsevier, Amsterdam, pp. 401-407.

Zaher, H., Pol, D., Carvalho, A.B., Riccomini, C., Campos, D., Navas, W., 2006. Re-description of the cranial morphology of *Mariliasuchus amarali*, and its phylogenetic affinities (Crocodyliformes, Notosuchia). American Museum Novitates 3512, 1-40

## ANEXO II

“Dal’ Bo, P.F.F., Basilici, G., Angélica, R.S., Ladeira, F.S.B., 2009. *Paleoclimatic interpretations from pedogenic calcretes in a Maastrichtian semi-arid eolian sand sheet palaeoenvironment: Marília Formation (Bauru Basin, southeastern Brazil).* *Cretaceous Research* 30, 659-675.”



*“The philosophical study of nature rises above the requirements of mere delineation, and does not consist in the sterile accumulation of isolated facts. The active and inquiring spirit of man may therefore be occasionally permitted to escape from the present into the domain of the past, to conjecture that which cannot yet be clearly determined, and thus to revel amid the ancient and ever-recurring myths of geology.”*

*Alexander von Humboldt*



# **PALEOCLIMATIC INTERPRETATIONS FROM PEDOGENIC CALCRETES IN A MAASTRICHTIAN SEMI-ARID EOLIAN SAND-SHEET PALEOENVIRONMENT: MARÍLIA FORMATION (BAURU BASIN, SE BRAZIL)**

Patrick Francisco Führ Dal' Bó<sup>1</sup>, Giorgio Basilici<sup>1</sup>, Rômulo Simões Angélica<sup>2</sup> and  
Francisco Sérgio Bernardes Ladeira<sup>3</sup>

<sup>1</sup> Departamento de Geologia e Recursos Naturais, Instituto de Geociências, Universidade Estadual de Campinas – Brazil (patrickdalbo@ige.unicamp.br; basilici@ige.unicamp.br).

<sup>2</sup> Faculdade de Geologia, Instituto de Geociências, Universidade Federal do Pará – Brazil (angelica@ufpa.br)

<sup>3</sup> Departamento de Geografia, Instituto de Geociências, Universidade Estadual de Campinas – Brazil (fsbladeira@ige.unicamp.br)

## **Abstract**

Stratigraphic and sedimentologic studies in continental successions do not always devote particular attention to the paleosols, in particular in arid or semi-arid paleoenvironments. The aim of this paper is to: i) describe in detail the macro and microscopic pedogenic features of four types of paleosol profiles with calcic horizons of the Marília Formation (Maastrichtian), and ii) elaborate paleoclimatic considerations based on the depth of the nodular calcic horizon and on the molecular weathering ratios of the main oxides. The Marília Formation, which crops out in the eastern portion of the Bauru Basin (São Paulo State, SE of Brazil), usually contains profiles of calcic paleosols developed over sandstone deposits which formed in a eolian sand sheet paleoenvironment. The type of calcium carbonate accumulation in paleosol horizons varies from thin discontinuous coatings on ped surfaces trough faint filaments in soil matrix to massive accumulations between coalesced nodules, which are associated respectively to the stages I, II, and III of calcic soil development morphology classification (Gile et al., 1966). Four carbonate paleosol profiles with prominent calcic horizons (Bk and Ck) and secondary argillic horizons (Bt and Btk) have been studied in Marília Formation: two near the homonymous city and other two around the Monte Alto plateau. Field data and petrographic, geochemical, and clay mineralogy analyses allowed to classify these four paleosol profiles as Aridisols and define some paleoclimate considerations on their development. Molecular weathering ratios relative to

calcification, hydrolysis, clay formation, salinization, and hydration of the paleosol profiles has been calculated to define the characteristic of the paleosols and the paleoclimatic proxies. Paleoprecipitations have been estimated by the application of an empirical equation that related this value to the depth of the Bk horizon.

Keywords: Pedogenic calcrete, Paleoclimate, Eolian sand sheet, Maastrichtian, Bauru Basin.

## **1. Introduction**

The terminology used in sedimentological and/or pedological studies for pedogenic calcrete profiles is quite various. The contrasting arguments between sedimentologists and pedologists created a confusion of terminology and application, which varies according to the region where the effective works have been developed, and the literature of the different areas of knowledge (Machette, 1985; Wright and Tucker, 1991).

Calcrete is considered as an accumulation of calcium carbonate that occurs near the terrestrial surface and that shows a great variety of forms and consistencies, from pulverulent, nodular to extremely harden and continuous layers. Caliche is considered here as synonymous of calcrete, according to the definition of Wright and Tucker (1991). The profiles and/or horizons of calcrete result from the cementation and displacive and replacive introduction of calcium carbonate into soil profiles and sediments, in areas where vadose and/or shallow phreatic groundwater become supersaturated in calcium carbonate (Wright and Tucker, 1991; Alonso-Zarza, 2003).

Presently, the pedogenic calcrete profiles cover approximately an area of  $2 \times 10^7$  sq. km. (13% of the terrestrial surface) (Yaalon, 1971). They are a prominent surface feature in those climatic zones where a seasonal moisture deficit occurs (Goudie, 1983). Ollier and Pain (1996) attest that the current formation of pedogenic calcrete is restricted to areas with annual precipitation limits lower than 500 mm, in which evapotranspiration processes necessarily exceeds the precipitation. The soil processes that take part in the formation of calcium carbonate profiles involve the conjunction of three prevailing solution movements that occur within the profile and in contiguous areas: vertical washing, diffuse capillary ascendancy and lateral transference (Gile et al., 1966). The last process, which involves the migration and lateral addition, is accepted as the most common. Other basic processes responsible for calcium carbonate accumulation in ground profiles are: precipitation, cementation, physical expansion (displacement) and substitution (Goudie, 1983; Machette, 1985; Wright and Tucker, 1991; Alonso-Zarza, 2003). Conventionally eolian dust is believed to be a major source of carbonate for pedogenic processes in arid zones (Machette, 1985).

Pedogenetic calcrete corresponds to the formation of a calcic (k) or petrocalcic (km) (if continuous and indurated) horizon in the terminology of soil scientists, and it is generally

associated to B and C soil horizons of the pedogenic profile (Schaetzl and Anderson, 2005). Calcretes typically occur within Aridisols, Vertisols, Alfisols, and Mollisols (Soil Survey Staff, 1999; Retallack, 2001). Resedimented conglomeratic calcretes appear to be less common in the stratigraphic record (Allen, 1986). Most of the studied calcretes are from pedogenic settings (Gile et al., 1966; Goudie, 1983; Machette, 1985; Wright and Tucker, 1991), but in some cases groundwater can form calcretes (Arakel, 1986). Pimentel et al. (1996) and Alonso-Zarza (2003) listed specific features that allow to distinguish between pedogenic and groundwater calcretes, based only on morphologic features, such as thin thickness profiles, ordered horizons, soil structures, abundant root traces and absence of disseminated reduction features.

This paper describes and discusses in detail the development of four types of Maastrichtian carbonate paleosol profiles of the Marília Formation, which are classified as Calcisols (according to Mack et al., 1993) or Aridisols (Soil Survey Staff, 1999).

The aim of this work is the: i) description of field and laboratory data of four paleosol profiles with calcrete horizons; ii) interpretation of paleoclimatic development conditions of the paleosols.

## **2. Stratigraphical and sedimentological setting**

The Bauru Basin (Fig. 1A) is an intracratonic basin developed upon the greatest basaltic effusion of the world (Serra Geral Formation, Late Jurassic – Early Cretaceous), which was formed during the South America – Africa plate opening. The Bauru Basin, Santonian-Maastrichtian in age (Fernandes and Coimbra, 1996), has an elliptical shape with an axis in NE direction. Thermal and lithostatic subsidence is considered the mechanism which generated the accommodation space (Riccomini, 1997). The sedimentary filling of this basin occurs over an area of 370,000 km<sup>2</sup> in mid-southeast Brazil with a maximum sedimentary thickness of 300 m (Fig. 1B).

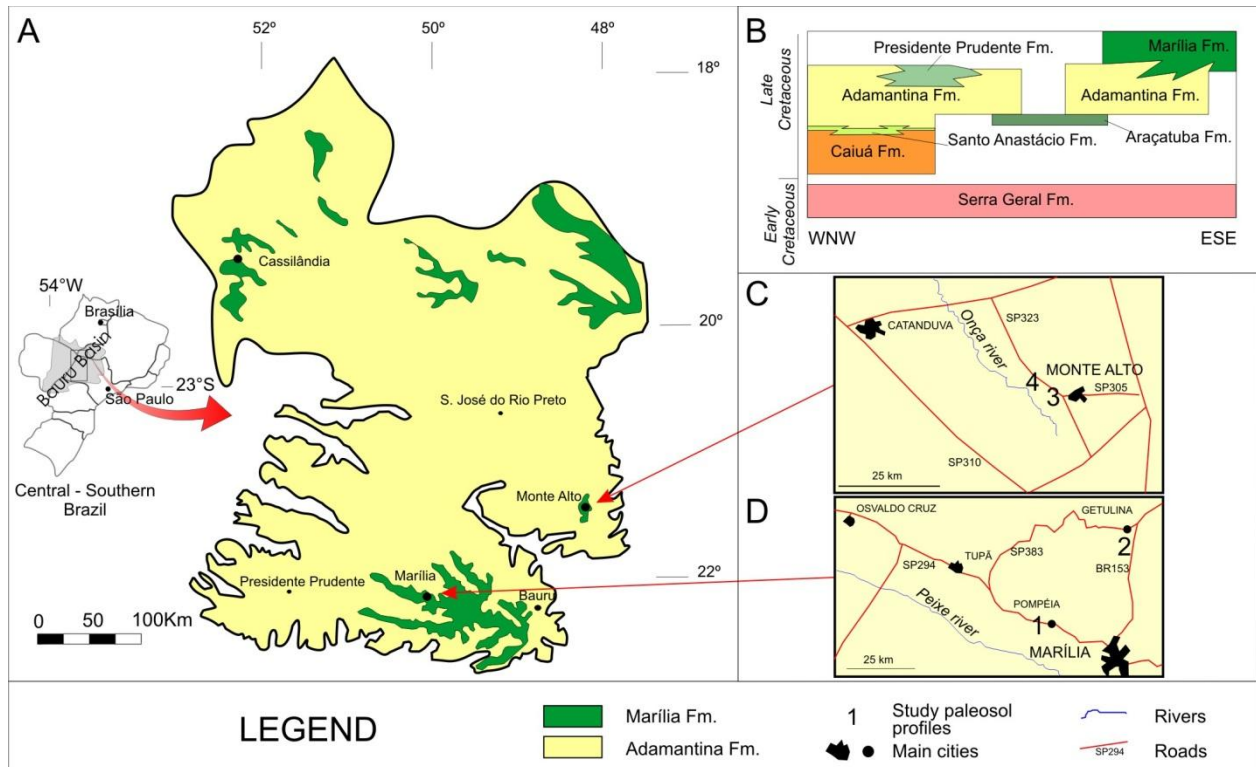


**Figure 1.** Geological and stratigraphic features of the study area. (A) Distribution of the Marília Formation in the central and northern part of the Bauru Basin. (B) Stratigraphical sketch of the Bauru Basin, simplified from Zaher et al. (2006). (C) Location of the sites where the Monte Alto 1 and Monte Alto 2 paleosol profiles were measured. (D) Location of the sites where the Serra da Flor Roxa and Serra de Lins paleosol profiles were measured.

A complex and not yet very clear stratigraphy characterizes the Bauru Basin. We studied the paleosol profiles in two areas: the Marília and the Monte Alto plateau (Fig. 1C, D), which are typical areas of the Marília Formation and display well preserved paleosol profiles with calcrete horizons. The Marília Formation (Maastrichtian) is the youngest unit of the Bauru Basin (Dias-Brito et al., 2001). It is characterized by a vertical succession of deposits and paleosols, which are represented by two depositional architectural elements (ephemeral fluvial deposits and sandstone wind rippled deposits), and one paleopedogenetic element (paleosols) (Fig. 2).

The sandstone wind rippled deposits (77% of the depositional record) (Fig. 2A, B) are made up of medium to fine and very fine sandstone, constituted principally of quartz grains and secondarily of lithic fragments and feldspars. Sandstone is well or very well sorted, and quartz grains have high sphericity and are well rounded, commonly exhibiting hematite coatings, probably associated with desert varnish. This lithofacies was interpreted here as wind ripples produced by the continuum migration of coarser grains concentrated at ripple crests over finer

grains, preferentially trapped in ripple-trough shadow zones or low-impact zones (Mountney, 2006). Bioturbation features are not common in this lithofacies, probably due to intense arid conditions that prevailed during deposition of wind ripples.

The ephemeral fluvial deposits (23% of the depositional record) (Fig. 2A, C) are made up of several episodes of sedimentation, characterized by conglomerate sandstone and sandstone conglomerate that form concave-up bottom and flat top sedimentary bodies (less than 3 km wide, more than 7 km long and up to 4 m thick). This lithofacies is organized in tabular beds, internally subdivided into a conglomerate lower portion and a sandstone upper portion, presenting a rough gradation. The lower portion is characterized by clast-supported conglomerate, constituted of rounded or subrounded basalt and quartzite clasts, at times with ventifact clasts. The unstructured conglomerate/sandstone bodies have been interpreted as ephemeral channels depositional episodes produced by high concentrated hydraulic flows. Planar laminated sandstone at the top of conglomerate/sandstone bodies can be interpreted as wind activity reworking ephemeral fluvial deposits, also testifying the ephemeral hydraulic flows.

The architectural element paleosol (Fig. 2A, D) constitute on average 65% of the Marília Formation. Aridisols profiles are the most representative pedotypes (*sensu* Retallack, 1998, 2001). They are developed on medium to fine well sorted sandstone (wind ripples deposits) with calcic (Bk and Ck) and secondarily argillic (Bt and Btk) horizons. Vertical transitions from paleosols to sediments are always marked by an abrupt horizontal erosional surface, underlined by frequent truncation of the profile that may result in the absence of A horizon.

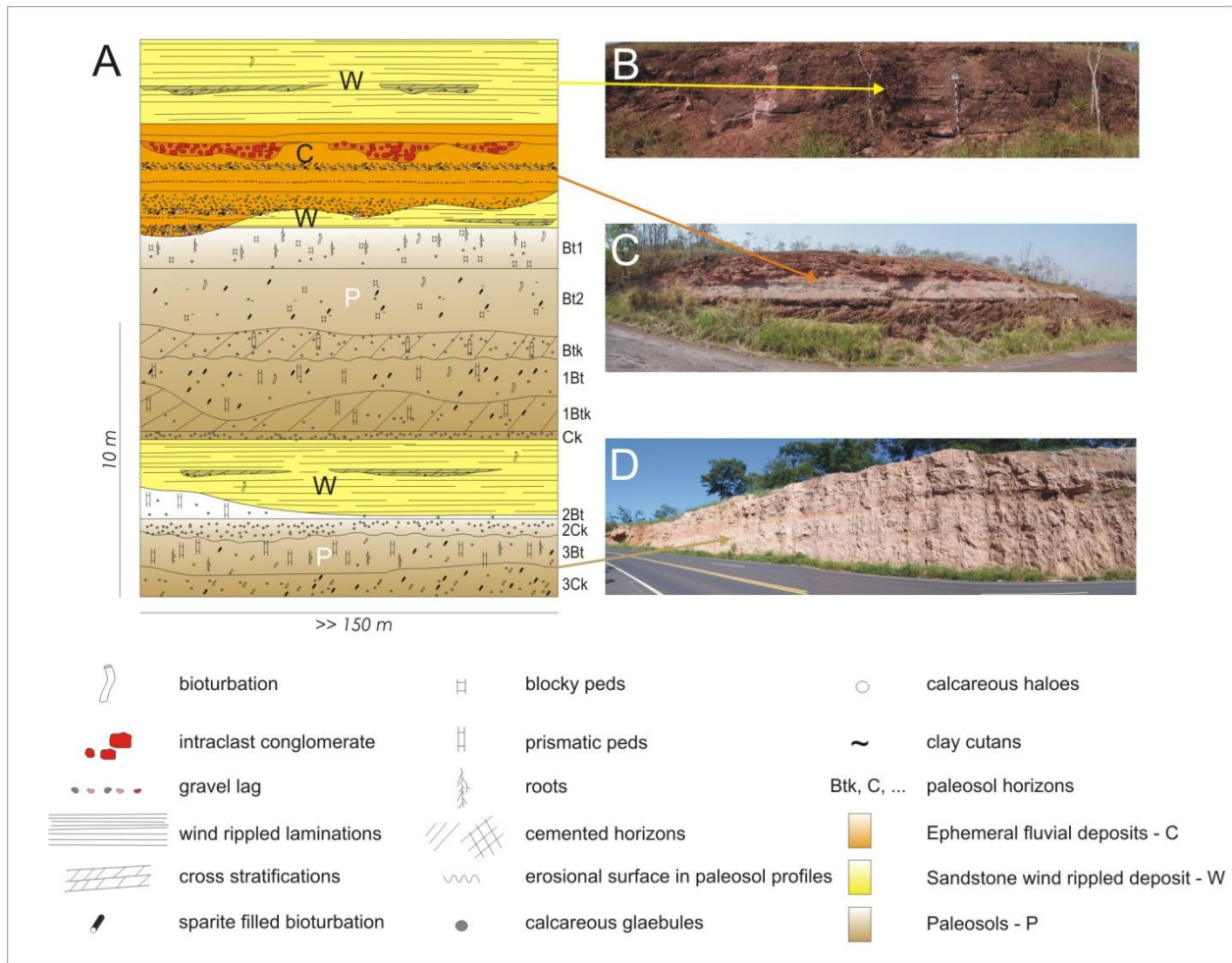


**Figure 2.** (A) Synthetic sketch of the architectural elements of the Marília Formation in the study area. Architectural elements: (B) Sandstone wind rippled deposits; (C) Ephemeral fluvial deposits; (D) Paleosols.

The Marília Formation is interpreted as an eolian sand sheet area, dominated by wind ripples deposition, pedogenesis and few ephemeral channels (Basilici et al., 2007). Previous works defined the Marília Formation as a wide alluvial fan, dominated by braided rivers and small lakes (Soares et al., 1980; Fernandes, 1998; Goldberg and Garcia, 2000).

Eolian sediments of the Marília Formation reflect periods of sedimentation followed by episodes of landscape stability and pedogenesis, with neglected sedimentation (Fig. 3). Episodes of sedimentation and soil development probably resulted respectively from cyclic decreases and increases in available moisture and vegetation covering. Alternations between drier to more humid periods result in phases with more prominent sedimentation or pedogenesis, respectively. During drier periods reduced vegetation covering and windier conditions made soil development

difficult (Fig. 3B, C), whereas in more humid phases the increased vegetation covering stabilized the landscape, increased soil moisture, reduced wind deflation and intensified soil development (Fig. 3A, D, E). Gustavson and Holliday (1999) described an analogous situation from the Late Tertiary of the Southern High Plains of Texas and New Mexico.

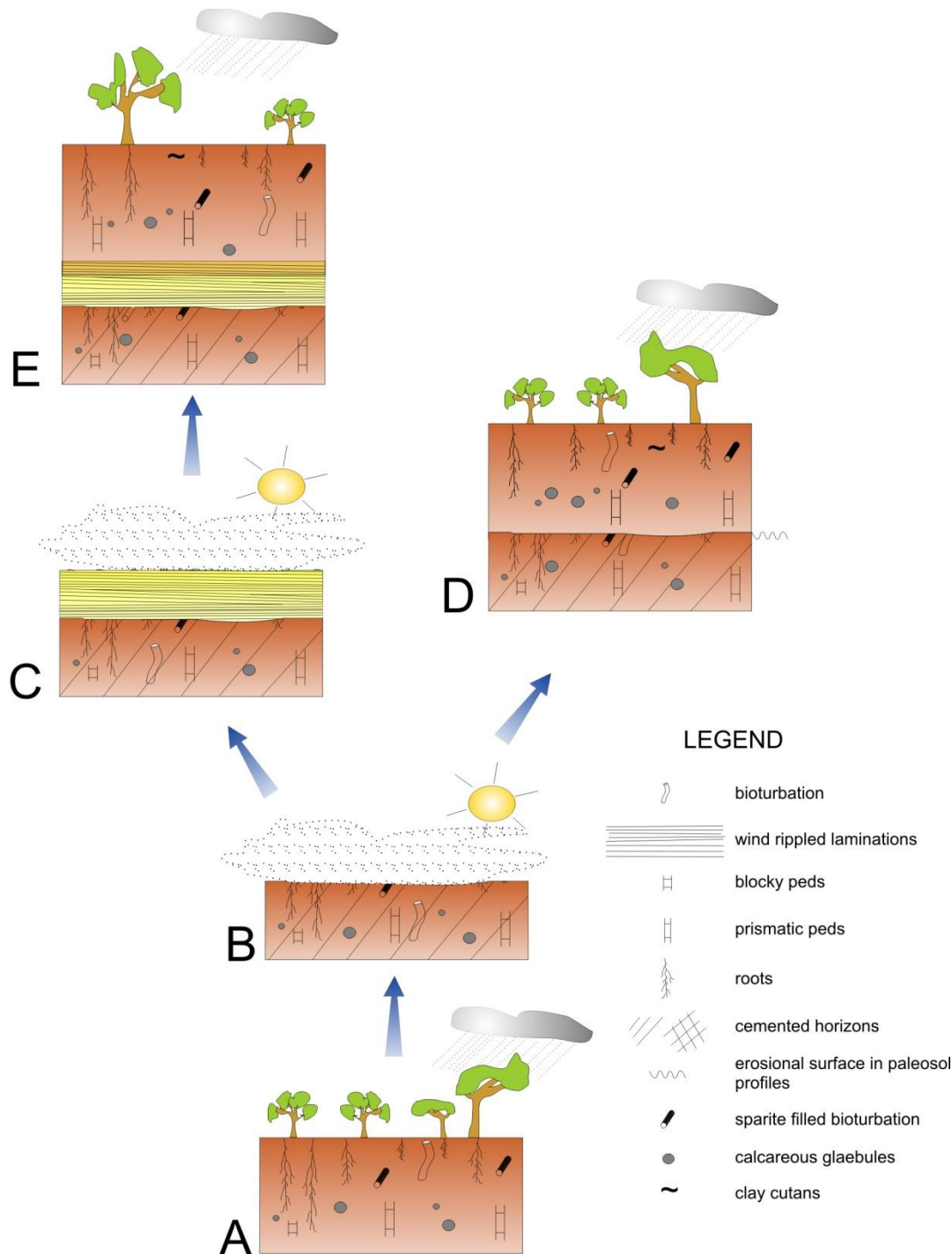


**Figure 3.** Model of the evolution of the Marília Formation, based on climatic phases from more humid to dry. (A) Paleosols (principally Aridisols) developed in more humid conditions. (B) In dry climatic phase, the disappearance of the vegetation induces the eolian erosion of the soil, the detrital production and the subsequent (C) deposition of wind rippled deposits on the eolian sand sheet. (D) The following humid climatic phase again leads to an intense pedogenesis of the recent deposits. (E) The pedogenesis can affect all the previous deposits, if this was very strong or if the thickness of the deposits was small, leaving only erosional surfaces as evidence of the dry climatic phase.

### **3. Methods**

The paleosols constitute from 30 to 85% of twenty measured and described sections. Four most representative paleosol profiles with well defined and preserved paleosol horizons were recognized and studied in detail, according to lithological, morphological and chemical properties observed in the field and/or laboratory. The first two (Serra da Flor Roxa and Serra de Lins paleosol profiles) are located near the Marília city (Fig. 1D). The other two (Monte Alto 1 and 2 paleosol profiles) are situated near the Monte Alto city (Fig. 1C).

All the paleosol profiles were described according to the field-guide of Lemos and Santos (1984) and following the description model of Retallack (1991). For each profile, four to eight representative samples of the main soil horizons were collected to confection of the thin sections and for X-ray Fluorescence Spectroscopy analyses. Thin sections were described following the terminology of Bullock et al. (1985). Chemical analyses of the major elements, obtained by X-ray fluorescence spectrometer (XRF), permitted to evaluate five molecular weathering ratios relative to calcification, hydrolysis, clay formation, salinization, and hydration of the paleosol profiles. The ratios were obtained by dividing the weight percentage of the involved oxides by its molecular weight, and than dividing the oxides as specified by the particular ratio.

Clay mineral analyses were carried out on analogous paleosol profiles of the same Marília Formation that out crop near the Cassilândia town (Fig. 1A), 400 km toward north from Monte Alto paleosol profiles. The use of these last data to interpret the paleoclimatic conditions of formation of the four described paleosols is suggested because: (1) the paleosols out cropping near Cassilândia belong to the same lithostratigraphic unit; (2) the parent material and the deposits alternated to the paleosols are analogous in all the examined successions; (3) the macroscopic features, the microfabric, and the distribution of the main chemical elements are similar in the paleosols of Cassilândia and in those described here. X-ray Powder Diffraction (XRD) analyses were carried out on whole-rock powder with a PANalytical X’Pert Pro MPD (PW3040/60) diffractometer. X-ray powder patterns were collected on randomly oriented powdered samples in  $\theta$ - $\theta$  scanning mode using Co K $\alpha$  radiation (45 kV, 40 MA,  $\lambda = 1.789 \text{ \AA}$ ), divergence slit  $1/2^\circ$ , anti-scatter slit  $1^\circ$ , Fe K $\beta$  Filter, with  $2\theta$  range of  $4$ – $75^\circ$  in steps of  $0.02^\circ$ . Their identification was further supported by SEM images.

Paleoprecipitation estimates were made based on depth of nodular calcic horizon (Bk) according to the methodology proposed for Jenny (1941) and later amplified by Retallack (1994, 2005). The depth of this horizon below the surface reflects the depth of soil wetting by available water. The following equation was used to quantify this parameter (Retallack, 1994, 2005):

$$P \text{ (precipitation; mm)} = 137.24 + 6.45D \text{ (depth; cm)} + 0.013D^2,$$

where determination coefficient  $R^2 = 0.52$  and standard error (*S.E.*) =  $\pm 147$  mm.

## 4. The paleosols of the Marília Formation

Four types of paleosol profiles are described in this section. The Serra da Flor Roxa and Monte Alto 1 profiles display a complete sequence of soil horizons: A-Bk1-Bk2-Btk-2Bk and A-Bk-Btk-C, respectively. The Serra de Lins and Monte Alto 2 paleosol profiles show an incomplete sequence of horizons: Bt-Btk-C-2Bk and Bt-Btk-Bt-C, respectively, without A horizon, probably truncated by eolian deflation.

### 4.1. Macroscopic description

The sedimentary succession that contains these four types of paleosol profiles is made up of cyclic interbedding of eolian deposits and paleosols. The deposits are formed by medium to fine-grained sandstone, laminated or with “ghosts” of planar parallel laminations, attributed to subcritically climbing wind ripples (Hunter, 1977). The deposits abruptly cover the top of the paleosol profiles, whereas the lower transition from the paleosol profiles to the deposits is gradual.

#### 4.1.1. Serra da Flor Roxa paleosol profile

The paleosol profile is 2.5 m thick; it shows a complete sequence of horizons A-Bk1-Bk2-Btk-2Bk (Fig. 4, Table 1). The last horizon 2Bk probably corresponds to an older truncated paleosol profile; thus this profile may be interpreted as pedocomplex (Catt, 1990). The texture is constituted by fine to medium sandstone with rare subangular to angular granules or small pebbles. Quartz grains and secondarily lithic fragments are the main constituents of the

sandstone. Quartz grains are usually subspherical, well rounded and coated with iron oxides, attributable to desert varnish (Oberlander, 1994). Quartzite and basalt are the most frequent conglomeratic clasts. The A horizon is thin (0-15 cm) and red (2,5YR5/6) to reddish orange (10R6/8) in color; normally it contains numerous sand-filled fine root traces with downward-tapering and bifurcations (0.5-1 cm wide and 3-5 cm long). Enrichment in organic matter was not observed. This horizon may be identified as an ochric epipedon. The boundary with adjacent B horizon is gradual to abrupt. In the B horizons, prismatic or angular to subangular blocky soil structures prevail. Prismatic structures vary from medium to coarse (2 to 10 cm) and can be broken into fine to medium (1 to 2 cm) blocky structures (Fig. 5A). These structures are hardened and cemented by calcium carbonate. They are only easy to crack in the ped contacts. The B horizon (15 to 209 cm) has been subdivided into Bk1 (15-89), Bk2 (89-104) and Btk (104-209) according to the differences in structures size, colors and calcareous glaebules content. The color varies from moderate orange pink (5YR8/4, Bk1) to light brown (5YR6/6, Bk2) to moderate orange pink (5YR8/4, Btk). Bioturbations are in general common. The ichnofossils are constituted of vertical sand filled, cylindrical shape tubes, 0.3-0.7 cm in diameter, more than 10 cm long. Frequently, micrite calcite encrusts the walls and cements the sand filling of the bioturbation tubes. Evidences of clay translocation are more evident in the Btk horizon, and include abundant clay cutans around the peds, pores filled with clays and little bridges of clay amongst the sand grains. Local macroscopic concentrations of  $\text{CaCO}_3$  (calcareous glaebules) are very common in these horizons, in particular in the Bk2 and 2Bk horizons. The glaebules vary from 0,5 to 3 cm in diameter, are roughly equidimensional, sometimes spherical or amygdaloidal in shape, with clear outer boundaries, very hardened internal structure; they are strongly reactive to HCl 10% (Fig. 5B). The transition from Btk to underlying 2Bk horizon is abrupt and irregular. The horizon color is pink (5YR7/4), and the high calcareous glaebules content (about 10-15% of the soil matrix surface) is responsible for the structureless massive soil structure. Bioturbation traces were no observed.

**Table 1.** Morphological properties of the Serra da Flor Roxa, Serra de Lins and Monte Alto 1 and Monte Alto 2 paleosol profiles.

Horizon	Depth (cm)	Munsell Color (moist)	Structure	Lower boundary	Carbonate nodules	Bioturbation features
<b>Serra da Flor Roxa</b>						
A	0-15	2,5YR5/6	massive	gradual to abrupt/irregular	few	common root traces
Bk1	15-89	5YR8/4	prismatic to angular blocky	gradual/irregular	common to frequent	common root traces
Bk2	89-104	5YR6/6	angular to subangular blocky	clear/irregular	common	rare root traces
Btk	104-209	5YR8/4	prismatic	abrupt/irregular	-	common root traces
2Bk	209-250	5YR7/4	massive	-	common	-
<b>Serra de Lins</b>						
Bt	0-22	5YR6/6	prismatic	clear/wavy	-	frequent root traces
Btk	22-33	7,5YR7/4	massive	clear/wavy	frequent	rare root traces
C	33-150	7,5YR7/4	massive	clear/wavy	rare	-
2Bk	150-200	7,5YR8/2	massive	-	frequent	-
<b>Monte Alto 1</b>						
A	0-16.5	2,5YR7/4	massive	clear/smooth	-	few root traces
Bk	16.5-32	7,5YR5/4	massive	clear/wavy	frequent	common krotovinas
Btk	32-65	7,5YR5/4	prismatic to subangular blocky	gradual/wavy	common	many krotovinas

C	65-77	7,5YR8/4	massive	-	-	-
<b>Monte Alto 2</b>						
Bt	0-20	7,5R7/4	prismatic to angular blocky	clear/smooth	-	frequent root traces
Btk	20-40	10R7/6	prismatic to angular blocky	clear/wavy	rare to common	common root traces
Bt	40-80	10R6,5/6	prismatic to angular blocky	clear to gradual/wavy	rare	rare root traces
C	80-135	2,5YR7/2	massive	-	rare	rare root traces

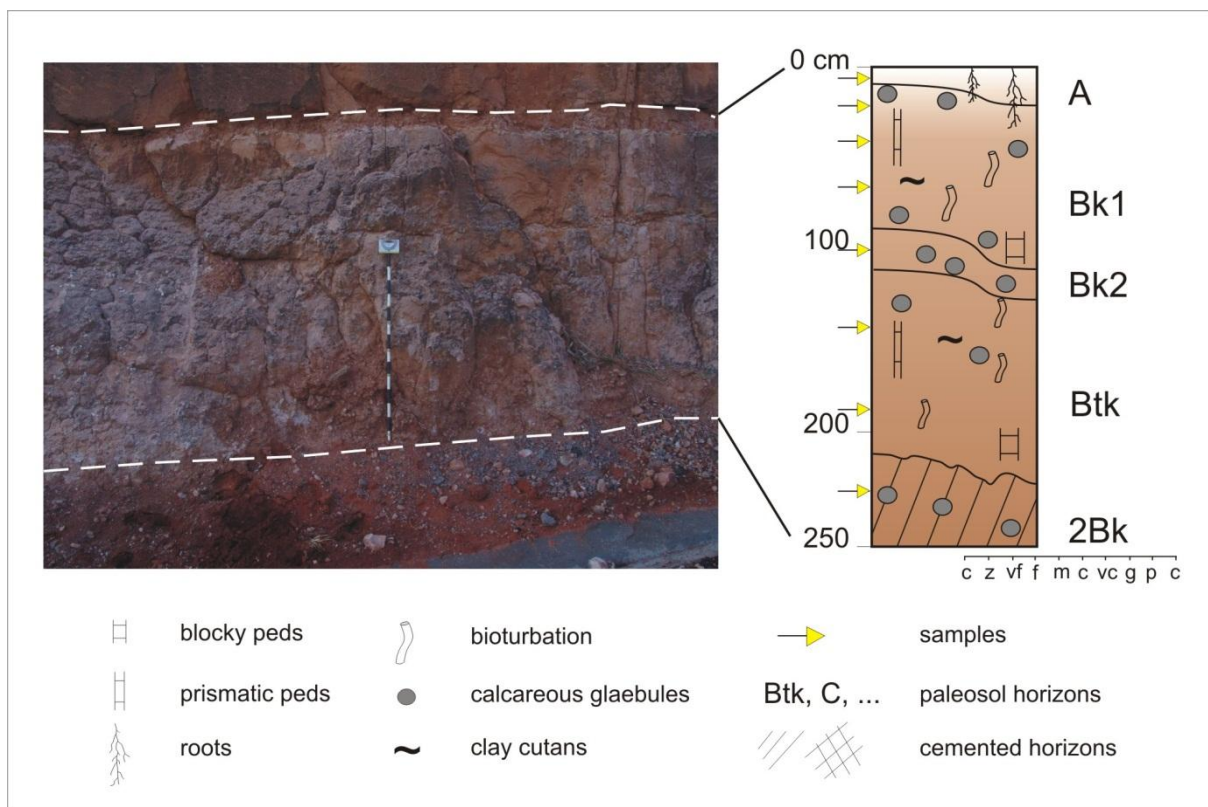


**Figure 4.** Serra da Flor Roxa paleosol profile. The location is in Figure 1A and D. For explanations see description in the text. Jacob staff is 1.5 m high.

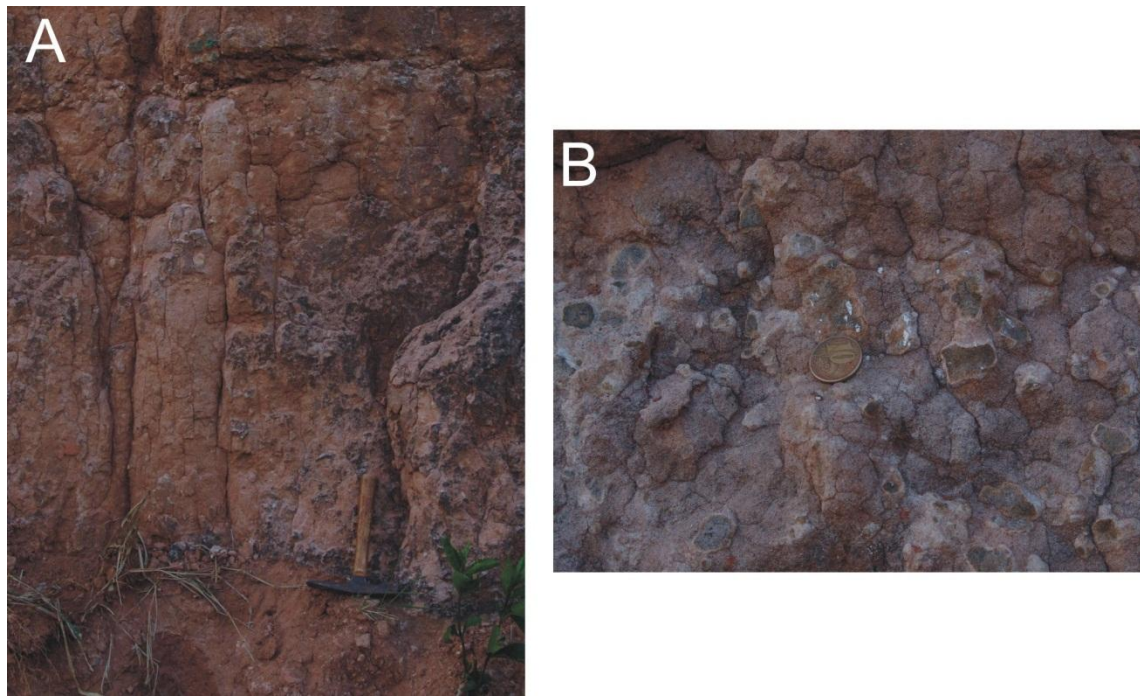


**Figure 5.** Serra da Flor Roxa paleosol profile. (A) Very coarse prismatic peds breaking into coarse angular blocky peds in the Btk horizon. Hammer is 28 cm. (B) Stage II of calcrete accumulation of Gile et al. (1966) in Bk2 horizon. Coin is 1.9 cm.

#### 4.1.2. Serra de Lins paleosol profile

This paleosol profile is 2 m thick; it is made up of a sequence of horizons Bt-Btk-C-2Bk, without A horizon preserved (Fig. 6; Table 1). The lower 2Bk horizon belongs to another paleosol profile. The texture of this paleosol profile is constituted of fine to medium well sorted sandstone, similar to that previously described for Serra da Flor Roxa paleosol profile. The Bt horizon is about 22 cm in thickness; it is light brown (5YR6/6) in color, and displays prismatic structures (Fig. 7). Many bioturbations are observed in this horizon, which consist of 2 cm wide and 10 cm long tubular shape traces (Fig. 7). In thin sections they exhibit form of vugs and channels. Calcareous glaebules do not occur in this horizon. Clay cutans are diffused around the prismatic peds, pointing out mechanical translocation of clay. This argillic horizon has been identified on the basis of field properties, such as the presence of clay coatings, pore infillings of clays, and bridging of sand grains by clay particles, and by the identification of microscopic illuvial textures (argillans). Btk horizon is reddish yellow (7,5YR7/4), 11 cm thick (22 to 33 cm). It is easily identified in the field due to the carbonate concentration, which forms a cemented

layer of coalesced nodules. The nodules and the matrix, which is strongly to moderately cemented, enable to classify this horizon as stage II of calcic soil morphology classification (Gile et al., 1966). Rare bioturbation traces, which can be related to root traces, consist of tubular forms, sand-filled, sometimes moderately encrusted by carbonate (Fig. 7). The boundary with the underlying C horizon is clear and wavy. This C horizon 118 cm thick (33 to 150 cm), reddish yellow (7,5YR7/4) in color. It is constituted of structureless fine sandstone (massive cemented structure). The boundary with the underlying horizon is abrupt and wavy, probably corresponding to an erosional surface. The 2Bk horizon is 50 cm thick, massive, and rich in calcareous glaebules that occupy up to 30% of the soil matrix. The color varies from pinkish white (7,5YR8/2) to dark grey (7,5YR4/1) when nodules are frequent. At times, the nodules display light red (10R6/8) coatings. Bioturbation traces have not been observed.

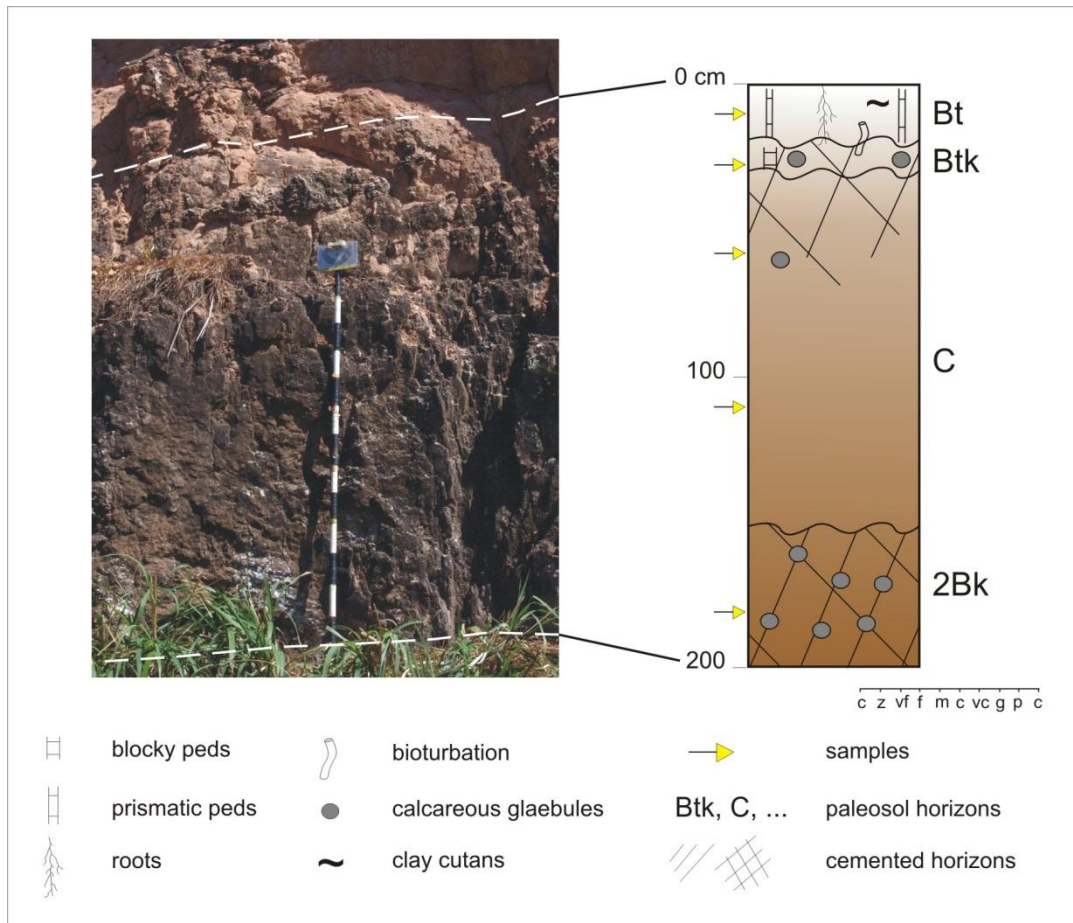


**Figure 6.** Serra de Lins paleosol profile. This profile lacks A horizon, probably due to eolian deflation. The location is in Figure 1A and D. For explanations see description in the text. Hammer is 28 cm.

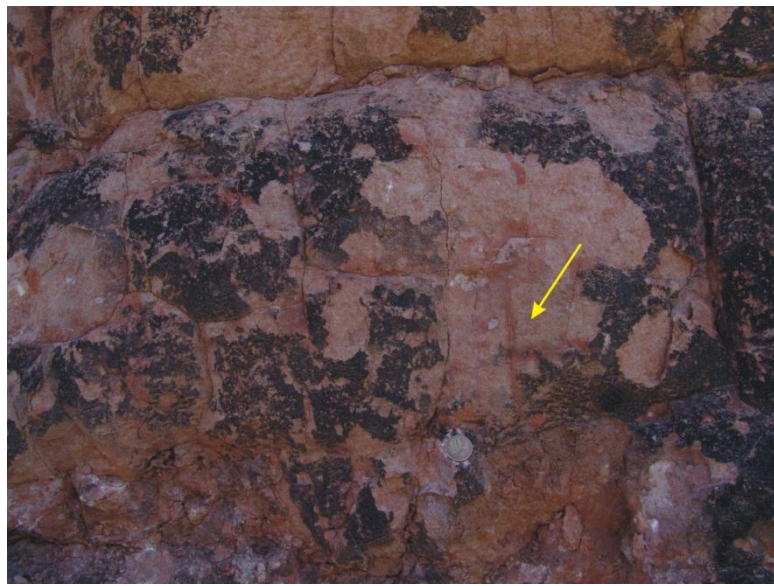


**Figure 7.** Serra de Lins paleosol profile. Prismatic structure and root traces (arrow). Coin is 1.9 cm.

#### 4.1.3. Monte Alto 1 paleosol profile

The paleosol profile is 0.77 m thick and is organized in a complete sequence of horizons: A-Bk-Btk-C (Fig. 8, Table 1). The texture is constituted of fine to medium well sorted sandstone. The A horizon (0-16.5 cm) is pale yellow (2,5YR7/4) in color and exhibits few bioturbation traces, related to calcite-filled root moulds. It may be identified as an ochric epipedon.

The transition with the underlying Bk horizon is clear and wavy, and marked by the appearance of carbonate nodules and krotovinas. Bk displays an intense carbonate nodulation, almost 50% of the soil matrix, which masks the original soil structure and appears massive. Soil matrix is moderate yellowish brown (7,5YR5/4) in color, and the nodules are sometimes white (7,5YR8/1) and grey (10YR5/1). The transition to the Btk horizon is gradual and wavy, and outlined by a very coarse primary prismatic structure (>10 cm) and by a secondary very coarse (>5 cm) subangular blocky substructure. Btk horizon color is moderate yellowish brown (7,5YR5/4), but also occurring disperse mottles, white (7,5YR8/1) in color, associated with incipient nodules formation (Retallack, 2001). Krotovinas (1 cm wide, 3 cm long) filled with fine sandstone, coming from the upper Bk material horizon, are frequent. The boundary to the lower

pink (7,5YR8/4) cemented C horizon is abrupt. Nodules and bioturbation traces disappear in this horizon.

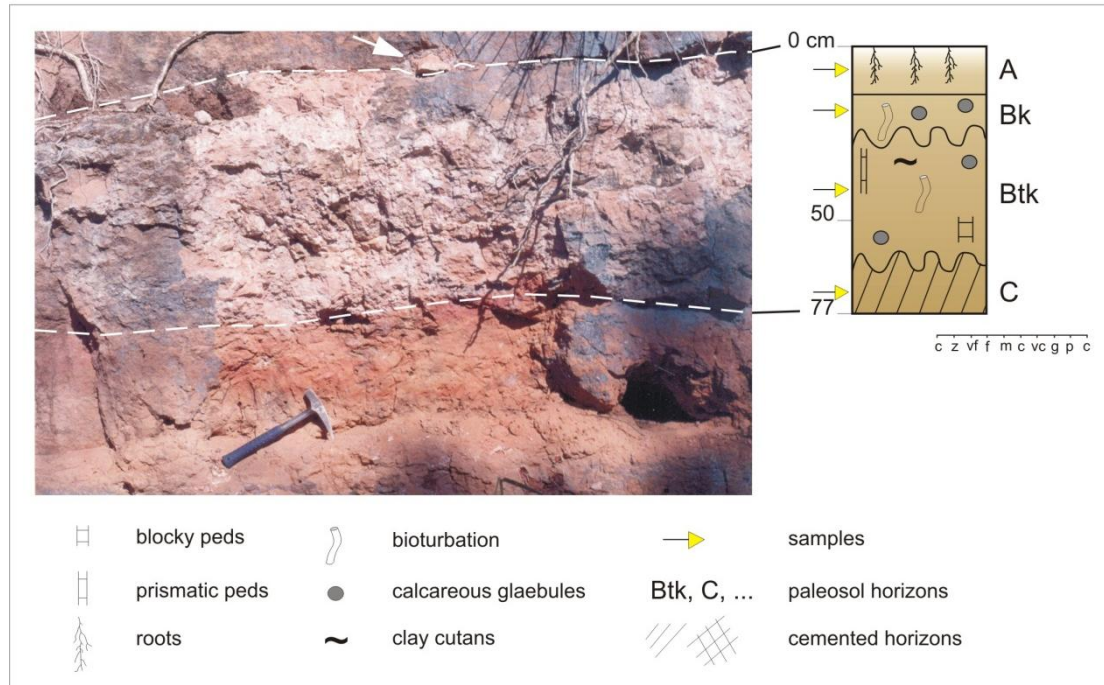


**Figure 8.** Monte Alto paleosol profile that shows a complete sequence of soil horizons: A-Bk-Btk-C. The top of this paleosol has an abrupt transition to eolian laminated sandstone, marked by centimeter intraformational mud clasts (white arrow). Hammer is 28 cm. For explanations see the text.

#### 4.1.4. Monte Alto 2 paleosol profile

This paleosol has a thickness of 135 cm. The A horizon is not preserved and the paleosol profile is constituted by a horizon sequence subdivided in Bt-Btk-Bt-C (Fig. 9, Table 1). The top of the profile is truncated by an erosive concave surface that is marked by intraformational carbonate nodules. The texture is constituted of fine to medium well sorted sandstone. The Bt horizon (0-20 cm) is light reddish brown (7,5R7/4) in color, and shows prominent very coarse (10-20 cm) prismatic and coarse (>5 cm) angular blocky structures (Fig. 9). Clay coatings are abundant; they commonly occur as incipient clay films that cover ped faces and joint sand grains. Carbonate nodules are absent and bioturbation traces (3 mm to 1 cm in diameter) are principally subspherical shape-tubes (<5 cm long) filled by sand and covered with clay films. The boundary to the lower Btk horizon is clear and smooth. Prismatic and blocky soil structures are continuous

with the underlying Btk horizon. Btk horizon (20-40 cm) displays some carbonate filaments and soft nodules (2 mm across). The color is light red (10R7/6) and bioturbation traces exhibit the same forms of the Bt horizon. The transition to underlying Bt horizon (40-80 cm) is clear and wavy. Prismatic and angular blocky pedes have greater dimensions than the overlying horizon (10-30 cm). Rare carbonate nodules occur especially in the upper portion of horizon, at the transition with Btk. The color is red (10R6,5/6) and the bioturbation traces are constituted of rare root traces with cylindrical (1-3 mm wide, 3 cm long), sand-filled tubes, encrusted by calcium carbonate. The transition to underlying C horizon (80-135 cm) is clear to gradual and wavy. This is a massive carbonate cemented horizon, reddish gray (2,5YR7/2) in color, and exhibits bioturbation traces concentrated in the upper transition to Bt horizon.

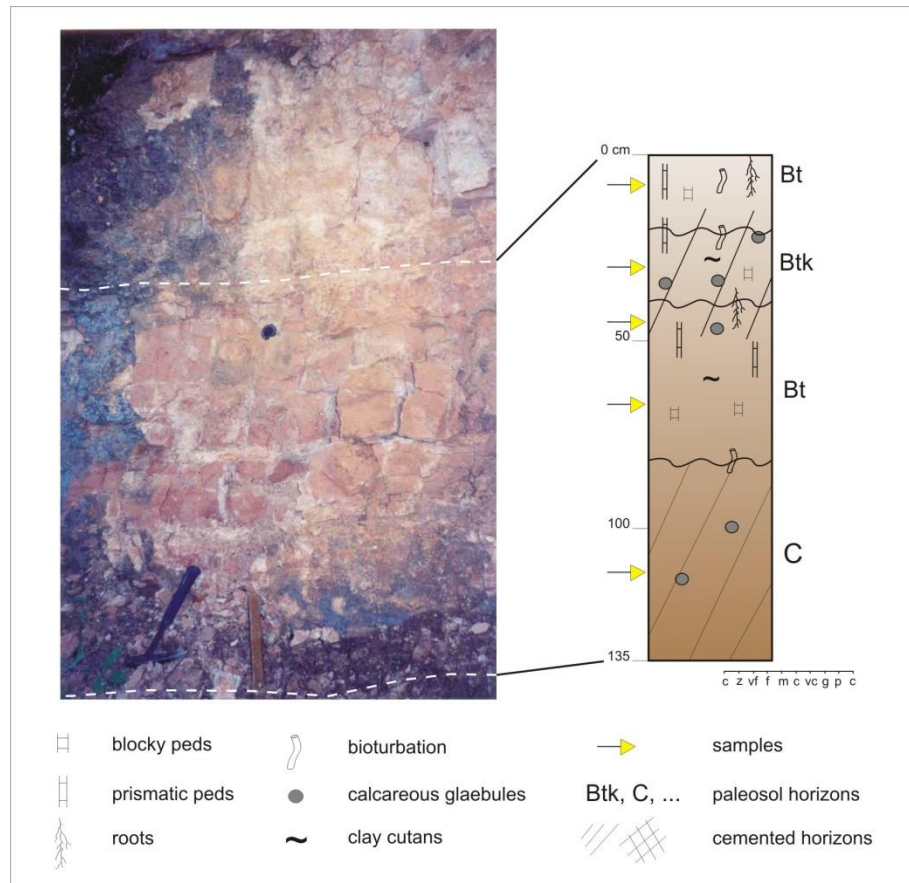


**Figure 9.** Monte Alto 2 paleosol profile. Hammer is 28 cm. A detailed description is in the text.

## 4.2. Microfabric characterization

The microfabric characterization is described for all the paleosol profiles, since they show analogous microscopic properties. The set of pedogenic calcrete microfeatures related herein are in accordance with K-fabric (Gile et al., 1965) or Alpha fabric (Wright, 1990).

The silt- and sand-size component (skeleton grains) of the horizons represents 65-80% of the thin sections area. Sand-size portion is constituted of very fine and fine-grained sand (>80%) and medium-grained sand (5-15%) with rounded to subrounded grains. Petrographic analyses show the following distribution: about 90% of monocrystalline quartz, 5% of feldspar, mica, zircon, clinopyroxene, olivine, and opaque minerals and 5% of lithic fragments of quartzite, basalt, and mudstone.

Quartz grains generally display smooth superficial texture, but many quartz grains may exhibit calcite dissolution features, responsible for external serrate morphologies. Some feldspar grains show calcite replacement features along the cleavage planes.

The plasmic fabric is constituted of clay and calcite microcrystals (<2  $\mu\text{m}$ ) and calcite macrocrystals (>5  $\mu\text{m}$ ). The plasmic portions, which are formed by anisotropic microcrystalline and sparry calcite crystals, are common in Bk horizons and are characterized by crystallitic birrefringent fabric (Fig. 10A).

Apedal pellicular and bridged grain structures, besides pedal subangular blocky structures are the most frequent identified microstructures. The apedal microstructures are formed by sand-grains coated or joined by fine iron and clay materials (Fig. 10B).

Clay coatings (argillans) correspond in the Bt and Btk horizons to illuvial features. The coatings occur principally on grain surface and in the walls of pores. The grain coating forms a coat of fine iron and clay around the grain surface, and exhibits variations from typic, capping, link capping and pendent. Coatings associated with the walls of pores were classified in typic and crescent (Bullock et al., 1985). The last is only characteristic of larger pores (0.5-5 mm) that formed specific places for water accumulation (Fig. 10C, D). Internally, the coatings may show microfissures and post-depositional iron segregation. In some cases, the Btk paleosol-coatings display internal calcite replacement (Fig. 10C, D). Hypocoatings are common calcite incipient coatings that occur in the groundmass and around external surface of grains. They are apparent in A horizons associated with biogenic features of the rhizosphere (Kraimer et al., 2005).

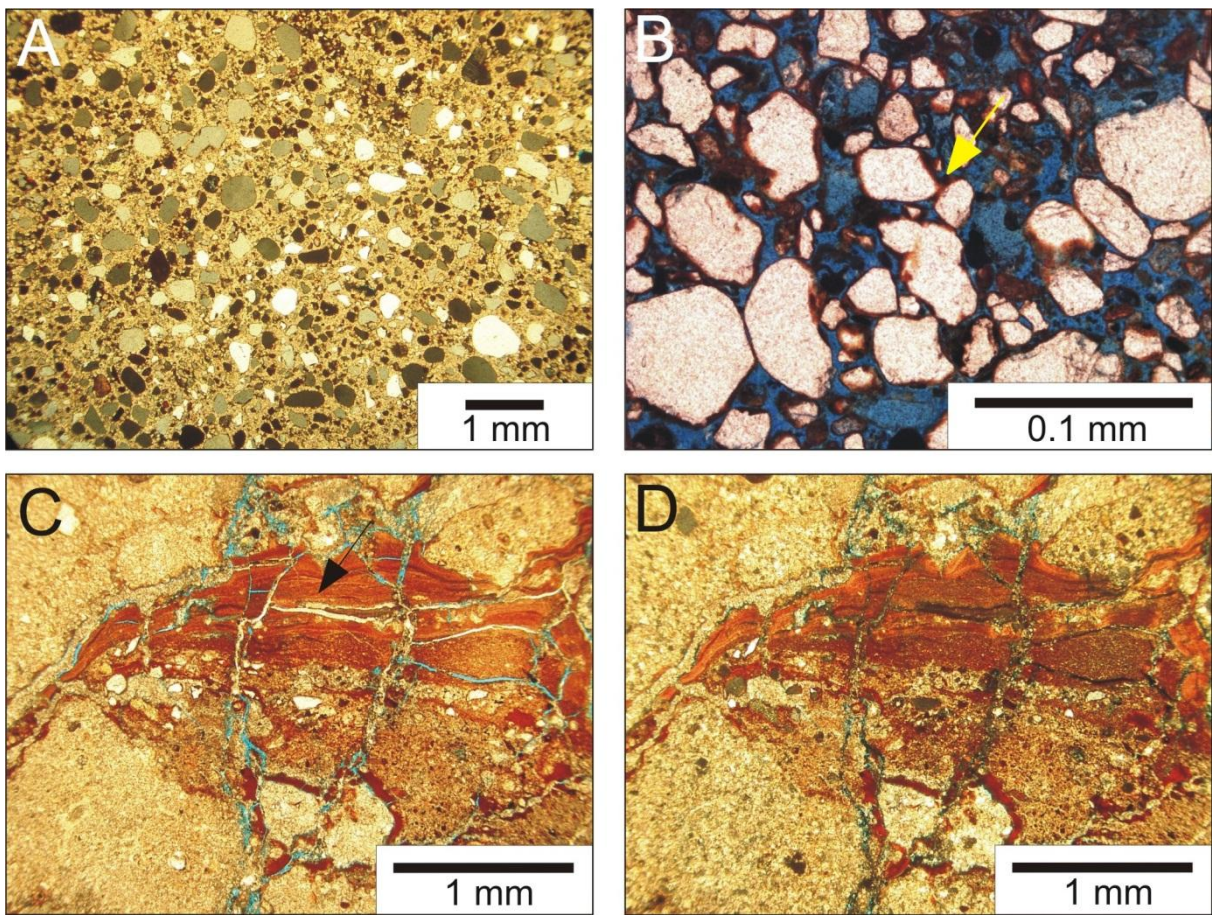


**Figure 10.** Photomicrographs of the paleosols. (A) Crystallitic birrefringent fabric in Bk horizon. (B) Pellicular and bridged grain structures. White arrow indicates in detail the apedal bridged grain microstructure. (C-D) Illuvial clay coatings associated with pore-walls, exhibiting post-depositional iron segregation and internal microfissures. Black arrow indicates a microfissure filled with microcrystalline calcite, which records the replacement processes in Btk horizon. (Photomicrographs A and D cross-polarized light. B and C, plane light).

Clay coatings (argillans) in Btk horizons are commonly observed alternating with calcite coatings (calcans) on the pore walls (Fig. 11).

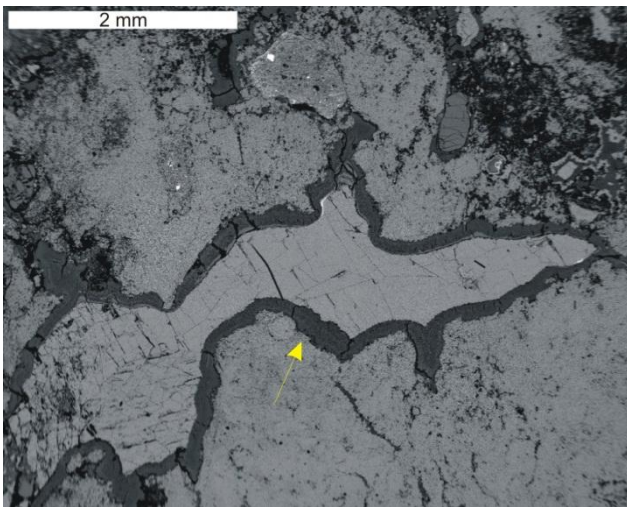


**Figure 11.** Scanning electron microscope (SEM) photomicrograph of a thin section from Btk Aridisols horizon. The internal walls of the vugs are coated by clay (arrow), whereas the internal portion is filled by sparry calcite.

Pedotubules are described according to the external shape and the internal pattern of infilling. These microfeatures have circular or elliptical shape with a diameter or b-axis of 0.5-4 mm. According to the internal pattern of infilling, pedotubules were subdivided in two classes: dense incomplete and loose discontinuous. Pedotubules are the unique evidence of biological activity in thin sections. Elliptical and circular pedotubules (granotubules) exhibit loose discontinuous sand-grained infill. They are associated to root activity that opened soil-cavities, subsequently filled by material from upper horizons (Fig. 12A, B). Another type of pedotubules (isotubules), which have an elliptical shape and dense incomplete infillings, were attributed to soil infauna organisms.

The nodules of calcite are distinguished as follow: typic, the most frequent (90%), halos, septaric and geodic, less frequent, (9 and 1%, respectively), according to their internal morphology. Fragmented coatings of ancient illuvial clay may form papules in the Bt horizons, but their distribution is not more than 1% of the thin section area. The nodules (0.5-4 mm across) are mainly composed of microcrystalline calcite and exhibit external subcircular or elliptical shape (Fig. 12C). In the Bk horizons, calcite nodules may reach until of 20% of the thin section area.

Crystalline pedofeatures are frequent in the Bk horizons. They consist of calcite inequigranular mosaic-crystals, 0.001-1.2 cm across, formed within the largest pores. Their distribution may reach 10% of the thin section area.

The Bk horizons display also floating framework grains in the microcrystalline calcite matrix (Fig. 12D). The introduction of calcite in the Bk soil-horizon may substitute siliciclastic material and, as a consequence of the calcite expansive growth, these horizons are characterized by calcite crystals with different sizes, forms and orientations (Tandon and Friend, 1989).

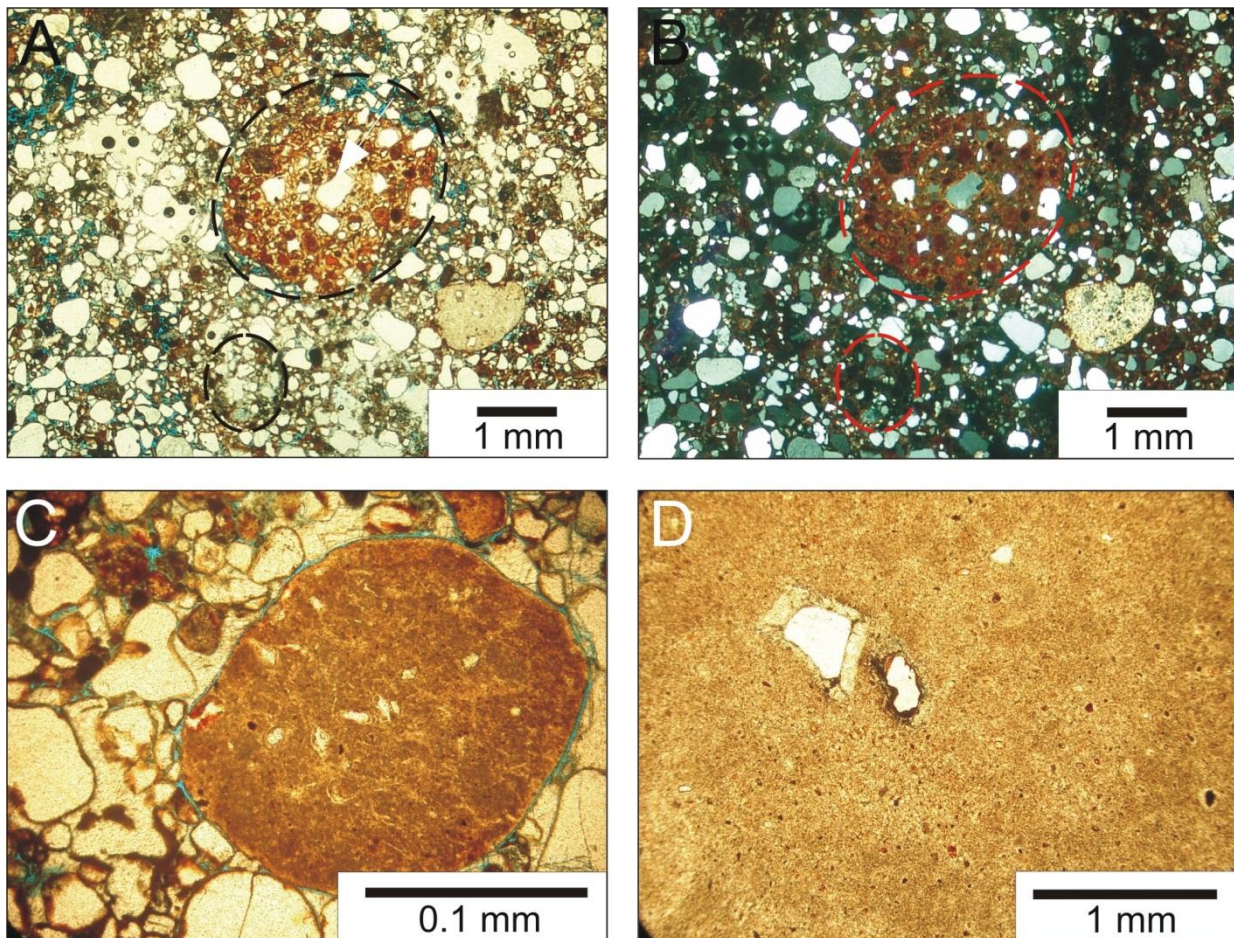


**Figure 12.** (A-B) Elliptical granotubule with loose discontinuous infilling (1.3 mm in diameter) and elliptical isotubule with dense incomplete infilling (3.2 mm in diameter) in Bt horizon. (C) Calcite nodule in Bk horizon. (D) Floating quartz framework grains in calcite matrix in Bk horizon. (Photomicrograph B, cross-polarized light. A, C and D, plane light).

#### 4.3. Geochemical composition

Chemical analyses, which are expressed as weight percent of the major elements, were carried out for the four described paleosol profiles. A total of 21 samples (four to seven samples per profile) were collected. The samples were collected based on the horizons described in the

field. The major elements values, obtained in weight percent of the major oxides, are tabulated in Table 2.

**Table 2.** Weight percentage of the major oxides within the Serra da Flor Roxa, Serra de Lins and Monte Alto 1 and Monte Alto 2 paleosol profiles.

Horizon	Depth (cm)	SiO <sub>2</sub>	TiO <sub>2</sub>	Al <sub>2</sub> O <sub>3</sub>	Fe <sub>2</sub> O <sub>3</sub>	MnO	MgO	CaO	Na <sub>2</sub> O	K <sub>2</sub> O	P <sub>2</sub> O <sub>5</sub>	LOI
<b>Serra da Flor Roxa</b>												
A	5	82.08	0.661	6.83	2.77	0.026	1.86	0.52	0.18	2.05	0.033	2.83
Bk1	17	59.15	0.32	3.89	1.38	0.089	1.62	16.9	0.09	1.09	0.022	15.89
Bk1	30	84.30	0.471	5.27	1.83	0.020	1.51	0.91	0.18	1.79	0.024	3.26
Bk1	60	87.29	0.416	4.89	1.54	0.019	1.54	0.30	0.17	1.68	0.020	2.18
Bk2	100	57.17	0.330	3.76	1.32	0.091	1.65	17.62	0.08	1.08	0.023	16.15
Btk	140	69.35	0.339	4.18	1.39	0.033	1.43	11.16	0.13	1.31	0.021	10.55
Btk	190	86.84	0.401	4.98	1.59	0.016	1.45	0.68	0.13	1.65	0.020	2.45
2Bk	225	49.25	0.260	2.82	1.05	0.125	1.33	23.41	0.05	0.93	0.025	20.10
<b>Serra de Lins</b>												
Bk	11	84.18	0.490	5.96	1.91	0.031	1.42	1.11	0.15	1.87	0.022	2.91
Btk	28	62.26	0.484	5.69	2.37	0.059	1.87	12.52	0.11	1.59	0.028	12.30
C	50	85.23	0.428	5.49	1.63	0.023	1.38	0.88	0.17	1.80	0.019	2.55
C	110	80.76	0.513	5.54	1.86	0.024	1.63	2.99	0.18	1.87	0.028	4.41
2Bk	180	71.21	0.246	3.27	0.97	0.030	1.00	11.55	0.12	1.41	0.022	10.32
<b>Monte Alto 1</b>												
A	7.5	84.08	0.53	4.79	1.94	0.05	1.17	1.15	0.58	2.35	0.03	3.31
Bk	20	68.46	0.75	4.92	3.07	0.07	2.63	7.27	0.40	2.32	0.07	10.03
Btk	40	56.85	0.87	6.41	3.81	0.08	2.38	12.98	0.28	2.32	0.09	13.94
C	65	79.10	0.72	6.81	3.03	0.05	1.97	0.63	0.63	2.72	0.05	4.30
<b>Monte Alto 2</b>												
Bt	10	71.17	0.67	5.17	2.14	0.05	1.74	7.37	0.37	2.13	0.02	9.16
Btk	30	43.59	0.42	4.05	1.55	0.05	2.47	24.04	0.11	1.06	0.02	22.65
Bt	46	77.68	0.67	6.54	2.46	0.05	3.19	3.44	0.39	1.97	0.03	3.57
Bt	70	69.97	0.66	6.22	2.38	0.04	2.09	6.83	0.39	1.98	0.04	9.37
C	110	78.15	0.75	5.77	2.70	0.05	2.34	1.79	0.46	2.24	0.02	5.74

$\text{SiO}_2$  is the most abundant oxide (Tab. 2). It has a constant distribution in all the four profiles ranging from 70 to 85%; it decreases to about 57 and 43% only when  $\text{CaO}$  increases.

The more relevant variations of sesquioxides are related to  $\text{CaO}$  variations (Tab. 2): they decrease when  $\text{CaO}$  increases. In general, iron and aluminum oxides increase toward the top of the Serra de Lins and Serra da Flor Roxa paleosols, whereas they decrease toward the top of the Monte Alto 1 and Monte Alto 2 paleosols.

The variation of  $\text{CaO}$  marks the concentration in carbonate nodules and the calcic horizons (Tab. 2). Minimum values of  $\text{CaO}$  were found where the A horizon is preserved at the top of the paleosols as in Monte Alto 1 and Serra da Flor Roxa profiles, underlining a strong lixiviation of this oxide.

$\text{MgO}$  is present in low amounts, showing small increases in correspondence of the Bk horizons attesting probable presence of dolomite.

$\text{K}_2\text{O}$  and  $\text{Na}_2\text{O}$  are distributed in minimal quantity. Although the distribution of these alkalis depends on the  $\text{CaO}$  concentration, a small increase toward the top of Serra da Flor Roxa and Serra de Lins paleosols is observable. On the contrary, the Monte Alto 1 and 2 paleosol profiles show a small decrease toward the top.

Molecular weight ratios provide an index for weathering in paleosols. Thus chemical data were used to estimate five molecular weathering ratios: calcification, hydrolysis, clay formation, salinization, and hydration of the paleosol profiles (Fig. 13). The guideline described in Retallack (1997, 2001) was followed in their calculation and interpretation.

The alkaline earths/alumina ratio  $(\text{CaO}+\text{MgO})/\text{Al}_2\text{O}_3$  was used as indicative of calcification of the horizons, because presence of dolomite was observed in X-ray diffraction analyses (Fig. 14A). In wetter soil,  $\text{Ca}^{2+}$  and  $\text{Mg}^{2+}$  can be readily flushed down. In drier setting,  $\text{Ca}^{2+}$  and  $\text{Mg}^{2+}$  is less readily leached and accumulates in Bk horizons giving higher  $\text{CaO}+\text{MgO}$  to  $\text{Al}_2\text{O}_3$  ratios (Machette, 1985; Retallack, 1997, 2001).

The base/alumina ratio  $(\text{CaO}+\text{MgO}+\text{K}_2\text{O}+\text{Na}_2\text{O})/\text{Al}_2\text{O}_3$  was used to define the former hydrolysis conditions of the paleosol formation. The obtained values (1.19 to 16.67) are always greater than 1, reaching very high values in correspondence of the calcic horizons. Base/alumina ratios reflect an alkaline developed soil. The abundance of carbonate and the absence of siderite

and calcium sulphate allow defining the pH conditions of the soil formation as moderately alkaline soil (pH 8-8.5) (Retallack, 2001).

Clay formation is indicated by the ratio alumina to silica ( $\text{Al}_2\text{O}_3/\text{SiO}_2$ ). This molecular weathering ratio shows very low values (0.027 to 0.066), when clayey soils usually have values higher than 0.3. The higher values in the study paleosol profiles were used to recognize the concentration of clays in Bt horizons.

Molecular weathering ratios of soda to potash ( $\text{Na}_2\text{O}/\text{K}_2\text{O}$ ) are relatively useful to define the degree of soil salinization. We used this ratio based on that sodium is generally more soluble and less altered during the diagenesis than the potassium. The obtained values are less than the unit and relatively constant (from 0.1 to 0.3). Such values and the absence of evaporite minerals or their pseudomorphs seem indicative of the absence of these processes during the soil formation.

The molecular weathering ratio expressed as ratio of silica to sesquioxides ( $\text{SiO}_2/\text{Al}_2\text{O}_3+\text{Fe}_2\text{O}_3$ ) may give a crude guide to former hydration of minerals in paleosols (Retallack, 2001). In the examined samples the value is included between 5.4 and 15.5, pointing out original soil conditions characterized by high quantity of silica with few hydrated minerals. Vertical trends of this ratio are not observed. The ratio decreases only in correspondence of the horizons with major clay content (Bt).

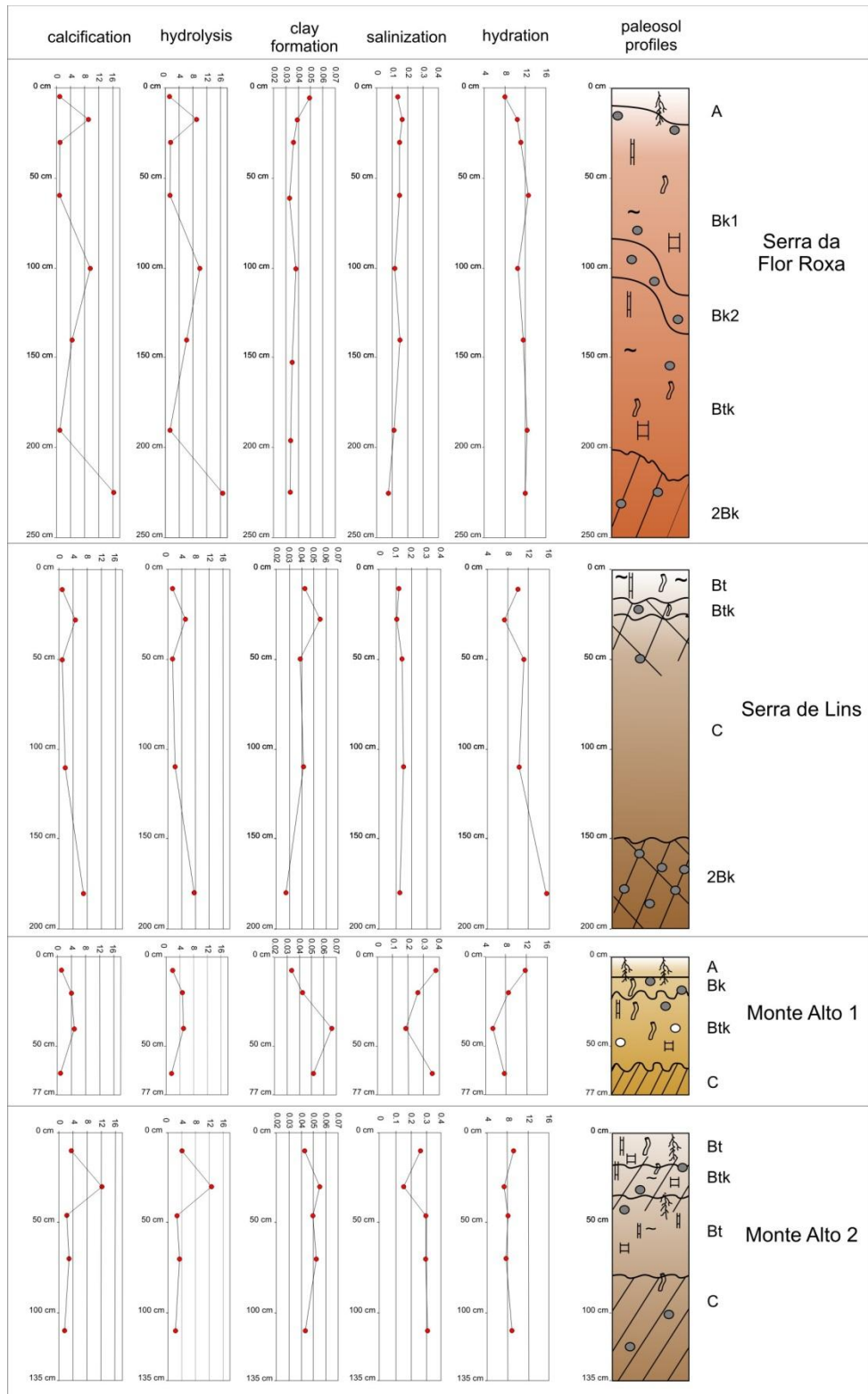


**Figure 13.** Molecular weathering ratios of the four study paleosol profiles. Data in weight percentage of the major oxides are in Table 1. Molecular weathering ratio formulae used:  $(\text{CaO} + \text{MgO})/\text{Al}_2\text{O}_3$  for calcification;  $(\text{CaO} + \text{MgO} + \text{K}_2\text{O} + \text{Na}_2\text{O})/\text{Al}_2\text{O}_3$  for hydrolysis;  $\text{Al}_2\text{O}_3/\text{SiO}_2$  for clay formation;  $\text{Na}_2/\text{K}_2\text{O}$  for salinization, and  $\text{SiO}_2/(\text{Al}_2\text{O}_3 + \text{Fe}_2\text{O}_3)$  for hydration.

#### **4.4. Clay mineralogy and stable isotopes discussion**

Clay mineral analyses were carried out in 21 samples of paleosol profiles near the town of Cassilândia (state of Mato Grosso do Sul, Fig. 1A).

The clay mineralogy is mainly constituted of palygorskite, smectite, and probably sepiolite (Fig. 14A, B). These analyses confirm the findings of previous authors that described palygorskite and smectite as being frequently occurring clay minerals of the Marília Formation (Suguio and Barcelos, 1983).

Few studies were executed on stable isotopes of C and O of the carbonates of the Bauru Group. Values in  $\delta^{18}\text{O}$  lighter than  $-5.5\text{\textperthousand}$  obtained from shell of ostracods point out fresh water lacustrine life conditions (Castro et al., 1999). Suguio (1973) examined the  $\delta^{18}\text{O}$  and  $\delta^{13}\text{C}$  of 39 of carbonates sampled in calcic horizons of paleosols of the Marília Formation from various localities in Minas Gerais, Goiás, and São Paulo states.  $\delta^{13}\text{C}$  values are between  $-7$  and  $-10\text{\textperthousand}$ , and in  $\delta^{18}\text{O}$  between  $-5$  and  $-7\text{\textperthousand}$ . Suguio (1973) attributed the  $\delta^{13}\text{C}$  values lighter than  $-8\text{\textperthousand}$  to diagenetic effects. Moreover, the author compared the  $\delta^{18}\text{O}$  of Marília calcic horizons with calcrete of Moçamedes Desert in Angola, which has values around  $-2\text{\textperthousand}$ . He interpreted this discordance as less arid conditions of formation of the calcretes in Marília Formation.

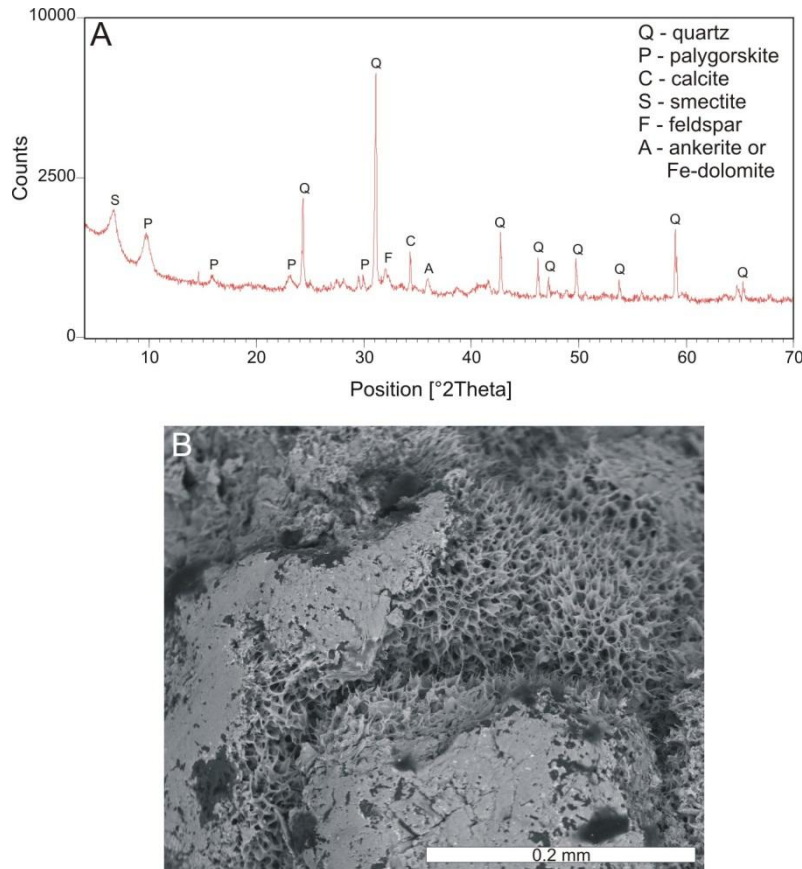


**Figure 14.** X-ray diffraction analysis from Aridisol paleosol profile of the Marília Formation that crops out near Cassilândia (Fig. 1A). This paleosol profile shows analogous micro- and macrofeatures as chemical composition of the studied Aridisols. (A) X-ray diffratograms of Btk Aridisol horizon. Smectite and palygorskite are the dominant clay minerals. (B) Scanning electron microscope (SEM) photomicrograph of smectite displaying a honeycomb structure.

#### 4.5. Paleosol interpretation

The high concentration of calcium carbonate in B horizons, which allows the identification of calcic (Bk), the occurrence of an ochric epipedon, and the occurrence of argillic B horizons (Bt) are the keys to interpreting these paleosol profiles as Aridisols (Soil Survey Staff, 2006). The formation and preservation of organic matter in A horizons could have been inhibited because of the arid paleoclimatic conditions and the deficit in soil moisture regime. The Aridisols are soils of arid or semi-arid climate, where the limited availability of soil moisture does not sustain a wide and large plant community.

The diagnostic horizons link these Aridisols with two specific suborders: i) Calcic suborder, which is characterized for calcic horizons (Bk and Ck) and, ii) Argid suborder, which is

identified by the presence of an argillic horizon (Bt and Btk). However, in considering the mix of calcic and argillic horizons in the four analyzed profiles, the most appropriate soil classification fall in Calcicardid great group, which are typically Arid soil profiles, that have been recharged with calcium carbonate from atmospheric influx (Soil Survey Staff, 1999). Calcic suborder has been identified for Monte Alto 1, paleosol profile. Serra de Lins, Monte Alto 2, and Serra da Flor Roxa paleosol profiles present an argillic horizon that typically characterizes Arid suborder. However, all these Arid suborder paleosol profiles exhibit arid calcic horizons (Bk and Ck). Thus, the genesis of this particular humid argillic soil horizon may be related to: i) the influence of occasional, exceptionally large precipitation events; ii) local variation in soil-forming processes such as more humid internal soil drainage, linked to gently inclined soil-morphology. Eghbal and Southard (1993) linked the development of argillic horizons in Aridisols to more humid climatic phases, even on flat and long stable surfaces.

The Btk horizon represents an intermediate position between more humid Bt and more arid Bk horizons. The presence of carbonates in argillic horizon is a common situation in desertic soils (Khormali et al., 2003). In some cases they may dominate the soil matrix, but more commonly they occur as nodules which have partially displaced the previously deposited clays. The accumulation of carbonate in argillic horizons is widely interpreted as being indicative of significant climate change from more humid to more arid conditions, with an accompanying reduction in depth of leaching (Nettleton and Peterson, 1983; Schaetzl and Anderson, 2005). Decalcification and clay translocation probably occur during the more humid climate because clay flocculates in the presence of carbonates and is followed by recalcification during subsequent drier periods.

Profiles with carbonate accumulations that have a diagenetic origin were excluded in our analysis. Instead, in all cases the analyzed paleosol profiles show typical pedogenetic features that enable us to classify them as pedogenic calcretes: ordered horizons in the paleosol profiles, thin calcrete profile thickness, prismatic, blocky and nodular soil structures, abundant root traces, absence of disseminated Fe-reduction features, such as pervasive mottling (Pimentel et al., 1996; Alonso-Zarza, 2003). Moreover, the microstructures related to Alpha calcretes (Wright, 1990) such as crystallarias, nodules, carbonate infillings, floating detrital grains, crystallitic fabric, hypocoatings, sparitic fringes, displacive carbonate growth features, and other macro and

microstructures linked to biogenic Beta calcretes, such as root traces and faunal burrows, are observed, thus rejecting the diagenetic origin of these calcrete horizons.

The macroscopic morphology of the calcic horizons allows to classify the paleosol profiles in a different degree of evolution according to the stages of Gile et al. (1966). Serra da Flor Roxa paleosol profiles show Bk horizons related to stage III (almost 50% of  $\text{CaCO}_3$  content) (Fig. 15A). Serra de Lins, Monte Alto 1, and Monte Alto 2 paleosol profiles display stage II and I in Bk and Btk horizons (almost 20% and <4% of  $\text{CaCO}_3$  content) (Fig. 5B, 15B). The stage I is characterized by few filaments in soil matrix and faint coatings of carbonate (<4% of  $\text{CaCO}_3$ ) in ped surfaces (Fig. 15B).

Palygorskite and sepiolite are common clay minerals in many ancient and present-day Aridisols with Bk horizons (Watts, 1980).

Aridisols are soils with low degree of development because the extreme environmental conditions and the deficiency of water. These last aspects inhibit the weathering processes and the hydrolysis values obtained by base/alumina ratios are in general higher than 1. The hydrolysis value obtained for these paleosols are consistent with their interpretation as Aridisols.

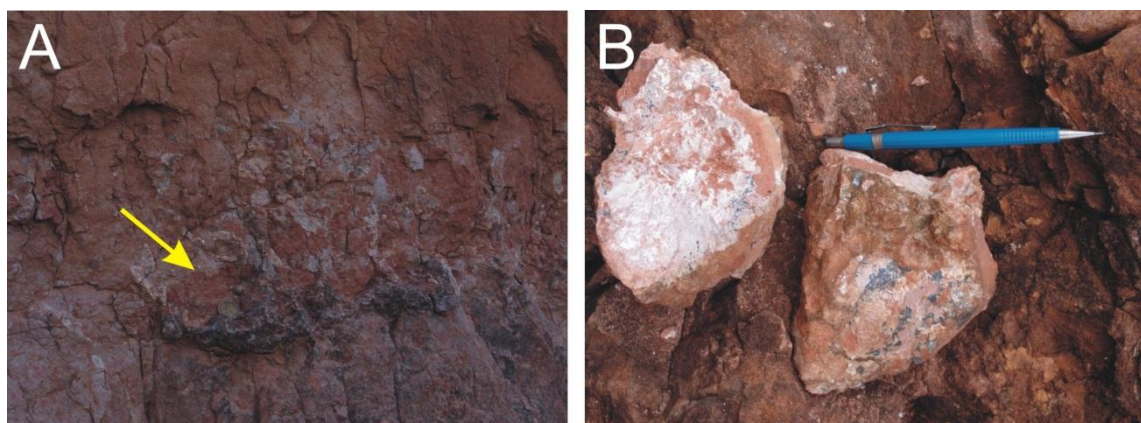


**Figure 15.** (A) High concentration of carbonate in Bk horizon of the Serra da Flor Roxa paleosol profile (arrow), which may be compared with phase III of calcic soil morphology of Gile et al. (1966). Coin is 1.9 cm. (B) Thin discontinuous coatings and encrustations on prismatic ped surfaces at stage I of Gile et al. (1966). Pencil is 14 cm.

## **5. Paleoclimatic considerations**

Different techniques have been used to determine the Cretaceous paleoclimate, including stable isotope composition (Ghosh et al., 1995), zonal circulation models (Barron and Washington, 1982), and fast ocean atmosphere model (FOAM) (Donnadieu et al., 2006).

In global terms, the climate at the end of the Cretaceous is considered much warmer than the present: high atmospheric CO<sub>2</sub> levels and temperatures, on average 10°C higher than at present (Donnadieu et al., 2006). Refined paleoclimatic models define a progressive warming from Aptian to Maastrichtian with reduced annual temperature variation and a low gradient of temperature from equator to poles (30° to -5°C) (Clarke and Jenkyns, 1999; Amiot et al., 2004; Donnadieu et al., 2006).

From the Late Jurassic the study area was characterized by an arid climate. Scherer (2000) and Scherer and Lavinia (2005, 2006) described eolian and eolian-fluvial depositional systems during the Late Jurassic and Early Cretaceous. Suguio and Barcelos (1983), Goldberg and Garcia (2000), and Dias-Brito et al. (2001) interpreted the paleoclimatic conditions of the Bauru Basin during the Late Cretaceous as hot and arid. Moreover, the contemporaneous uplifting of a regional geographic barrier towards SE and NE (the Serra do Mar and Alto Paranaíba mountains, respectively) acted as topographic highlands, probably inhibiting the free passage of oceanic humid winds, thus contributing with the increased continental aridity (Andreis et al., 1999; Goldberg and Garcia, 2000).

In this paper some paleoclimatic parameters recorded in paleosols classified as Aridisols were tested with the goal of increasing the information of the Late Cretaceous climate during the sedimentation of the Marília Formation: i) the depth of the Bk horizon, ii) the molecular weathering ratios, and iii) the clay mineralogy. The depth of the carbonate nodular horizon (Bk) as originally proposed for Jenny (1941) and modified by Retallack (1994; 2005) was used as proxy for paleoprecipitation estimates. The molecular weathering ratios expressed in calcification, hydrolysis, and salinization (Retallack, 1997; Sheldon et al., 2002) were used to define climate controlled chemical processes and testing the paleoprecipitation values. The clay mineralogy is a proxy on the paleoclimatic conditions, because the kinds of clays that form in the soil as product of hydrolysis of weatherable minerals can be related to the amount of precipitation and the temperature.

The free carbonate in soils usually forms a distinctive calcareous layer or calcic (Bk) horizon (Birkeland, 1999). The position of this horizon within the soil profile reveals the depth of wetting of the soil by available water (Retallack, 2001). Therefore, in dry climates the calcic horizon is closer to the surface than in wetter ones (Machette, 1985).

Following Retallack (1994; 2005), the depth of the carbonate nodular horizon (Bk) in soils ( $D$ , in cm) could be correlated with mean annual precipitation ( $P$ , in mm), so that Bk horizons are deep in subhumid regions, and shallow in arid or semi-arid regions. Retallack (2005) studied 807 profiles distributed in arid and semi-arid regions of the world and expressed this relationship:

$$P = 137.24 + 6.45D + 0.013D^2,$$

where determination coefficient  $R^2 = 0.52$ , and standard error ( $S.E.$ ) =  $\pm 147$  mm.

The depth of the Bk horizon is defined as the depth to the horizon where nodules or other forms of carbonate dominate the fabric of the profile, and the thickness of soil with nodules is the interval between shallowest and deepest nodules (Retallack, 1994, 2005).

The application of this equation, that is the calculus of the minimum paleoprecipitation values at the moment of carbonate nodules formation (Retallack, 1994), was possible only for Monte Alto 1 and Serra da Flor Roxa paleosol profiles, because it requires the complete preservation of the original soil sequence A-B-C horizons.

The Serra da Flor Roxa profile shows depth of the carbonate nodular horizon  $D = 15$  cm, while Monte Alto 1 profile presents  $D = 16.5$  cm. Replacing such values in the following equation  $P = 137.24 + 6.45D + 0.013D^2$ , the respective paleoprecipitation values were found:  $P = 236.91$  mm and  $P = 247.19$  mm, both subject to a standard error ( $S.E.$ ) of  $\pm 147$  mm.

The mean annual precipitation (MAP) of these two paleosol profiles shows average index around 240 mm of rainfall; thus, pointing out semi-arid to arid conditions prevailing during profiles formation and evolution. These data are consistent with the other interpretations, based on sedimentary, geochemical and paleontological features of the Marília Formation (Suguió and Barcelos, 1983; Fernandes, 1998; Goldberg and Garcia, 2000; Dias-Brito et al., 2001; Basilici et al., 2007).

Some difficulties arise in using the depth of the Bk horizon as a paleoprecipitation indicator. Firstly, the paleosol profile may be eroded before its complete burial (Retallack, 2001).

Second, the original thickness can be modified by compaction of the paleosol after deep burial. Third, the higher atmospheric CO<sub>2</sub> of Late Cretaceous (Berner, 1990; Nordt et al., 2003) could deepen the Bk horizons, and thus alter the values of mean annual precipitation. Nevertheless, we may consider the first and the second aspects irrelevant in this case to paleoprecipitation estimates. Indeed, we considered: i) only complete paleosol profiles, where the presence of the A horizon suggests absence or small erosion of the profile; ii) the compaction of well sorted sandy paleosol may be regarded as minimal. The third aspect (higher atmospheric CO<sub>2</sub>), if compared with a same paleoprecipitation value in modern soil, determined a deepening and thinning of the Bk horizon. Therefore, the inferred value of the mean annual rainfall may be considered as maximum values.

Molecular weathering ratio has been analyzed in all the paleosol profiles, with the aim to testing the paleoprecipitations values obtained from the calculus of the depth of calcic horizons and define climate controlled chemical processes.

Chemical analyses of major element (Table 2), expressed as weight percent, were used to calculate alkaline earths/alumina, base/alumina, and soda/potash ratios (Fig. 13), which reflect the primary calcification, the hydrolysis, and the salinization processes that occurred within the profile.

The results of the molecular weathering ratio indicate that Bk and Btk horizons suffered intense calcification processes, whereas these processes were less intense in the A and C horizons (Fig. 13). Bk and Btk horizons show the maximum index (4.83 to 16.28), whereas A horizons have the lesser values (0.82 to 1.05) and C (0.89 to 2.84) (Fig. 13). This variability of the values probably results from the external source of calcium carbonate and the atmospheric addition of either eolian dust or carbonate dissolved in rainwater is believed as the probably source (Machette, 1985; Dixon, 1994). Dissimilarity between calcification index presented in the A and B horizons are in accordance with the calculated paleoprecipitation values, that leached calcium from A horizon and subsequently accumulated in B horizons. Low values of Na<sub>2</sub>O, K<sub>2</sub>O, and MgO indicate that there was enough water to remove most of these exchangeable cations from the profile, but it was not sufficient to remove calcium from the Bk and Btk horizons.

Data on base/alumina ratio corroborate the previous hypothesis. In fact, the highest concentration of bases occurs in Bk and Btk (4.68 to 16.67) horizons, inasmuch as the upper A and lower C (1.19 to 3.29) horizons show the minimum values (Fig. 13).

The studied paleosol profiles do not show evaporite minerals either pseudomorphs of evaporite crystals. The molecular weathering ratio of soda/potash ( $\text{Na}_2\text{O}/\text{K}_2\text{O}$ ) that is an indicator of salinization is very mild in the examined profiles (Fig. 13). These values are always less than 1 (0.08 to 0.37), and point out salt-unaffected soil formation.

Smectite is a clay mineral that forms in parent material of felsic composition when the mean annual rainfall is less than 500 mm (Retallack, 2001). Palygorskite and sepiolite are two rare fibrous clay minerals that evidence warm and dry environmental conditions. These were found in the Bt and Btk horizons within arid-climate soils, as Aridisols (Singer and Galan, 1984; Botha and Hughes, 1992; Calvo et al., 1999). Retallack (2001) claims that palygorskite constitutes most of the clay fraction in Morocco soils, where the annual precipitation is less than 300 mm. Palygorskite and sepiolite are also associated with soils that have Bk horizons. In this case, their formation is favored by the precipitation of low-Mg calcite that, by increasing the content of Mg ions, allows the authigenic precipitation of palygorskite and sepiolite or the alteration of smectite in palygorskite (Watts, 1980). Suguio and Barcelos (1983) assert that the calcrete horizons and palygorskite clay minerals indicate that the deposits of the Bauru Basin were formed in a warm and dry paleoclimate.

Clay cutans (argillans), concentrated in Bt horizons, are related to clay illuviation into the soils, thus pointing out rainfall phases. Periodical phases of precipitation are indicated also by the presence of Vertisols in the Marília Formation (Goldberg and Garcia, 2000; Basilici et al., 2007), which are characterized by Bss horizons with slickensides. This kind of paleosol marks periodical phases of shrinking and swelling of the clay content of the soil caused by wetting and drying of the soil as consequence of the periodical precipitations.

In conclusion, the climate of the Late Cretaceous of SE Brazil was semi-arid. Indeed, although the climate during the genesis of the Marília Formation was generally dry, it may also be thought of as being characterized by a periodicity, perhaps seasonality, of the precipitation, evidenced mainly by the depth of the Bk horizons, by the clay illuviation (Bt and Btk horizons) and by the occurrence of Vertisols (Mack and James, 1994; Mermut et al., 1996).

## 6. Conclusions

The Marília Formation, Maastrichtian of the Bauru Basin, is constituted of an interbedding of deposits and paleosols. These latter comprise 30 to 85% of the twenty measured sections. The sediments are mainly composed of wind rippled deposits and secondarily of ephemeral fluvial channel deposits. Most of the paleosols are classified as Aridisols. The Marília Formation is interpreted as an eolian sand sheet area subjected alternatively to prevalent wind sedimentation or pedogenesis.

Four paleosols profiles from the Marília Formation were described. They are marked by the presence of horizons with prominent concentration of calcium carbonate and secondarily by the occurrence of argillic horizons. They have been classified as Aridisols, in Calcic and Argic suborders, respectively (Soil Survey Staff, 1999).

These characteristics, coupled with an A-Bk/Btk profile, ochric over calcic diagnostic horizons, root traces, and hematite oxides commonly coating sand grains, indicate that the paleosols of the Marília Formation might have formed under desert shrub or dry woodland environment (Oberlander, 1994; Retallack, 1994).

The depth of the Bk horizons, the molecular weathering ratios, the mineralogy of the clay fractions, and the sedimentological data were used as proxies to obtain paleoclimatic information on Late Cretaceous of the SE Brazil during the deposition of the Marília Formation.

The depth to the nodular calcic Bk horizon has been used as data for determining paleoprecipitation values. Mean annual precipitation (MAP) expressed low values, around 300 to 200 mm ( $S.E \pm 147$  mm) of rainfall, pointing out semi-arid to arid conditions. The results of the molecular weathering ratio, expressed in calcification  $(CaO+MgO)/Al_2O_3$  and hydrolysis  $(CaO+MgO+K_2O+Na_2O)/Al_2O_3$  ratios, indicate that Bk and Btk horizons suffered intense calcification processes and display greatest base concentration. Low values of weight percent of  $Na_2O$ ,  $K_2O$ , and  $MgO$  within the paleosol profiles indicate also that there was enough water to remove most of these exchangeable cations from the profile, but not sufficient to remove calcium from the Bk and Btk horizons. Low values of soda/potash ratios and the absence of evaporite minerals or their pseudomorphs suggest the lack of salinization processes during the soil formation.

Clay minerals also evidence arid conditions of development of the paleosols. Smectite, and above all palygorskite and sepiolite are clay mineral formed in dry environmental conditions.

Nevertheless, clay coatings in Bt and Bss horizons in Vertisols suggest periodical rainfall, and confirm the obtained information from depth of the Bk horizons.

These findings on the paleoclimate of the Marília Formation are in accordance with the sedimentary data of the Marília Formation (Fernandes, 1998; Goldberg and Garcia, 2000; Basilici et al., 2007) that interpreted it as a sand sheet area, characterized by eolian sedimentation and secondarily by sporadic deposition within ephemeral rivers.

In conclusion, the macro- and microfeatures, mineralogical, and geochemical analysis of four paleosols with calcic horizons attributed to Aridisols, allowed to interpret the paleoclimate of the Marilia Formation as characterized by a semi-arid regime with scarce and periodical precipitation.

### Acknowledgements

We are very grateful to FAPESP (Fundação de Amparo à Pesquisa do Estado de São Paulo) which financed this research (projects number 07/00140-6 and 07/02079-2).

### 7. References

- Allen, J.R.L., 1986. Pedogenic calcretes in the Old Red Sandstone facies (Late Silurian-Early Carboniferous) of the Anglo-Welsh area, southern Britain. In: Wright, V.P. (Ed.). *Paleosols: Their Recognition and Interpretation*. Blackwell Scientific Publications, Oxford, pp. 58-86.
- Alonso-Zarza, A.M., 2003. Palaeoenvironmental significance of palustrine carbonates and calcretes in the geological record. *Earth-Science Reviews* 60, 261-298.
- Amiot, R., Lécuyera, C., Buffetaut, E., Fluteau, F., Legendre, S., Martineau, F., 2004. Latitudinal temperature gradient during the Cretaceous Upper Campanian–Middle Maastrichtian:  $\delta\text{O}18$  record of continental vertebrates. *Earth and Planetary Science Letters* 226, 255-272.
- Andreis, R.R., Capilla, R., Reis, C.C., 1999. Considerações estratigráficas e composição dos arenitos da Formação Marília (Cretáceo Superior) na região de Uberaba. In: Boletim, 5º Simpósio sobre o Cretáceo do Brasil. Serra Negra, pp. 449-456.
- Arakel, A.V., 1986. Evolution of calcrete in palaeodrainages of the lake Napperby area, central Australia. In: Chivas, A.R., Torgersen, T., Eowler, J.M. (Eds.). *Palaeoenvironment of Salt Lakes. Palaeogeography, Palaeoclimatology, Palaeoecology* 54, 283-303.

- Barron, E.J., Washington, W.M., 1982. Cretaceous climate: a comparison of atmospheric simulations with the geologic record. *Palaeogeography, Palaeoclimatology, Palaeoecology* 40, 103-133.
- Basilici, G., Ladeira, F.S.B., Dal' Bó, P.F.F., 2007. Aeolian/fluvial and paleosol climatic sequences in an ancient sand sheet: Marília Formation, Late Cretaceous of the Bauru Basin, Brazil. In: Abstracts, 25th International Association of Sedimentologists Meeting, International Association of Sedimentologists. Patras, pp. 49.
- Berner, R.A., 1990. Atmospheric carbon dioxide levels over Phanerozoic time. *Science* 249, 1382-1385.
- Birkeland, P.W., 1999. Soils and Geomorphology. 3rd ed., Oxford University Press, New York, 430 pp.
- Botha, G.A., Hughes, J.C., 1992. Pedogenetic palygorskite and dolomite in late Neogene sedimentary succession, northwestern Transvaal, South Africa. *Geoderma* 53, 139-154.
- Bullock, P., Fedoroff, N., Jongerius, A., Stoops, G., Tursina, T., 1985. Handbook for soil thin section description. Waine Research Publications, Wolverhampton, 152 pp.
- Calvo, J.P., Blanc-Valleron, M.M., Rodriguez-Arandía, J.P., Rouchy, J.M., Sanz, M.E., 1999. Authigenic clay minerals in continental evaporitic environments. In: Thiry, M., Simon-Coinçon, R. (Eds.). *Palaeoweathering, Palaeosurfaces and Related Continental Deposits*. IAS Special Publication, 27, 129-151.
- Castro de, J.C., Dias-Brito, D., Musacchio, E.A., Suarez, J., Maranhão, M.S.A.S., Rodrigues, R., 1999. Arcabouço estratigráfico do Grupo Bauru no oeste Paulista. In: Boletim, 5º Simpósio sobre o Cretáceo do Brasil. Serra Negra, pp. 509-515.
- Catt, J.A., 1990. Paleopedology manual. *Quaternary International* 6, 1-95.
- Clarke, L.J., Jenkyns, H.C., 1999. New oxygen isotope evidence for long-term Cretaceous climatic change in the southern Hemisphere. *Geology* 27, 699-702.
- Dias-Brito, D., Musacchio, E.A., Castro, J.C. de., Maranhão, M.da.S., Suarez, J.M., Rodrigues, R., 2001. Grupo Bauru: uma unidade continental do Cretáceo no Brasil – concepções baseadas em dados micropaleontológicos, isotópicos e estratigráficos. *Revue de Paléobiologie* 20 (1), 245-304.
- Dixon, J.C., 1994. Aridic soils, patterned ground, and desert pavements. In: Abrahams, A.D., Parsons, A.J. (Eds.). *Geomorphology of desert environments*. Chapman and Hall, London, pp. 64-81.

- Donnadieu, Y., Pierrehumbert, R., Jacob, R., Fluteau, F., 2006. Modelling the primary control of paleogeography on Cretaceous climate. *Earth and Planetary Science Letters* 248 (1/2), 426-437.
- Eghbal, M.K., Southard, R.J., 1993. Micromorphological evidence of polygenesis of three Aridisols, western Mojave Desert, California. *Soil Science Society of America Journal* 57, 1041-1050.
- Fernandes, L.A., 1998. Estratigrafia e evolução geológica da parte oriental da Bacia Bauru (Ks, Brasil). Unpublished PhD thesis, Universidade de São Paulo, São Paulo, 216 pp.
- Fernandes, L.A., Coimbra, A.M., 1996. A Bacia Bauru (Cretáceo Superior, Brasil). *Anais da Academia Brasileira de Ciências* 68 (2), 195-205.
- Ghosh, P., Bhattacharya, S.K., Jani, R.A., 1995. Palaeoclimate and palaeovegetation in central India during the Upper Cretaceous based on stable isotope composition of the paleosol carbonates. *Palaeogeography, Palaeoclimatology, Palaeoecology* 114, 285-296.
- Gile, L.H., Peterson, F.F., Grossman, R.B., 1965. The K horizon: a master soil horizon of carbonate accumulation. *Soil Science* 99, 74-82.
- Gile, L.H., Peterson, F.F., Grossman, R.B., 1966. Morphological and genetic sequences of carbonate accumulation in desert soils. *Soil Science* 101, 347-354.
- Goldberg, K., Garcia, A.J.V., 2000. Palaeobiogeography of the Bauru Group, a dinosaur-bearing Cretaceous unit, northeastern Paraná Basin, Brazil. *Cretaceous Research* 21, 241-254.
- Goudie, A.S., 1983. Calcrete. In: Goudie, A.S., Pye, K. (Eds.). *Chemical sediments and geomorphology: precipitates and residual in near-surface environment*. Academic Press, London, pp. 93-131.
- Gustavson, T.C., Holliday, V.T., 1999. Eolian sedimentation and soil development on semi-arid to subhumid grassland, Tertiary Ogallala and Quaternary Blackwater Draw Formations, Texas and New Mexico High Plains. *Journal of Sedimentary Research* 69 (3), 622-634.
- Hunter, R.E., 1977. Basic types of stratification in small eolian dunes. *Sedimentology* 24, 361-387.
- Jenny, H.J., 1941. Factors of soil formation. McGraw-Hill, New York, 281 pp.
- Khormali, F., Abtahi, A., Mahmoodi, S., Stoops, G., 2003. Argillic horizon development in calcareous soils of arid and semiarid regions of southern Iran. *Catena* 53, 273-301.
- Kraimer, R.A., Monger, H.C., Steiner, R.L., 2005. Mineralogical distinctions of carbonates in desert soils. *Soil Science Society of America Journal* 69, 1773-1781.

Lemos, R.C. de., Santos, R.D. dos., 1984. Manual de descrição e coleta de solo no campo. 3rd ed., Sociedade Brasileira de Ciência do Solo, Campinas, 84 pp.

Machette, M.N., 1985. Calcic soils of the southwestern United States. In: Weide, D.L. (Ed.). Soils and quaternary geology of the southwestern United States. Geological Society of America, Special Paper, 203, 1-21.

Mack, G.H., James, W.C., 1994. Paleoclimate and the global distribution of paleosols. *The Journal of Geology*, 102, 360-366.

Mack, G.H., James, W.C., Monger, H.C., 1993. Classification of paleosols. *Geological Society of America Bulletin* 105, 129-136.

Mermut, A.R., Padmanabham, E., Eswaran, H., Dasog, G.S., 1996. Pedogenesis. In: Ahmad, N., Mermut, A. (Eds.). Vertisols and technologies for their management. *Developments in Soil Science* 24, 43-61.

Mountney, N.P., 2006. Aeolian facies model. In: Posamentier, H.W., Walker, R.G. (Ed.). Facies models revisited. *SEPM Special Publication* 84, 19-83.

Nettleton, W.D., Peterson, F.F., 1983. Aridisols. In: Wilding, L.P., Smeckand, N.E., Hall, G.F., (Eds.). *Pedogenesis and Soil Taxonomy; II. The Soil Orders*. Elsevier, Amsterdam, pp. 165-215.

Nordt, L., Atchley, S. and Dworkin, S., 2003. Terrestrial evidence for two greenhouse events in the latest Cretaceous. *GSA Today*, December 2003, 4-9.

Oberlander, T.M., 1994. Rock varnish in deserts. In: Abrahams, A.D., Parsons, A.J. (Eds.). *Geomorphology of desert environments*. Chapman and Hall, London, pp. 106-119.

Ollier, C., Pain, C., 1996. Regolith, soils and landforms. John Wiley and Sons, Chichester, 316 pp.

Pimentel, N.L., Wright, V.P., Azevedo, T.M., 1996. Distinguishing early groundwater alteration effects from pedogenesis in ancient alluvial basins: examples from the Palaeogene of southern Portugal. *Sedimentary Geology* 105, 1-10.

Retallack, G.J., 1991. Miocene paleosols and ape habitats of Pakistan and Kenia. Oxford University Press, New York, 346 pp.

Retallack, G.J., 1994. The environmental factor approach to the interpretation of paleosols. In: Amundson, R., Harden, J., Singer, M. (Eds.). *Factors of soil formation: a fiftieth anniversary retrospective*. Soil Science Society of America Special Publication 33, 31-64.

Retallack, G.J., 1997. A colour guide to paleosols. John Wiley and Sons, Chichester, 175 pp.

Retallack, G.J., 1998. Core concepts of paleopedology. *Quaternary International* 51/52, 203-212.

- Retallack, G.J., 2001. Soils of the past: an introduction to paleopedology. Allen and Unwin, London, 520 pp.
- Retallack, G.J., 2005. Pedogenic carbonate proxies for amount and seasonality of precipitation in paleosols. *Geology* 33 (4), 333-336.
- Riccomini, C., 1997. Arcabouço estrutural e aspectos do tectonismo gerador e deformador da Bacia Bauru no estado de São Paulo. *Revista Brasileira de Geociências* 27 (2), 153-162.
- Schaetzl, R.J., Anderson, S., 2005. Soils: genesis and geomorphology. University Press, Cambridge, 832 pp.
- Scherer, C.M.S., 2000. Eolian dunes of the Botucatu Formation (Cretaceous) in southernmost Brazil: morphology and origin. *Sedimentary Geology* 137, 63-84.
- Scherer, C.M.S., Lavinia, E.L.C., 2005. Sedimentary cycles and facies architecture of aeolian-fluvial strata of the Upper Jurassic Guará Formation, southern Brazil. *Sedimentology* 52, 1323-1341.
- Scherer, C.M.S., Lavinia, E.L.C., 2006. Stratigraphic evolution of a fluvial-eolian succession: The example of the Upper Jurassic-Lower Cretaceous Guará and Botucatu formations, Paraná Basin, southernmost Brazil. *Gondwana Research* 9, 475-484.
- Sheldon, N.D., Retallack, G.J., Tanaka, S., 2002. Geochemical climofunctions from North American soils and application to paleosols across the Eocene-Oligocene boundary in Oregon. *The Journal of Geology* 100, 687-696.
- Singer, A., Galan, E. (Eds.), 1984. Palygorskite-sepiolite: occurrence, genesis, uses. Elsevier, Amsterdam, 352 pp.
- Soares, P.C., Landim, P.M.B., Fúlfaro, V.J., Sobreiro Neto, A.F., 1980. Ensaio de caracterização estratigráfica do Cretáceo no estado de São Paulo: Grupo Bauru. *Revista Brasileira de Geociências* 10, 177-185.
- Soil Survey Staff, 1999. Soil taxonomy. Handbook, U.S. Department of Agriculture 436, 869 pp.
- Soil Survey Staff, 2006. Keys to soil taxonomy. 10th ed., U.S. Department of Agriculture, Natural Resource Conservation Service, 332 pp.
- Suguio, K., 1973. Formação Bauru. Calcários e sedimentos detriticos associados. Unpublished Livre Docêncie Thesis, Universidade de São Paulo, 236 pp.
- Suguio, K., Barcelos, J.H., 1983. Calcretes of the Bauru Group (Cretaceous), Brazil: petrology and geological significance. *Boletim IG, São Paulo*, 14, 31-47.

- Tandon, S.K., Friend, P.F., 1989. Near-surface shrinkage and carbonate replacement processes, Arran Cornstone Formation, Scotland. *Sedimentology* 36, 1113-1126.
- Watts, N.L., 1980. Quaternary pedogenetic calcretes from Kalahari (southern Africa): mineralogy, genesis and diagenesis. *Sedimentology* 27, 661-686.
- Wright, V.P., 1990. A micromorphological classification of fossil and recent calcic and petrocalcic microstructures. In: L.A. Douglas (Ed.). *Soil micromorphology: a basic and applied science. Developments in soil science*, vol. 19. Elsevier, Amsterdam, pp. 401-407.
- Wright, V.P., Tucker, M.E. 1991. Calcretes: an introduction. In: Wright, V.P., Tucker, M.E. (Eds.). *Calcretes*. Blackwell, Oxford, pp. 1-22.
- Yaalon, D.H., 1971. Soil-forming processes in time and space. In: Yaalon, D.H. (Ed.). *Paleopedology: origin, nature and dating of paleosols*. International Society of Soil Science and Israel University Press, Jerusalem, pp. 29-39.
- Zaher, H., Pol, D., Carvalho, A. B., Riccomini, C., Campos, D., Navas, W., 2006. Re-description of the cranial morphology of *Mariliasuchus amarali*, and its phylogenetic affinities (Crocodyliformes, Notosuchia). *American Museum Novitates* 3512, 1-40.

## ANEXO III

“Dal’ Bo, P.F.F. & Basilici, G., 2010. *Estimativas de paleoprecipitação e gênese de feições cárnicas e argílicas em paleossolos da Formação Marília (Neocretáceo da Bacia Bauru).* *Geociências* 29(1): 33-47.”



*“We know more about the movement of celestial bodies than about the soil underfoot.”*

*Leonardo Da Vinci*



# **ESTIMATIVAS DE PALEOPRECIPITAÇÃO E GÊNESE DE FEIÇÕES CÁLCICAS E ARGÍLICAS EM PALEOSSOLOS DA FORMAÇÃO MARÍLIA (NEOCRETÁCEO DA BACIA BAURU)**

Patrick Francisco Führ Dal' Bó & Giorgio Basilici

Departamento de Geologia e Recursos Naturais, Instituto de Geociências, Universidade Estadual de Campinas (UNICAMP). Rua João Pandiá Calógeras, 51, CEP 13083-970, Cx. Postal 6152. Campinas, SP.

Endereços eletrônicos: patrickdalbo@ige.unicamp.br; basilici@ige.unicamp.br.

**Resumo** – O presente estudo tem por objetivo investigar a gênese de feições que indicam a concentração de carbonato de cálcio e outras que indicam a concentração de feições iluviais de ferro e argila, que ocorrem em paleossolos da Formação Marília. Regra geral, essas feições estão concentradas em dois horizontes de paleossolo, as feições cálcicas em horizontes Bk de *Aridisols* e as argílicas em horizontes Bt de *Aridisols* e *Alfisols*. Para tanto, foram estudados 19 perfis de paleossolos, contando com 3 horizontes Bk e 11 horizontes Bt. Nestes horizontes selecionados, procedeu-se com a caracterização da macro- e micromorfologia, da geoquímica, e análises de microscopia eletrônica de varredura. As estimativas de paleoprecipitação foram obtidas por meio de dois métodos indiretos de análise: profundidade de ocorrência de nódulos carbonáticos em horizontes Bk e geoquímica dos horizontes Bt. Postula-se, neste artigo, que a gênese de ambas as feições está ligada a atuação de processos pedogenéticos pretéritos e que as paleoprecipitações tiveram papel preponderante como fator de controle à gênese e diferenciação dessas feições nos paleossolos estudados.

**Palavras-chave:** paleossolos; estimativas de paleoprecipitação; gênese de feições cálcicas e argílicas; Formação Marília.

**Abstract** – *Paleoprecipitation estimates and genesis of calcic and argillic features in paleosols of the Marília Formation (Neocretaceous of the Bauru Basin).* This paper aims to investigate the genesis of calcic and argillic features which occur in paleosols of the Marília Formation. In a general sense, these features are concentrated in two paleosol horizons, the calcic features in Bk Aridisols horizons and argillic features in Bt Aridisols and Alfisol horizons. In this paper 19 paleosol profiles were studied and detail macro and micromorphological, geochemical, and SEM analyses were performed on 3 Bk and 11 Bt horizons. The paleoprecipitation estimates were inferred following two climofunctions, depth-to-carbonate from Bk and chemical composition from Bt horizons. By comparing the calcic and argillic features of these horizons with modern soil horizons this study demonstrates that these features were pedogenically formed and that paleoprecipitation was an important forcing factor in the genesis and principally in the differentiation of these features.

**Keywords:** paleosols; paleoprecipitation estimates; genesis of calcic and argillic features; Marília Formation.



## **1. Introdução**

Uma grande variedade de técnicas que se apóiam em registros representativos (*proxy records*) vêm sendo desenvolvidas nos últimos anos com o objetivo de quantificar os principais parâmetros atmosféricos (composição da atmosfera, regimes de paleoeventos, paleotemperaturas e índices pluviométricos passados) que afetaram a conformação dos climas pretéritos. Neste contexto, os paleossolos são utilizados para a interpretação paleoclimática como indicadores de estimativas anuais de paleoprecipitação (*Mean annual precipitation – MAP*) e estimativas anuais de paleotemperatura (*Mean annual temperature - MAT*). A interpretação de regimes climáticos do passado com o uso de paleossolos é baseada principalmente na identificação de feições pedogênicas que estudos com solos modernos mostraram possuir significado paleoclimático. No presente estudo, serão utilizadas duas técnicas para calcular os índices de paleoprecipitação que ocorreram durante o desenvolvimento de dois tipos de horizontes de paleossolos na Formação Marília: profundidade de ocorrência de nódulos carbonáticos (*depth-to-carbonate rainfall estimates - DTC*) para horizontes cálcicos Bk e índice de alteração química (*chemical index of alteration without potassium - CIA-K*) para horizontes argílicos Bt.

Nos paleossolos da Formação Marília é comum a ocorrência de feições pedogênicas que indicam a concentração e remobilização secundária de carbonato de cálcio (feições de cristalização, dissolução, substituição, descarbonatação e recarbonatação). Atualmente, solos com horizontes cálcicos e petrocálcicos são amplamente distribuídos em áreas áridas e semi-áridas por toda a superfície terrestre (Goudie, 1973) e paleossolos que apresentam horizontes cálcicos são considerados ótimos indicadores paleoclimáticos e paleoambientais (Goudie, 1983; Wright & Tucker, 1991; Alonso-Zarza, 2003).

A iluviação de argila é outro importante processo pedogênico registrado nos paleossolos da Formação Marília. As partículas de argila se movem nos solos em estado de suspensão durante a ocorrência das frentes de molhamento e ficam retidas nas superfícies das unidades estruturais ou paredes dos poros após a completa evaporação e/ou absorção da água que as carregavam. Essas feições de iluviação são freqüentes em horizontes argílicos, que por definição, são horizontes subsuperficiais que exibem evidências de iluviação de argila e apresentam um percentual maior no conteúdo de argila do que os horizontes superiores do mesmo perfil (Soil Survey Staff, 1999).

A formação de horizontes argílicos envolve tipicamente três processos pedogênicos: dispersão, translocação e acumulação (Eswaran & Sys, 1979). O regime climático da área é determinante aos processos de gênese e transporte das partículas de argila. Em climas úmidos, os horizontes argílicos se desenvolvem predominantemente por alteração do material de origem, ao passo que em climas áridos, o aporte das partículas de argila ocorre preponderantemente via adição eólica (Rust, 1983).

A presença de horizontes pedogênicos que exibem intercalações e superposições de feições de concentração de carbonato de cálcio e argílicas são comuns nos paleossolos estudados. Horizontes cálcicos que contêm feições de iluviação de argila são comumente interpretados como resultado de mudanças climáticas (Reheis, 1987). Gile *et al.* (1966) indicam que as feições de iluviação de argila foram formadas primeiramente em condições climáticas mais úmidas e posteriormente foram recobertas por feições de concentração de carbonato de cálcio quando as condições climáticas se tornaram mais secas. Situações em que ocorrem feições de iluviação de argila recobrindo as de carbonato de cálcio são interpretadas como produto de mudanças climáticas de períodos mais secos para úmidos (Khormali *et al.*, 2003), porém são raramente reportadas na literatura (Bronger *et al.*, 1998). Segundo Gile *et al.* (1966), o carbonato de cálcio deve ser completamente removido do perfil para ocorrer a iluviação de argila, devido à tendência da argila em flocular na presença de carbonatos. Porém, Holliday (1985) indicou que as partículas de argila podem ser translocadas mesmo em solos que apresentam altas concentrações de carbonato de cálcio e, apesar da tendência da argila em flocular na presença de íons de Ca, caso os solos possuam macroporos e canais livres, acompanhados de disponibilidade de água superior às perdas por evapotranspiração, os processos de iluviação de argila podem ocorrer. O Na desempenha um papel importante no desenvolvimento desses processos em ambientes áridos, pois possui um alto efeito dispersivo sobre as argilas.

Os objetivos deste estudo são: a) calcular os índices de paleoprecipitação que ocorreram durante a formação dos horizontes cálcicos e argílicos, b) evidenciar os principais processos pedogenéticos que agiram na gênese de tais horizontes.

## 2. Área de estudo

Os trabalhos foram desenvolvidos principalmente em três setores da Bacia Bauru: na porção centro-oeste do estado de São Paulo, nas imediações do município de Marília, na porção centro-norte do estado de São Paulo, nas proximidades do município de Monte Alto, e na porção noroeste da bacia, entre os municípios de Cassilândia (MS), Itajá (GO), Itarumã (GO) e Quirinópolis (GO) (Figura 1). Os pontos estudados estão listados e geograficamente referenciados na Tabela 1 e indicados no mapa da Figura 1.

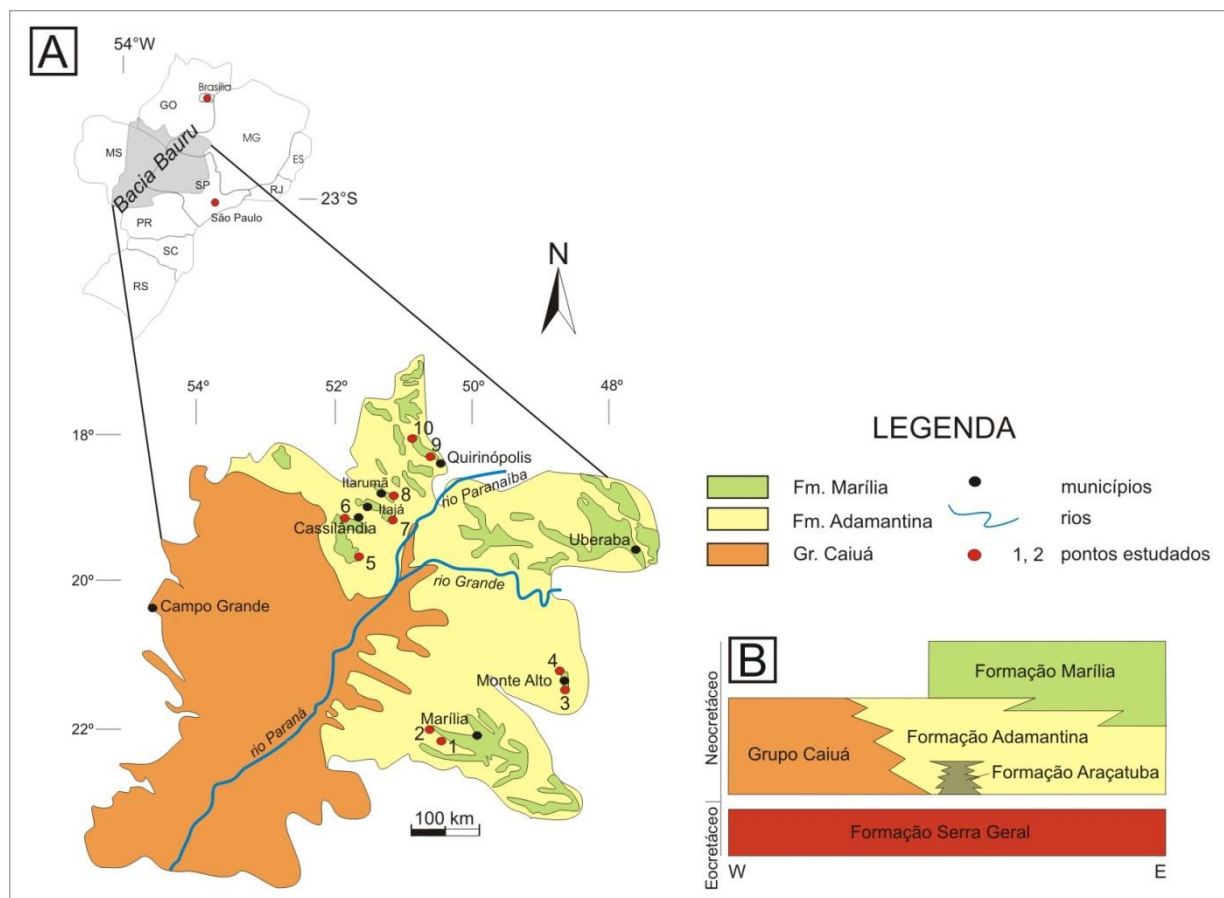


**Figura 1.** A) Mapa geológico simplificado mostrando a distribuição das unidades da Bacia Bauru e pontos estudados na Formação Marília. B) Relações estratigráficas entre as unidades da Bacia Bauru (modificado de Fernandes, 1998).

**Tabela 1.** Coordenadas geográficas dos pontos estudados (vide mapa da Figura 1).

Ponto	Coordenadas Geográficas
1	50°11'25"S, 22°22'40"W
2	50°04'05"S, 22°15'25"W
3	48°32'58"W, 21°15'14"S
4	48°32'41"W, 21°15'25"S
5	51°25'23"W, 19°23'32"S
6	51°38'56"W, 19°05'46"S
7	51°34'19"W, 19°03'02"S
8	51°18'29"W, 18°52'42"S
9	50°28'45"W, 18°07'32"S
10	51°01'21"W, 18°02'40"S

### 3. Contexto geológico e estratigráfico

A área de estudo está situada na Bacia Bauru. A Bacia Bauru é uma bacia sedimentar intracratônica, desenvolvida durante o Cretáceo Superior (Santoniano-Maastrichtiano), na porção centro-sul da Plataforma Sul-Americana. A bacia possui forma aproximadamente elíptica com eixo maior na direção nordeste e cobre uma extensão de aproximadamente 370.000 km<sup>2</sup>, que abrange o oeste do estado de São Paulo, nordeste do Mato Grosso do Sul, sudeste do Mato Grosso, sul de Goiás e oeste de Minas Gerais. Suas maiores espessuras preservadas ultrapassam os 300 m, como em sondagens realizadas na Estrutura de Piratininga, onde foram atravessados 324 m de sedimentos da Formação Marília (Santos *et al.*, 1980), mas em média são da ordem de 100 m (Paula e Silva, 2003).

O substrato da Bacia Bauru é formado por rochas vulcânicas da Formação Serra Geral, de idade entre 133 e 130 Ma (Renne *et al.*, 1992). A sucessão sedimentar (com rochas vulcânicas associadas) da bacia é separada dos derrames basálticos da Formação Serra Geral por não-conformidade (Fernandes & Coimbra, 2000). O mecanismo que gerou a depressão sobre a qual se acumularam os sedimentos da bacia tem sido interpretado como de natureza mecânica (Batezelli, 2003), devido a processos de reativação de lineamentos do embasamento Pré-Cambriano, e termal (Milani, 1997; Riccomini, 1997), como produto de reajustes flexurais negativos da litosfera, ocorridos após a acomodação e resfriamento da pilha de basaltos da Formação Serra Geral.

A Bacia Bauru é subdividida em dois grupos: Caiuá e Bauru. As relações estratigráficas entre os dois grupos ainda é tema bastante controverso. Alguns autores defendem a tese da interdigitação e contemporaneidade dos grupos (Fernandes & Coimbra, 1996; Fernandes, 1998; Fernandes & Coimbra, 2000), enquanto outros, baseados no reconhecimento de uma superfície de descontinuidade regional, denominada de Geossolo Santo Anastácio (Fúlfaro *et al.*, 1999), e dados paleomagnéticos (Ernesto *et al.*, 2006), entendem que os dois grupos se depositaram em intervalos distintos: Grupo Caiuá no Eocretáceo (Aptiano/Albiano) e o Grupo Bauru no Neocretáceo (Campaniano-Maastrichtiano), separados por superfícies de discordância de milhões de anos.

Numerosos trabalhos têm procurado hierarquizar do ponto de vista estratigráfico as diferentes unidades que afloram na Bacia Bauru. A subdivisão proposta por Soares *et al.* (1980) para o estado de São Paulo, em quatro formações, da base para o topo: Caiuá, Santo Anastácio, Adamantina e Marília, alcançou grande aceitação dos pesquisadores em função de sua operacionalidade em campo (Etchebehere *et al.*, 1993; Dias Brito *et al.*, 2001). Porém, principalmente a partir da década de 1990, surgem novos trabalhos com propostas de inclusão, reformulação e exclusão de unidades da Bacia Bauru (Fernandes, 1992, 1998; Fernandes & Coimbra 1994, 1996, 2000; Batezelli 1998, 2003; Paula e Silva, 2003). Dentre as principais proposições dos autores citados estão a inclusão das formações Uberaba (Hasui, 1968), que só aflora na região do Triângulo Mineiro, e Araçatuba (Zaine *et al.*, 1980) no Grupo Bauru e a reclassificação da Formação Caiuá na categoria de Grupo Caiuá (Fernandes, 1992).

O presente estudo irá se restringir à caracterização geológica e estratigráfica da Formação Marília, unidade superior do Grupo Bauru, pois se trata da unidade que é o objeto de estudo.

A Formação Marília é constituída por arenitos muito finos a médios e raros depósitos de arenitos conglomeráticos. Os arenitos são bem selecionados, bem arredondados e exibem alta esferecidade, predominantemente constituídos por quartzo e secundariamente por fragmentos líticos (Basilici *et al.*, 2009). Possui espessura máxima preservada de 160 a 180 m em superfície (Soares *et al.*, 1980; IPT, 1981) na cidade de Marília (SP) e 233 m em subsuperfície na cidade de Lupércio (SP) (Paula e Silva, 2003). A idade de deposição admitida é Maastrichtiano (74-65 Ma). Esta idade foi obtida através de correlações estratigráficas com vertebrados fósseis do gênero *Aeolosaurus* (Santucci e Bertini, 2001), por relacionamentos estratigráficos e biogeográficos com

diferentes taxa de ostracodes e carófitos (Dias-Brito *et al.*, 2001), e dados paleomagnéticos (Tamrat *et al.*, 2002).

## 4. Métodos

### 4.1. Aquisição de dados em campo

Em campo, foram levantadas 10 seções estratigráficas, que estão indicadas na Figura 1 (pontos estudados). Os paleossolos representam 66% da espessura total das seções, nas quais os outros 25% são formados por depósitos eólicos de arenito com lamination plano-paralela e 9% por depósitos de arenito conglomerático, atribuídos a deposição de canais efêmeros. Informações adicionais sobre a descrição das seções podem ser encontradas em Dal' Bó (2008) e Basilici *et al.* (2009).

Os paleossolos foram identificados em campo com base no reconhecimento de feições diagnósticas como rizólitos, estruturas e horizontes de solo, e variações texturais entre os horizontes pedogênicos (Catt, 1990; Retallack, 2001). A descrição morfológica seguiu em parte os critérios estabelecidos no *Soil Survey Manual* (Soil Survey Staff, 1993), considerando as adaptações propostas para a descrição de paleossolos (Catt, 1990) e, modificações de Birkeland (1999). A taxonomia dos horizontes e perfis está de acordo com o *US Soil Taxonomy* (Soil Survey Staff, 1999), por se tratar de um sistema mais apropriado à classificação de paleossolos (Kraus, 1999; Sheldon & Tabor, 2009).

Adicionalmente às descrições de campo, foram coletadas amostras indeformadas e orientadas, representativas dos principais horizontes e tipos de paleossolos, para a confecção de lâminas delgadas e exames por microscopia eletrônica de varredura (MEV). Outras amostras dos mesmos horizontes foram coletadas para as análises químicas e mineralógicas.

### 4.2. Micromorfologia e MEV

A confecção das seções delgadas foi realizada no Laboratório de Lamination do IG/Unicamp. Devido ao alto grau de desagregabilidade das amostras, mesmo que em sua maior parte cimentadas por carbonato de cálcio, foi necessária a impregnação com resina de poliéster,

que promoveu o endurecimento do material por polimerização, viabilizando a confecção das lâminas sem perda significativa de material. Os procedimentos empregados na descrição das lâminas delgadas seguiram as proposições de Bullock *et al.* (1985) e Castro (2002), realizados sistematicamente sobre amostras da base para o topo dos perfis, inicialmente com auxílio de lupa binocular e posteriormente ao microscópio óptico de luz polarizante.

As análises de microscopia eletrônica de varredura foram realizadas no Laboratório de Microscopia Eletrônica de Varredura do IG/Unicamp, sob as mesmas lâminas que foram analisadas ao microscópio óptico de luz polarizante. As lâminas foram pulverizadas com um filme fino de carbono. O equipamento utilizado foi um MEV LEO 430 acoplado a um espectrômetro de energia EDS, que possibilitou a observação das feições pedogênicas em escala de micrômetros.

#### **4.3. Análises químicas e mineralógicas**

A determinação dos elementos químicos maiores foi obtida mediante a análise por Fluorescência de Raios-X (XRF, equipamento Philips, PW2404) em discos de vidro com aproximadamente 1 grama de amostra fundida em matriz de tetraborato de lítio. As análises foram realizadas no Laboratório de Geoquímica Analítica do IG/Unicamp. O principal objetivo dessas análises foi o de auxiliar na melhor caracterização dos horizontes de paleossolos e, contribuir para o conhecimento das formas de alteração do material de origem, que foi determinado com o uso de equações de alteração (Maynard, 1992).

A mineralogia dos horizontes de paleossolos foi determinada através de Difração de Raios-X (método do pó), que foi realizada no Laboratório de Raios-X do Centro de Geociências da Universidade Federal do Pará. O equipamento utilizado foi um difratômetro PW3040/60 equipado com ânodo de cobre ( $\text{CoK}\alpha$ ), monocromador ( $\text{FeK}\beta$ ), gerador de tensão com 40 kV e gerador de corrente 35 mA. As características dos minerais foram identificadas a partir da interpretação dos difratogramas gerados, utilizando-se o software APD - *Automatic Powder Diffraction* da marca Philips. Adicionalmente, utilizou-se também o programa Minerva, que consiste em um banco de dados do *International Center for Diffraction Data* com as principais características dos minerais, permitindo a comparação difratométrica dos picos dos minerais com padrões difratométricos de fases cristalinas individuais caracterizadas. Lâminas orientadas, com

amostras de granulação inferior a <2 µm foram utilizadas para a caracterização dos argilominerais presentes.

#### 4.4. Paleoprecipitação

Para verificar as estimativas anuais de paleoprecipitação, foram empregados dois métodos distintos. O primeiro método empregado consiste na determinação da profundidade (D, *depth* em cm) de um horizonte no qual ocorre a maior concentração de nódulos carbonáticos (horizonte Bk) e/ou em relação a um horizonte no qual o carbonato de cálcio é dominante na matriz do solo. A relação entre a profundidade desses horizontes com índices de precipitação (P, *precipitation* em mm) foi descrita pela primeira vez em 1941 (Jenny, 1941). O autor citado escolheu uma série de solos com horizontes cárnicos nos *Great Plains* norte-americanos que apresentavam pouca variabilidade nos principais fatores de formação dos solos: vegetação de gramíneas, topografia plana, material de origem derivado de acumulações de *loess* carbonático e idade determinada (<14 Ka), porém submetidos a diferentes regimes climáticos (climossequência). A principal conclusão do autor foi de que os horizontes cárnicos eram mais profundos nas áreas que apresentavam maiores índices pluviométricos e mais superficiais nas áreas mais secas.

Em 2005, Retallack (2005) expandiu a base de dados de Jenny (1941) e Arkley (1963) para 807 solos com horizontes cárnicos distribuídos em todos os continentes e definiu a seguinte equação para determinar os índices de precipitação de acordo com a profundidade dos horizontes cárnicos Bk:

$$P \text{ (mm)} = 137.24 + 6.45D + 0.013D^2,$$

na qual  $R^2 = 0.52$  (coeficiente de determinação) e  $s = \pm 147 \text{ mm}$  (desvio padrão).

Esta equação vem sendo largamente utilizada em estudos que procuram estabelecer estimativas de paleoprecipitação em paleossolos que apresentam horizontes cárnicos (Retallack, 2007; Cleveland *et al.*, 2008). No presente estudo, a equação foi aplicada a 3 perfis de paleossolos que apresentaram as seguintes características: a) horizonte superficial A preservado, b) contato superior com outros paleossolos e/ou litofácies sem evidência de erosão.

O segundo método empregado consiste na aplicação de uma equação exponencial que relaciona os índices de precipitação (MAP) com os índices de alteração química (CIA-K) de

horizontes argílicos Bt. O primeiro passo para a aplicação da equação é o cálculo dos índices de alteração química. Esse índice foi originalmente proposto por Nesbitt & Young (1982), como segue a equação:  $CIA = 100 \times ((Al_2O_3 / (Al_2O_3 + CaO + Na_2O + K_2O)))$ , em % de massa molar. A aplicação desse índice sem o óxido de potássio foi sugerida por Maynard (1992), com o objetivo de controlar os efeitos do metassomatismo do potássio em paleossolos.

Sheldon *et al.* (2002) propuseram a seguinte equação:

$$MAP (\text{mm}) = 221e^{0,0197(CIA-K)},$$

na qual  $R^2 = 0.72$  (coeficiente de determinação) e  $s = \pm 182 \text{ mm}$  (desvio padrão).

Altos valores de CIA-K refletem altos valores de precipitação e consequentemente os solos foram submetidos a intensos processos de alteração química. Em geral, tais processos culminaram com a lixiviação dos elementos solúveis alcalinos e alcalinos terrosos e com a concentração de elementos menos solúveis como o alumínio. Índices de alteração química iguais a 100 (CIA-K = 100) são equivalentes às estimativas de precipitação de aproximadamente 1585 mm/ano (Sheldon *et al.*, 2002).

Neste estudo, o cálculo da paleoprecipitação por meio de índices de alteração química foi conduzido em 11 horizontes Bt.

## 5. Paleossolos da Formação Marília

Na Formação Marília, foram reconhecidas 4 ordens de paleossolos: *Aridisols*, *Alfisols*, *Entisols* e *Vertisols*. Contudo, neste estudo, apenas os perfis de *Aridisols* e *Alfisols* serão abordados em detalhe, pois possuem significado paleoclimático, e a gênese das feições cálcicas e argílicas estão associadas ao desenvolvimento desses perfis.

### 5.1. *Aridisols*

Os *Aridisols* correspondem ao tipo de paleossolo mais freqüente na área de estudo; foram descritos 18 perfis, que representam 43% da espessura da Formação Marília (Figura 2A).

Os perfis apresentam espessuras variáveis de 0,3 m a 7 m. Em geral, os perfis apresentam seqüência de horizontes Bt/Btk/Bk(ou Bkm)/C(ou Ck). Poucos perfis apresentam o horizonte

superficial A preservado; em muitos casos, este horizonte foi decapitado por atividade de erosão eólica. As cores variam de vermelho (10R5/8), vermelho-claro (10R6/8) a bruno-avermelhado (10R4/6). As texturas arenosas são preponderantes, com granulação predominante de areia fina a média. As estruturas pedogênicas (peds) variam de acordo com os horizontes; em geral exibem estruturação forte, com alto grau de desenvolvimento e tamanhos grandes, podendo atingir mais de 40 cm de diâmetro nos horizontes B (Figura 2B). Estruturas granulares muito grandes (2 cm a 4 cm de diâmetro) podem ser vistas nos horizontes A. Nos horizontes B (Bt e Btk) prevalecem as estruturas grande a muito grande prismática e em blocos sub- e angulares. Em alguns casos, as estruturas prismáticas primárias podem ser quebradas em estruturas em blocos angulares secundárias, que revelam o alto grau de desenvolvimento pedogênico. Outras estruturas como laminar e maciça estão associadas a horizontes Bkm e C, Ck, respectivamente.

As superfícies dos peds freqüentemente apresentam revestimentos (*coatings*) de filmes pretos (N3) de oxihidróxidos de manganês e revestimentos de carbonato de cálcio. Muitas vezes ambos os revestimentos ocorrem associados, preenchendo a porosidade de bioturbação dos horizontes. Nos horizontes Bt, o revestimento pode ter um aspecto brilhante e ceroso, devido à infiltração mecânica de argilas que se acumulam nas superfícies dos peds, preenchem a porosidade e, podem formar pontes de argila entre os grãos de areia.

O principal agente cimentante dos horizontes é o carbonato de cálcio. Os horizontes mostram graduação entre horizontes fracamente cimentados (Bt), fortemente (Btk e Ck) a extremamente cimentados (Bk e Bkm). Freqüentemente as concentrações de carbonato de cálcio formam glébulas, em sua maioria nódulos e algumas septárias. Os nódulos possuem estrutura interna indiferenciada, são macios a duros, brancos, com dimensões que variam de <1 cm a 5 cm de diâmetro, e possuem formas subesféricas, elipsoidais, amigdaloidais e irregulares. Outros tipos de glébulas, como os halos glebulares, são macios, brancos, pequenos (0,2 cm a 1 cm de diâmetro) e irregulares. Em alguns casos, os nódulos podem ocupar até 50% do volume dos horizontes, formando horizontes endurecidos de calcrete pedogênico (Figura 2C).



**Figura 2.** Feições pedogênicas descritas nos *Aridisols*. A) Visão geral de um afloramento com diversos perfis de *Aridisols* superpostos. Ponto 1 na figura 1. B) Estrutura prismática muito grande em horizontes Btk. Ponto 2 na figura 1. C) Nódulos endurecidos e coalescentes de carbonato de cálcio em horizonte Bk, formando horizontes de calcreto pedogênico. Ponto 6 na figura 1.

Estruturas de bioturbação como rizólitos, crotovinas, halos de redução e escavações animais são comuns principalmente nos horizontes superiores dos paleossolos (A, B). Os icnofósseis exibem diversas estruturas que foram discriminadas com base na forma dos relevos de limite, presentes na base (hiporrelevo) e topo (epirrelevo) das camadas, que assumem formas côncavas ou convexas. Em geral, correspondem a estruturas cilíndricas alongadas na vertical, com ramificações laterais e afinamento para a base, como os rizólitos, que podem atingir até 10

cm de comprimento e diâmetros que variam de 0,5 cm no topo a 0,2 cm na base das ramificações.

Escavações meandrantes com disposição horizontal a oblíqua em relação ao substrato, podendo entrecruzar-se, com dimensões e configurações variadas e preenchimento diferente da matriz; são menores ainda, de 0,1 cm a 0,2 cm de diâmetro e no máximo 14 cm de comprimento, e foram atribuídas à atividade de organismos vermiformes do icnogênero *Planolites* (Figura 3). Outras estruturas com formas subesféricas em planta e tubulares longitudinalmente, como as crotovinas (Figura 4), foram diferenciadas com base no contraste de cor e granulação entre o material da matriz e do preenchimento. Freqüentemente, o preenchimento das bioturbações é composto por areia fina ou média e calcita espática.

A transição entre os horizontes é clara a gradual com superfície de separação ondulada a irregular. Quando a transição é de forma abrupta e plana, essa é marcada pela intensa concentração de nódulos carbonáticos em um horizonte ou separada por superfícies de erosão planas suborizontais. Alguns perfis de *Aridisols* são do tipo *compound* (Duchaufour, 1982) ou *multistorey* (Morrison, 1967), separados por superfícies de erosão planas suborizontais, causadas pela deflação eólica. Estes perfis não mostram poligenia, e apresentam sucessão vertical marcada por horizontes diagnósticos distintos, que evidenciam diferentes episódios alternados de sedimentação, pedogênese e erosão. Os perfis do tipo *polygenetic* ou *composite* (Morrison, 1967) indicam a superposição de diferentes fases de evolução pedogênica, marcadas em afloramento por perfis espessos que exibem recorrência de características similares em horizontes distintos do mesmo perfil.



**Figura 3.** Estruturas de bioturbação produzidas por animais vermiformes sedimentívoros do icnogênero *Planolites*. Ponto 6 na figura 1.



**Figura 4.** Crotovina descrita em Aridisol, com clara diferenciação de cor entre a matriz do paleossolo e do material de preenchimento. Ponto 7 na figura 1.

## 5.2. *Alfisols*

Apenas um perfil representativo da ordem dos *Alfisols* foi descrito na Formação Marília. Este perfil possui 3,57 m de espessura e ocorre próximo ao município de Itajá (GO). O perfil

encontra-se sobreposto a uma sucessão poligenética composta por 5 perfis de *Aridisols*, da qual é separado por uma superfície erodida plana levemente inclinada gerada por deflação eólica. O perfil apresenta apenas seqüência de horizontes Bt/Btk (Figura 5). As cores predominantes são vermelho (10R4/8), bruno-avermelhado (10R4/6) e vermelho-claro (10R7/8). A textura é arenosa, com granulação de areia fina nos horizontes superiores Bt e areia média nos horizontes inferiores Btk. As estruturas pedogênicas apresentam alto grau de desenvolvimento e tamanhos grandes. As estruturas dos horizontes Bt e Btk variam de grande a muito grande em blocos sub- e angulares, com estruturação secundária moderada de média a grande em blocos sub- e angulares (Figura 6).

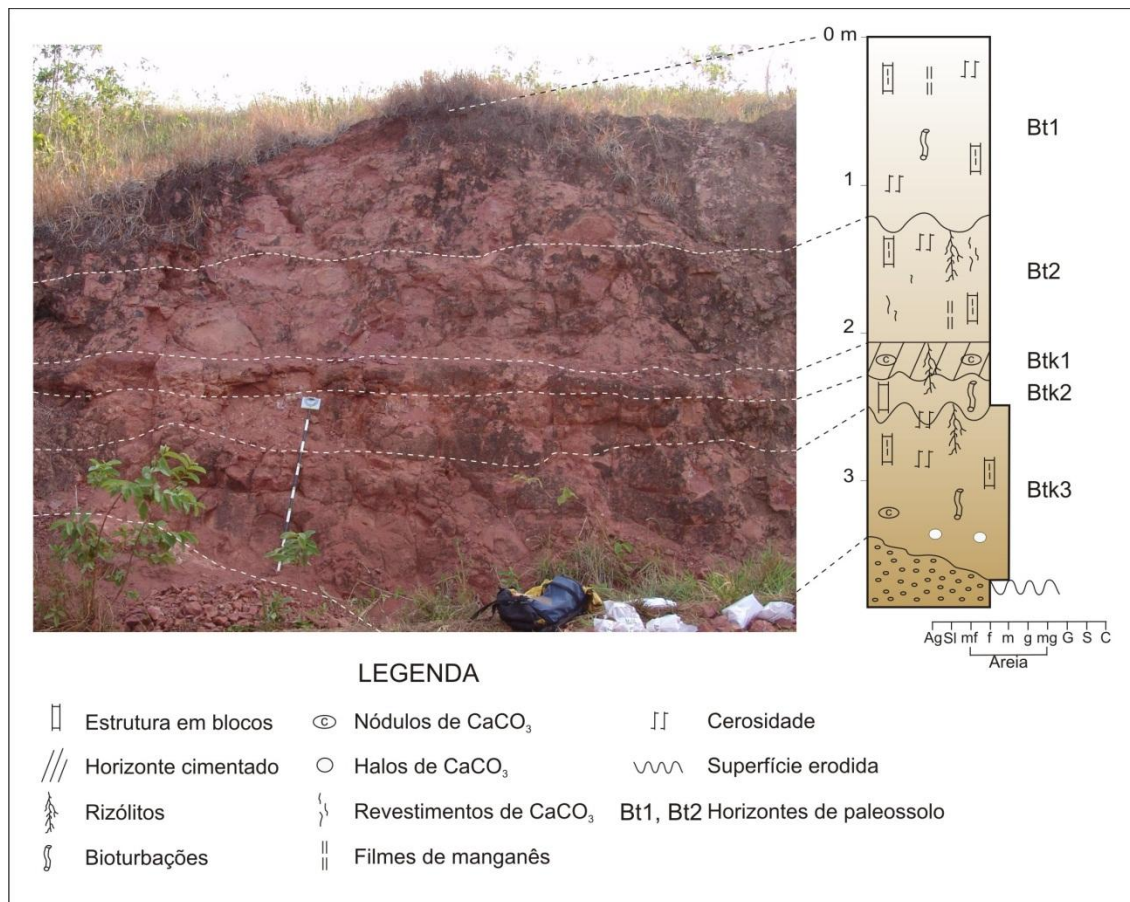


**Figura 5.** Perfil de *Alfisol* que ocorre próximo ao município de Itajá (GO). Ponto 7 na figura 1.

Os revestimentos mais comuns são filmes pretos (N3) de oxihidróxidos de manganês e cerosidade que ocorrem em todos os horizontes. Revestimentos de carbonato de cálcio ocorrem exclusivamente nos horizontes Btk.

Os horizontes se apresentam cimentados por carbonato de cálcio e mostram graduação entre horizontes fracamente (Bt), fortemente (Btk2 e Btk3) a extremamente cimentados (Btk1). Glébulas de carbonato de cálcio ocorrem apenas nos horizontes Btk e exibem variações entre nódulos e halos glebulares. Os nódulos possuem estrutura interna indiferenciada, são macios a duros, brancos, com dimensões que variam de <0,1 cm a 3,5 cm de diâmetro e formas subesféricas, elipsoidais e amigdaloidais. Os halos glebulares são macios, brancos, pequenos a médios (0,4 cm a 0,7 cm de diâmetro) e irregulares.

Estruturas de bioturbação ocorrem em todos os horizontes. Os rizólitos exibem estruturas em tubos cilíndricos alongados na vertical e apresentam ramificações laterais com afinamento em direção a base das ramificações. Os diâmetros variam de 1 cm a 1,2 cm no eixo principal e 0,4 cm a 0,6 cm nas ramificações, com comprimento máximo de 18 cm (Figura 7). Outras escavações que ocorrem nos horizontes Bt foram atribuídas à atividade de artrópodes do icnogênero *Macanopsis*. Estas escavações são subcilíndricas e ocorrem dispostas verticalmente ao substrato, não-ramificadas e apresentam extremidade basal arredondada (possível icnito de habitação). Os diâmetros são menores que dos rizólitos, usualmente 0,5 cm de diâmetro e 2,4 cm a 4 cm de comprimento. As bioturbações estão preenchidas em sua maior parte por areia fina e calcita microcristalina.

A transição entre os horizontes ocorre principalmente de forma clara a gradual com superfície de separação ondulada.



**Figura 6.** Estrutura em blocos muito grande, descrita no horizonte Bt1 do perfil de *Alfisol* da figura 5.



**Figura 7.** Rizólito descrito no horizonte Btk3 do perfil de *Alfisol* da figura 5.

## 6. Estimativas de paleoprecipitação

Os cálculos de estimativas de paleoprecipitação foram realizados com o uso da profundidade de horizontes cálcicos Bk e por meio de índices de alteração química de horizontes Bt. O uso dos índices de alteração química de horizontes Bt na área de estudo se mostrou mais profícuo, pois se baseia nas características dos horizontes B e não requer a preservação completa dos perfis, portanto pode ser aplicado mesmo em perfis com o horizonte superficial A erodido.

A aplicação dos resultados das estimativas de paleoprecipitação para a construção de uma série temporal de variabilidade paleoclimática na Formação Marília é problemática, pois faltam datações e marcadores estratigráficos que permitam a correlação das diferentes áreas de exposição da formação. Os resultados apresentados neste estudo refletem dois momentos distintos de evolução paleoclimática durante a deposição e formação de solos na Formação Marília e contrastam com estudos anteriores que admitiam o imperativo de paleoclimas áridos durante toda a evolução dessa formação (Soares *et al.*, 1980; Suguio & Barcelos, 1983).

As estimativas de paleoprecipitação calculadas com a profundidade de horizontes cálcicos apresentaram valores médios de 240 mm/ano (Figura 8). Estes valores são consistentes com a observação das feições macro- e micromorfológicas que ocorrem nestes horizontes.

As estimativas realizadas por meio da geoquímica de horizontes Bt apresentaram considerável incremento na quantidade de chuvas, com valores médios de 824 mm/ano (Figura 8, Tabela 2).

Estes valores refletem um momento distinto de evolução da Formação Marília, no qual os carbonatos depositados em fases mais secas passaram a sofrer lixiviação e o processo dominante se tornou a iluviação de ferro e argila e a formação de horizontes Bt.

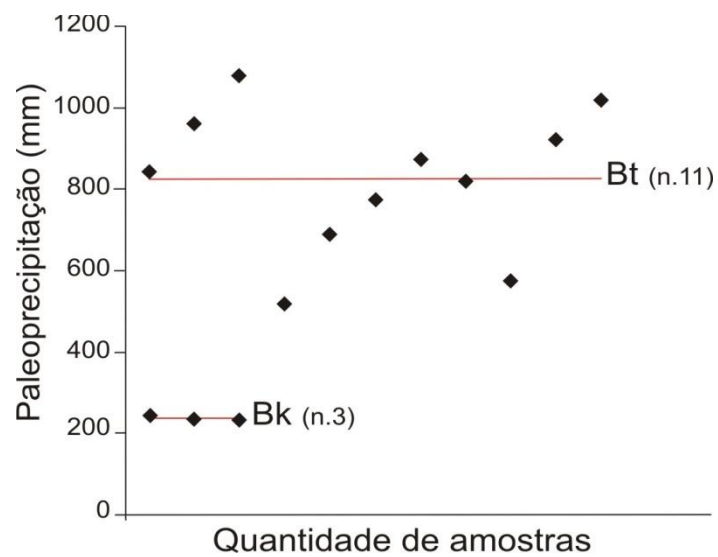


**Figura 8.** Estimativas de paleoprecipitação calculadas nos horizontes Bk e Bt. A linha vermelha disposta na horizontal indica a média dos valores obtidos.

**Tabela 2.** Dados geoquímicos dos horizontes Bt (% em peso).

Perfil/ Amostra	SiO <sub>2</sub>	TiO <sub>2</sub>	Al <sub>2</sub> O <sub>3</sub>	Fe <sub>2</sub> O <sub>3</sub>	MnO	MgO	CaO	Na <sub>2</sub> O	K <sub>2</sub> O	P <sub>2</sub> O <sub>5</sub>	LOI	Total	CIA-K <sup>a</sup>	MAP <sup>a</sup>
<b>Alfisol (Itajá – GO)</b>														
<b>Bt1 (P2H1)</b>	83,08	1,02	3,87	3,51	0,04	2,64	0,92	0,09	1,27	0,05	3,80	100,3	68,00	843
<b>Bt2 (P2H2)</b>	82,44	1,31	4,75	4,34	0,04	1,83	0,74	0,16	1,66	0,05	3,08	100,4	74,70	962
<b>Aridisol (Itajá – GO)</b>														
<b>Bt1 (CI2)</b>	82,29	1,26	5,12	4,52	0,06	1,68	0,53	0,17	1,78	0,08	2,81	100,3	80,46	1078
<b>Bt2 (CI6)</b>	72,70	1,35	5,36	4,46	0,04	3,02	3,71	0,17	2,01	0,07	6,72	99,6	43,27	518
<b>Bt3 (CI7)</b>	74,45	1,66	5,95	5,28	0,10	2,89	2,19	0,21	2,11	0,09	5,40	100,3	57,89	691
<b>Bt4 (CI9)</b>	75,37	1,25	6,55	4,42	0,06	3,05	1,87	0,20	2,34	0,09	5,10	100,3	63,72	775
<b>Aridisol (Monte Alto – SP)</b>														
<b>Bt1 (MA2)</b>	87,35	0,47	4,74	1,74	0,08	0,47	0,61	0,59	2,22	0,03	1,68	99,98	69,56	870
<b>Bt2 (MA10)</b>	85,02	0,46	5,48	1,60	0,05	0,76	0,78	0,81	2,57	0,03	2,42	99,98	66,62	821
<b>Bt3 (MA12)</b>	77,68	0,67	6,54	2,46	0,05	3,19	3,44	0,39	1,97	0,03	3,57	99,99	48,67	576
<b>Aridisol (Marília – SP)</b>														
<b>Bt1 (SLN1)</b>	84,18	0,49	5,96	1,91	0,03	1,42	1,11	0,15	1,87	0,02	2,91	100	72,54	922
<b>Bt2 (FRX6)</b>	86,84	0,40	4,98	1,59	0,01	1,45	0,68	0,13	1,65	0,02	2,45	100,2	77,58	1018

<sup>a</sup> CIA-K = 100 x (Al<sub>2</sub>O<sub>3</sub>/(Al<sub>2</sub>O<sub>3</sub>+CaO+Na<sub>2</sub>O)); MAP (mm) = 221e<sup>0,0197(CIA-K)</sup>.

A presença de paligorsquita como argilomineral dominante nos horizontes Bt analisados indica que o material utilizado para a difração possui carbonatos em sua composição, pois a presença de paligorsquita em horizonte iluvial Bt é um indício de que o horizonte possui pequenos nódulos ou filamentos iluviais de carbonato de cálcio em torno de grãos (Figura 9). A paligorsquita nesses horizontes ocorre aprisionada na estrutura cristalina das calcitas que formam os pequenos nódulos e filamentos (Khademi & Mermut, 1999). Já nos horizontes Bk, a presença de paligorsquita é associada aos processos de neoformação da paligorsquita em horizontes cálcicos ricos em Mg e Si sob condições de pH>8 (Singer, 1989). Segundo Paquet & Millot (1972), a paligorsquita é um argilomineral instável em solos submetidos a índices de precipitação

superiores a 300 mm e se transforma, em sua maioria, em esmectita. Khormali & Abtahi (2003) mostraram que o fato da paligorsquita ser o argilomineral preponderante nos horizontes argílicos do sul do Irã está associado ao aprisionamento da paligorsquita na estrutura cristalina da calcita, que se deposita nos horizontes Bt após os processos de iluviação das argilas.

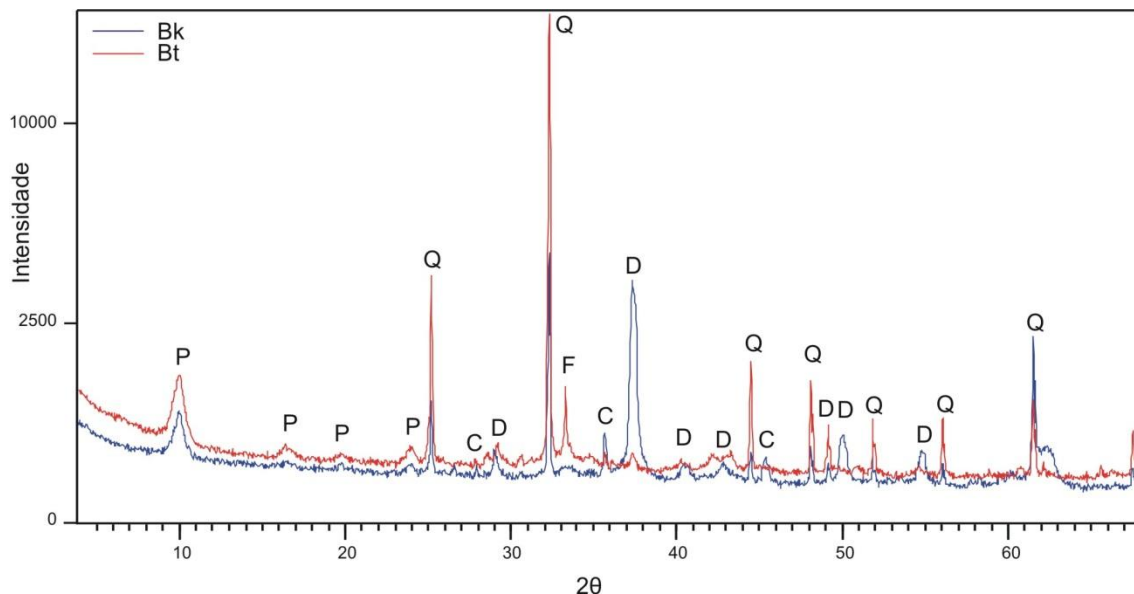


**Figura 9.** Difratograma de DRX em lâminas orientadas (fração <2 µm) de amostras de horizonte Bk de *Aridisol* e Bt de *Alfisol* (ponto 7 na Figura 1). A maior intensidade dos picos obtida na amostra do horizonte Bt (em vermelho) está associada à maior concentração de óxidos e hidróxidos de Fe de baixa cristalinidade ou amorfos na amostra. P = paligorsquita; Q = quartzo; C = calcita; D = dolomita; F = feldspato.

## 7. Gênese das feições cárnicas

A gênese de feições que indicam a concentração de carbonato de cálcio em paleossolos desenvolvidos sobre material de origem eólica não carbonático, como o caso dos paleossolos da Formação Marília, emerge uma série de questões. A possibilidade de que o carbonato de cálcio tenha origem geogênica, ligada à atividade do lençol freático, foi descartada com base no reconhecimento de diversas feições exclusivas da atividade pedogenética: distribuição irregular do carbonato de cálcio nos perfis (alguns perfis exibem estágios distintos de concentração, como revestimentos, nódulos e lâminas endurecidas), presença de cutâs de calcita (calcãs) sobre cutâs de ferro e argila (ferriargilãs), ocorrência de cimentação em pontes e meniscos ligando os grãos do arcabouço, ocorrência disseminada de nódulos típicos (órticos) de calcita microcristalina e

ausência de nódulos ou bandas de calcita espática seguindo os planos de estratificação. Pimentel *et al.* (1996) listaram uma série de atributos que permitem a distinção entre as formas de concentração de carbonato de cálcio ligadas à atividade de percolação de águas enriquecidas em CaCO<sub>3</sub> e outras exclusivas à pedogênese. Segundo os autores, o reconhecimento de feições diagnósticas da pedogênese como perfis pouco espessos (2 a 3 m) organizados em horizontes, estruturas pedogênicas (nodular, laminar, prismática e blocos) e rizólitos, somados a ausência de feições disseminadas de redução de ferro, como mosqueamento proeminente, e ausência de variações mineralógicas entre os carbonatos e outros minerais de origem evaporítica no mesmo perfil (dolomita, gipsita, halita) permite essa distinção. A observação de microfeições com textura do tipo alfa (Wright, 1990), como cristalárias, nódulos, preenchimentos, grãos do arcabouço “flutuantes”, estruturas plásicas cristalíticas, hipocutâs, franjas de calcita espática e feições de crescimento expansivo (*displacive*) e outras ligadas à origem biogênica com textura do tipo beta como tubos de raízes (Figura 10), escavações animais e filamentos de fungos calcificados (Figura 11), corroboram a origem pedogênica dos perfis estudados.

A principal fonte de CaCO<sub>3</sub> para o desenvolvimento de perfis pedogênicos com acumulações de carbonato de cálcio é a poeira eólica (Goudie, 1973). Poeiras ricas em íons de Ca se acumulam na superfície dos perfis e são dissolvidas pelas águas de chuva. A combinação entre os íons de cálcio com o ácido carbônico, derivado em grande parte do CO<sub>2</sub> liberado pela respiração das raízes das plantas, formará o CaCO<sub>3</sub> que irá se precipitar no perfil de solo a uma profundidade relativa à quantidade de água disponível na frente de molhamento (Jenny, 1941). A taxa de acumulação do CaCO<sub>3</sub> em perfis pedogênicos está ligada a espessura dos horizontes Bk e BCk (Bockheim & Douglass, 2006). Machette (1985) quantificou que a taxa média de acumulação de CaCO<sub>3</sub> por adição de poeira eólica, em três áreas dos estados do Novo México e Utah (EUA), foi de 0,2 g de CaCO<sub>3</sub> por cm<sup>2</sup> por 10<sup>3</sup> anos. Estas taxas são similares às calculadas posteriormente por Eghbal & Southard (1993) em *Aridisols* com horizontes cálcicos desenvolvidos no deserto de Mojave (Califórnia). O mecanismo de lixiviação de bicarbonatos e íons de cálcio, referido por Goudie (1983) como modelo de eluviação (*per descensum model*), é aqui postulado como o principal agente de concentração dos carbonatos e consequentemente de formação das feições cálcicas nos paleossolos da Formação Marília.

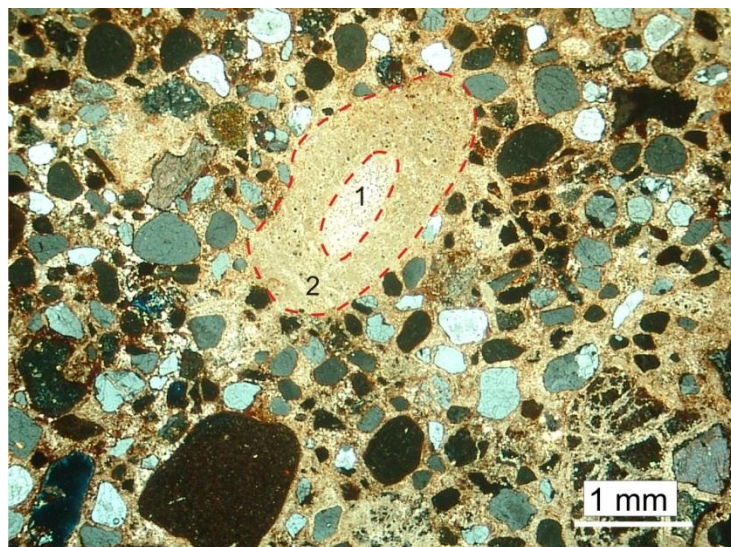


**Figura 10.** Feição elipsoidal produzida por raiz em lâmina de horizonte Bk de *Aridisol* (ponto 7 na figura 1). O processo de calcificação ocorreu de forma diferenciada na estrutura radicular. O número 1 indica a calcificação no parênquima medular e o número 2 mostra a calcificação no parênquima cortical.

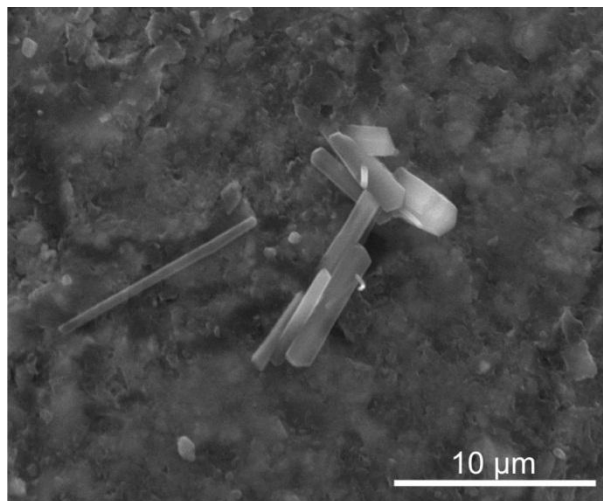


**Figura 11.** Imagem obtida em MEV de calcitas com formas aciculares (*needle-fibre calcite*) associada a filamentos de fungos calcificados que ocorrem no interior de tubos de raízes em horizonte Bk de *Aridisol*. Ponto 2 na figura 1.

## 8. Gênese das feições argílicas

Grande parte das feições argílicas observadas ocorrem nos horizontes Bt e Btk. Nos 11 horizontes Bt estudados, o percentual de cutâs de iluviação (ferriargilás) que ocorrem na matriz dos paleossolos foi superior a 1% da área das lâminas delgadas, que é o percentual mínimo

requerido a classificação de um horizonte argílico (Soil Survey Staff, 1999). Nos horizontes Btk, esses percentuais podem ser menores, devido ao alto conteúdo de Ca em alguns horizontes, que devem ter provocado a floculação das argilas e assim inibiram a formação de ferriargilás iluviais.

Em campo, os ferriargilás, referidos como cerosidade, ocorrem revestindo as paredes dos peds, na forma de filmes finos em torno de grãos siliciclásticos, e formando pontes que preenchem a porosidade e unem os grãos. Em lâminas, ocorrem sob a superfície de grãos livres e preenchendo a porosidade de empilhamento e canais. Os ferriargilás de grãos livres apresentam variações entre cutâs de capeamento e de ligação. Os ferriargilás de canais foram classificados em típicos e crescentes. Este último, só ocorre em poros funcionais maiores, que formaram uma espécie de baía e foram capazes de aprisionar água por mais tempo, provocando um hidromorfismo temporário que permitiu a desestabilização das ligações ferro-argila, facilitando assim a migração e deposição do ferro e posteriormente da argila (Cooper & Vidal-Torrado, 2000). Internamente, esses cutâs apresentam laminação, microfissuração e segregação pós-deposicional de ferro (Figura 12).

A acumulação de argila em horizontes de solo de ambientes áridos tem sido atribuída à deposição de poeira eólica na superfície dos solos, com posterior desenvolvimento e espessamento de horizontes argílicos ao longo do tempo (Wells *et al.*, 1987). Os cálculos de paleoprecipitação indicaram valores mínimos de 518 mm/ano durante o desenvolvimento dos horizontes Bt. Estes valores são considerados suficientes para causar a eluviação de grande parte dos carbonatos e formação de um horizonte argílico, mesmo em curto período de tempo. Holliday (1985) descreveu uma série de horizontes argílicos desenvolvidos sobre depósitos de dunas eólicas no Texas (EUA), com idades aproximadas de 450 anos, em áreas onde os índices de precipitação não ultrapassam os 468 mm/ano.

O modelo de formação dos horizontes argílicos parece seguir os mesmos pressupostos de formação dos horizontes cálcicos: a) deposição de poeiras eólicas, b) iluviação do material. A diferenciação nos processos ocorreu devido ao incremento nos índices de paleoprecipitação que, nos horizontes argílicos, favoreceram a dispersão coloidal das argilas, com posterior translocação e acumulação. Provavelmente, os processos de substituição dos ferriargilás por carbonato de cálcio foram de tamanha intensidade nos horizontes Btk que não é possível a observação dessas feições mesmo em lâminas delgadas.

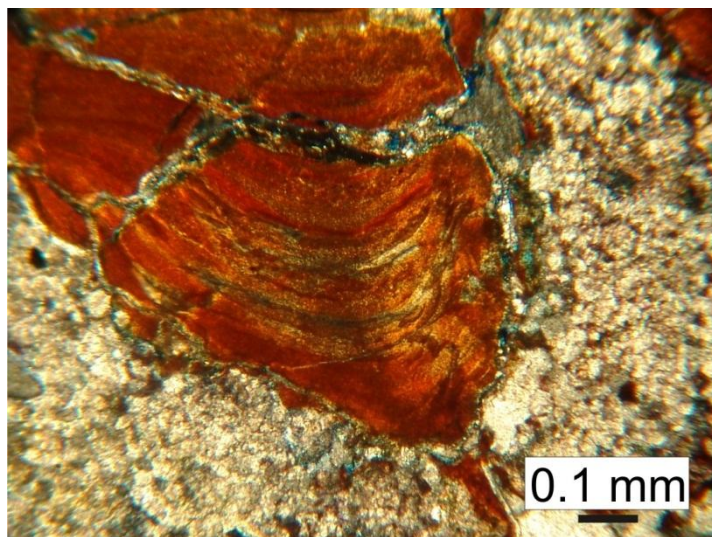


**Figura 12.** Ferriargilã iluvial descrito no horizonte Bt2 do perfil de *Alfisol* da figura 2, mostrando laminação interna, microfissuração e segregação pós-deposicional de ferro.

## 9. Conclusões

A análise de feições macro- e micromorfológicas, em conjunto com a análise da geoquímica de duas ordens de paleossolos na Formação Marília, revelou que a gênese das concentrações secundárias de carbonato de cálcio, bem como das associadas à concentração de ferro e argila, foram controladas por processos pedogênicos que permitiram a diferenciação e concentração dessas feições em horizontes cárpicos Bk de *Aridisols* e argílicos Bt de *Aridisols* e *Alfisols*. O principal fator de controle a diferenciação dos processos pedogênicos que culminaram com a formação desses horizontes nos paleossolos estudados foi o clima. As estimativas de paleoprecipitação revelaram dois momentos distintos de evolução paleoclimática da Formação Marília, um caracterizado por momentos de maior aridez, com índices de paleoprecipitação em torno de 240 mm/ano, que permitiram o desenvolvimento de horizontes cárpicos e outro com valores médios de 824 mm/ano, suficientes para a lixiviação dos carbonatos e favorecimento dos processos de dispersão, translocação e acumulação de argilas nos horizontes argílicos.

Provavelmente, o regime climático que prevaleceu durante a evolução da Formação Marília foi semi-árido, devido à preponderância dos carbonatos nos horizontes de paleossolo. Os momentos de maior pluviosidade parecem ser pontuais, e estariam ligados a condições sazonais mais úmidas. A ocorrência de horizontes argílicos Btk em *Aridisols* e *Alfisols* que

apresentam feições cárnicas e argílicas superpostas reforça a interpretação de sazonalidade do clima. Porém, a ausência de um marco estratigráfico nos paleossolos estudados, somado à ausência de um controle temporal entre as fases de iluviação e lixiviação dos carbonatos, não permite, nesse momento, uma reconstrução paleoclimática em termos de freqüência e períodos de duração das fases mais úmidas e secas, impossibilitando a investigação das causas que provocaram as variações paleoclimáticas.

## Agradecimentos

Os autores agradecem à Fundação de Amparo à Pesquisa do Estado de São Paulo (processos 07/00140-6 e 07/02079-2) pelo auxílio financeiro, ao Conselho Nacional de Desenvolvimento Científico e Tecnológico pela concessão da bolsa de doutorado ao primeiro autor e a *International Association of Sedimentologists* pelo auxílio financeiro através do *PhD Grant* ao primeiro autor.

## 10. Referências bibliográficas

- ALONSO-ZARZA, A.M. Palaeoenvironmental significance of palustrine carbonates and calcretes in the geological record. **Earth-Science Reviews**, v. 60, p. 261-298, 2003.
- ARKLEY, R.J. Calculation of carbonate and water movement in soil from climatic data. **Soil Science**, v. 96, p. 239-248, 1963.
- BASILICI, G.; DAL' BO, P.F.F.; LADEIRA, F.S.B. Climate-induced sediment-palaeosol cycles in a Late Cretaceous dry aeolian sand sheet: Marília Formation (North-West Bauru Basin, Brazil). **Sedimentology**, v. 56, p. 1876-1904, 2009.
- BATEZELLI, A. **Redefinição litoestratigráfica da unidade Araçatuba e da sua extensão regional na Bacia Bauru no estado de São Paulo**. Rio Claro, 1998. 110 p. Dissertação (Mestrado) - Instituto de Geociências e Ciências Exatas, Universidade Estadual Paulista.
- BATEZELLI, A. **Análise da sedimentação cretácea no triângulo mineiro e sua correlação com áreas adjacentes**. Rio Claro, 2003. 183 p. Tese (Doutorado) - Instituto de Geociências e Ciências Exatas, Universidade Estadual Paulista.
- BIRKELAND, P.W. **Soils and Geomorphology**, 3rd edition. New York: Oxford University Press, 430 p., 1999.
- BOCKHEIM, J.G. & DOUGLASS, D.C. Origin and significance of calcium carbonate in soils of southwestern Patagonia. **Geoderma**, v. 136, p. 751-762, 2006.

BRONGER, A.; WINTER, R.; SEDOV, S. Weathering and clay mineral formation in two Holocene soils and in buried paleosols in Tadzhikistan: towards a Quaternary paleoclimatic record in Central Asia. **Catena**, v. 34, p. 19-34, 1998.

BULLOCK, P.; FEDOROFF, N.; JONGERIUS, A.; STOOPS, G.; TURSINA, T. **Handbook for soil thin section description**. Wolverhampton: Waine Research Publications, 152 p., 1985.

CASTRO, S.S. **Micromorfologia de solos: bases para descrição de lâminas delgadas**. Campinas: Universidade Estadual de Campinas, 143 p., 2002.

CATT, J.A. Paleopedology manual. **Quaternary International**, v. 6, p. 1-95, 1990.

CLEVELAND, D.M.; NORDT, L.C.; ATCHLEY, S.C. Paleosols, trace fossils, and precipitation estimates of the uppermost Triassic strata in northern New Mexico. **Palaeogeography, Palaeoclimatology, Palaeoecology**, v. 257, p. 421-444, 2008.

COOPER, M. & VIDAL-TORRADO, P. Gênese de ferri-argilás em horizontes B texturais de uma seqüência de solos sobre diabásio em Piracicaba (SP). **Scientia Agricola**, v. 57, n.4, p. 745-750, 2000.

DAL' BO, P.F.F. **Inter-relação paleossolos e sedimentos em lençóis de areia eólica da Formação Marília (noroeste da Bacia Bauru)**. Campinas, 2008. 99 p. Dissertação (Mestrado) – Instituto de Geociências, Universidade Estadual de Campinas.

DIAS-BRITO, D.; MUSACCIO, E.A.; CASTRO, J.C.; MARANHÃO, M.S.; SUAREZ, J.M.; RODRIGUES, R. Grupo Bauru: uma unidade continental do Cretáceo no Brasil – concepções baseadas em dados micropaleontológicos, isotópicos e estratigráficos. **Revue de Paléobiologie**, v. 20, n. 1, p. 245-304, 2001.

DUCHAUFOUR, P. **Pedology: pedogenesis and classification**. London: George Allen & Unwin, 187 p., 1982.

EGHBAL, M.K. & SOUTHARD, R.J. Micromorphological evidence of polygenesis of three Aridisols, western Mojave Desert, California. **Soil Science Society of America Journal**, v. 57, p. 1041-1050, 1993.

ERNESTO, M.; BATEZELLI, A.; SAAD, A.R.; ETCHEBEHERE, M.L.C.; FÚLFARO, V.J. Início da sedimentação suprabasáltica na Bacia do Paraná: paleomagnetismo do Grupo Caiuá (oeste de São Paulo e noroeste do Paraná). In: SIMPÓSIO DO CRETÁCEO DO BRASIL, 7 e SIMPÓSIO DO TERCIÁRIO DO BRASIL, 1. **Boletim...** Serra Negra, 2006, p. 48.

ESWARAN, H. & SYS, C. Argillic horizon formation in low activity clay soils, formation and significance to classification. **Pedologie**, v. 29, p. 175-190, 1979.

ETCHEBEHERE, M.L.C.; SILVA, R.B.; SAAD, A.R.; RESENDE, A.C. Reavaliação do potencial do Grupo Bauru para evaporitos e salmouras continentais. **Geociências**, v. 12, p. 333-352, 1993.

FERNANDES, L.A. **A cobertura cretácea suprabasáltica no estado do Paraná e pontal do paranapanema (SP): os grupos Bauru e Caiuá**. São Paulo, 1992. 171 p. Dissertação (Mestrado) - Instituto de Geociências, Universidade de São Paulo.

FERNANDES, L.A. **Estratigrafia e evolução geológica da parte oriental da Bacia Bauru (Ks, Brasil)**. São Paulo, 1998. 216 p. Tese (Doutorado) - Instituto de Geociências, Universidade de São Paulo.

FERNANDES L.A. & COIMBRA A.M. O Grupo Caiuá (Ks): revisão estratigráfica e contexto deposicional. **Revista Brasileira de Geociências**, v. 24, n. 3, p. 164-176, 1994.

FERNANDES, L.A. & COIMBRA, A.M. A Bacia Bauru (Cretáceo Superior, Brasil). **Anais da Academia Brasileira de Ciências**, v. 68, n. 2, p. 195-205, 1996.

FERNANDES, L.A. & COIMBRA, A.M. Revisão estratigráfica da parte oriental da Bacia Bauru (Neocretáceo). **Revista Brasileira de Geociências**, v. 30, n. 4, p. 717-728, 2000.

FÚLFARO, V.J.; ETCHEBEHERE, M.L.C.; PERINOTTO, J.A.J.; SAAD, A.R. Santo Anastácio: um Geossolo cretácico na Bacia Caiuá. In: **SIMPÓSIO SOBRE O CRETÁCEO DO BRASIL, 5, SIMPOSIO SOBRE EL CRETÁCICO DE AMÉRICA DEL SUR, 1. Boletim...** Serra Negra, 1999, p. 125-130.

GILE, L.H.; PETERSON, F.F.; GROSSMAN, R.B. Morphological and genetic sequences of carbonate accumulation in desert soils. **Soil Science**, v. 101, p. 347-354, 1966.

GOUDIE, A.S. **Duricrusts in Tropical and Subtropical Landscapes**. Oxford: Claredon, 174 p., 1973.

GOUDIE, A.S., Calcrete. In: GOUDIE, A.S. & PYE, K. (Eds.). **Chemical Sediments and Geomorphology: Precipitates and Residual in Near-Surface Environment**. London: Academic Press, p. 93-131, 1983.

HASUI, Y. A Formação Uberaba. In: CONGRESSO BRASILEIRO DE GEOLOGIA, 22, 1968, Belo Horizonte. **Anais...** Belo Horizonte, Sociedade Brasileira de Geologia, 1968, p. 167-179.

HOLLIDAY, V.T. Morphology of late Holocene soils at the Lubbock Lake archeological site, Texas. **Soil Science Society of American Journal**, v. 49, p. 938-946, 1985.

IPT - INSTITUTO DE PESQUISAS TECNOLÓGICAS DO ESTADO DE SÃO PAULO. **Mapa Geológico do Estado de São Paulo, 1:500.000**. Nota explicativa. São Paulo, 126 p., 1981.

- JENNY, H.J. **Factors of soil formation**. New York: McGraw-Hill, 281 p., 1941.
- KHADEMI, H. & MERMUT, A.R. Submicroscopy and stable isotope geochemistry of carbonates and associated palygorskite in Iranian Aridisols. **European Journal of Soil Science**, v. 50, p. 207-216, 1999.
- KHORMALI, F. & ABTAHI, A. Origin and distribution of clay minerals in calcareous arid and semi-arid soils of Fars Province, southern Iran. **Clay Minerals**, v. 38, p. 511-527, 2003.
- KHORMALI, F.; ABTAHI, A.; MAHMOODI, S.; STOOPS, G. Argillic horizon development in calcareous soils of arid and semiarid regions of southern Iran. **Catena**, v. 53, p. 273-301, 2003.
- KRAUS, M.J. Paleosols in clastic sedimentary rocks: their geologic applications. **Earth-Science Reviews**, v. 47, p. 41-70, 1999.
- MACHETTE, M.N. Calcic soils of the southwestern United States. In: WEIDE, D.L. (Ed.). **Soils and Quaternary Geology of the Southwestern United States**. Geological Society of America Special Paper, v. 203, p. 1-21, 1985.
- MAYNARD, J.B. Chemistry of modern soils as a guide to interpreting Precambrian paleosols. **Journal of Geology**, v. 100, p. 279-289, 1992.
- MILANI E.J. **Evolução tectono-estratigráfica da Bacia do Paraná e seu relacionamento com a geodinâmica fanerozóica do gondwana sul-ocidental**. Porto Alegre, 1997. 254 p. Tese (Doutorado) – Universidade Federal do Rio Grande do Sul.
- MORRISON, R.B. Principles of Quaternary soil stratigraphy. In: MORRISON, R.B. & WRIGHT, H.E. (Eds.). **Means of Correlation of Quaternary Successions**. International Union for Quaternary Research, v. 9, p. 1-69, 1967.
- NESBITT, H.W. & YOUNG, G.M. Early Proterozoic climates and plate motions inferred from major element chemistry of lutites. **Nature**, v. 299, p. 715-717, 1982.
- PAQUET, H. & MILLOT, C. Geochemical evolution of clay minerals in the weathered products and soils of Mediterranean climates. In: INTERNATIONAL CLAY CONFERENCE. **Proceedings...** Madrid, Spain, 1972, p. 199-202.
- PAULA E SILVA, F. **Geologia de subsuperfície e hidroestratigrafia do Grupo Bauru no estado de São Paulo**. Rio Claro, 2003. 166 p. Tese (Doutorado) - Instituto de Geociências e Ciências Exatas, Universidade Estadual Paulista.
- PIMENTEL, N.L.; WRIGHT, V.P.; AZEVEDO, T.M. Distinguishing early groundwater alteration effects from pedogenesis in ancient alluvial basins: examples from the Palaeogene of southern Portugal. **Sedimentary Geology**, v. 105, p. 1-10, 1996.

REHEIS, M.C. Climatic implications of alternating clay and carbonate formation in semiarid soils of south-central Montana. **Quaternary Research**, v. 27, p. 270-282, 1987.

RENNE, P.R.; ERNESTO, M.; PACCA, I.G.; COE, R.S.; GLEN, J.; PRÉVOT, M.; PERRIN, M. Rapid eruption of the Parana flood volcanism, rifting of southern Gondwanaland and the Jurassic-Cretaceous boundary. **Science**, v. 258, p. 975-979, 1992.

RETALLACK, G.J. **Soils of the Past**, 2nd edition. Oxford: Blackwell, 404 p., 2001.

RETALLACK, G.J. Pedogenic carbonate proxies for amount and seasonality of precipitation in paleosols. **Geology**, v. 33, p. 333-336, 2005.

RETALLACK, G.J. Cenozoic paleoclimate on land in North America. **Journal of Geology**, v. 115, p. 271-294, 2007.

RICCOMINI, C. Arcabouço estrutural e aspectos do tectonismo gerador e deformador da Bacia Bauru no estado de São Paulo. **Revista Brasileira de Geociências**, v. 27, n. 2, p. 153-162, 1997.

RUST, R.H. Alfisols. In: WILDING, L.P.; SMECK, N.E.; HALL, G.F. (Eds.). **Pedogenesis and Soil Taxonomy II. The Soil Orders**. Developments in Soil Science 11B. Amsterdam: Elsevier, p. 253-281, 1983.

SANTOS, P.R.; RODRIGUES, M.E.; LUZ, O.T. **A Estrutura de Piratininga: mapeamento geológico de detalhe**. São Paulo, Paulipetro – Consórcio CESP/IPT, 17 p., 1980.

SANTUCCI, R.M. & BERTINI, R.J. Distribuição paleogeográfica e biocronológica dos Titanossauros (Saurischia, Sauropoda) do Grupo Bauru, Cretáceo Superior do sudeste brasileiro. **Revista Brasileira de Geociências**, v. 31, n. 3, p. 307-314, 2001.

SHELDON, N.D. & TABOR, N.J. Quantitative paleoenvironmental and paleoclimatic reconstruction using paleosols. **Earth-Science Reviews**, v. 95, p. 1-52, 2009.

SHELDON, N.D.; RETALLACK, G.J.; TANAKA, S. Geochemical climofunctions from North American soils and application to paleosols across the Eocene–Oligocene boundary in Oregon. **Journal of Geology**, v. 110, p. 687-696, 2002.

SINGER, A. Palygorskite and sepiolite group minerals. In: DIXON, J.B. & WEED, S.B. (Eds.). **Minerals in Soil Environment**, 2nd edition. Soil Science Society of America Book Series 1, p. 829-872, 1989.

SOARES, P.C.; LANDIM, P.M.B.; FÚLFARO, V.J.; SOBREIRO NETO, A.F. Ensaio de caracterização estratigráfica do Cretáceo no estado de São Paulo: Grupo Bauru. **Revista Brasileira de Geociências**, v. 10, p. 177-185, 1980.

SOIL SURVEY STAFF. **Soil Survey Manual**. Soil Conservation Service. U.S. Department of Agriculture Handbook 18. Washington, DC, 437 p., 1993.

SOIL SURVEY STAFF. **Soil Taxonomy**, 2nd edition. U.S Department of Agriculture, Natural Resource Conservation Service 436. Washington, DC, 871 p., 1999.

SUGUIO, K. & BARCELOS, J.H. Calcretes of the Bauru Group (Cretaceous), Brazil: petrology and geological significance. **Boletim do Instituto de Geociências da Universidade de São Paulo**, v. 14, p. 31-47, 1983.

TAMRAT, E.; ERNESTO, M.; FÚLFARO, V.J.; SAAD, A.R.; BATEZELLI, A.; OLIVEIRA, A.F. Magnetoestratigrafia das formações Uberaba e Marília (Grupo Bauru) no triângulo mineiro (MG). In: SIMPÓSIO SOBRE O CRETÁCEO DO BRASIL, 6 e SIMPOSIO SOBRE EL CRETÁCICO DE AMÉRICA DEL SUR, 2. **Boletim...** São Pedro, 2002, p. 323-327.

WELLS, S.G.; MCFADDEN, L.D.; DOHRENWEND, J.C. Influence of late Quaternary climatic changes on geomorphic and pedogenic processes on a desert piedmont, eastern Mojave Desert, California. **Quaternary Research**, v. 27, p. 130-146, 1987.

WRIGHT, V.P. A micromorphological classification of fossil and recent calcic and petrocalcic microstructures. In: DOUGLAS, L.A. (Ed.). **Soil Micromorphology: a Basic and Applied Science**. Developments in Soil Science 19. Amsterdam: Elsevier, p. 401-407, 1990.

WRIGHT, V.P. & TUCKER, M.E. Calcretes: an introduction. In: WRIGHT, V.P., TUCKER, M.E. (Eds.). **Calcretes**. Oxford: Blackwell, p. 1-22, 1991.

ZAINA, J.E.; BARBOUR, Jr.E.; NEGREIROS, J.H.; RODRIGUES, M.E.; BARRETO, M.L.K.; ETCHEBEHERE, M.L.C.; OLIVEIRA, M.S.; LUZ, O.T.; ANTONINI, S.A.; MUZARDO, V.A. **Geologia do Bloco 38 e 44: Região de Araçatuba, Tupã e Marília**. São Paulo, Relatório Paulipetro, 50 p., 1980.



## ANEXO IV

“Dal’ Bo, P.F.F. & Basilici, G., 2010. *Interpretação paleoambiental da Formação Marília na porção noroeste da Bacia Bauru: relações entre sedimentação e paleopedogênese em um antigo lençol de areia eólica. Geociências, no prelo.*”



*“It is not the strongest of the species that survives, nor the most intelligent that survives. It is the one that is the most adaptable to change.”*

*Charles Robert Darwin*



# **INTERPRETAÇÃO PALEOAMBIENTAL DA FORMAÇÃO MARÍLIA NA PORÇÃO NOROESTE DA BACIA BAURU: RELAÇÕES ENTRE SEDIMENTAÇÃO E PALEOPEDOGÊNESE EM UM ANTIGO LENÇOL DE AREIA EÓLICA**

Patrick Francisco Führ Dal' Bó & Giorgio Basilici

Departamento de Geologia e Recursos Naturais, Instituto de Geociências, Universidade Estadual de Campinas (UNICAMP). Rua João Pandiá Calógeras, 51, CEP 13083-970, Cx. Postal 6152. Campinas, SP.

Endereços eletrônicos: patrickdalbo@ige.unicamp.br; basilici@ige.unicamp.br.

**Resumo** – A Formação Marília (Maastrichtiano), que aflora na porção noroeste da Bacia Bauru (estados de Goiás e Mato Grosso do Sul), é interpretada como um antigo sistema de lençol de areia eólica. A sucessão vertical estudada, com 170 m de espessura, é caracterizada por alternâncias de perfis de paleossolos, arenitos muito finos a médios e raros corpos de arenitos conglomeráticos. Quatro ordens de paleossolos foram identificadas: *Aridisols*, *Alfisols*, *Vertisols* e *Entisols*, que representam 66% do total da espessura da formação. Os depósitos foram individualizados em três litofácies: Arenito com laminação plano-paralela, Arenitos conglomeráticos e Arenito com estratificação cruzada acanalada de base côncava. Arenito com laminação plano-paralela é a litofácie mais comum descrita na área de estudo; esta forma corpos com estratificação cavalgante transladante subcrítica e é atribuída à deposição de areias com marcas onduladas eólicas. Superfícies erodidas, atribuídas à deflação eólica, marcam o contato inferior desta litofácie com o topo de perfis de *Aridisols* e *Alfisols*, indicando importantes mudanças nas condições paleoambientais, que foram responsáveis por fases distintas de construção dos corpos geológicos. Períodos caracterizados por maior aridez paleoclimática foram determinantes à construção dos lençóis de areia, caracterizados por deposição eólica em amplas superfícies morfológicas instáveis e pouco vegetadas; enquanto que, períodos com maior disponibilidade hídrica assistiram à reativação de canais efêmeros com transporte e deposição fluvial e a expansão da cobertura vegetal que propiciava a estabilização da superfície morfológica e a consequente formação de solos sobre os depósitos eólicos.

**Palavras-chave:** depósitos eólicos; paleossolos; lençóis de areia eólica; Formação Marília.

**Abstract** – *Paleoenvironmental interpretation of the Marília Formation in the northwestern portion of the Bauru Basin: Relationships between sedimentation and paleopedogenesis in an ancient eolian sand sheet.* The Marília Formation (Maastrichtian) along the outcropping belt in the northwestern portion of the Bauru Basin (Goiás and Mato Grosso do Sul states), is interpreted as an ancient eolian sand sheet. The vertical succession, ca 170 m thick, is made up of paleosols, very fine- to medium-grained sandstone and rare sandy conglomerate bodies. Four paleosol orders were identified: Aridisols, Alfisols, Vertisols, and Entisols. They represent 66% of the thickness of the Marília Formation. The deposits were discriminated in three lithofacies: Planar parallel laminated sandstone, Sandy conglomerates, and Scoured trough cross-stratified sandstone. The first, which forms bodies of sandstone characterized by subcritically climbing translatent strata, is the most common lithofacies. Eroded deflation surfaces divide the upper boundary from Aridisols and Alfisols to wind-generated deposits and mark an important change in paleoenvironmental conditions. Two alternating phases, controlled by variations in the paleoclimate, characterized the paleoenvironment of the Marília Formation: an arid phase, marked by prevalent eolian deposition was responsible for the construction of the eolian sand sheet, and a more humid phase in which occurred intense and prolonged pedogenesis of the previous eolian deposits, as well as active fluvial transport and deposition.

**Keywords:** eolian deposits; paleosols; eolian sand sheet; Marília Formation.

## **1. Introdução**

Lençóis de areia eólica ocorrem em ambientes desérticos, e são caracterizados por morfologias planas a levemente onduladas, nas quais não ocorrem dunas com faces de avalanche (Bagnold, 1941). Kocurek & Nielson (1986) estudaram 6 áreas deposicionais modernas de lençóis de areia eólica na América do Norte e listaram uma série de cinco fatores responsáveis à obstrução da construção de dunas nessas áreas: presença de sedimentos de granulação grossa (areia grossa a cascalhos), cimentação superficial, nível do lençol freático próximo à superfície, inundações periódicas e cobertura vegetal.

Os processos eólicos de sedimentação e erosão em ambientes de lençóis de areia eólica ocorrem preferencialmente em áreas caracterizadas por índices de precipitação inferiores a 250 mm/ano; áreas áridas segundo Köeppen (1948), em regiões de clima quente (Kocurek & Nielson, 1986) ou frio (Koster, 1988). A ação efetiva do vento em remover e transportar sedimentos sobre o substrato arenoso inconsolidado é facilitada nessas áreas em virtude da escassa cobertura vegetal. A atuação de processos pedogenéticos responsáveis à formação de solos depende exclusivamente da interação entre dois fatores de controle: escassez de aporte sedimentar e estabilização da superfície morfológica (Lancaster, 1993). Como consequência da estabilização da superfície, é comum em sucessões sedimentares continentais dominadas por depósitos eólicos a ocorrência de feições pedogênicas intercaladas a estruturas biogênicas como pistas, pegadas, escavações animais e rizólitos (Loope, 1988).

A Formação Marília, Neocretáceo da Bacia Bauru, exposta nos estados de Goiás e Mato Grosso do Sul, foi anteriormente interpretada como produto de deposição de leques aluviais e sistemas lacustres efêmeros (Barcelos, 1984; Fulfaro *et al.*, 1994; Batezelli, 2003; Batezelli *et al.*, 2006) e recentemente revisada por Basilici *et al.* (2009) e Basilici & Dal' Bo (2010), que a reinterpretaram como um antigo lençol de areia eólica, caracterizado pela cíclica alternância vertical de depósitos eólicos e paleossolos.

O presente estudo tem por objetivo a caracterização paleopedológica e sedimentológica da Formação Marília, que aflora nos estados de Goiás e Mato Grosso do Sul, visando a) o reconhecimento e descrição de diferentes tipos/perfis de paleossolos e litofácies, b) a definição das características genéticas dos paleossolos e sedimentos, e c) a definição de fatores paleoambientais que condicionaram os momentos de sedimentação e paleopedogênese. Para tal,

foi estudada uma área com aproximadamente 15.000 km<sup>2</sup>, entre os estados de Goiás e Mato Grosso do Sul, na qual foram medidas 13 seções estratigráficas, por um total de 170 m de espessura. Os perfis de paleossolos representam 66% da freqüência relativa de distribuição por espessura nas seções medidas, enquanto as litofácies respondem por 34%.

## 2. Área de estudo

A área de estudo está localizada na porção noroeste da Bacia Bauru, entre os estados de Goiás e Mato Grosso do Sul, na faixa de afloramentos da Formação Marília (Figura 1A). Nesta porção da bacia afloram as formações Santo Anastácio, pertencente ao Grupo Caiuá (Fernandes & Coimbra, 1994), e Adamantina e Marília, unidades superiores do Grupo Bauru (Barcelos, 1984) (Figura 1B).

A Formação Marília foi reportada pela primeira vez na literatura por Almeida & Barbosa (1953), na ocasião estudando a então Série Bauru no estado de São Paulo, na região das serras de Santana, Itaqueri, São Carlos e Cuscuzeiro. Barcelos (1984) e posteriormente Barcelos & Suguio (1987), em estudos sobre a distribuição das unidades do Grupo Bauru além do estado de São Paulo, ampliaram os limites então conhecidos da Formação Marília no estado de São Paulo e Triângulo Mineiro, para áreas do sul de Goiás e nordeste de Mato Grosso do Sul. Segundo a proposição dos autores, as áreas de afloramento da Formação Marília estariam restritas às porções mais elevadas de escarpas e planaltos regionais, ao modo que, as rochas da Formação Adamantina ocupariam as porções topograficamente mais suavizadas e os fundos de vales. Na área de estudo, a Formação Marília possui uma espessura máxima de 190 m (CPRM, 2004), e é caracterizada por arenitos muito finos a grossos e raros depósitos de arenitos conglomeráticos. Os arenitos são bem selecionados, bem arredondados e exibem alta esfericidade, predominantemente constituídos por quartzo e secundariamente por fragmentos líticos de basalto e quartzito (Basilici *et al.*, 2009; Basilici & Dal' Bo, 2010).

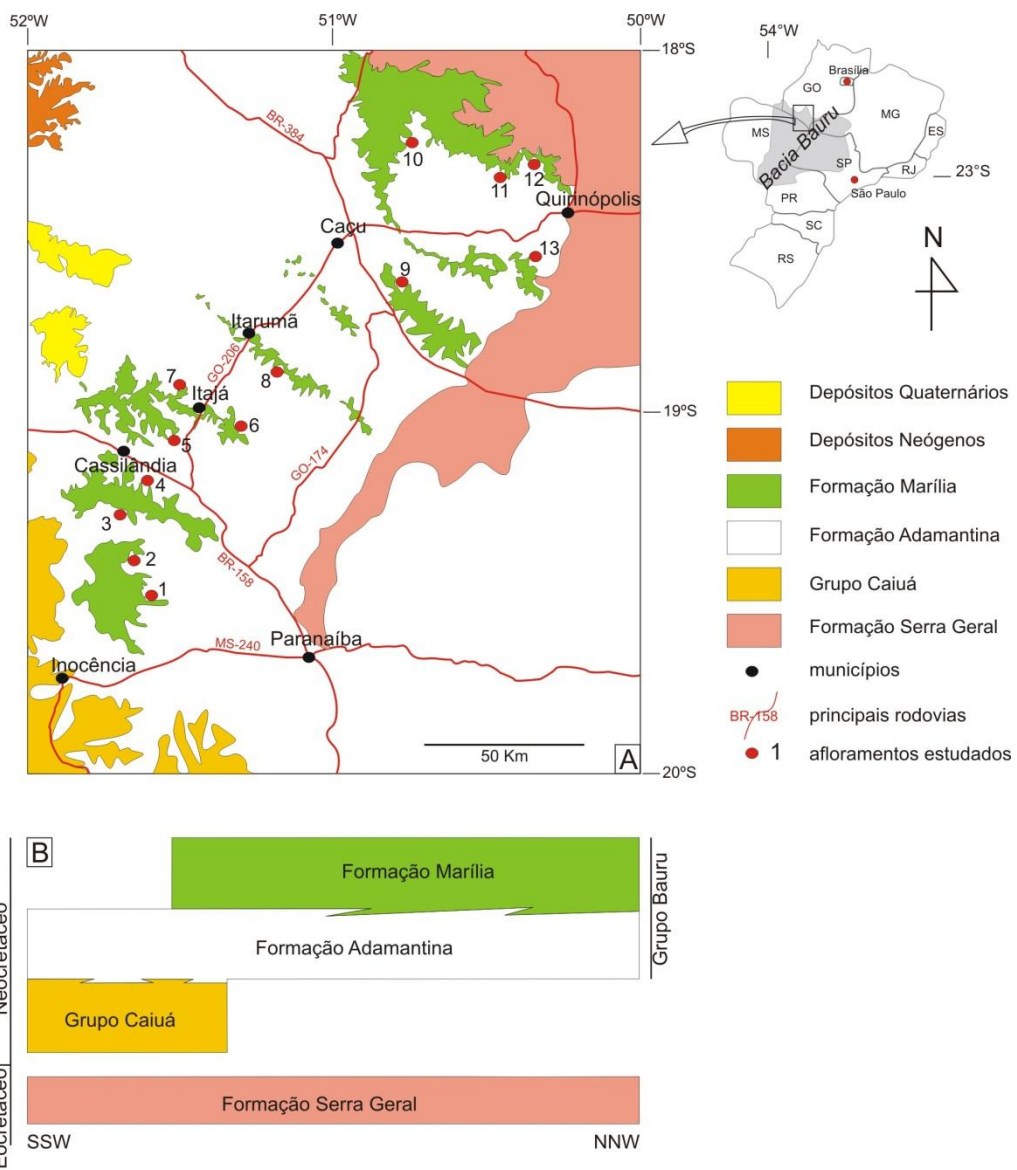


**Figura 1.** Localização da área de estudo na porção noroeste da Bacia Bauru. A) Mapa geológico simplificado com a localização dos pontos estudados na Formação Marília (modificado de CPRM, 2004). B) Relações estratigráficas entre as unidades na área de estudo (modificado de CPRM, 2004).

### 3. A Formação Marília na porção noroeste da Bacia Bauru

Em campo, foram medidas 13 seções estratigráficas, com as respectivas localizações assinaladas na Figura 1A. A análise paleopedológica e a análise de fácies permitiram a identificação e a discriminação de quatro ordens de paleossolos (*Aridisols*, *Alfisols*, *Vertisols* e

*Entisols*) e três litofácies (Arenito com laminação plano-paralela, Arenitos conglomeráticos e Arenito com estratificação cruzada acanalada de base côncava) (Tabela 1).

**Tabela 1.** Freqüências relativas em percentagem por espessura (170 m total medido) de paleossolos e litofácies no registro geológico.

Elementos	% Paleossolos	% Litofácies	% Total do registro geológico
<i>Aridisols</i>	84,5	-	55,8
<i>Alfisols</i>	10,7	-	7
<i>Vertisols</i>	2,7	-	1,8
<i>Entisols</i>	2,1	-	1,4
Arenito com laminação plano-paralela	-	68,5	23,3
Arenitos conglomeráticos	-	26	8,8
Arenito com estratificação cruzada acanalada de base côncava	-	5,5	1,9
Total	-	-	100

### 3.1. Paleossolos

Os paleossolos foram identificados em campo com base no reconhecimento de feições diagnósticas como rizólitos, estruturas e horizontes de solo, e variações texturais entre os horizontes pedogênicos (Catt, 1990; Retallack, 2001). A descrição morfológica seguiu os critérios estabelecidos no *Soil Survey Manual* (Soil Survey Staff, 1993), e a taxonomia de horizontes e perfis está de acordo com o *US Soil Taxonomy* (Soil Survey Staff, 1999).

#### 3.1.1. *Aridisols*

Os *Aridisols* correspondem ao tipo de paleossolo mais freqüente na área de estudo; representam 84,5% da espessura dos paleossolos e 55,8 da espessura total da Formação Marília (Figura 2).

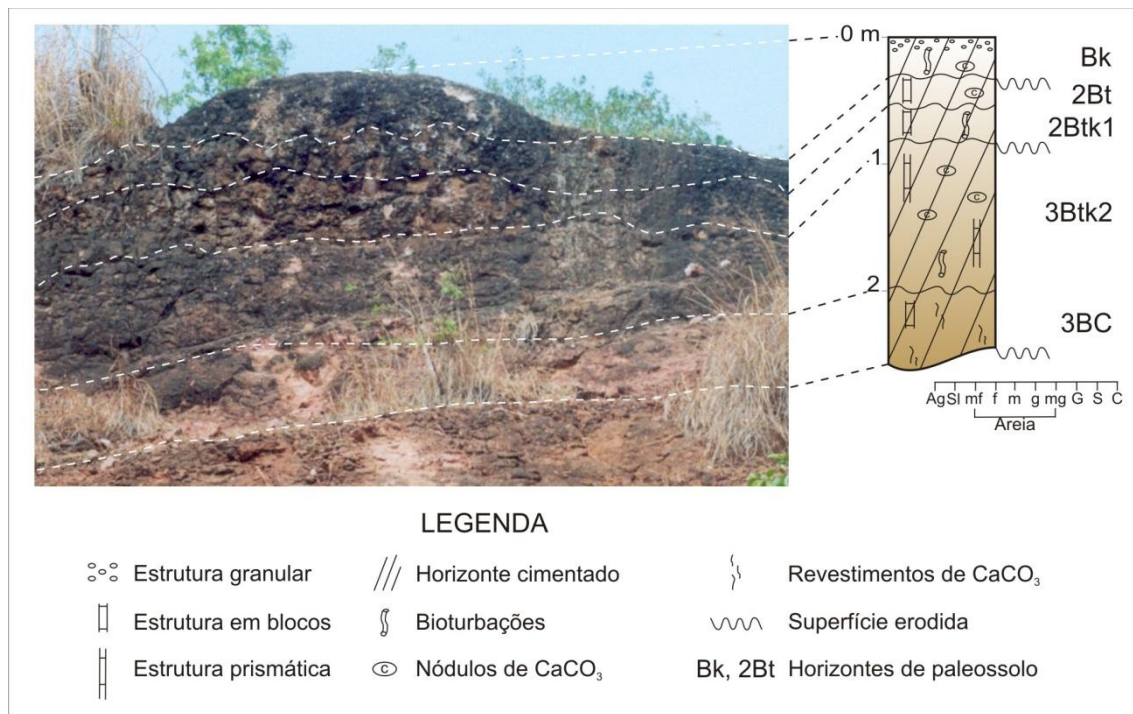


**Figura 2.** Perfil de *Aridisol* descrito próximo ao município de Itajá (GO). Ponto 7 na Figura 1A.

Os perfis apresentam espessuras variáveis de 0,3 m a 7 m. Em geral, os perfis exibem seqüência de horizontes Bt/Btk/Bk(ou Bkm)/C(ou Ck). Poucos perfis apresentam o horizonte superficial A preservado; em muitos casos, a porção superior dos perfis é marcada por uma superfície erodida com concentração de seixos. As cores variam de vermelho (10R5/8), vermelho-claro (10R6/8) a bruno-avermelhado (10R4/6). As texturas arenosas são preponderantes, com granulação predominante de areia fina a média. As estruturas pedogênicas variam de acordo com os horizontes; em geral exibem estruturação forte, com alto grau de desenvolvimento e tamanhos grandes (Figuras 3 e 4).



**Figura 3.** Estrutura prismática muito grande, descrita em perfil de *Aridisol*. Ponto 7 na Figura 1A.



**Figura 4.** Estrutura laminar incipiente, com 1 mm a 2 mm de espessura, descrita em perfil de *Aridisol*. Ponto 11 na Figura 1A.

Na superfície das estruturas pedogênicas podem ocorrer revestimentos de filmes pretos (N3) de oxihidróxidos de manganês e revestimentos de carbonato de cálcio.

Nos horizontes Btk, Bk, Bkm e Ck ocorrem nódulos de calcita, em sua maioria com organização interna típica (indiferenciada) e por vezes com formas de halos e septárias. Os nódulos são macios a duros, brancos, e possuem dimensões que variam de <1 cm a 5 cm de

diâmetro, e formas subesféricas, elipsoidais, amigdaloidais e irregulares. Os halos são macios, brancos, pequenos (0,2 cm a 1 cm de diâmetro) e irregulares. As septárias são duras, brunovermelhadas, grandes (2 cm a 5 cm de diâmetro), elipsoidais ou irregulares e possuem um padrão de fraturas radiais preenchidas por calcita microcristalina.

Evidências de atividade biológica, atestadas por estruturas de bioturbação, ocorrem concentradas principalmente nos horizontes A e B. Em geral, estas correspondem a estruturas cilíndricas alongadas na vertical, com ramificações laterais e afinamento para a base, como os rizólitos, que podem atingir até 10 cm de comprimento e diâmetros que variam de 0,5 cm no topo a 0,2 cm na base das ramificações. Freqüentemente, o preenchimento das bioturbações é composto por areia fina ou média e calcita espática.

A transição entre os horizontes é clara a gradual com superfície de separação ondulada a irregular. Quando a transição ocorre de forma abrupta e plana, essa é marcada pela intensa concentração de nódulos de calcita em um horizonte ou separada por superfícies erodidas com morfologia plana subhorizontal.

### **3.1.1.2. Interpretação**

*Aridisols* são solos típicos de regiões semi-áridas e áridas, caracterizadas por índices de precipitação anuais inferiores a 500 mm (Nettleton & Peterson, 1983).

A disponibilidade hídrica limitada, onde a evapotranspiração freqüentemente excede às precipitações, conduz ao retardo dos processos de alteração química dos perfis e favorece a ocorrência de horizontes subsuperficiais enriquecidos em minerais secundários e sais solúveis a profundidades menores que 1 m. Os *Aridisols* que apresentam horizontes com concentrações secundárias de carbonato de cálcio podem ser classificados como calcretes pedogênicos (Goudie, 1973) ou *Calcisols* (Mack *et al.*, 1993).

Os calcretes pedogênicos são formados por horizontes bem diferenciados de acumulações secundárias de CaCO<sub>3</sub>, em escala macro- e microscópica. A progressiva acumulação de CaCO<sub>3</sub> nos perfis pedogênicos é indicada por diferentes estágios morfológicos (Gile *et al.*, 1966; Bachman & Machette, 1977), que variam de acordo com a disponibilidade de íons de cálcio, atividade de organismos, relação entre precipitação/evapotranspiração, tempo de evolução e tipo de material de origem.

Nos perfis estudados, foram observados horizontes de calcrete pedogênico representativos dos seis estágios morfológicos característicos de paleossolos com texturas finas e médias.

O primeiro estágio evolutivo observado é marcado por acumulações incipientes de carbonato de cálcio, de aspecto pulverulento, com filamentos e revestimentos sobre as unidades estruturais e poucas impregnações em torno de raízes e grãos. No segundo estágio, o desenvolvimento dos solos conduziu a maior concentração de carbonatos por difusão e translocação, culminando com a formação de nódulos pequenos e irregulares, que não ultrapassam 10% em volume dos horizontes (Figura 5). O contínuo crescimento dos nódulos conduziu à formação de horizontes cimentados e endurecidos com nódulos coalescentes apresentando cimentação internodular por calcita espática (estágio III). O quarto estágio de evolução é marcado pela ocorrência de um horizonte petrocálcico Bkm com estruturas laminares menos espessas que <1 cm. No quinto estágio evolutivo, as estruturas laminares apresentam espessuras superiores a 1 cm e passam a ocorrer pisólitos de carbonato de cálcio. O último estágio (VI) é caracterizado pela ocorrência de pisólitos, diferentes gerações de lâminas e fragmentos angulares “brechosos” de carbonato de cálcio (Figura 6). Tal estágio foi reconhecido em horizontes petrocálcicos e, indica que as diferentes formas e morfologias presentes nestes horizontes podem ser produto da ação de múltiplos episódios de exposição, erosão e recimentação.



**Figura 5.** Exemplo representativo da concentração de carbonato de cálcio em horizontes pedogênicos de *Aridisols*: estágio II de concentração, marcado por nódulos pequenos e irregulares, descrito no ponto 4 na Figura 1A.



**Figura 6.** Exemplo representativo da concentração de carbonato de cálcio em horizontes pedogênicos de *Aridisols*: estágio VI, horizonte petrocálcico com aspecto “brechoso”, devido a diversos fragmentos angulares de calcrete, descrito no ponto 5 na Figura 1A.

### **3.1.2. *Alfisols***

Foi descrito apenas um perfil da ordem dos *Alfisols*; porém, os *Alfisols* representam 10,7% da espessura dos paleossolos.

O perfil possui 3,57 m de espessura, e apresenta seqüência de horizontes Bt/Btk (Figura 7). As cores predominantes são vermelho (10R4/8), bruno-avermelhado (10R4/6) e vermelho-claro (10R7/8). A textura é arenosa, com granulação de areia fina nos horizonte superiores Bt e areia média nos horizontes inferiores Btk. As estruturas pedogênicas apresentam alto grau de desenvolvimento e tamanhos grandes. As estruturas dos horizontes Bt e Btk variam de grande a muito grande em blocos sub- e angulares, com estruturação secundária moderada de média a grande em blocos sub- e angulares.

Na superfície das estruturas pedogênicas podem ocorrer revestimentos de filmes pretos (N3) de oxihidróxidos de manganês e cerosidade, que é mais evidente nos horizontes Bt.

Nos horizontes Btk ocorrem nódulos de calcita, que exibem variações entre nódulos típicos e halos. Os nódulos típicos são macios a duros, brancos, e possuem dimensões que variam de <0,1 cm a 3,5 cm de diâmetro e formas subesféricas, elipsoidais e amigdaloidais. Os halos são macios, brancos, pequenos a médios (0,4 cm a 0,7 cm de diâmetro) e irregulares.

Evidências de atividade biológica, atestadas por estruturas de bioturbação, ocorrem em todos os horizontes. As principais estruturas são os rizólitos, que formam tubos cilíndricos alongados na vertical e apresentam ramificações laterais com afinamento em direção a base das ramificações. Os diâmetros dos rizólitos variam de 1 cm a 1,2 cm no eixo principal e 0,4 cm a 0,6 cm nas ramificações, com comprimento máximo de 18 cm. As bioturbações estão preenchidas em sua maior parte por areia fina e calcita microcristalina.

A transição entre os horizontes ocorre principalmente de forma clara a gradual com superfície de separação ondulada.

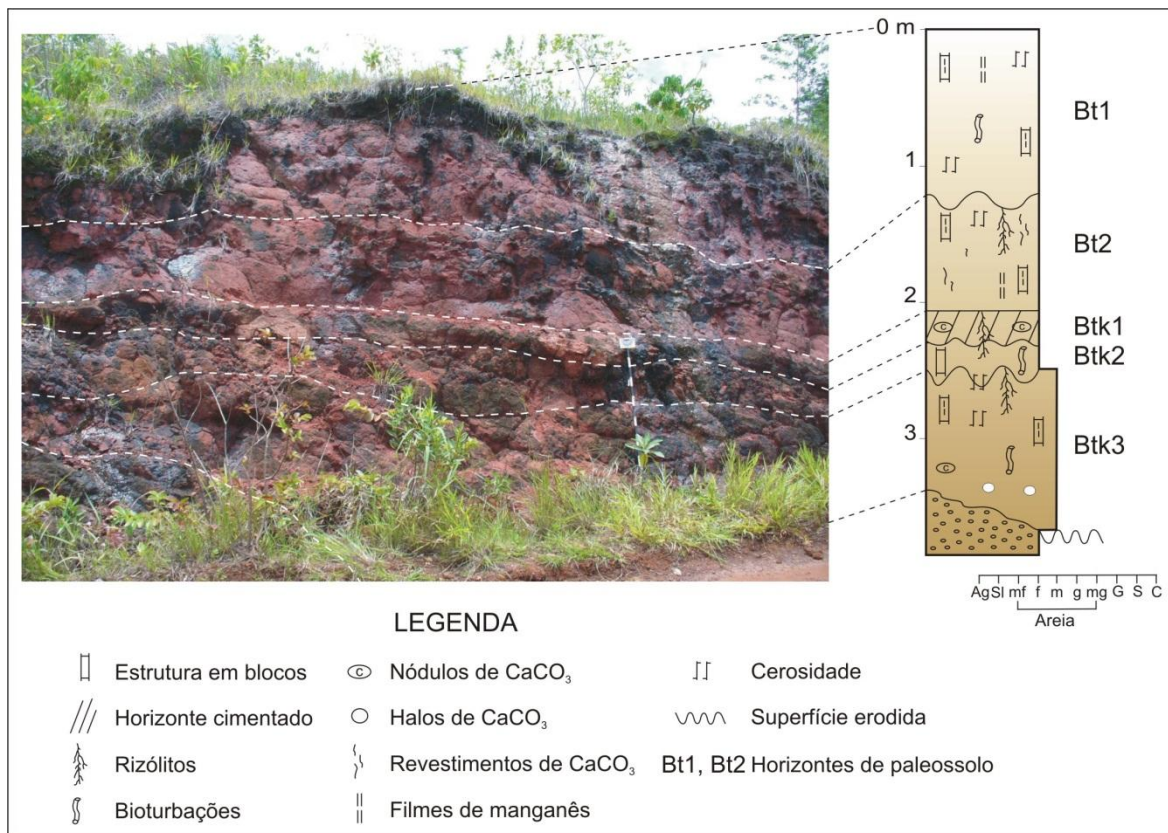


**Figura 7.** Perfil de *Alfisol* descrito próximo ao município de Itajá (GO). Ponto 7 na Figura 1A.

### 3.1.2.1. Interpretação

*Alfisols* são solos típicos de áreas florestadas e são caracterizados pela ocorrência de horizontes subsuperficiais Bt enriquecidos em conteúdo de argila iluvial e que apresentam saturação por bases igual ou superior a 35% (Soil Survey Staff, 1999). Em paleossolos, a saturação por bases pode ser obtida através de dois indicadores: o primeiro considera a ocorrência de um horizonte com nódulos de carbonato de cálcio em profundidade superior a 1 m a partir do topo do perfil (Retallack, 2001). O segundo indicador, que usa de índices de alteração química, é eficaz também a diferenciação entre esses perfis e perfis de *Ultisols*, que também possuem horizontes subsuperficiais Bt enriquecidos em argila iluvial. Segundo Sheldon *et al.* (2002), os horizontes B de *Alfisols* possuem relações molares entre os óxidos de cálcio, magnésio, potássio e sódio divididos por óxido de alumínio ( $\Sigma$ bases/Al = ((CaO+MgO+Na<sub>2</sub>O+K<sub>2</sub>O)/Al<sub>2</sub>O<sub>3</sub>)) maiores que 0,5, enquanto que, em *Ultisols* tal relação seria menor que 0,5.

O perfil analisado apresenta dois horizontes Bt ricos em argila iluvial (percentual de argila iluvial maior que 1% em área de lâminas delgadas) (Dal' Bo & Basilici, 2010), possui um horizonte Btk1 com concentração de nódulos de carbonato de cálcio em profundidade superior a 1 m a partir do topo do perfil e todos os horizontes B exibem relações molares entre os óxidos de bases/alumina superiores ao índice de 0,5 (Figura 8), respondendo assim aos requisitos necessários à classificação deste perfil como *Alfisol*.

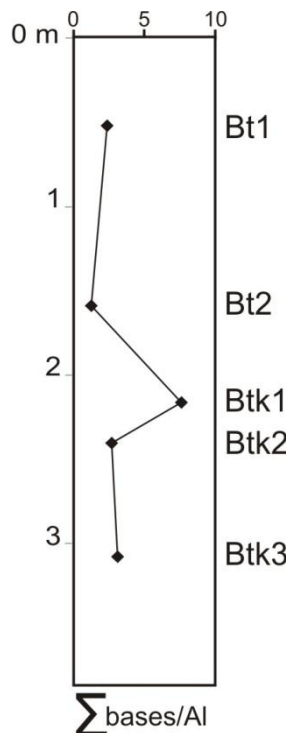


**Figura 8.** Relações molares entre os óxidos de Ca, Mg, K e Na divididos por óxido de Al em perfil de *Alfisol* descrito no ponto 7 na Figura 1A.

### 3.1.3. *Vertisols*

Os *Vertisols* representam 2,7% da espessura dos paleossolos nas seções medidas.

Os perfis possuem espessuras de 0,4 a 0,74 m, e exibem apenas horizontes Bss e Ck (Figura 9). Horizontes A não foram observados; o topo dos perfis é marcado por superfícies erodidas com morfologia plana a levemente ondulada. As cores variam de vermelho-claro (7,5R7/6), laranja (7,5YR7/6, 7,5YR6/6) a bruno-claro (7,5YR5/8), com mosqueamento cinzento-claro (10YR8/1), abundante (>20% em volume da matriz do horizonte) e proeminente, com contraste conspícuo entre o matiz dos horizontes e o matiz do mosqueado. As texturas

variam de argilosa nos horizontes Bss a arenosa, com variações de granulação entre areia fina e média nos horizontes Ck. As estruturas presentes nos horizontes Bss apresentam estruturação forte, tamanhos grandes e formas de blocos sub- e angulares. Superfícies de fricção cortam as estruturas com ângulos de inclinação de 30-50° em relação à horizontal e definem formas cuneiformes ou paralelepípedicas. Os horizontes Ck não apresentam estruturas pedogênicas e possuem aspecto maciço devido à intensa cimentação por carbonato de cálcio.

Os revestimentos são apenas de carbonato de cálcio e ocorrem nos horizontes Bss e Ck, sob a forma de películas que envolvem os grãos e filamentos que recobrem a superfície das estruturas.

Nódulos de calcita ocorrem nos horizontes Bss e Ck, porém nos horizontes Bss são comuns os nódulos típicos, duros, brancos, com dimensões pequenas (<0,1 cm de diâmetro) e formas subesféricas e irregulares, enquanto nos horizontes Ck, ocorrem os halos, macios a duros, brancos, pequenos (<1 cm de diâmetro) e irregulares.

Evidências de atividade biológica são raras e se concentram nas porções superiores dos horizontes Bss. Em geral, são estruturas de bioturbação com formatos tubulares alongados na vertical e diâmetros que variam de 0,4 cm a 0,6 cm. O preenchimento das bioturbações pode ser por material lamítico, areia fina ou calcita microcristalina.

A transição entre os horizontes é clara com superfície de separação irregular.

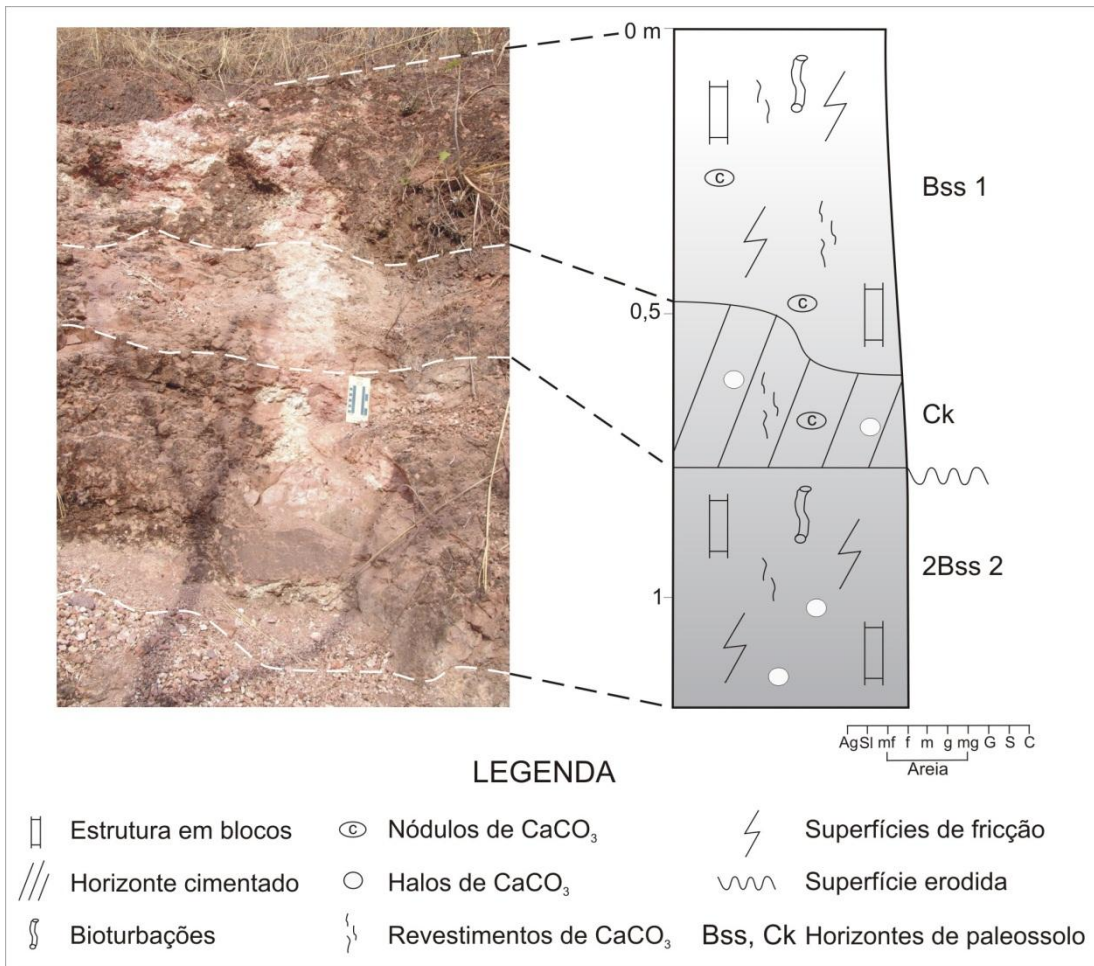


**Figura 9.** Perfil de *Vertisol* descrito próximo ao município de Quirinópolis (GO). Ponto 12 na Figura 1A.

### 3.1.3.1. Interpretação

Os *Vertisols* formam perfis homogêneos, com distinção incipiente de horizontes e transição interna irregular, caracterizados por possuírem conteúdo de argila maior que 30% na matriz do solo e superfícies de fricção em profundidades de até 1 m a partir da superfície dos perfis (Soil Survey Staff, 1999). São característicos de regiões com sazonalidade climática bem marcada, com alternância de estações úmidas e secas. Não são encontrados em climas extremamente áridos ou extremamente úmidos e, os índices anuais de precipitação variam, em geral, de 180-1520 mm (Retallack, 2001).

A alternância entre períodos úmidos e secos tem influência na formação de grande parte das feições e estruturas pedogênicas dos *Vertisols*. Devido ao alto conteúdo de argilas expansivas,

principalmente do grupo das esmectitas, que possuem altos coeficientes de extensibilidade linear (COLE), esses perfis sofrem periodicamente modificações de volume. Durante os períodos secos, sofrem contração do material pedológico, resultando em rachaduras profundas no perfil, que são posteriormente preenchidas por sedimentos ou materiais de horizontes superiores. Tais materiais são incorporados aos perfis durante os períodos úmidos, caracterizados por forte expansão das argilas e formação de uma série de feições diagnósticas dos *Vertisols*: superfícies de fricção proeminentes, estruturas com formas cuneiformes ou paralelepípedicas e microrrelevo gilgai.

O reconhecimento de perfis de paleossolos da ordem dos *Vertisols* é baseado principalmente no alto conteúdo de argilas expansivas e em feições morfológicas: rachaduras de dessecção, estruturas pedogênicas com formas cuneiformes ou paralelepípedicas, microrrelevo gilgai, diques clásticos e superfícies de fricção (Mack & James, 1992; Mack *et al.*, 1993). Embora a esmectita represente o principal argilomineral descrito em *Vertisols*, outros argilominerais como a paligorsquita, vermiculita, ilita e clorita também podem ser freqüentes (Coulombe *et al.*, 1996).

As feições diagnósticas que permitiram a interpretação dos perfis descritos como *Vertisols* foram: a) superfícies de fricção que cortam as estruturas e produzem formas cuneiformes nos horizontes Bss (Figuras 10 e 11), b) alto percentual de argila nos horizontes Bss ( $\leq 73\%$ ), c) abundância de argilas expansivas na fração de argila fina ( $< 0,2 \mu\text{m}$ ) na matriz do solo nos horizontes Bss (esmectita, paligorsquita e sepiolita) (Basilici *et al.*, 2009).

Perfis de *Vertisols* que possuem horizontes Bss com nódulos de carbonato de cálcio em até 20% em volume da matriz dos horizontes, foram descritos por Khadkikar *et al.* (1998) em depósitos aluviais de clima semi-árido no oeste da Índia e denominados de *calcic Vertisols* (Vanstone, 1991) ou *vertic Calcisols* (Gustavson, 1991).

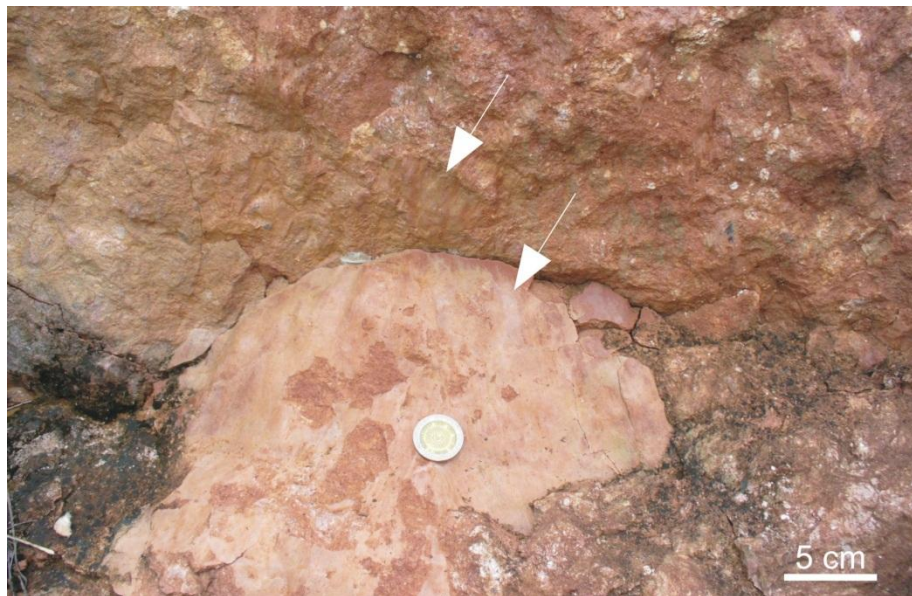


**Figura 10.** Superfícies de fricção em horizonte Bss de *Vertisol*. Ponto 8 na Figura 1A.



**Figura 11.** Detalhe de estrutura pedogênica cuneiforme com superfícies polidas e estriadas provocadas por ação de superfícies de fricção. Ponto 8 na Figura 1A.

### 3.1.4. *Entisols*

Os *Entisols* formam perfis com espessuras que variam de 0,3 m a 1,25 m. A freqüência de distribuição por espessura é de 2,1% dos paleossolos.

Os perfis exibem seqüência de horizontes A/C(ou Ck), marcados pela ausência de horizontes diagnósticos B. As cores variam de vermelho-claro (2,5YR6/8), vermelho (10R5/8) a bruno-avermelhado (2,5YR5/8), com porções cinzento-claro (7,5YR8/1) associadas a halos e nódulos de calcita. As texturas variam desde areia fina, média e grossa a areia com cascalho, com grânulos e seixos de basalto e quartzito concentrados nos horizontes C. Os horizontes não exibem estruturas pedogênicas, apresentando porções de grão simples (não-coerentes) e outras maciças, em virtude da cimentação por carbonato de cálcio.

Os horizontes C mostram “fantasmas” de laminações plano-paralelas sempre que desenvolvidos sobre os depósitos da litofácie Arenito com laminação plano-paralela e grânulos e seixos quando associados à litofácie Arenito com estratificação cruzada acanalada de base côncava (Figura 12).

Apenas revestimentos incipientes de carbonato de cálcio na matriz e películas de óxidos de ferro em torno de grãos foram observados. Não há evidências de movimentação mecânica de argilas, nem filmes de oxihidróxidos de manganês.

Nódulos de calcita ocorrem concentrados nos horizontes Ck. Os nódulos são em sua maioria halos, macios a duros, brancos, pequenos a grandes (<1 cm a 3 cm de diâmetro) e possuem formas irregulares.

Evidências de atividade biológica são raras e quando ocorrem, estão concentradas nos horizontes A. Em geral, correspondem à porosidade de bioturbação e possuem formas subesféricas, dimensões de 0,1 cm a 0,3 cm de diâmetro e exibem preenchimento por areia fina com cores diferentes da matriz dos horizontes.

A transição entre os horizontes é clara e gradual com superfície de separação suave ondulada.

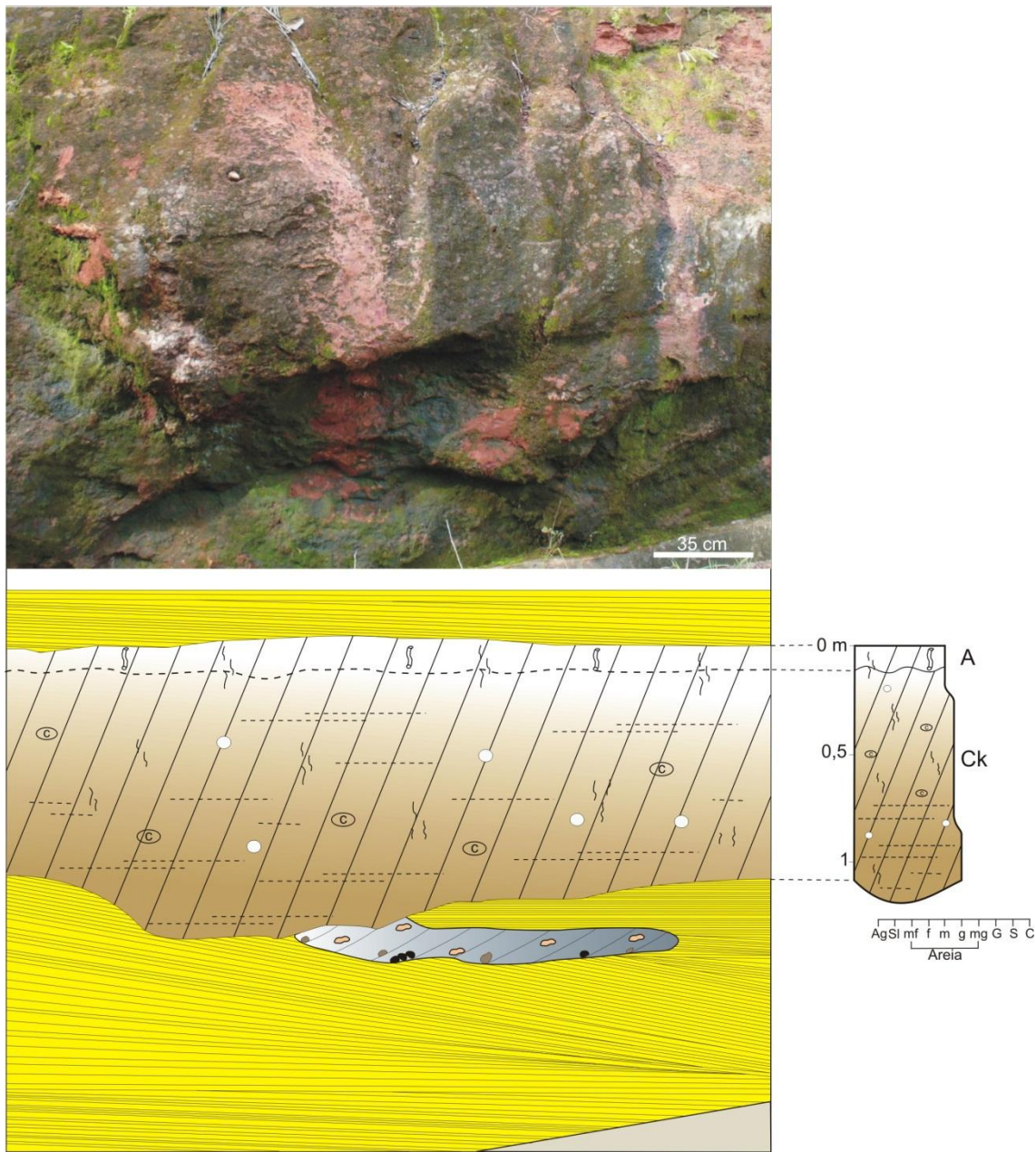


**Figura 12.** Esquema ilustrativo de perfil de *Entisol* desenvolvido sobre os depósitos eólicos da litofácie Arenito com laminação plano-paralela. Em meio à litofácie ocorre um corpo lenticular da litofácie Arenito com estratificação cruzada acanalada de base côncava. Ponto 8 na Figura 1A.

### 3.1.4.1. Interpretação

Os *Entisols* são caracterizados por baixo grau de evolução pedogênica. Comumente formam perfis com horizontes superficiais delgados e ócricos, e não possuem horizontes B

diagnósticos ou estruturas pedogênicas (Soil Survey Staff, 1999). Podem se desenvolver sobre qualquer material de origem, clima ou situação topográfica (Retallack, 2001). Essa ordem de solos representa o estágio inicial de alteração do material originário em solo, podendo evoluir para quaisquer outras ordens de solo, a depender do tempo, material de origem, posição topográfica e condições climáticas (Schaetzl & Anderson, 2005).

A ausência de horizontes B diagnósticos e estruturas pedogênicas são fatores que evidenciam o baixo grau de evolução dos perfis. Os horizontes A foram classificados como epipedons ócricos por apresentarem espessura reduzida, cores claras e ausência de matéria orgânica que possibilitaria a sua classificação em outros tipos de epipedons como melânicos, úmbricos, mólicos ou hísticos (Soil Survey Staff, 1999). Nestes horizontes, a atividade biológica, mesmo que de forma incipiente, obliterou as estruturas sedimentares primárias, que podem ser observadas nos horizontes C, que guardam muitas características similares ao material de origem como cor e textura.

O tempo e/ou as condições ambientais desfavoráveis (altas taxas de sedimentação e/ou erosão) foram os principais fatores que determinaram a formação de *Entisols* na Formação Marília. A presença de nódulos e halos de calcita permite afirmar que a gênese destes perfis ocorreu de forma concomitante aos *Aridisols*, representando perfis de *Aridisols* incipientes.

### **3.2. Depósitos**

#### **3.2.1. Arenito com laminação plano-paralela – depósitos arenosos com marcas onduladas eólicas**

A litofácies Arenito com laminação plano-paralela é a mais comum descrita na área de estudo, constitui 68,5% dos depósitos e 23,3% da espessura total da Formação Marília. Esta litofácies forma pacotes de geometria tabular, com 0,9 m a 6,5 m de espessura e continuidade lateral maior que 50 m (Figura 13A). Apenas camadas lenticulares da litofácies Arenito com estratificação cruzada acanalada de base côncava podem interromper o desenvolvimento lateral e vertical desta litofácies. A granulação varia de areia muito fina a grossa, predominantemente constituída por grãos de quartzo, feldspatos e fragmentos líticos de basalto. Os grãos de areia que formam os arenitos são bem selecionados, bem arredondados e exibem alta esfericidade. Esta

litofácie é caracterizada por arenitos com laminações plano-paralelas horizontais ou de ângulo baixo (Figura 13B). Estas laminações são identificáveis por pequenas diferenças de granulação: lâminas (<2 mm) formadas por arenitos muito finos a finos intercaladas com camadas finas (0,2 cm a 2 cm) de arenitos médios a grossos. Tanto as lâminas como as camadas finas possuem continuidade lateral limitada, adelgacando e desaparecendo para as bordas. As camadas mais finas podem exibir graduação inversa; mais visível em seções cortadas de forma oblíqua em respeito aos planos de estratificação (Figura 13C). O padrão de bimodalidade observado entre as camadas, com lâminas de areia de granulação fina na base das camadas se alternando a lâminas de areia de granulação grossa no topo das camadas, forma laminações denominadas de risca de agulha (*pin stripe lamination*) (Fryberger & Schenk, 1988) (Figura 13C). Muito raramente são observadas laminações cruzadas em um único *set*. Superfícies erodidas horizontais ou de ângulo baixo dividem *sets* de laminações plano-paralelas com espessuras entre 20 cm a 50 cm (Figura 13D).

O limite inferior desta litofácie com os paleossolos é sempre assinalado por uma superfície erodida subhorizontal ou inclinada de ângulo baixo, enquanto o limite superior possui uma transição difusa com os paleossolos e erodida com as outras litofácies.

Vestígios de atividade biológica não são freqüentes; visualmente não ultrapassam 5% da superfície em área das seções. Os icnofósseis mais observados foram estruturas de bioturbação em forma de tubos cilíndricos alongados na vertical, com dimensões de 5 mm a 10 mm de diâmetro, e preenchimento por areia fina e média.

Nódulos de calcita, em sua maioria halos, macios, brancos, pequenos (1 mm a 5 mm de diâmetro) e irregulares, ocorrem disseminados por toda a extensão da litofácie. Clastos intraformacionais constituídos por nódulos de calcita, duros, brancos, pequenos a grandes (<1 cm a 3 cm de diâmetro) e com formas arredondadas, ocorrem em meio à litofácie, organizados em linhas ou camadas.

A textura superficial de grãos de quartzo, de granulação de areia média a grossa, observada ao microscópio eletrônico de varredura (MEV), mostra o alto grau de arredondamento dos grãos de quartzo e a textura superficial fosca. Algumas feições produzidas pela abrasão eólica, como fraturas conchoidais (*dish-shaped conchoidal fractures*) também podem ser observadas na superfície dos grãos (Figura 13E).

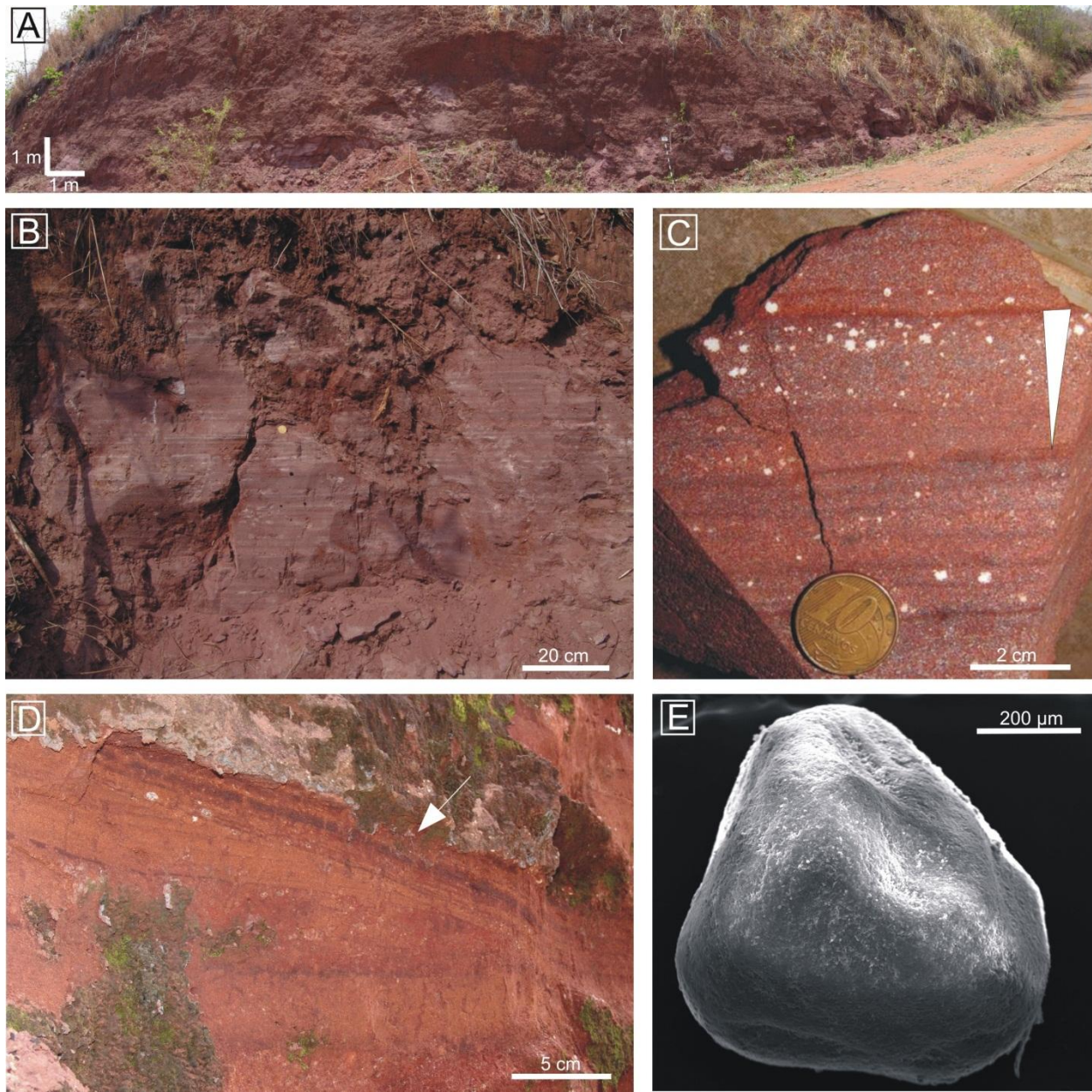


**Figura 13.** Características da litofácie Arenito com laminação plano-paralela. A) Visão geral de um afloramento da litofácie, mostrando a continuidade lateral dos depósitos por mais de 50 m. B) Laminações plano-paralelas horizontais ou de ângulo baixo produzidas por deposição de areias com marcas onduladas eólicas. C) Laminação riscada de agulha e detalhe de um *set* exibindo gradação inversa. D) Superfície de truncamento de ângulo baixo dividindo *sets* de laminações plano-paralelas. E) Grão de quartzo exibindo fraturas conchoidais produzidas por abrasão eólica. Fotos A e B, ponto 8 na Figura 1A; fotos C, D e E, ponto 5 na Figura 1A.

### **3.2.1.1. Interpretação**

Esta litofácie é interpretada como produto da deposição de areias com marcas onduladas eólicas, que formaram estratificação cavalgante transladante subcrítica (*subcritically climbing translatent strata*) (Hunter, 1977). Bagnold (1941) e Hunter (1977) observaram que pequenas marcas onduladas assimétricas formadas em superfícies expostas ao transporte eólico produziam laminationes plano-paralelas caracterizadas por variações de granulação: lâminas de areia muito fina a fina e lâminas de areia média a grossa. A contínua migração das cristas das ondulações promove a formação de lâminas caracterizadas por gradação inversa, na qual laminationes cruzadas produzidas por avalanche são dificilmente reconhecíveis devido ao alto grau de seleção das areias. As superfícies erodidas que truncam os *sets* de laminationes plano-paralelas são geradas por mudanças no sentido ou velocidade dos ventos (Hunter, 1977; Mountney, 2006).

Os grãos de areia que constituem os arenitos são bem selecionados, bem arredondados, e exibem superfícies foscas, e outras feições superficiais descritas que indicam deposição por ação de processos eólicos (Mahaney, 2002). O processo de deflação eólica origina superfícies erodidas subhorizontais ou levemente inclinadas, como as observadas no contato inferior desta litofácie (Hunter, 1977).

### **3.2.2. Arenitos conglomeráticos – depósitos de canais efêmeros**

Esta litofácie representa 26% dos depósitos e é constituída por arenitos, arenitos conglomeráticos e conglomerados arenosos. Esta litofácie forma corpos sedimentares com até 4 m de espessura, organizados em camadas tabulares ou lenticulares achatadas caracterizadas por geometria basal côncava e topo plano (Figura 14A). A base das camadas é marcada por superfícies erodidas com formas onduladas, responsáveis por variações de espessura das camadas de 0,1 m a 1,8 m. As camadas são subdivididas internamente em duas porções, uma inferior de conglomerado e outra superior de arenito. Os conglomerados exibem gradação incipiente e matriz arenosa similar as areias que formam a porção superior de arenitos (Figura 14B). Os conglomerados são sustentados por clastos, constituídos predominantemente de basalto e quartzito. A média do tamanho das maiores partículas ( $MpS$ ) varia, da base para o topo, de 11 cm a 0,5 cm, respectivamente. A matriz é abundante, pobemente selecionada, e apresenta

granulação de areia média a grossa, com predomínio da fração grossa. É composta por grãos bem arredondados de quartzo e fragmentos líticos. Os conglomerados exibem raros seixos oblatos com faces planas imbricados a(t) b(i). Na fração de seixos e pequenos calhaus, dois tipos de ventifacts podem ser observados: a) clastos de basalto e quartzito com faces planas, b) clastos de basalto com crateras de impacto (Figura 14C).

A porção superior das camadas é formada por arenitos médios a grossos e conglomerados arenosos, pobemente selecionados, que se sobrepõem de forma gradacional aos conglomerados da porção inferior. Em alguns casos, o limite superior das camadas pode apresentar contatos abruptos com a litofácie Arenito com laminação plano-paralela, atestados por arenitos com laminações plano-paralelas que cortam o topo dos depósitos de conglomerados (Figura 14D).

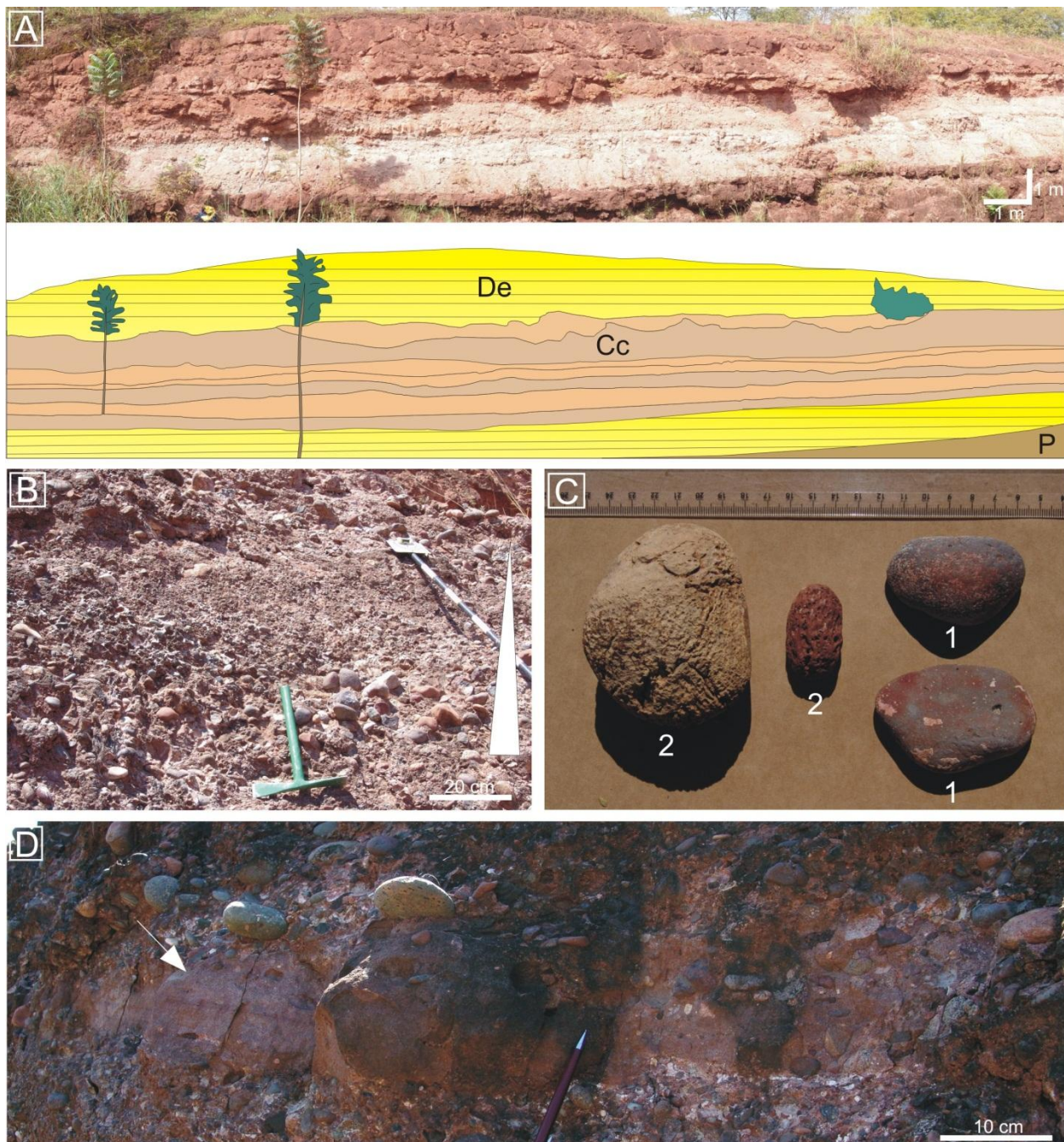


**Figura 14.** Características da litofácies Arenitos conglomeráticos. A) Depósitos de canais efêmeros organizados em camadas de geometria tabular (P, paleossolos; Cc, corpos canalizados; De, depósitos eólicos). B) Camadas de conglomerado mostrando gradação incipiente. C) Clastos com faces planas (1) e clastos com crateras de impacto (2). D) Seta indicando a porção superior de um set da litofácies Arenitos conglomeráticos cortado por depósitos da litofácies Arenito com laminação plano-paralela. Fotos A-D, ponto 5 na Figura 1A.

### **3.2.2.1. Interpretação**

A textura e a organização geométrica do conjunto das camadas, organizadas em geometria basal côncava e topo plano, indicam deposição por fluxos hidráulicos em estruturas canalizadas.

Fluxos hidráulicos turbulentos formaram as superfícies erodidas côncavas na base de canais. O padrão de imbricação  $a(t)$   $b(i)$  de seixos oblatos é ligado a transporte de carga de fundo por atividade hidráulica, comum na deposição de barras cascalhentas em lençol (Harms *et al.*, 1975). Sedimentos grossos e pobemente selecionados sugerem fluxos deposicionais rápidos, sem tempo suficiente para desenvolver estruturas típicas de depósitos de canais fluviais, como conglomerados sustentados por clastos com arcabouço aberto (*open framework*) e ausência de matriz. Os episódios deposicionais foram gerados por fluxos altamente concentrados e intermitentes, indicados pelo alto conteúdo de matriz; ausência de organização de clastos; inexistência de estratificações cruzadas; esporádica orientação preferencial de clastos, exibindo poucos clastos imbricados e organização arquitetural simples. A presença de graduação incipiente ocorreu provavelmente nas fases finais de deposição, como resultado da diminuição gradual da energia dos fluxos. Os arenitos com grãos arredondados, bem selecionados, e laminationes plano-paralelas, que truncam o topo das camadas de conglomerados, foram interpretados como resultado de retrabalhamento por atividade eólica em fase de exposição subárea dos depósitos fluviais, reforçando a hipótese de fluxos esporádicos em canais efêmeros.

O mapeamento geológico das feições canalizadas, baseado na distribuição dos depósitos em afloramentos estudados próximos ao município de Itajá (GO), possibilitou a reconstrução paleogeográfica dos canais efêmeros (Figura 15).

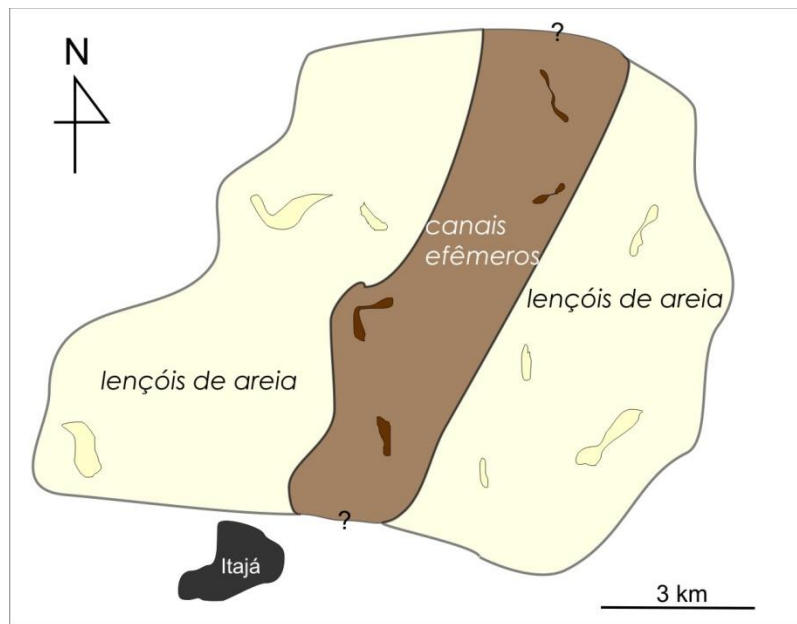


**Figura 15.** Mapa de reconstrução paleogeográfica dos canais fluviais efêmeros baseado na distribuição de afloramentos estudados.

### 3.2.3. Arenito com estratificação cruzada acanalada de base côncava – depósitos de inundação instantânea

Esta litofácies representa 5,5% dos depósitos e forma pacotes de geometria lenticular, caracterizada por base côncava e topo plano. É constituída por arenitos médios a grossos e arenitos conglomeráticos pobemente selecionados. Ocorre interestratificada aos depósitos da litofácies Arenito com laminação plano-paralela e possui espessuras que variam de 0,05 m a 0,35 m e continuidade lateral menor que 20 m. Os arenitos são constituídos por grãos de quartzo bem arredondados, esféricos e com superfícies foscas. Os grânulos e seixos que compõem os arenitos conglomeráticos são principalmente de basalto, quartzito, nódulos de calcita e intraclastos lamíticos.

As camadas são formadas por um ou dois *sets* de estratificações cruzadas acanaladas. Na porção superior destas camadas que contêm as estratificações, podem ocorrer camadas finas de arenitos lamíticos com 2 cm a 10 cm de espessura e dezenas de metros de desenvolvimento lateral, que exibem pequenas gretas de dessecação preenchidas por areia fina (Figura 16).



**Figura 16.** Litofácies Arenito com estratificação cruzada acanalada de base côncava. Detalhe de gretas de dessecação preenchidas por areia fina que ocorrem no topo de camadas finas de arenitos lamíticos. Ponto 8 na Figura 1A.

### 3.2.3.1. Interpretação

As estruturas sedimentares descritas são indicativas de fluxos aquosos. Fluxos turbulentos produziram a erosão do substrato e foram responsáveis pela conformação da geometria côncava encontrada na base desta litofácies. Após a erosão do substrato e formação de escavações côncavas, pequenas dunas de geometria 3-D preencheram essas depressões depositando areias finas, médias e grossas com estratificação cruzada acanalada, semelhantes às estruturas de corte-e-preenchimento.

A interpretação desta litofácies como produto de depósitos de inundação instantânea em porções mais rebaixadas da topografia interna dos lençóis de areia é corroborada por depósitos mal selecionados com clastos grossos, extensão e espessura limitada (<20 m de extensão lateral e <0,35 m de espessura), retrabalhamento dos depósitos eólicos da litofácies Arenito com laminação plano-paralela e, limite superior da litofácies marcado por nível de arenitos lamíticos mostrando o decréscimo de energia dos fluxos ao final da deposição.

#### 4. Reconstrução paleoambiental e interpretação das relações entre sedimentos e paleossolos

A sucessão sedimentar da Formação Marília, exposta na porção noroeste da Bacia Bauru, é caracterizada por alternâncias verticais de paleossolos, depósitos eólicos e depósitos fluviais, que possuem uma distribuição em média por espessura de 66%, 23,3%, 10,7%, respectivamente, em 13 seções estratigráficas medidas, que perfazem uma espessura total de 170 m.

Os depósitos foram divididos em três litofácies: Arenito com laminação plano-paralela, Arenitos conglomeráticos e Arenito com estratificação cruzada acanalada de base côncava. Os paleossolos foram classificados de acordo com o *US Soil Taxonomy* (Soil Survey Staff, 1999) em quatro ordens, que refletem os principais fatores de formação dos solos (Jenny, 1941): *Aridisols* e *Alfisols* associados ao clima; *Vertisols* ao material de origem e topografia e *Entisols* ao tempo de formação. A participação de organismos nos processos de formação dos solos foi mais ativa nas duas primeiras ordens, atestada pela maior freqüência de bioturbações e devido ao maior grau de evolução e diferenciação dos horizontes pedogênicos nestas ordens.

A transição vertical entre os paleossolos e os depósitos é sempre abrupta e erodida, atestada pela freqüente ausência de horizontes A nos paleossolos. Lateralmente, devido à continuidade limitada dos depósitos, é possível observar a superposição de perfis de paleossolo separados internamente por superfícies erodidas (Figura 17).

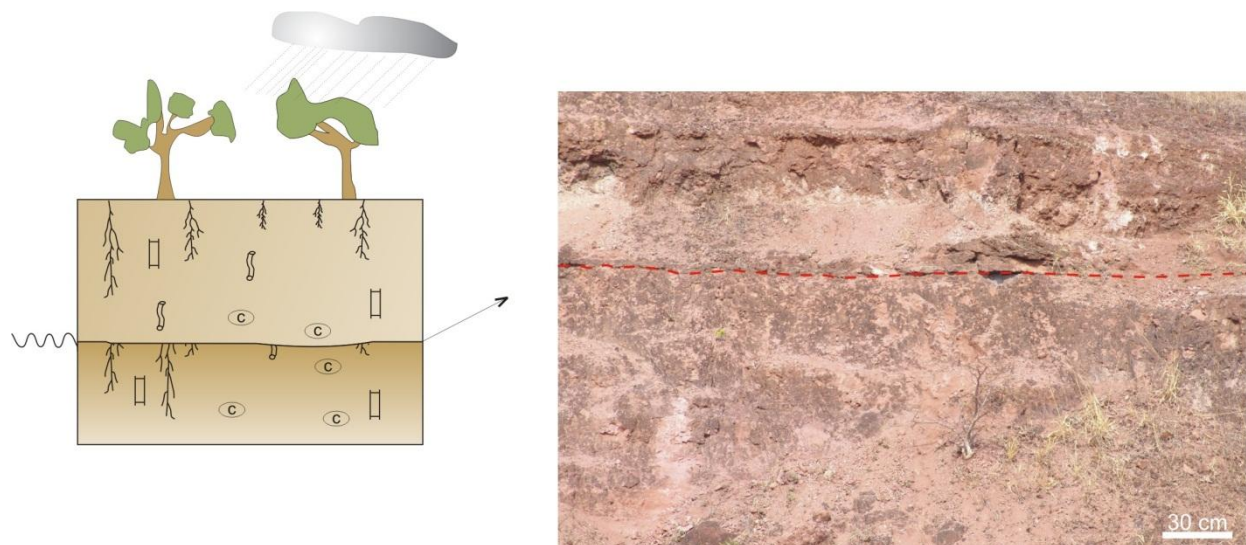


**Figura 17.** Superfície erodida em meio à paleossolo, separando dois perfis de *Aridisols*. Ponto 11 na Figura 1A.

As superfícies erodidas, que ocorrem na base dos depósitos eólicos e separam os corpos eólicos dos perfis de *Aridisols*, *Alfisols* e *Entisols*, possuem formas planas suborizontais e, possivelmente foram geradas por atividade de deflação eólica. Em alguns casos, tais superfícies podem assumir formas levemente onduladas, devido à presença de horizontes subsuperficiais Bk endurecidos, que atuaram como superfícies cimentantes e não permitiram a completa erosão dos perfis de *Aridisols*. As superfícies erodidas com base côncava que cortam de forma indiscriminada o topo dos perfis de *Aridisols* ocorrem associadas aos depósitos da litofácie Arenitos conglomeráticos e, têm origem na escavação produzida por ação de fluxos hidráulicos.

Alguns perfis de *Aridisols* superpostos são separados internamente por superfícies erodidas planas suborizontais. Em tais casos, possivelmente as taxas de sedimentação foram superiores às de pedogênese, resultando no progressivo enterramento do perfil e da superfície erodida, desenvolvendo perfis semelhantes aos denominados por Marriott & Wright (1993) de *compound-truncated profiles*. Estes perfis não mostram poligenia, e apresentam sucessão vertical marcada por horizontes diagnósticos distintos, que evidenciam diferentes episódios alternados de sedimentação, pedogênese e erosão.

Felix-Henningsen *et al.* (2003) descreveram no oeste sul-africano perfis de paleossolo com horizontes de calcrete pedogênico truncados por superfícies erodidas semelhantes aos da Formação Marília. Estes autores atribuíram a formação das superfícies erodidas à ação de períodos com predominante atividade de erosão eólica, dominante durante as fases mais secas de ciclos paleoclimáticos do Pleistoceno e Holoceno.

Gustavson & Winkler (1988) e Gustavson & Holliday (1999) descreveram superfícies de deflação eólica intercaladas à paleossolos e depósitos eólicos nos altiplanos do Texas e Novo México (EUA). Segundo os autores, a deflação ocorre durante os períodos caracterizados por índices pluviométricos muito baixos, seguidos de vegetação escassa e presença de ventos fortes e constantes. No entanto, a ocorrência de deposição eólica estaria sujeita a disponibilidade dos sedimentos de serem removidos e transportados pelo vento. Neste contexto, os autores identificaram uma sucessão com 110 m de espessura caracterizada por diversos episódios de deflação, alternados com sedimentação eólica e pedogênese. Para os autores, os episódios de sedimentação eólica teriam sido ativos durante os períodos mais secos de ciclos paleoclimáticos, enquanto as fases de desenvolvimento de solos estiveram restritas aos períodos com maior umidade disponível. A redução na cobertura vegetal seria a causa da exposição das superfícies à

ação dos ventos, capazes de mobilizar e transportar clastos durante os períodos mais quentes e secos e, conduzir a formação de superfícies de deflação cobertas por sedimentação eólica. Durante os períodos mais frios e úmidos, o aumento da cobertura vegetal tornaria a superfície novamente estável, com conseqüente redução da deflação eólica e favorecimento do desenvolvimento de solos.

Tchakerian (1991) e Lancaster & Tchakerian (1996) apresentaram um modelo de evolução semelhante para o deserto de Mojave, no oeste norte-americano, onde os episódios de formação de solos se alternam com episódios de sedimentação eólica. De acordo com os autores, os episódios de formação de solos representam períodos mais úmidos marcados por estabilidade geomórfica e ausência de sedimentação eólica. Estes períodos, com milhares de anos de duração, representariam pausas nos processos de sedimentação e erosão e, seriam responsáveis pela formação de superfícies estratigráficas de caráter regional.

Na área de estudo, a litofácie Arenito com laminação plano-paralela representa a fase de sedimentação eólica, que provavelmente cobriu uma superfície de alguns quilômetros de extensão, e foi lateralmente contígua a áreas deflacionares. Em afloramento, é possível rastrear as superfícies de deflação que cortam os perfis de paleossolos por mais de 50 m. As superfícies que cortam os perfis de *Aridisols* e *Alfisols*, provavelmente indicam a transição entre importantes fases de evolução do lençol de areia, pois ambas as ordens de paleossolos indicam períodos de formação com ordens de grandeza superiores há  $10^3$  anos (Birkeland, 1999), indicando diferentes fases de estabilização da superfície do lençol de areia (Figura 18).

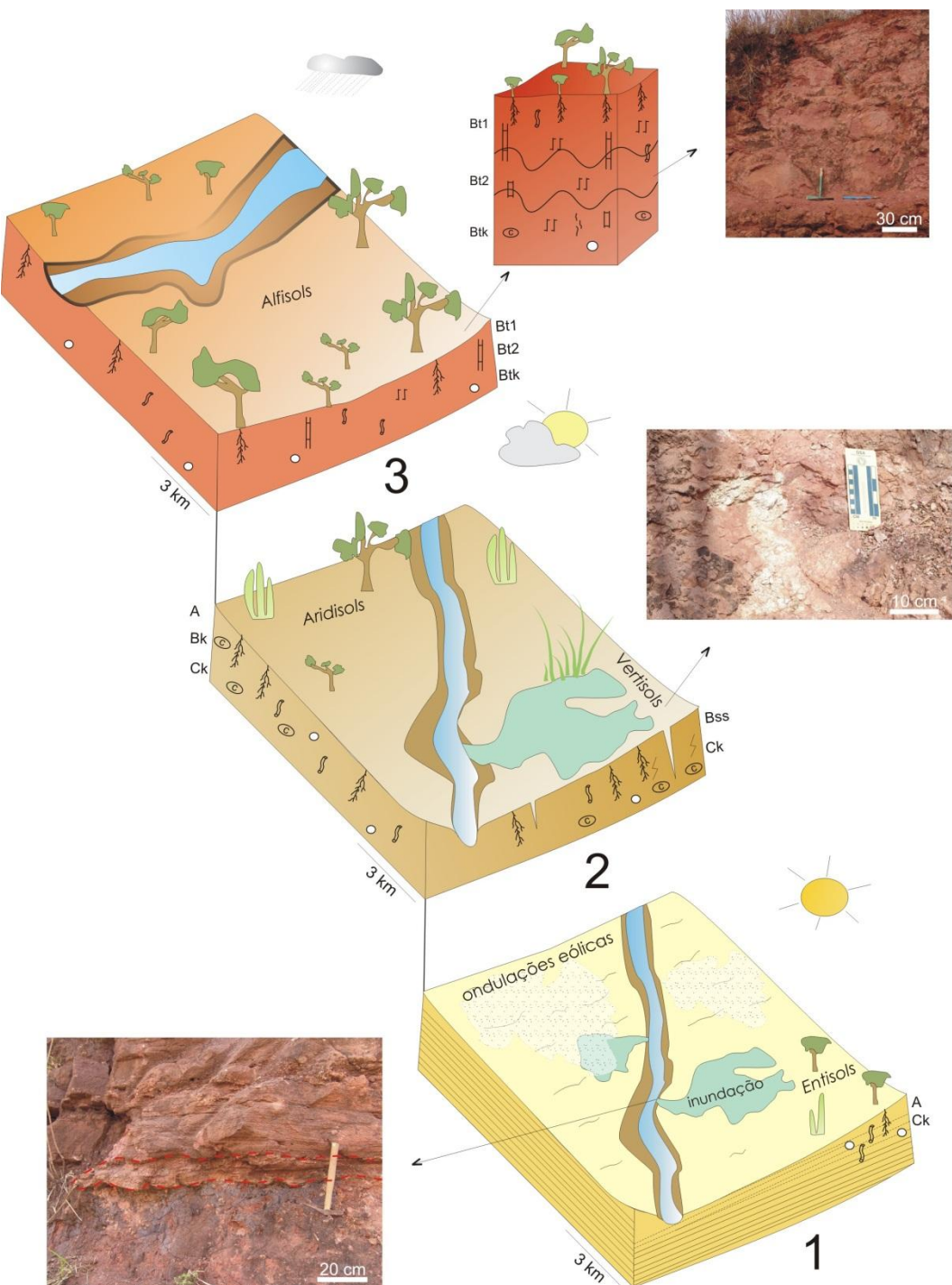


**Figura 18.** Modelo de evolução paleoambiental da Formação Marília na porção noroeste da Bacia Bauru, baseado em diferentes fases de construção dos corpos geológicos: (1) Fase mais seca, caracterizada por deposição eólica contígua ao desenvolvimento de *Entisols* e pequenos corpos de inundação, (2) desenvolvimento de *Aridisols* em fase climática menos seca que a anterior e *Vertisols* em porções mais próximas aos depósitos de inundação, e (3) fase de maior umidade atmosférica, caracterizada por perfis de *Alfisols* bem desenvolvidos. Admite-se que a deposição fluvial foi mais ativa em (2) e (3).

No modelo evolutivo proposto por Lancaster (1994), para o deserto de Mojave, os paleossolos mais desenvolvidos, com horizontes Bt e Bk, teriam evoluído em condições climáticas mais úmidas, nas quais a associação de paleossolos com depósitos fluviais sugeriria que a deposição fluvial também teria ocorrido em períodos com maior disponibilidade hídrica. Nestes períodos, a formação de solos predominaria em áreas intercanais, dotadas de umidade o suficiente para suportar o desenvolvimento de uma cobertura vegetal (Tchakerian & Lancaster, 2002). A maior atividade dos canais fluviais pode ser também um importante elemento à geração de sedimentos para a posterior deposição eólica (Kocurek & Lancaster, 1999).

Na Formação Marília, o modelo de construção de corpos geológicos envolve duas fases temporais distintas, que se alternam ciclicamente, e possuem a mesma grandeza espacial: a) fase de sedimentação eólica, caracterizada por depósitos arenosos com marcas onduladas eólicas, b) fase de pedogênese, que compreende dois períodos temporais distintos, ambos caracterizados por maior umidade atmosférica que a fase de sedimentação eólica. Durante os períodos mais áridos, se desenvolveram os perfis de *Aridisols* e *Entisols*, enquanto o desenvolvimento de *Alfisols* esteve condicionado a um aumento significativo na umidade atmosférica. Não é possível determinar se os perfis de *Vertisols* se desenvolveram durante os períodos mais secos ou úmidos, pois essa ordem de solo não possui significado climático e, apenas registra a variação sazonal entre condições mais secas e úmidas, porém tais variações podem ser provocadas por mudanças no nível do lençol freático e não necessariamente indicam mudanças nos regimes pluviométricos (Ahmad, 1983). A ordem de grandeza temporal envolvida nos processos de formação também difere das ordens de *Aridisols* e *Alfisols*, pois ao contrário das duas ordens, os *Vertisols* podem se desenvolver em intervalos temporais pequenos, apresentando clara diferenciação de horizontes em menos de 1.000 anos (Yaalon & Kalmar, 1978).

Transições laterais entre paleossolos e depósitos das litofácies Arenito com laminação plano-paralela e Arenito com estratificação cruzada acanalada de base côncava nunca foram observadas. Admite-se, que a ausência de tais transições ocorra em razão de dois fatores: a) ambas as litofácies constituem o material de origem dos paleossolos, b) as litofácies possuem continuidade lateral limitada e, perfis de paleossolos podem ocorrem superpostos, com superfícies erodidas separando os diferentes perfis, ou em casos de perfis com evidência de poligenia, sem superfície de separação visível.

Não foi possível verificar a natureza da transição entre os paleossolos e a litofácie Arenitos conglomeráticos, pois os depósitos desta litofácie nunca formam o material de origem dos paleossolos e a transição superior dos perfis em relação aos depósitos é marcada por superfície erodida. Aparentemente, esta litofácie não possui uma organização geométrica em meio às litofácies ou perfis de paleossolos, e ocorre de forma indiscriminada nas seções.

A identificação da origem dos sedimentos que formaram os depósitos eólicos ainda é incerta, assim como a capacidade dos rios em transportar e armazenar os sedimentos e a capacidade dos ventos em remover e transportar as areias que serviram à construção dos lençóis de areia. O suprimento de sedimentos (fornecimento) ocorreu provavelmente durante os períodos mais úmidos (períodos de maior atividade fluvial). Porém, nestes períodos, os sedimentos devem ter permanecido confinados em canais fluviais efêmeros e pequenos corpos marginais (depósitos de inundação), em razão da disponibilidade limitada e da baixa capacidade de transporte pelo vento em condições mais úmidas. Portanto, ao mesmo tempo em que aumentavam as taxas de suprimento nos períodos mais úmidos, a disponibilidade e a mobilidade dos sedimentos diminuía, em consequência do aumento dos índices de precipitação, que elevavam o nível médio do lençol freático e propiciavam o aumento da cobertura vegetal. Nos períodos mais secos, o suprimento de sedimentos diminuía, porém os sedimentos retidos nos canais efêmeros passaram a sofrer mobilização e transporte pelo vento. Nestes períodos de deflação eólica, os horizontes superficiais decapitados dos solos também forneceram material ao transporte eólico.

A freqüência dos eventos de deposição eólica pode estar diretamente associada aos depósitos de canais efêmeros e depósitos de inundação. Corpos lacustres ou de *sabkha* – que poderiam atuar como níveis de base locais ou regionais – e, poderiam ter permitido a acumulação e o armazenamento de sedimentos, para a deflação e deposição eólica, não foram encontrados.

A falta de dados paleoclimáticos e cronológicos inviabiliza a quantificação das taxas de suprimento e disponibilidade de sedimentos que atuaram na construção dos lençóis de areia eólica. A capacidade de transporte, que é função da força dos ventos, também é um fator de difícil quantificação. A ampliação da área de estudo, assim como a comparação com sistemas análogos modernos, pode constituir elementos adicionais à identificação da área fonte de sedimentos e contribuir para a melhor compreensão dos fatores que controlaram os episódios de deposição eólica.

## **5. Considerações finais**

A análise da sucessão vertical da Formação Marília na porção noroeste da Bacia Bauru revelou que depósitos eólicos e perfis de paleossolos constituem os principais corpos geológicos que ocorrem na Formação Marília. O contexto paleoambiental no qual se formaram os depósitos envolveu ampla sedimentação eólica em extensas superfícies de lençóis de areia. A morfologia da superfície, com característica essencialmente plana, permitiu a deposição de areias em pequenas estruturas onduladas assimétricas ou pequenas dunas sem faces de avalanche, que formaram corpos tabulares com estratificação cavalgante transladante subcrítica. A superfície era recortada por poucos e rasos canais fluviais efêmeros, que permitiram a formação de corpos conglomeráticos, contribuíram a deposição de areias mais grossas à superfície dos lençóis e formaram estruturas canalizadas que permitiram o armazenamento temporário de sedimentos, para a posterior deflação e deposição eólica. Alternados a tais eventos de sedimentação, ocorreram outros caracterizados por estabilidade da superfície morfológica e pedogênese dos corpos previamente depositados. Mudanças paleoclimáticas, que afetaram diretamente a disponibilidade hídrica do sistema, controlaram as diferentes fases de sedimentação eólica e desenvolvimento de solos. Durante as fases mais úmidas, com o crescimento e expansão da cobertura vegetal, houve a estabilização da superfície morfológica, que inibiu a atividade de deflação eólica e permitiu a formação de solos que se diferenciaram em quatro ordens de acordo com as variações nos fatores de formação de solos, que foram determinadas principalmente pelo clima, material de origem e tempo de formação.

## **Agradecimentos**

Os autores agradecem à Fundação de Amparo à Pesquisa do Estado de São Paulo (processos 07/00140-6 e 07/02079-2) pelo auxílio financeiro, ao Conselho Nacional de Desenvolvimento Científico e Tecnológico pela concessão da bolsa de doutorado ao primeiro autor e a *International Association of Sedimentologists* pelo auxílio financeiro através do *PhD Grant* e *Travel Grant* ao primeiro autor.

## **6. Referências bibliográficas**

- AHMAD, N. Vertisols. In: WILDING, L.P.; SMECK, N.E.; HALL, G.F. (Eds.), **Pedogenesis and Soil Taxonomy II. The Soil Orders**. Amsterdam: Elsevier, p. 91-123, 1983.
- ALMEIDA, F.F.M. & BARBOSA, O. **Geologia das quadrículas de Piracicaba e Rio Claro**. Rio de Janeiro: Boletim da Divisão de Geologia de Minas, Departamento Nacional de Produção Mineral, v. 143, p. 1-96, 1953.
- BACHMAN, G.O. & MACHETTE, M.N. **Calcic soils and calcretes in the southwestern United States**. United States Geological Survey: Open-File Report, v. 77-797, 163 p., 1977.
- BAGNOLD, R.A. **The Physics of Blow Sand and Desert Dunes**. London: Methuen, 265 p., 1941.
- BARCELOS, J.H. **Reconstrução paleogeográfica da sedimentação do Grupo Bauru baseada na sua redefinição estratigráfica parcial em território paulista e no estudo preliminar fora do estado de São Paulo**. Rio Claro, 1984. 190 p. Tese (Livre Docência) - Instituto de Geociências e Ciências Exatas, Universidade Estadual Paulista.
- BARCELOS, J.H. & SUGUIO, K. Correlação e extensão das unidades litoestratigráficas do Grupo Bauru, definidas em território paulista e nos estados de Minas Gerais, Goiás, Mato Grosso do Sul e Paraná. In: SIMPÓSIO REGIONAL DE GEOLOGIA, 6. **Atas...** Rio Claro, 1987, p. 313-321.
- BASILICI, G.; DAL' BO, P.F.F.; LADEIRA, F.S.B. Climate-induced sediment-palaeosol cycles in a Late Cretaceous dry aeolian sand sheet: Marília Formation (North-West Bauru Basin, Brazil). **Sedimentology**, v. 56, p. 1876-1904, 2009.
- BASILICI, G. & DAL' BO, P.F.F. Anatomy and controlling factors of a Late Cretaceous aeolian sand sheet: the Marília and the Adamantina formations, NW Bauru Basin, Brazil. **Sedimentary Geology**, v. 226, p. 71-93, 2010.
- BATEZELLI, A. **Análise da sedimentação cretácea no triângulo mineiro e sua correlação com áreas adjacentes**. Rio Claro, 2003. 183 p. Tese (Doutorado) - Instituto de Geociências e Ciências Exatas, Universidade Estadual Paulista.
- BATEZELLI, A.; SAAD, A.R.; PERINOTTO, J.A.J.; FULFARO, V.J. Análise estratigráfica aplicada à porção norte e nordeste da Bacia Bauru (Cretáceo Superior). **Revista Brasileira de Geociências**, v. 36, p. 253-268, 2006.
- BIRKELAND, P.W. **Soils and Geomorphology**, 3rd edition. New York: Oxford University Press, 430 p., 1999.
- CATT, J.A. Paleopedology manual. **Quaternary International**, v. 6, p. 1-95, 1990.

COULOMBE, C.E.; DIXON, J.B.; WILDING, L.P. Mineralogy and chemistry of Vertisols. In: AHMAD, N. & MERMUT, A. (Eds.), **Vertisols and Technologies for their Management**. Amsterdam: Elsevier, v. 24, p. 115-200, 1996.

CPRM – COMPANHIA DE PESQUISA DE RECURSOS MINERAIS - SERVIÇO GEOLÓGICO DO BRASIL. **Carta geológica do Brasil ao milionésimo. Folha SE22-Goiânia**. Brasília: Programa Geologia do Brasil, CPRM, CD-ROM, 2004.

DAL' BO, P.F.F. & BASILICI, G. Estimativas de paleoprecipitação e gênese de feições cárnicas e argílicas em paleossolos da Formação Marília (Neocretáceo da Bacia Bauru). **Geociências**, v. 29, p. 33-47, 2010.

FELIX-HENNINGSEN, P.; KANDEL, A.W.; CONARD, N.J. The significance of calcretes and paleosols on ancient dunes of the western Cape, South Africa, as stratigraphic markers and paleoenvironmental indicators. In: FÜLEKY, G. (Ed.), **Papers of the 1st International Conference on Archaeology and Soils**, p. 45-52, 2003.

FERNANDES, L.A. & COIMBRA, A.M. O Grupo Caiuá (Ks): revisão estratigráfica e contexto deposicional. **Revista Brasileira de Geociências**, v. 24, n. 3, p. 164-176, 1994.

FRYBERGER, S.G. & SCHENK, C.J. Pin stripe lamination: a distinctive feature of modern and ancient eolian sediments. **Sedimentary Geology**, v. 55, p. 1-15, 1988.

FULFARO, V.J.; PERINOTTO, J.A.J.; BARCELOS, J.H. A margem goiana do Grupo Bauru: implicações na litoestratigrafia e paleogeografia. In: SIMPÓSIO SOBRE O CRETÁCEO DO BRASIL, 3. **Boletim...** Rio Claro, 1994, p. 81-84.

GILE, L.H.; PETERSON, F.F.; GROSSMAN, R.B. Morphological and genetic sequences of carbonate accumulation in desert soils. **Soil Science**, v. 101, p. 347-354, 1966.

GOUDIE, A.S. **Duricrusts in Tropical and Subtropical Landscapes**. Oxford: Clarendon, 174 p., 1973.

GUSTAVSON, T.C. Buried Vertisols in lacustrine facies of the Pliocene Fort Hancock Formation, Hueco Bolson, west Texas and Chihuahua, Mexico. **Geological Society of America Bulletin**, v. 103, p. 448-460, 1991.

GUSTAVSON, T.C. & HOLLIDAY, V.T. Eolian sedimentation and soil development on semi-arid to subhumid grassland, Tertiary Ogallala and Quaternary Blackwater Draw Formations, Texas and New Mexico High Plains. **Journal of Sedimentary Research**, v. 69, n. 3, p. 622-634, 1999.

GUSTAVSON, T.C. & WINKLER, D.A. Depositional facies of the Miocene-Pliocene Ogallala Formation, northwestern Texas and eastern New Mexico. **Geology**, v. 16, p. 203-206, 1988.

HARMS, J.C.; Southard, J.B.; Spering, D.R.; Walker, R.G. **Depositional Environments as Interpreted from Primary Sedimentary Structures and Stratification Sequences**. Dallas: Society of Economic Paleontologists and Mineralogists, SEPM Short Course, v. 2, 153 p., 1975.

HUNTER, R.E. Basic types of stratification in small eolian dunes. **Sedimentology**, v. 24, p. 361-387, 1977.

JENNY, H.J. **Factors of soil formation**. New York: McGraw-Hill, 281 p., 1941.

KHADKIKAR, A.S.; MERH, S.S.; MALIK, J.N.; CHAMYAL, L.S. Calcretes in semi-arid alluvial systems: formative pathways and sinks. **Sedimentary Geology**, v. 116, p. 251-260, 1998.

KOCUREK, G. & LANCASTER, N. Aeolian system sediment state: theory and Mojave Desert Kelso dune field example. **Sedimentology**, v. 46, p. 505-515, 1999.

KOCUREK, G. & NIELSON, J. Conditions favourable to the formation of warm-climate aeolian sand sheets. **Sedimentology**, v. 33, p. 795-816, 1986.

KÖEPPEN, W. **Climatología: Con un Estudio de los Climas de la Tierra**. Pánuco: Fondo de Cultura Económica, 478 p., 1948.

KOSTER, E.A. Ancient and modern cold-climate aeolian sand deposition: a review. **Journal of Quaternary Science**, v. 3, n. 1, p. 69-83, 1988.

LANCASTER, N. Origins and sedimentary features of supersurfaces in the northwestern Gran Desierto sand sea. In: PYE, K. & LANCASTER, N. (Eds.), **Aeolian Sedimentation, Ancient and Modern**. Oxford: International Association of Sedimentologists, Special Publication, v. 16, p. 71-83, 1993.

LANCASTER, N. Controls on aeolian activity: some new perspectives from the Kelso Dunes, Mojave Desert, California. **Journal of Arid Environments**, v. 27, p. 113-124, 1994.

LANCASTER, N. & TCHAKERIAN, V.P. Geomorphology and sediments of sand ramps in the Mojave Desert. **Geomorphology**, v. 17, p. 151-166, 1996.

LOOPE, D.B. Rhizoliths in ancient aeolianites. **Sedimentary Geology**, v. 56, p. 301-314, 1988.

MACK, G.H. & JAMES, W.C. **Paleosols for Sedimentologists**. Cincinnati: Geological Society of America, Short Course Notes, 127 p., 1992.

MACK, G.H.; JAMES, W.C.; MONGER, H.C. Classification of paleosols. **Geological Society of America Bulletin**, v. 105, p. 129-136, 1993.

MAHANEY, W.C. **Atlas of Sand Grain Surface Textures and Applications**. Oxford: Oxford University Press, 237 p., 2002.

MARRIOTT, S.B. & WRIGHT, V.P. Paleosols as indicators of geomorphic stability in two Old Red Sandstone alluvial suites, South Wales. **Journal of the Geological Society of London**, v. 150, p. 1109-1120, 1993.

MOUNTNEY, N.P. Aeolian facies model. In: POSAMENTIER, H.W. & WALKER, R.G. **Facies Models Revisited**. Tulsa: Society for Sedimentary Geology, Special Publication, v. 84, p. 19-83, 2006.

NETTLETON, W.D. & PETERSON, F.F. Aridisols. In: WILDING, L.P.; SMECK, N.E.; HALL, G.F. (Eds.), **Pedogenesis and Soil Taxonomy II. The Soil Orders**. Amsterdam: Elsevier, p. 165-215, 1983.

RETALLACK, G.J. **Soils of the Past**. Oxford: Blackwell, 404 p., 2001.

SCHAETZL, R.J. & ANDERSON, S.N. **Soils: Genesis and Geomorphology**. Cambridge: University Press, 832 p., 2005.

SHELDON, N.D.; RETALLACK, G.J.; TANAKA, S. Geochemical climofunctions from North American soils and application to paleosols across the Eocene-Oligocene boundary in Oregon. **Journal of Geology**, v. 110, p. 687-696, 2002.

SOIL SURVEY STAFF. **Soil Survey Manual**. Soil Conservation Service. U.S. Department of Agriculture Handbook 18. Washington, DC, 437 p., 1993.

SOIL SURVEY STAFF. **Soil Taxonomy**, 2nd edition. U.S Department of Agriculture, Natural Resource Conservation Service 436. Washington, DC, 871 p., 1999.

TCHAKERIAN, V.P. Late Quaternary aeolian geomorphology of the Dale Lake sand sheet, southern Mojave Desert, California. **Physical Geography**, v. 12, n. 4, p. 347-369, 1991.

TCHAKERIAN, V.P. & LANCASTER, N. Late Quaternary arid/humid cycles in the Mojave Desert and western Great Basin of North America. **Quaternary Science Reviews**, v. 21, p. 799-810, 2002.

VANSTONE, S.D. Early Carboniferous (Mississippian) paleosols from southwest Britain: influence of climatic change on soil development. **Journal of Sedimentary Petrology**, v. 6, n. 4, p. 445-457, 1991.

YAALON, D.H. & KALMAR, D. Dynamics of cracking and swelling clay soils: displacement of skeletal grains, optimum depth of slickensides, and rate of intra-pedonic turbation. **Earth Surface Processes and Landforms**, v. 3, n. 1, p. 31-42, 1978.

## ANEXO V

“Basilici, G. & Dal’ Bo, P.F.F., 2010. *Anatomy and controlling factors of a Late Cretaceous aeolian sand sheet: The Marília and the Adamantina formations, NW Bauru Basin, Brazil.* *Sedimentary Geology* 226, 71-93.”



*“The man of knowledge must be able not only to love his enemies but also to hate his friends.”*

*Friedrich Nietzsche*



# **ANATOMY AND CONTROLLING FACTORS OF A LATE CRETACEOUS AEOLIAN SAND SHEET: THE MARÍLIA AND THE ADAMANTINA FORMATIONS, NW BAURU BASIN, BRAZIL**

Giorgio Basilici & Patrick Francisco Führ Dal' Bó

*DGRN/IG – Unicamp, Cidade Universitária, 13083-870, Campinas (SP), Brazil, (Tel.*

*55.19.35215121. Fax: 55.19.32891562. E-mail: basilici@ige.unicamp.br;*

*patrickdalbo@ige.unicamp.br)*

## **Abstract**

Few previous studies have given significant consideration to the palaeosols in aeolian sand sheet sedimentary successions and, mainly, to their palaeoenvironmental and stratigraphic meaning in interaction with the deposits. These themes are considered in this study that deals with the depositional architecture and the factors controlling the construction, accumulation and preservation of an ancient aeolian sand sheet, that form part of the Adamantina and Marília formations, in the Bauru Basin (Late Cretaceous, Brazil). In the NW portion of the Bauru Basin, these two units, *ca* 220 m thick, consist of sandstone, and secondarily of sandy conglomerate and mudstone, and are characterised by vertically alternated palaeosols and deposits. Facies analyses of the deposits and macroscopic characterisation of the palaeosols in 45 outcrops were integrated with laboratory analyses that consisted in descriptions of slabs of rock samples, petrographic analyses, clay mineralogy determination, geochemical analyses of the major oxides, and micromorphological characterisation of the palaeosols. Three architectural elements were recognised: palaeosols, wind-ripple-dominated aeolian sand sheet deposits, and ephemeral river deposits. The palaeosols constitute 66% of the entire sedimentary succession, and consist principally of Aridisols and, subordinately, of Alfisols, Vertisols, and Entisols. The wind-ripple-dominated aeolian sand sheet deposits (25%) are composed of sandstone, organised in translatent climbing wind-ripple strata, and secondarily of sandstone and mudstone deposited by infrequent floods. The ephemeral river deposits (9%) consist of sandy conglomerates 4 m thick and *ca* 2 km wide. Wind-ripple-dominated aeolian sand sheet deposits formed during relatively dry climate period on an unstable topographic surface of an aeolian sand sheet, where aeolian deposition or erosion prevailed. Palaeosols and ephemeral river deposits formed in a more humid climate

period on a stable topographic surface of the aeolian sand sheet. Six bounding surfaces permitted the subdivision of the study formations into genetic geological bodies, revealing different spatial and temporal orders. Two first order surfaces separate mature palaeosol profiles (Aridisols, Alfisols, and Vertisols) from overlying aeolian deposits or other mature palaeosol profiles. A second order surface separates immature palaeosols (Entisols) from overlying aeolian deposits. A third order surface constitutes the channel bottom. A fourth order surface is located at the bottom of flood deposits. A fifth order surface divides translatent wind-ripple. The constructional phase of the aeolian sand sheet occurred during the relatively dry climate period, when the available sediment was supplied from the material originally deposited by rivers and stored during a more humid period (primary supply), and by soil erosion during a drier climate (secondary supply). The accumulation surface was controlled during the drier climate by cemented Bk horizons over Aridisols and by the force of the wind blowing over the other soils or deposits. Otherwise, during the more humid climate, the accumulation surface was a stabilised surface represented by the soil. Preservation was dominated by tectonically induced subsidence and burial.

Keywords: Aeolian sand sheet, Palaeosols, Climatic cycles, Aeolian bounding surfaces, Bauru Basin, Late Cretaceous.

## **1. Introduction**

An aeolian sand sheet is defined as a flat or gently-undulating sandy surface above which dunes do not form (Fryberger et al., 1979; Kocurek and Nielson, 1986; Mountney, 2006); it is common in dryland areas in both hot and cold climates. The inhibition of dune formation can be influenced by sparse vegetation, high ground-water level, coarse-grained sediments, armoured or cemented surfaces, and a scarce supply and availability of sediments (Kocurek and Nielson, 1986; Breed et al., 1987).

Aeolian sand sheets form significant part of several of the world's major present-day desertic systems and constitute a portion of ergs, as in the case of the Namibia sand seas (Lancaster, 1994), or of other depositional systems such as alluvial fans, ephemeral rivers, playa-lakes, and beaches (Kocurek and Nielson, 1986; Breed et al., 1987; El-Baz et al., 2000). In other cases, they constitute most of the desertic area, as is the case of the Gran Desierto (Mexico) (Lancaster et al., 1987). Aeolian sand sheets commonly have a stabilised topographic surface on which soils form, leading to growth of sparse vegetation. However, they can also constitute unstable topographic surfaces where the changes are dominated by aeolian erosion or sedimentation. The depositional or erosional processes in both ancient and present-day aeolian sand sheet areas are widely described in the literature (e.g. Fryberger et al., 1979; Kocurek and Nielson, 1986; Breed et al. 1987; Langford and Chan, 1989; Trewin, 1993; Kocurek and Lancaster, 1999; El-Baz et al., 2000; Chakraborty and Chakraborty, 2001; Mountney and Russell, 2004; Scherer and Lavinia, 2005; Cain and Mountney, 2009). Nevertheless, little emphasis has been given to the phases of stability and pedogenesis in these areas (Gustavson and Wrinkler, 1988; Gustavson and Holliday, 1999) and to the study of succession, with alternating periods of topographic stability and instability (Basilici et al., 2009).

The objects of this study are the Adamantina and Marília formations (Late Cretaceous), which are the upper units of the NW portion of the Bauru Basin, located in south-east of Brazil (Fig. 1). They are interpreted in this paper as deposited in a desertic system characterised by an extensive aeolian sand sheet.

The main purposes of this study are to define an anatomic organisation and a sequential evolution of the Adamantina and Marília formations. To reach these results the specific objectives are to: (1) provide sedimentologic and palaeopedologic data about these formations;

(2) define the architecture and the sequential organisation found in this aeolian sand sheet deposits; and (3) interpret the construction, accumulation and preservation of this aeolian sand sheet, on the basis of the models of Kocurek (1999), Kocurek and Lancaster (1999), and Kocurek (2003).

To reach these objectives, 13 stratigraphic sections, each 6 to 40 m thick, were measured and analysed in detail and other 32 outcrops were examined over an area of some 15,000 km<sup>2</sup> between the towns of Cassilândia and Quirinópolis (Fig. 1). Limited expositions of the sedimentary succession of the Adamantina and Marília formations obliged a research over an extensive area. However, substantial differences in sediments and palaeosols have never been observed, suggesting the same depositional environment developed for all the 15,000 km<sup>2</sup>. In the field, the sediments were described according to facies analysis methods. 15 slabs of rock samples and 11 thin sections analyses of the sediments contributed to the definition of the mechanisms of transport and deposition, and petrographical characterisation. Pedological structures, horizons, roots and other biogenic traces, colour, and texture have been used to recognise and describe palaeosol profiles in the field (Birkeland, 1999; Retallack, 2001). 35 thin sections, 14 X-ray diffraction, 33 geochemical analyses of palaeosol samples, and 24 SEM analyses of clay minerals helped to distinguish the palaeosol horizons and identify the palaeosol profiles. Sediments are interpreted using comparison with analogous lithofacies and applying principles of hydraulic. The palaeosols are classified according to the US Soil Taxonomy (Soil Survey Staff, 1999). The comparison of the genetic conditions of sediments and palaeosols has been used to interpret the palaeoenvironmental characteristics, the depositional architecture, and the evolution of the aeolian sand sheet.

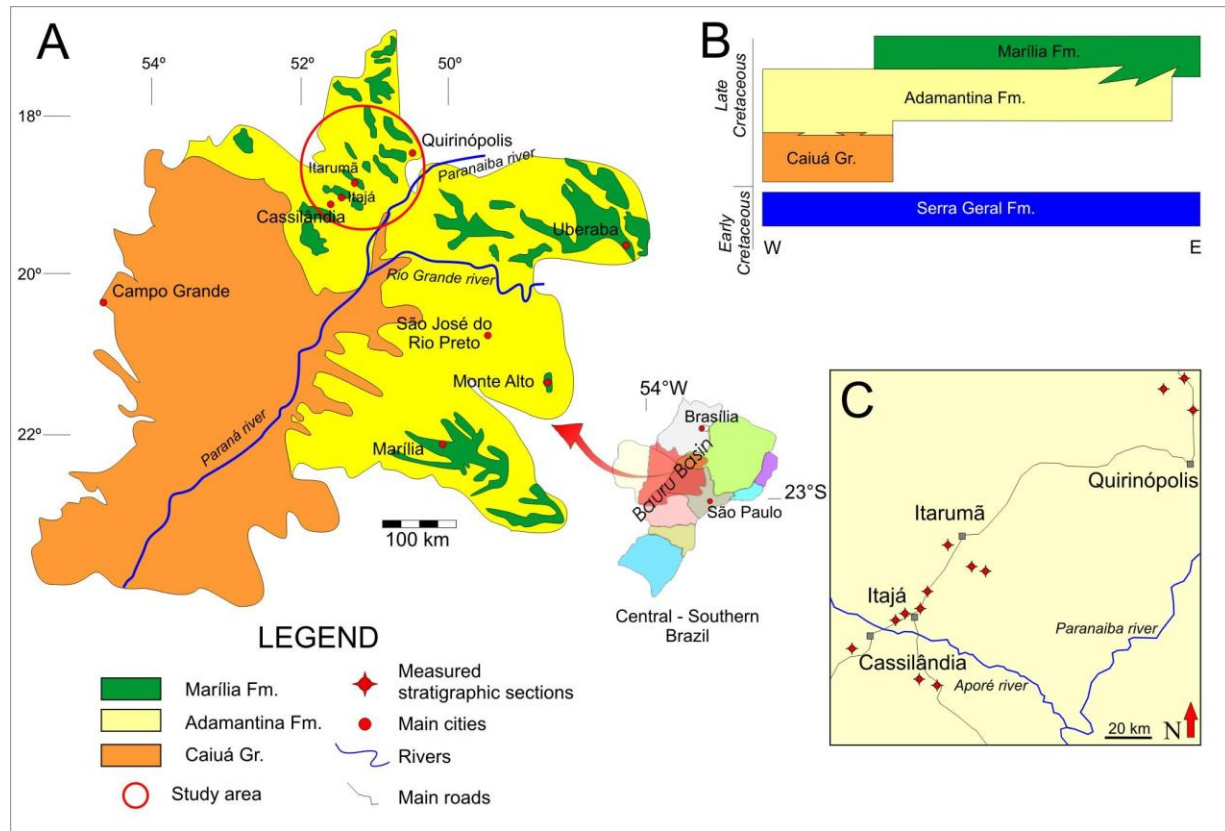


**Figure 1.** (A) Simplified map of the Bauru Basin and location of the study area in the NW of the basin. Modified after Fernandes and Coimbra (1996) and CPRM – Serviço Geológico do Brasil (2004). (B) Stratigraphic synthesis of the Bauru Basin, modified after CPRM – Serviço Geológico do Brasil (2004) and Zaher et al. (2006). (C) Detailed map of the location of the 13 measured sections.

## 2. Adamantina and Marília formations

The Adamantina and Marília formations are the youngest units of the Bauru Basin (Late Cretaceous). This is the last of the great sedimentary basins developed during the Palaeo-Mesozoic eras in southeastern Brazil (Fig. 1). It overlies the world's largest basaltic effusion, dated Early Cretaceous (Serra Geral Formation) (Renne et al., 1992; Turner et al., 1994), which was generated during the break-up of the Gondwana supercontinent.

Studies of the dynamic and temporal development of the Bauru Basin are not abundant, although it is generally accepted that thermal and lithostatic subsidence led to the creation of the accommodation space of the basin (Riccomini, 1997). The sedimentary succession has a maximum thickness of 330 m, and is located above the area of maximum thickness of the Serra Geral Formation (Zalán et al., 1991). Based on the age of the Serra Geral Formation and on

palaeontological data (Dias-Brito, 2001; Carvalho et al., 2005), the sedimentary succession of the Bauru Basin has been attributed to Santonian-Maastrichtian ages (Fernandes and Coimbra, 1996). The sedimentary filling is characterised by a not well defined succession of lithostratigraphic units (CPRM – Serviço Geológico do Brasil, 2004; Zaher et al., 2006), the simplified stratigraphy of which is shown in Fig. 1.

The area of study is located in the northwestern portion of the Bauru Basin (Fig. 1). Here, above the Serra Geral Formation, only the Adamantina and Marília formations crop out. These two formations are composed prevalently of sandstone (quartz arenite, sublitharenite or litharenite) interbedded with mudstone, gravelly sandstone, and sandy conglomerate (Fúlfaro and Perinotto, 1996; Fernandes and Coimbra, 2000; Goldberg and Garcia, 2000; CPRM – Serviço Geológico do Brasil, 2004). The Adamantina Formation differs from the Marília Formation in that it is characterised by finer-sized sediments and by the absence of the sandy conglomerate. The former is interpreted as having been formed in a mixed fluvial-aeolian depositional system, whereas the latter represents the deposition of alluvial megafans draining towards the west (Fúlfaro and Perinotto, 1996; Fernandes and Coimbra, 2000; Goldberg and Garcia, 2000).

In the area of study, the Adamantina and Marília formations are respectively 30 and 190 m thick (CPRM – Serviço Geológico do Brasil, 2004). Nevertheless, during the research activity it was verified that these two units are indistinguishable in the field, as they are characterised by the same lithofacies, architectural elements and sequential organisation. The two units are therefore herein described together. Moreover, in this study, the palaeoenvironmental interpretation differs from Fernandes and Coimbra (1999; 2000), Fúlfaro and Perinotto (1996), and Goldberg and Garcia (2000), because special emphasis has been given to the palaeosols, which constitute 66% of the sedimentary succession, and to the aeolian deposits, which constitute most of the remaining 34% of the sedimentary lithofacies.

### **3. Architectural elements**

The Adamantina and Marília formations have been subdivided into three architectural elements: palaeosols, wind-ripple-dominated aeolian sand sheet deposits, and ephemeral river deposits. The vertical frequency distribution in the 13 sections is respectively: 66, 25, and 9%. These architectural elements have been described according to the definition of Miall (1985;

1990) and following the subdivisions of Miall (1996), North (1996), and Mountney (2006) for alluvial and aeolian depositional systems. A description and genetic interpretation of these three architectural elements follows.

### **3.1. Palaeosols**

The palaeosols constitute the predominant architectural element. They vary from 0.3 to 3.8 m in thickness, and commonly consist of the superimposition of more than one palaeosol profile, separated by erosional deflation surfaces. The upper boundary to ephemeral river or wind-ripple-dominated aeolian sand sheet deposits is an erosional surface; whereas the lower boundary to these same architectural elements is always gradual. Unfavourable exposure allows the verification of lateral continuities only up to 50 m, but stratigraphic correlations between the studied sections suggest the continuity of this element for lateral distances of at least several kilometres (Fig. 2).

The palaeosol profiles were classified using the US Soil Taxonomy (Soil Survey Staff, 1999). This system of classification is preferred, because the key for classification is based on pedogenic features and the diagnostic horizons, which are preserved in the palaeosols. Four types have been recognised in the sections investigated and are classified as: Aridisols, Entisols, Vertisols, and Alfisols.

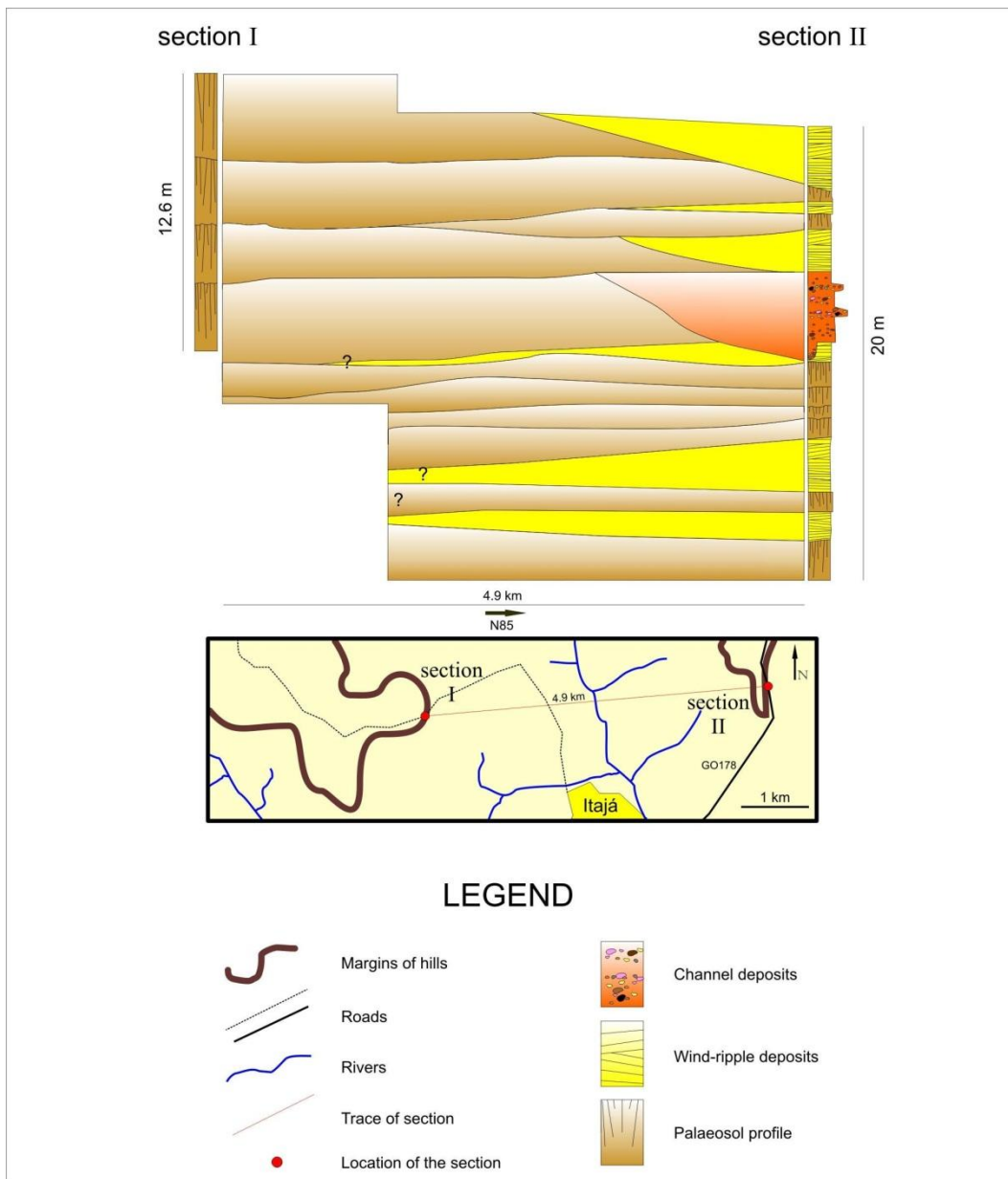


**Figure 2.** Stratigraphic correlation of two measured sections near the town of Itajá. A detailed field analysis verified that the strata are perfectly horizontal and faults do not exist between the two sections. Wind-ripple-dominated aeolian sand sheet deposits show a limited lateral continuity, though do reveal a lenticular shape. According to the depositional model presented here, erosional surfaces between palaeosol profiles may be correlated to the bottom of wind-ripple deposits.

### 3.1.1. Aridisols

The Aridisols (Fig. 3) constitute the most widely spread types. On average, they constitute 84.5% of the thickness of this architectural element. These Aridisols have a fine- to medium-grained sandstone texture, from moderately to well sorted. Petrographical analyses of six samples showed that the parent material is a sublitharenite (Pettijohn et al., 1987): the detrital grains are composed of, on average, monocristalline quartz (76.1%), basalt fragments (13.7%), polycristalline quartz (3.7%), opaque minerals (2.5%), fragments of calcareous nodules eroded from previous palaeosols (1.5%), feldspars (1%), and metamorphic fragments (1.5%) (Fig. 4A). The detrital grains are frequently well rounded and sub-spherical.

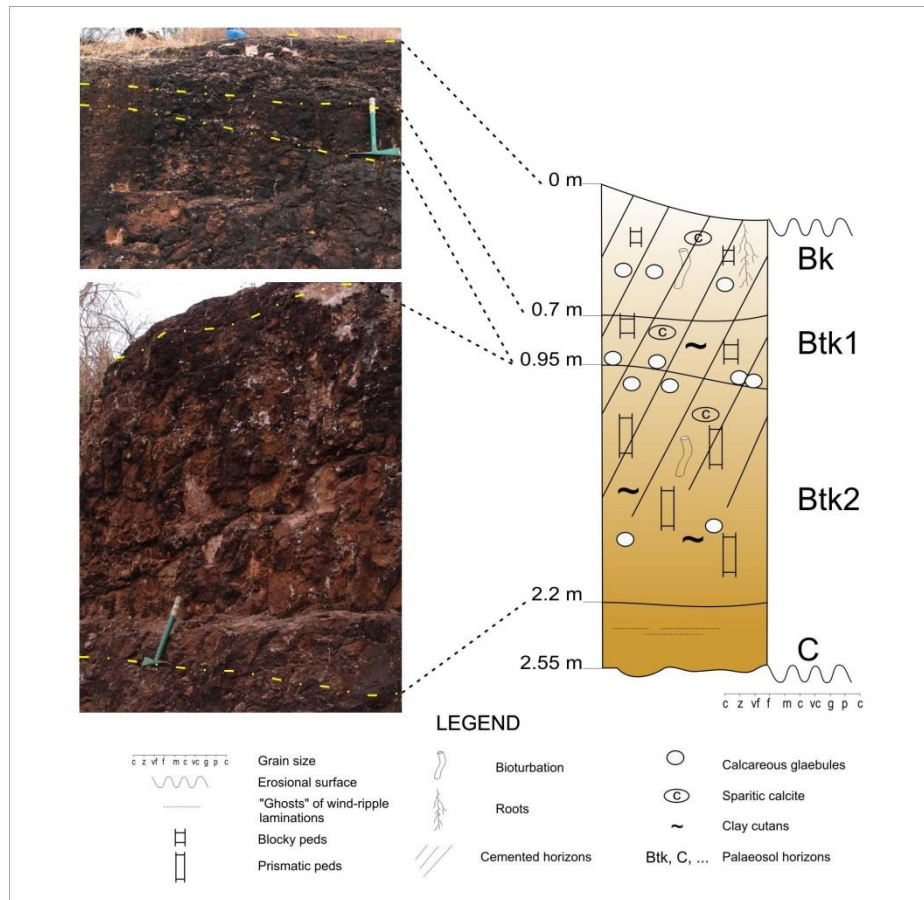


**Figure 3.** Palaeosol profile of Aridisol that crops out near the town of Itajá. Hammer: 0.31 m.

The Aridisols profiles have a thickness of 0.3 to 3 m and show a complete sequence of horizons A/Bt/Btk/Bk (or Bkm)/C (or Ck). However, the A horizon is commonly absent, but the

Bk or Btk horizon is always present. When present, the A horizon is <0.1 m in thickness, reddish orange (10R6/6 or 10R6/8), and structureless, or on rare occasions with a structure of weak medium to coarse granular peds or moderate medium blocky peds. The B horizon is 0.2 to 1.3 m thick, with a colour varying from reddish brown (10R4/4) to red (10R4/6) or light red (10R7/8). In this horizon, argillic (Bt or Btk), calcic (Bk), and petrocalcic (Bkm) horizons can be distinguished. The argillic horizons contain illuviated clay, in the form of clay cutans (argillans) that cover ped faces, coat the sandy grains (Fig. 5A and B), and fill the pores (Fig. 5C). X-ray diffraction and EDS analyses showed that most of the clays are composed of smectite (Fig. 5A), palygorskite, and probably sepiolite (Basilici et al., 2009). According to field estimations, the calcium carbonate varies from slightly calcareous through calcareous to very calcareous, making it possible to recognise the Btk, Bk and Bkm horizons, respectively. Calcium carbonate appears as thin filaments (calcans) that cover peds, pores and/or grain surfaces (Fig. 5B) (Btk horizon), through isolated or coalescent nodules (Btk or Bk horizons), to continuous layers with calcium carbonate >70% (Bkm horizon). Within the Bk horizon, strong medium to coarse subangular blocky peds and strong very coarse prismatic peds with secondary moderate medium to fine blocky peds are the most frequent pedogenic structures (Fig. 6A), although, at times, platy peds may occur (Fig. 6B).

The C horizon is 0.3-0.5 m thick, red (7,5R4/9, 7,5R4/6 or 7,5R4/4) in colour, and structureless, or with “ghosts” of planar parallel laminations, which were interpreted as translatent climbing wind-ripple deposits. The calcium carbonate content varies from very weak to strong (cf. Retallack, 1988), and it is characterised by isolated nodules.

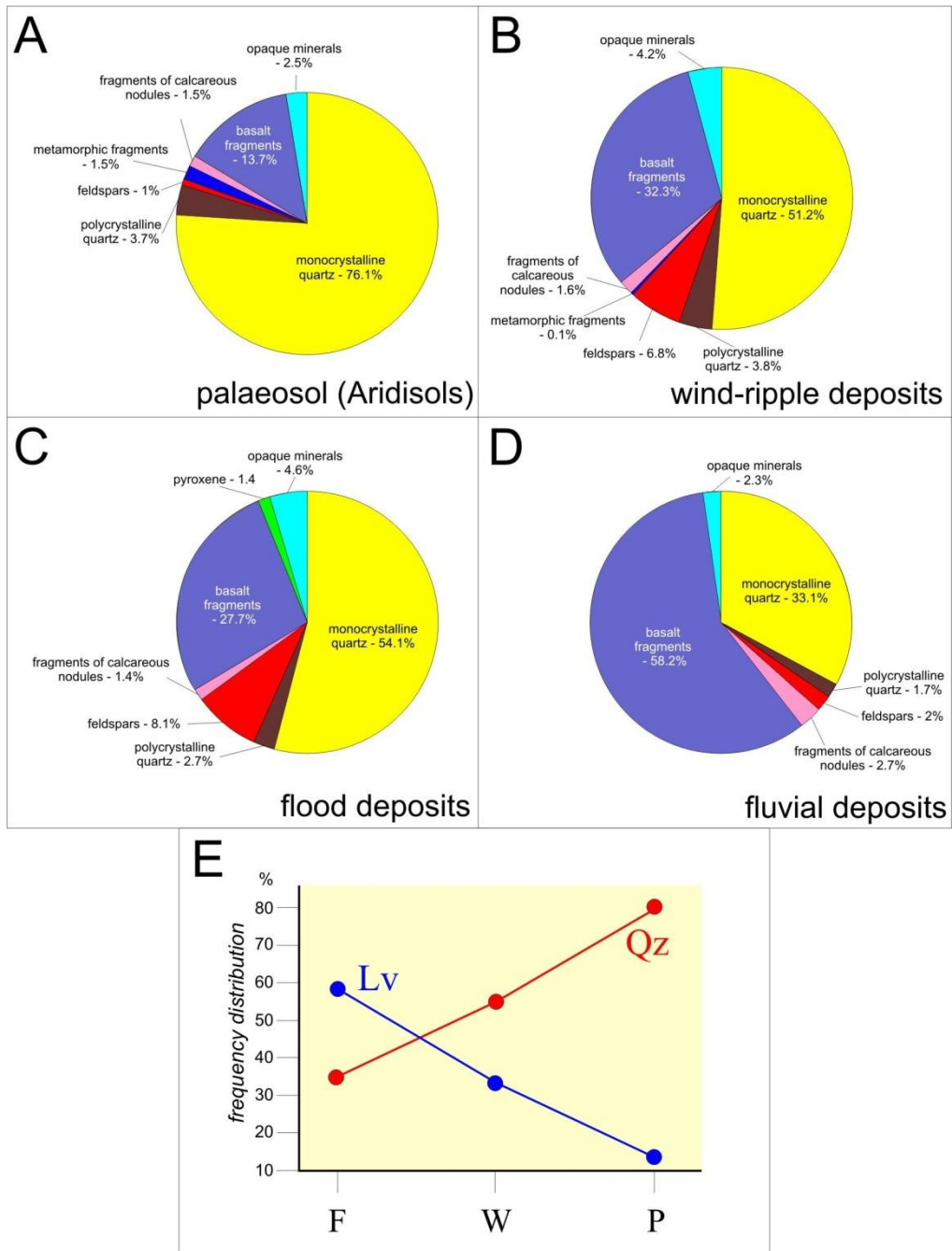


**Figure 4.** Petrographic assemblage of the main minerals of (A) palaeosols (Aridisols), (B) wind-ripple deposits, (C) flood deposits, and (D) fluvial deposits. See text for descriptions. (E) Distribution of the two main mineral components (Qz: monocrystalline plus polycrystalline quartz; Lv: basalt fragments) within the three architectural elements (F: ephemeral river deposits; W: wind-ripple-dominated aeolian sand sheet deposits; P: palaeosols). Note the decrease of basalt fragments and the increase in quartz from ephemeral river deposits through wind-ripple-dominated aeolian sand sheet deposits to palaeosols.

### **3.1.1.1. Interpretation.**

This type was classified as an Aridisol for the following reasons (Soil Survey Staff, 2006): (1) the A horizon can be classified as an ochric epipedon, as it is thin and light in colour, without meeting the criteria for the other seven epipedons; (2) the high content of calcium carbonate allows the identification of the Bk and Bkm horizons; (3) illuviated clay features identify the Bt horizons.

Climate and time have a strong influence on the generation of Aridisols. These soils are typical of regions where the precipitation to evapotranspiration ratio is less than one, thus allowing the precipitation of mineral salts, such as calcium carbonate, within the soil profile. At present, Aridisols are typical of areas with a precipitation of less than 500 mm/y (Wright and Tucker, 1991; Watson, 1992; Retallack, 2001). Estimates of palaeoprecipitation, based on the depth of the nodular Bk calcic horizon in relation to the palaeosol upper surface (Retallack, 2005), suggest values of around 250 mm/y (Dal' Bó et al., 2009). Therefore, the climate recorded by Aridisols probably corresponds to semi-arid conditions in Köppen's classification; these conclusions are confirmed by the presence of illuviated clay in the Bt horizons (Nettleton and Peterson, 1983; Watson, 1992). Moreover, the clay minerals palygorskite and sepiolite are frequently found in dry climate soils (Watson, 1992).

The time of development for these palaeosol profiles cannot be determined. However, many elements suggest a pedogenesis of more than  $10^3$  years, as explained below. Soil maturity is often estimated from the development of the Bk horizon (Gile et al., 1966; Nettleton and Peterson, 1983; Machette, 1985; Monger et al., 1991). The Bk horizon of this palaeosol can be classified as stage III, indicating mature palaeosol and suggesting of a development history ranging from several thousand to a few hundred thousand years. This estimate is not universally adaptable to all Aridisols, however, because the development stage does not depend only on time, but also on other factors such as carbonate availability, the precipitation/evapotranspiration ratio, the parent material, the soil texture, and the activity of organisms. The diversified horizons, well-developed pedogenic structures, clay illuviation, and the occurrence of palygorskite, smectite, and sepiolite clay minerals also suggest a long period of soil development (cf. Watts, 1980; Retallack, 1988; Wright, 1989).

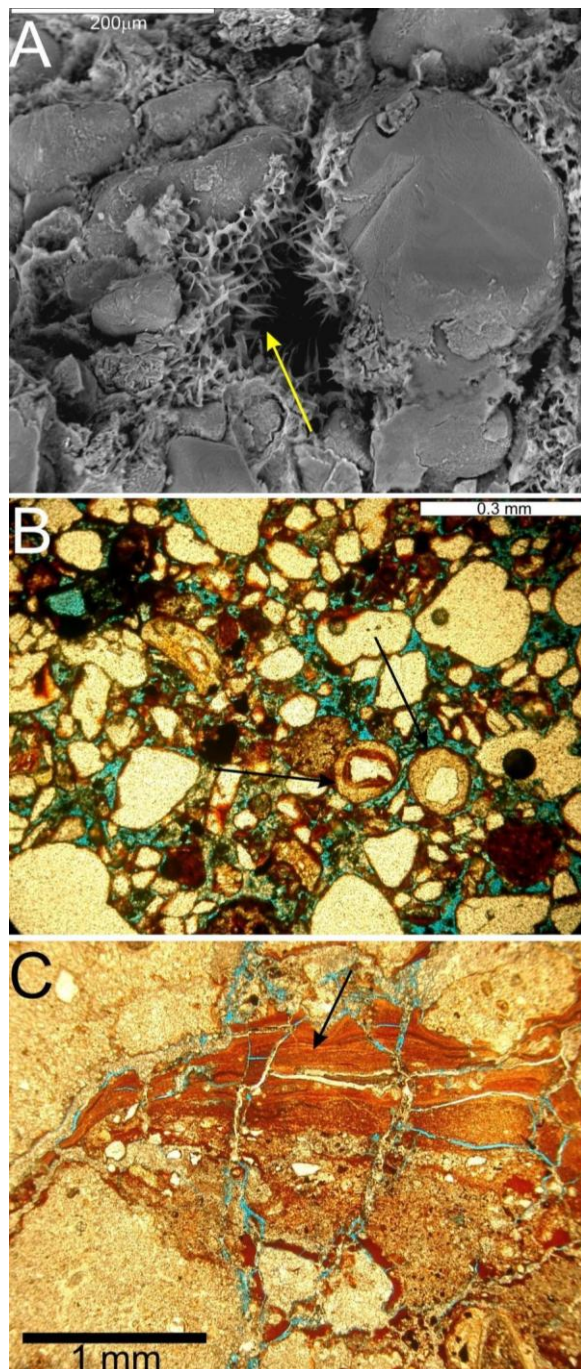


**Figure 5.** Aridisols. (A) Smectite clay minerals (arrow) cover quartz grains as clay cutans in Bt or Btk horizons of Aridisols. (B) Thin section of Btk horizon. The arrows indicate quartz grains covered with alternating darker cutans of clay (argillans) and brighter calcite cutans (calcans). (C) Illuvial clay cutans (arrow) associated with pore-walls that exhibit post-depositional iron segregation. Crossed polarised light.

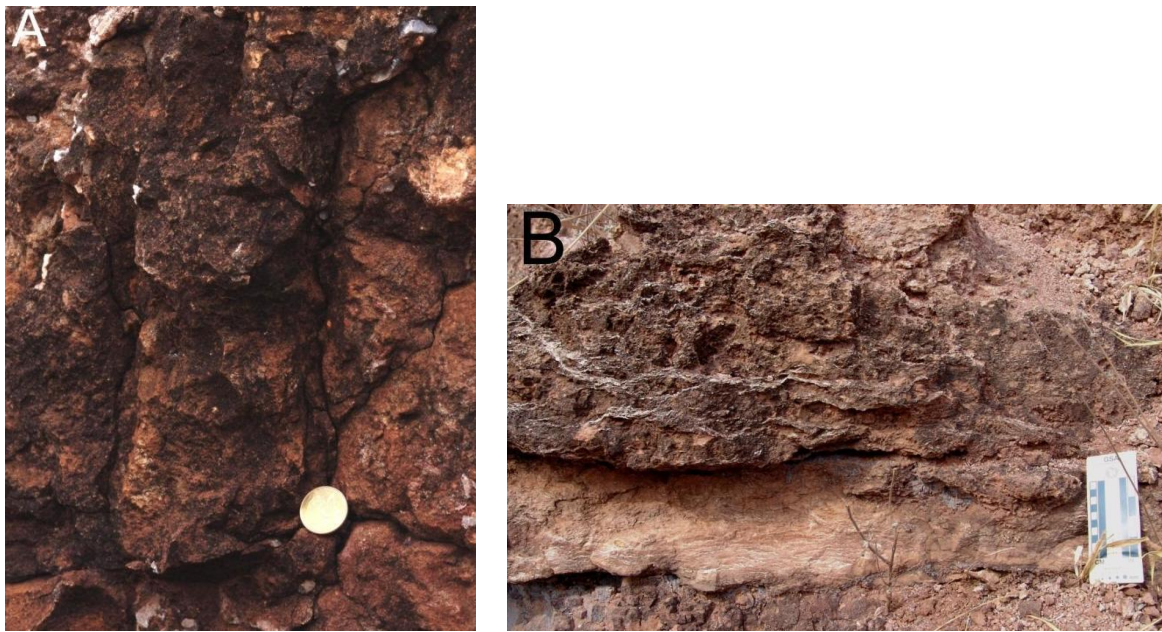


**Figure 6.** (A) Prismatic peds in Btk horizon of Aridisols. Coin: 20 mm. (B) Platy peds in Bk horizon of Aridisols.

### 3.1.2. Entisols

The Entisols (Fig. 7) constitute 0.3-0.5 m thick profiles and account for only 2.1% of the palaeosols thickness. They are found interlayered with sandstone deposits of translatent wind-ripple strata. The texture consists of fine- to medium-grained sandstone, with a petrographic assemblage analogous to that of Aridisols. The palaeosol profiles consist of a sequence of A/Ck horizons. The A horizon is  $\leq 0.1$  m thick, has a sandy texture and is light red (2,5YR6/8) or reddish brown (2,5YR5/8) in colour. It is structureless, with a few calcareous cutans that bridge between the sandy grains. Bioturbation is rare; on the palaeosol section area is less than 3%. This consists in sandstone filled cylindrical tube, up to 60 mm long and 1 to 10 mm across, vertical or oblique. The upper boundary is abrupt, whereas the transition to the C horizon is clear to gradual (cf. Soil Survey Staff, 1993). The Ck horizon is 0.2-0.4 m thick, red (10R4/8 or 10R5/8) in colour, and reveals some calcareous nodules (5-10 mm across) (Fig. 8). “Ghosts” of translatent climbing wind-ripple strata are common in this horizon.

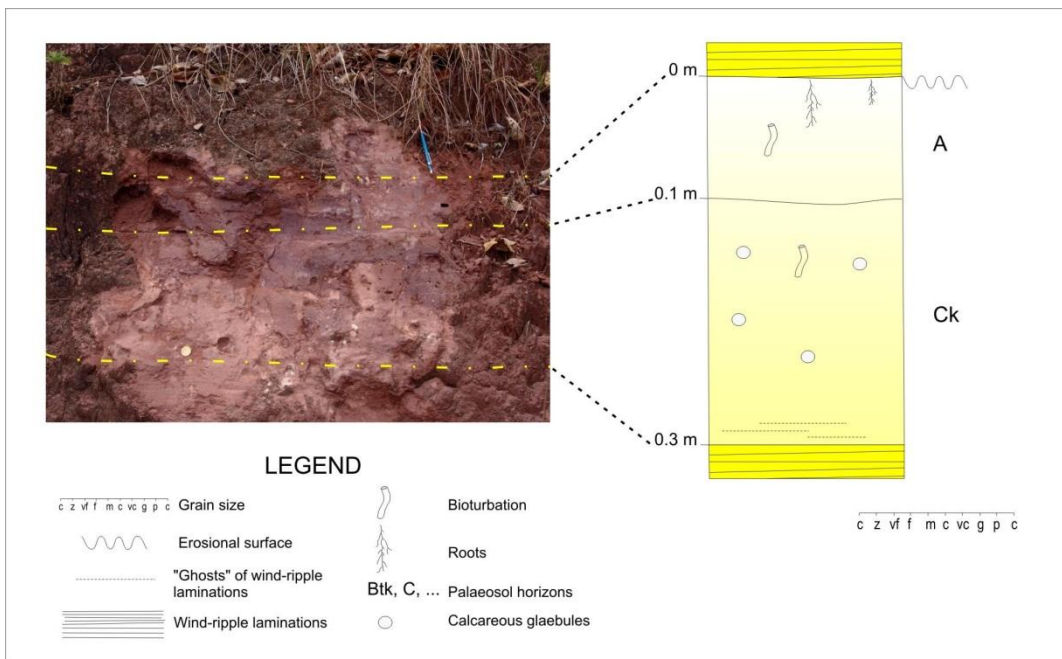


**Figure 7.** Palaeosol profile of Entisols, which crops out near the town of Itarumã. Pencil: 0.14 m.

### 3.1.2.1. Interpretation

The Entisols are soils with slight development. Diagnostic criteria are (1) the absence of a B horizon and of pedogenic structures, (2) a thin soil profile, (3) an ochric epipedon A horizon, and (4) the absence of other features employed to define other soil orders (Grossman, 1983; Soil Survey Staff, 2006). A short development time is the main controlling factor in the genesis of Entisols; although dry climate and resistant to weathering parent material may contribute to their formation (Watson, 1992). The rare bioturbation implies short time of development of the soil as also harsh life conditions.

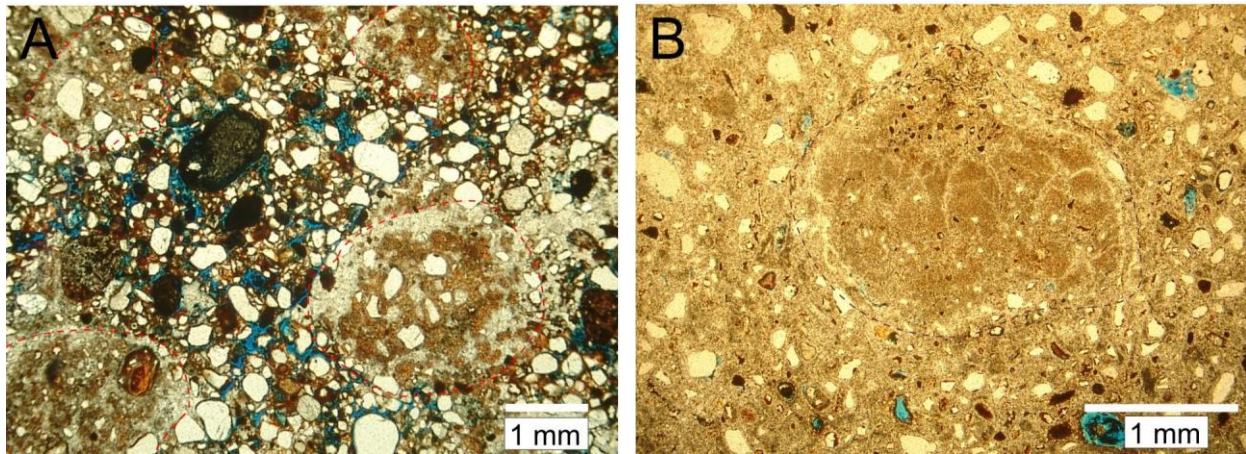


**Figure 8.** Entisols. Thin section showing nodule formation in Entisols. The nodules (marked by dashed lines) vary from halos of weakly impregnative microcrystalline calcite (A) to strongly impregnative typic nodules (B). Photomicrographs in plane polarised light.

### 3.1.3. Vertisols

The Vertisols (Fig. 9) constitute only 2.7% of the palaeosols. Their texture comprises a sandy mudstone, corresponding to a parent material probably originating from flood deposits, as discussed below. The palaeosol profiles are 0.4 to 0.74 m thick. The A horizon is always absent, probably truncated by aeolian deflation, since these profiles are sharply overlain by wind-rippled deposits. Vertisol profiles consist of a sequence of Bss/Ck horizons. The Bss horizon, 0.4 to 0.48 cm thick, is light red (7,5R7/6) or red (7,5R5/8) in colour. The texture of this horizon is, on average, 73% clay, 18% silt, and 9% sand. X-ray diffraction, MEV and EDS analyses of the finer clay fraction show that the clay is constituted by smectite, palygorskite and probably sepiolite (Fig. 10A and B) (Basilici et al., 2009). The Bss horizon is characterised by moderate medium subangular blocky peds separated by slickenside surfaces (Fig. 10C), dipping 30–50°, which identify a subsuperficial pedogenic structure known as mukkara. Calcium carbonate cutans (calcans) and nodules occur in this horizon. The Bss/Ck transition is clear and wavy to irregular (cf. Soil Survey Staff, 1993). The Ck horizon is 0.26 m thick; it is structureless, dark red (7,5R3/8 or 7,5R3/6) in colour, and weakly cemented by calcium carbonate.

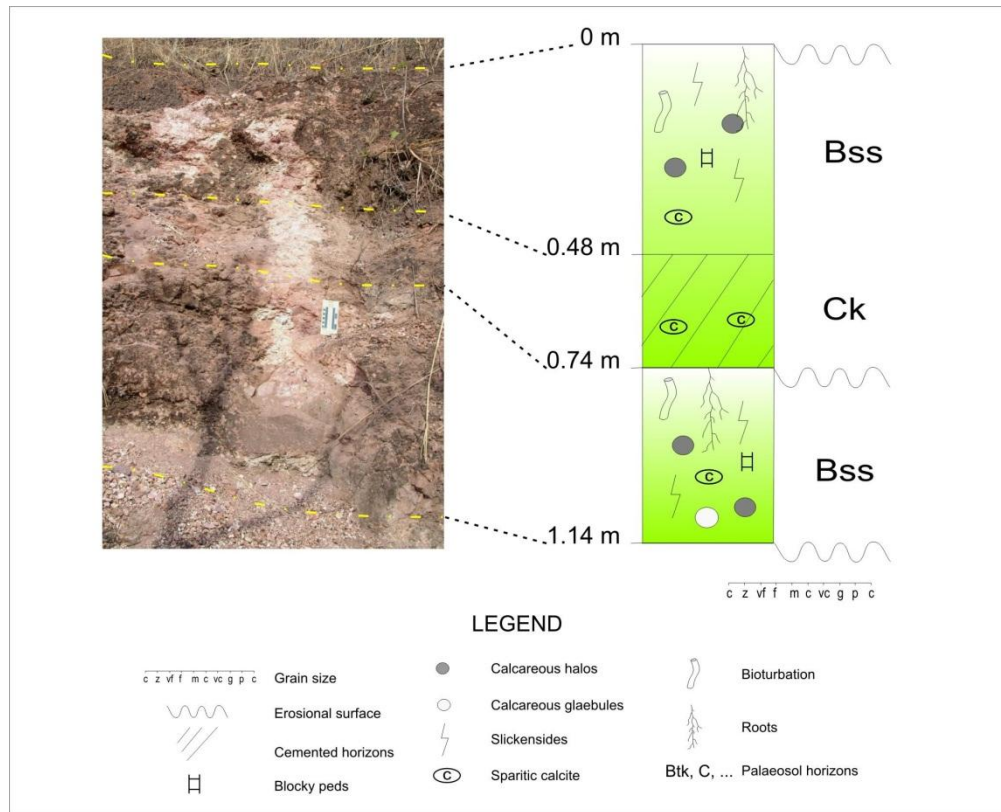


**Figure 9.** Two superimposed profiles of Vertisols, which crop out near the town of Quirinópolis.

### 3.1.3.1. Interpretation

This type is interpreted as Vertisol due to (1) the presence of wedge-shaped pedes, separated by slickenside planes, (2) the clay texture, and (3) the presence of expansive clay minerals (cf. Ahmad, 1983; Mack and James, 1992; Mack et al., 1993; Mermut et al., 1996; Schaetzl and Anderson, 2005). Vertisol formation is strongly controlled by a parent material with a high percentage (>30%) of expansive clay minerals in the fine fraction. Vertisols are not associated with any particular climatic conditions, but they do indicate periodic wetting and drying of the soil, with consequent swelling and shrinking to produce the wedge-shape structure (Ahmad, 1983; Soil Survey Staff, 1999). Wetting and drying of the soil may occur after periodic precipitation or due to water table variations (Retallack, 2001; Heidari et al., 2008).

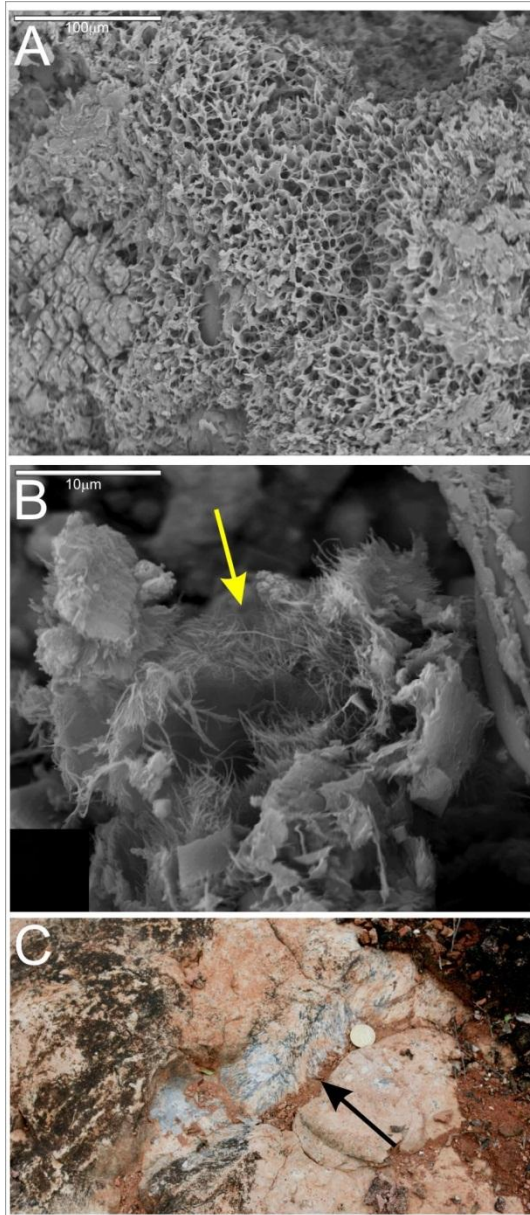


**Figure 10.** Vertisols. (A) Scanning electron microscope (SEM) photomicrograph of smectite displaying a honeycomb structure. Smectite constitutes the bulk of clay minerals of Vertisols in Bss horizon, and is also present in Aridisols, but in lesser proportion. (B) SEM photomicrograph of fibrous clay mineral (arrowed) in Bss horizon of Vertisols. The chemical composition displays in order of abundance  $\text{SiO}_2$ ,  $\text{MgO}$ , and  $\text{Al}_2\text{O}_3$ , that allows the interpretation of this clay mineral as palygorskite. (C) Slickensides (arrow) in Bss horizon of Vertisols. Coin: 20 mm.

### 3.1.4. Alfisols

Only one Alfisol profile, which is located in the upper portion of the succession studied, was recognised (Fig. 11). The palaeosol profile is *ca* 4 m thick, with a parent material consisting

of well-sorted, fine- to medium-grained sandstone, showing well rounded grains. Most of the grains were quartz, and secondarily lithic fragments, petrographically very similar to the Aridisols. The profile found here is characterised by a sequence of Bt/Btk horizons. The Bt horizon has a sandy texture and is reddish brown (10R5/4) or dull reddish brown (10R6/3). This horizon shows very strong coarse prismatic and/or subangular blocky peds, 0.3-0.77 m across. Manganese oxyhydroxides (mangans) and calcium carbonate cutans (calcans) separate the ped surfaces. Bioturbation is very common. Some of this is composed of sandstone-filled vertical cylindrical tubes, more than 0.1 m long, that decrease downwards in diameter from 8 to 5 mm, they are often ramified (Fig. 12). This bioturbation is distributed for all the palaeosol profile. Smaller bioturbation consists of sandstone filled cylindrical tubes, a few centimetres long and 2 mm across, also often ramified, and displaying manganese oxyhydroxide concentration in the central portion. In section this smaller bioturbation is more abundant than the other, but it is restricted to the Bt1 and to the upper portion of the Bt2 horizons. Both types of bioturbation may be interpreted as root traces. Each Btk horizon is 0.15 m thick and is orange (5YR7/6) or dull orange (5YR7/4) in colour. Soft or weakly indurated calcium carbonate nodules are found in these horizons, with a surface distribution around 10%. These horizons are clearly identified by the molecular weathering ratios relative to calcification and hydrolysis, which represents an increase in bases in relation to alumina (Fig. 13 and Tab.1). The boundaries of the horizons are gradual to diffuse, and generally wavy (cf. Soil Survey Staff, 1993).

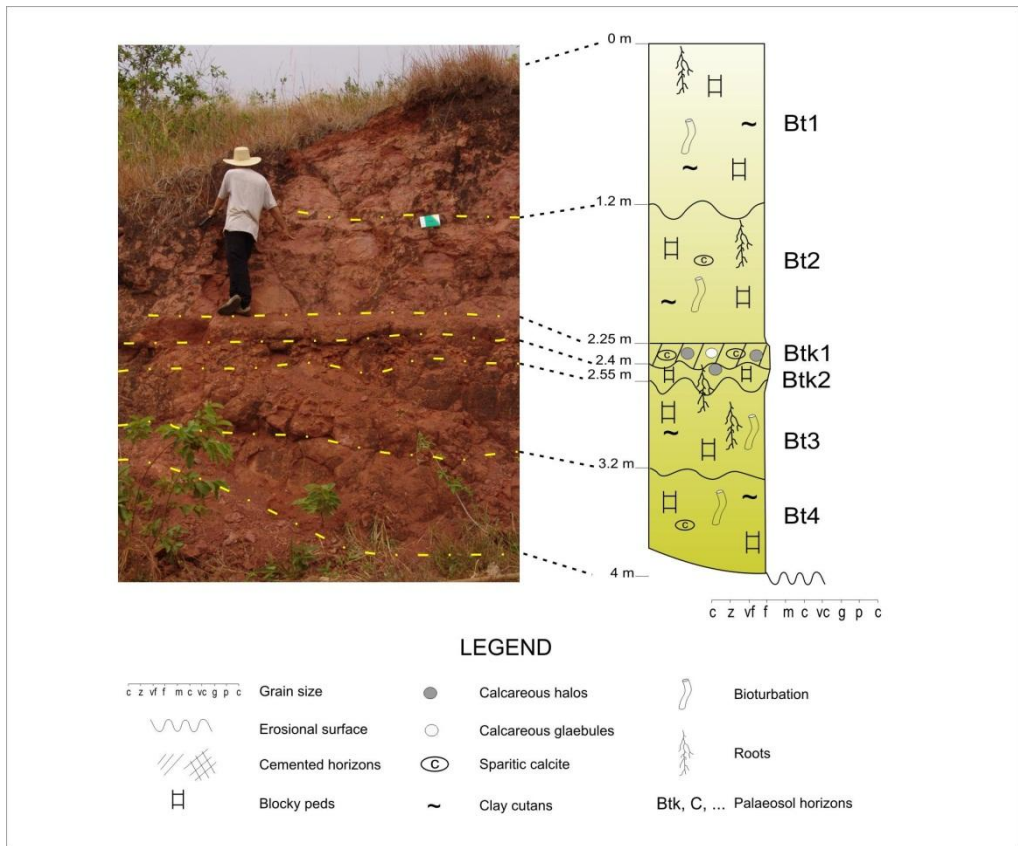


**Figure 11.** Palaeosol profile of Alfisol. This profile is exposed near the town of Itajá.



**Figure 12.** Root trace from the Bt horizon of Alfisols of figure 11, tapering downwards and branching laterally (arrowed), which is filled with fine- medium-grained sandstone. Coin: 20 mm.

### **3.1.4.1. Interpretation**

This type was considered to be an Alfisol for the following reasons: (1) the Bt horizon is dominant and very thick; (2) the upper portion of the palaeosol profile is characterised by eluviation processes up to 2.25 m from the top, as revealed by the high hydration molecular weathering ratio and the increase in downwards clay formation (Fig. 13); (3) the Btk horizon, located at a minimum depth of 2.25 m from the top of the palaeosol profile, is very thin and delineated by calcification and hydrolysis molecular weathering ratios (Fig. 13); (4) root traces are quite abundant and characterised by a bimodal distribution in size (Fig. 12). This evidence indicates a relatively more humid climate during soil formation, and a dense vegetation cover. Moreover, the pattern of bimodal distribution in size of the root traces may be associated to seasonally dry climate; in these conditions a superficial network of small roots is active during the more humid season and greater and deeper roots sustain the trees during the drier period (Retallack, 1983; 1991; 2001). Such as Alfisol profile can be used to define: (1) more humid conditions of aeolian sand deposition and (2) a long period of soil development, probably much greater than  $10^3$  years (Rust, 1983).

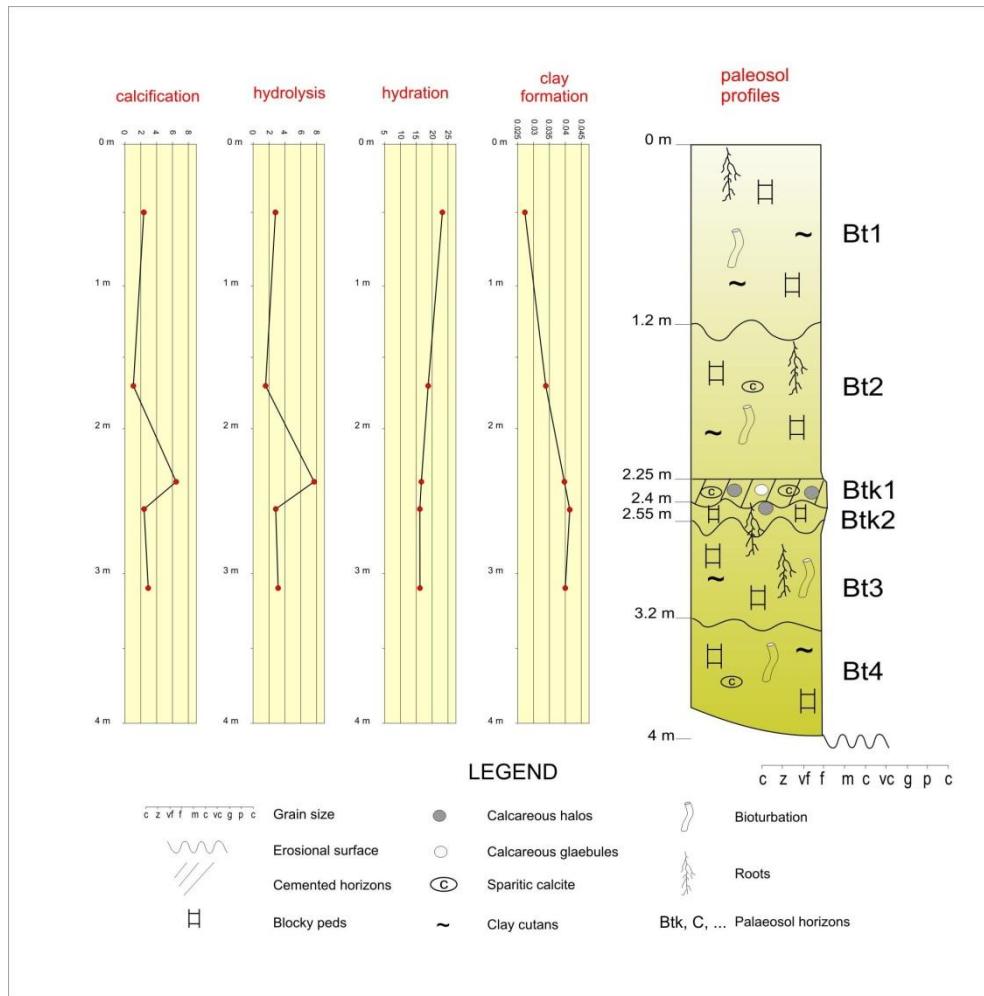


**Figure 13.** Molecular weathering ratios of the Alfisol profile of figure 11. Data in weight percentage of the major oxides are in Table 1. The following molecular weathering ratio formulae were used:  $(\text{CaO} + \text{MgO})/\text{Al}_2\text{O}_3$  for calcification;  $(\text{CaO} + \text{MgO} + \text{K}_2\text{O} + \text{NaO})/\text{Al}_2\text{O}_3$  for hydrolysis;  $\text{SiO}_2/(\text{Al}_2\text{O}_3 + \text{Fe}_2\text{O}_3)$  for hydration;  $\text{Al}_2\text{O}_3/\text{SiO}_2$  for clay formation.

**Table 1.** Weight percentage of the major oxides within the Alfisol profile of figure 11.

Horizon	depth (m)	$\text{SiO}_2$	$\text{TiO}_2$	$\text{Al}_2\text{O}_3$	$\text{Fe}_2\text{O}_3$	$\text{MnO}$	$\text{MgO}$	$\text{CaO}$	$\text{Na}_2\text{O}$	$\text{K}_2\text{O}$	$\text{P}_2\text{O}_5$	LOI	Total
Bt1	0.5	83.08	1.02	3.87	3.51	0.042	2.64	0.92	0.09	1.27	0.058	3.80	100.3
Bt2	1.7	82.44	1.31	4.75	4.34	0.046	1.83	0.74	0.16	1.66	0.051	3.08	100.4
Btk1	2.3	61.18	1.03	4.11	3.56	0.058	4.50	10.31	0.09	1.23	0.054	13.60	99.7
Btk2	2.55	75.56	1.36	5.25	4.41	0.082	3.40	2.21	0.10	1.49	0.055	6.04	100.0
Bt3	3.2	74.47	1.36	5.05	4.48	0.069	3.15	3.36	0.14	1.62	0.072	6.38	100.2

### **3.2. Wind-ripple-dominated aeolian sand sheet deposits**

Wind-ripple-dominated aeolian sand sheet deposits are composed of sandstone formed largely by wind-ripple strata, but with the contribution of flood deposits. They are 0.55 to 13.5 m thick and extend laterally for from 50 m to few kilometres, and are characterised by marked variations in thickness and lateral extension (Fig. 2). The transition to overlaying ephemeral river deposits is an erosional surface, whereas the upwards transition from underlying river deposits is gradual.

This architectural element is formed by two lithofacies: translatent wind-ripple strata and flood deposits. The first lithofacies is the more abundant in the sedimentary record (68.5%), and consists of very fine- to coarse-grained sandstone, moderately to well-sorted, with a bimodal distribution. The petrographical assemblage consists of the same components as the Aridisols, although with greater frequency of basaltic rock fragments and fewer quartz grains (Fig. 4B). According to the classification of Pettijohn et al. (1987), such a sandstone can be classified as lithoarenite. It is organised in thin strata, from 1 to 20 mm thick, with laminae of very fine-grained sandstone with small haematite grains separating the thicker strata with weak inverse grading (Fig. 14A). Each single stratum pinches out laterally in a few metres. These strata form cosets of planar to low-angle parallel stratification, 0.2-2.5 m thick, which are separated by analogous cosets with erosional surfaces (Fig. 14B). Bioturbation is uncommon, though where present consists of sandstone-filled vertical tubes, with circular or elliptical sections, some 2-10 mm across.

Flood deposits are uncommon in this element (5.5% of the sedimentary record) and are characterised by poorly or very poorly-sorted, medium- to coarse-grained sandstone with rare small pebbles. The petrographical features are identical to those of the wind-ripple strata (Fig. 4C). This lithofacies is characterised by lenticular strata, up to 0.5 m thick, extending laterally by no more than 20 m. The erosional bottom surface is characterised by small troughs, not more than 0.1 m deep. Cross-stratified sets, not more than 0.15 m high, form the strata. Thin strata of sandy mudstone may cover the cross-stratified sets, or simply occur interbedded within the wind-ripple strata; desiccation cracks are common on their top surfaces (Fig. 14C).

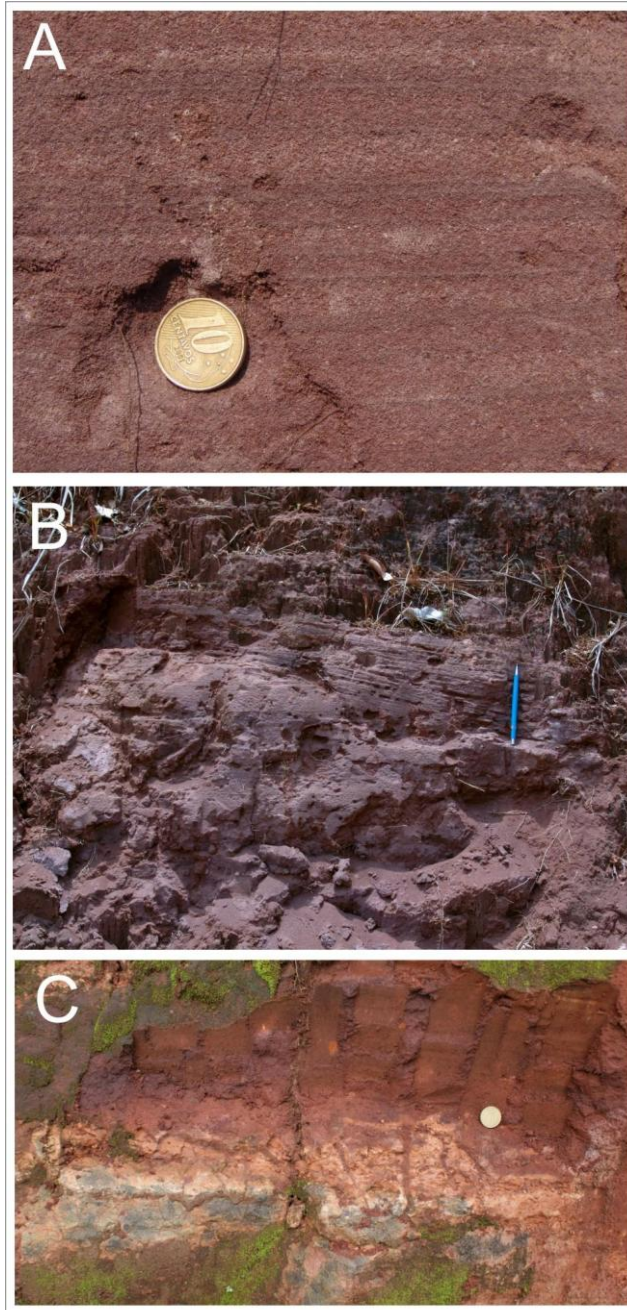


**Figure 14.** Wind-ripple-dominated aeolian sand sheet deposits. (A) Translatent wind-ripple strata are characterised by thin laminae of very fine sandstone deposited into the ripple-trough shadow zone. Coin: 20 mm. (B) Cosets of wind-ripple deposits separated by erosional surfaces of fourth order. Pencil: 0.14 m. (C) Flood deposits are characterised by muddy deposits with desiccation crack structures. Coin: 20 mm.

### **3.2.1. Interpretation**

Planar or low-angle parallel strata correspond to subcritically climbing translatent strata (Hunter, 1977) which have formed as the result of wind ripple migration. The thin laminae of very fine sandstone that separate the sets represent the sand deposited into the ripple-trough shadow zone. Weak inverse grading of the sets arose from the accumulation of coarse grains concentrated on or near the ripple crest. Moreover, moderate sorting and the apparent bimodal distribution of grain sizes is typical of sand sheets that are dominated by wind ripples (Breed et al., 1987; Mountney, 2006). The cosets of planar or low-angle parallel strata, separated by erosional surfaces, correspond to different phases in the accumulation of climbing aeolian sand ripples, brought about by changes in velocity and/or direction of the wind. Thin, brief cosets might correspond to coppice dunes, as observed in present-day sand sheets, but thicker and longer cosets are related to an extensive flat body of climbing aeolian ripples.

The erosional bottom surface, the cross-stratifications corresponding to small 3-D dunes, the mudstone with desiccation cracks at the top, and the shape of the beds all suggest that the flood deposits were formed by non-channelised floods, characterised by a relatively rapidly waning flow and surface desiccation (Trewin, 1993; Chakraborty and Chakraborty, 2001; Fisher et al., 2007). The sediments supplied, coarser and poorly-sorted, suggest greater competence and a relatively higher rate of sedimentation than do the aeolian ripples; however, the similar petrographic features of the two lithofacies indicate local provenance, probably resulting from highly concentrated rainfalls, rather than the wide-spread flooding of active fluvial channels.

The predominance of the deposition of aeolian ripples and the absence of dune deposits in this architectural element constitutes an essential feature of aeolian sand sheets. The sand sheet was subjected to phases of erosion and sedimentation on an unstable surface, where sparse and/or temporally variable vegetation and animal communities, identified by rare bioturbation traces, were insufficient to generate a stabilised pedogenic surface. The absence of adhesion structures (Kocurek and Fielder, 1982) and contorted laminations suggest that the water table was well beneath the depositional surface.

### **3.3. Ephemeral river deposits**

Ephemeral river deposits constitute an element up to 4 m thick, *ca* 2 km wide, and several kilometres long. The lower boundary is an abrupt concave-up surface, whereas the upper boundary is flat, forming an apparently sharp transition to aeolian deposits, locally marked by gravel lags. River deposits constitute uncommon, isolated bodies, that never show interbedding with translatent wind-ripple strata. This element accounts for 26% of the sedimentary record.

Sandy conglomerate, gravelly sandstone, and fine- to coarse-grained sandstone constitute this lithofacies. The conglomerate is clast-supported, with maximum particle size from 1100 to 5 mm, decreasing towards the top of the beds; some flattened clasts show a(t) b(i) imbrication (Walker, 1975). Weakly graded conglomerate beds are common (Fig. 15A), but open work structure was not observed. The sandstone is poorly- or very poorly-sorted, and its petrographic features are dominated by 58.2% basaltic fragments and 34.8% quartz minerals, typical of a lithoarenite (Fig. 4D). The petrographical distribution of this sandstone is also reflected in the composition of the conglomerate, with dominantly basaltic pebbles and cobbles and secondarily sandstone ones. The ephemeral river deposits are formed by flattened lenticular beds, 0.3 to 1.1 m thick, a few metres to more than 50 m long in the palaeocurrent direction, which is evident at both bottom and top erosional surfaces (Fig. 15B). Each river deposit is formed of various layers, roughly grading from sandy conglomerate to sandstone. At times, the sandstone at the top of the beds displays planar laminations attributed to aeolian ripples (Fig. 15C). Neither bioturbation nor pedogenesis marks were observed within this architectural element. Palaeocurrent information is not abundant. However, a detailed geological map of a channel body (Basilici et al., 2009, cf. their figure 6B) reveals a fluvial channel axis at N20°, and flat pebble imbrications from three ephemeral river deposits indicate flow towards the north (Fig. 16).

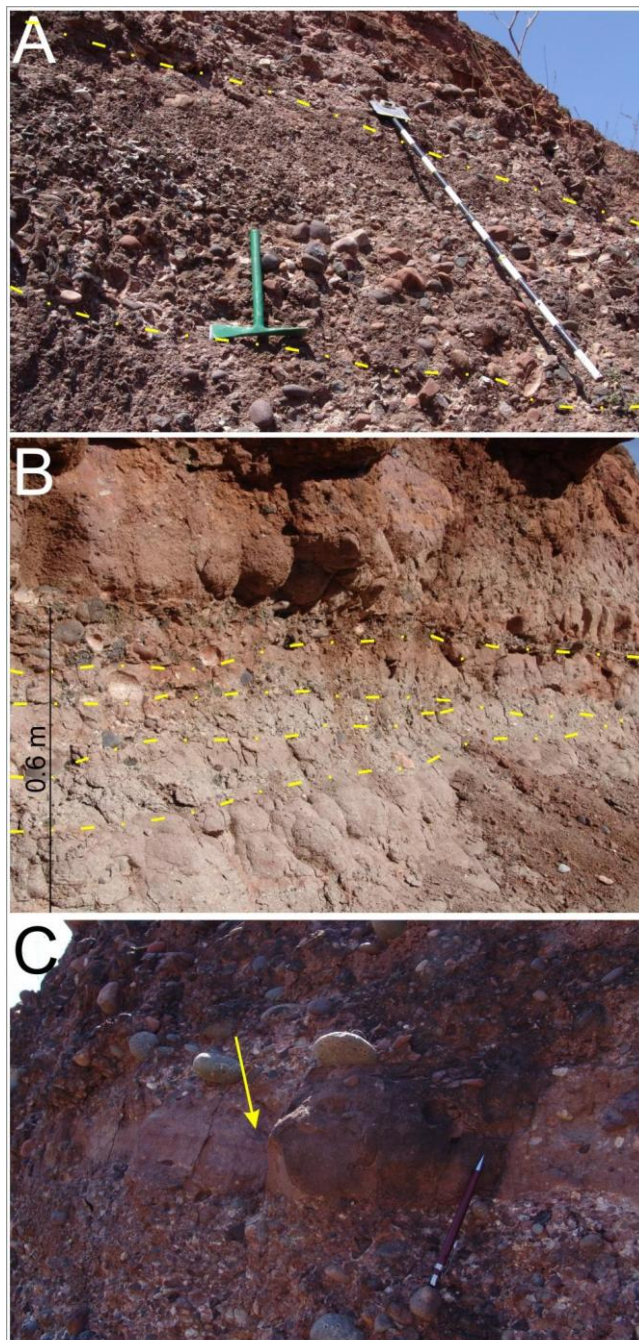


**Figure 15.** Ephemeral river deposits. (A) Roughly graded sandy conglomerate beds. The dashed lines highlight the bottom and the top of the bed. Hammer: 0.31 m. (B) Lenticular gravelly sandstone beds that compose the fill of a river channel. The dashed lines highlight the erosional bottom of the beds. (C) Sandstone with translatent wind-ripple strata (arrowed) at the top of a sandy conglomerate graded bed. Note the erosional surface that partially cut the sandstone bed.

### **3.3.1. Interpretation**

The planar-concave shape of this sedimentary body suggests that the depositional processes took place within a channelised structure. Since the fabric of the conglomerate, which is characterised by imbricated pebbles, a clast-supported structure and graded beds, suggests deposition by hydraulic transport flow (Rees, 1968; Walker, 1975; Blair, 1999), it is evident that this architectural element can be interpreted as the fill of a river channel. The relative simplicity of the depositional macroforms, that are identifiable as gravel-sheet bars, the absence of open work structure and cross-stratifications indicate non-persistent flow conditions within the channelised structure (Tooth, 2000; Jain et al., 2005). These ephemeral flow conditions are also clear in the upper sandstone portion of the strata, where planar laminations are ascribed to aeolian ripples, suggesting the reworking of fluvial sands by the wind.

The sandy conglomerate of this architectural element is similar to the lithofacies C of Blair (2003), described for the channels of the giant Cucomungo fan (California, USA), a present-day depositional system localised in an arid climate. However, the ephemeral river deposits here record a fluvial system that was not associated with alluvial fans nor an arid climate, because there is no interbedding with muddy debris flows, as is the case of the Cucomungo fan; moreover, it does not involve intense aeolian reworking, which would have yielded conglomerate lag deposits, and destroyed the previous fluvial deposits, as Krapf et al. (2005) observed for ephemeral braided-rivers of the arid NW of Namibia. Furthermore, the absence of bioturbation and pedogenic features suggest that the depositional processes were superimposed on each other within a relatively short time span, though the climate may have contributed to restrain the processes of pedogenesis and bioturbation.

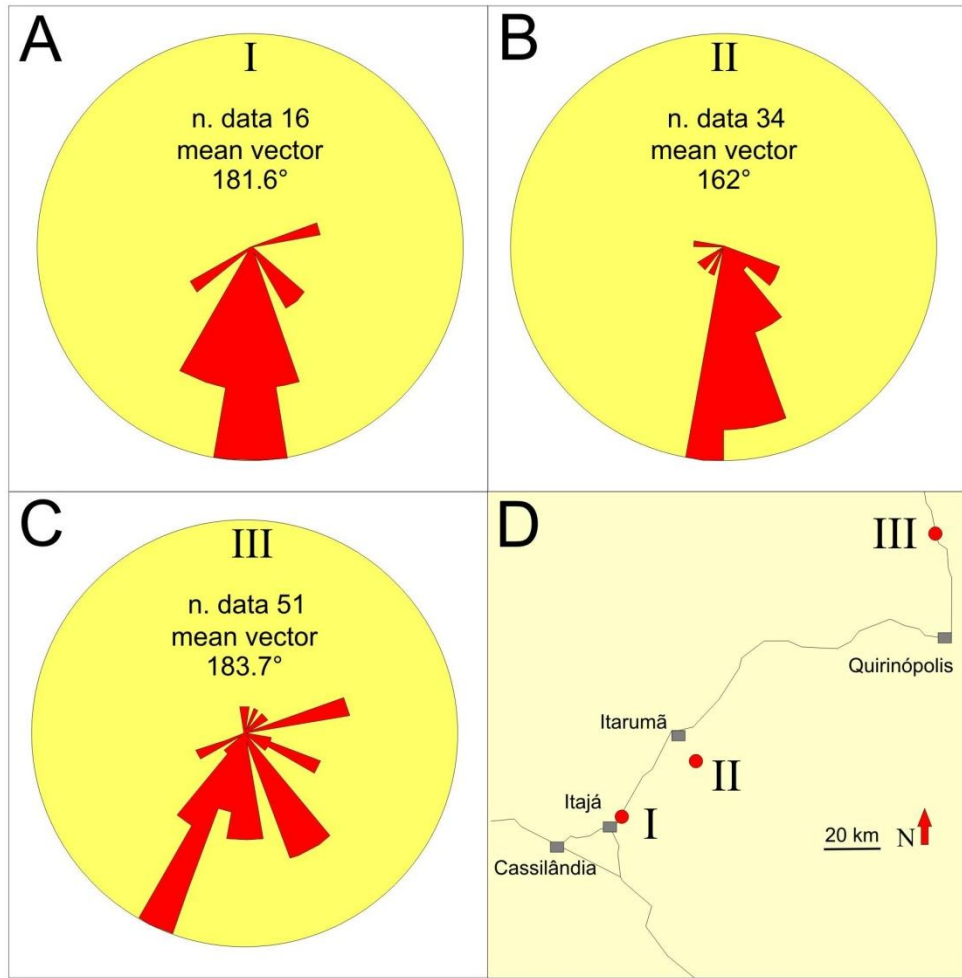


**Figure 16.** Circular histograms depicting the dips of imbricated flattened pebbles of two ephemeral rivers deposits cropping out near Itajá (A, site I), Itarumã (B, site II), and Quirinópolis (C, site III). (D) Location of the outcrops. Data outline river flows towards north.

#### 4. Sequential organisation and erosional bounding surfaces

In all the stratigraphic sections measured, palaeosols and wind-ripple-dominated aeolian sand sheet deposits are organised in a cyclical sequence, which is characterised by the vertical interbedding of the two architectural elements (Fig. 17). The transitions between palaeosols and deposits are erosional at the bottom of the wind-ripple-dominated aeolian sand sheet deposits and gradual at the bottom of the palaeosols. These transitions can be traced laterally in outcrop for more than 50 m. However, the stratigraphic correlations between sections up to 4.9 km across indicate that the wind-ripple-dominated aeolian sand sheet deposits have a lateral continuity limited to only a few kilometres, and that they are probably replaced by erosional surfaces, which

separate different palaeosol profiles (Fig. 2 and 17). In fact, cyclical sequences between the two architectural elements are sometimes replaced laterally by cyclical sequences between palaeosol profiles, whose transition is highlighted out by an erosional surface and the superposition of a C horizon over an A or B horizon (Fig. 17). Sheet-shaped ephemeral river deposits are found to be randomly scattered throughout the two formations, with no apparent preferential distribution in the sedimentary succession (Fig. 17).

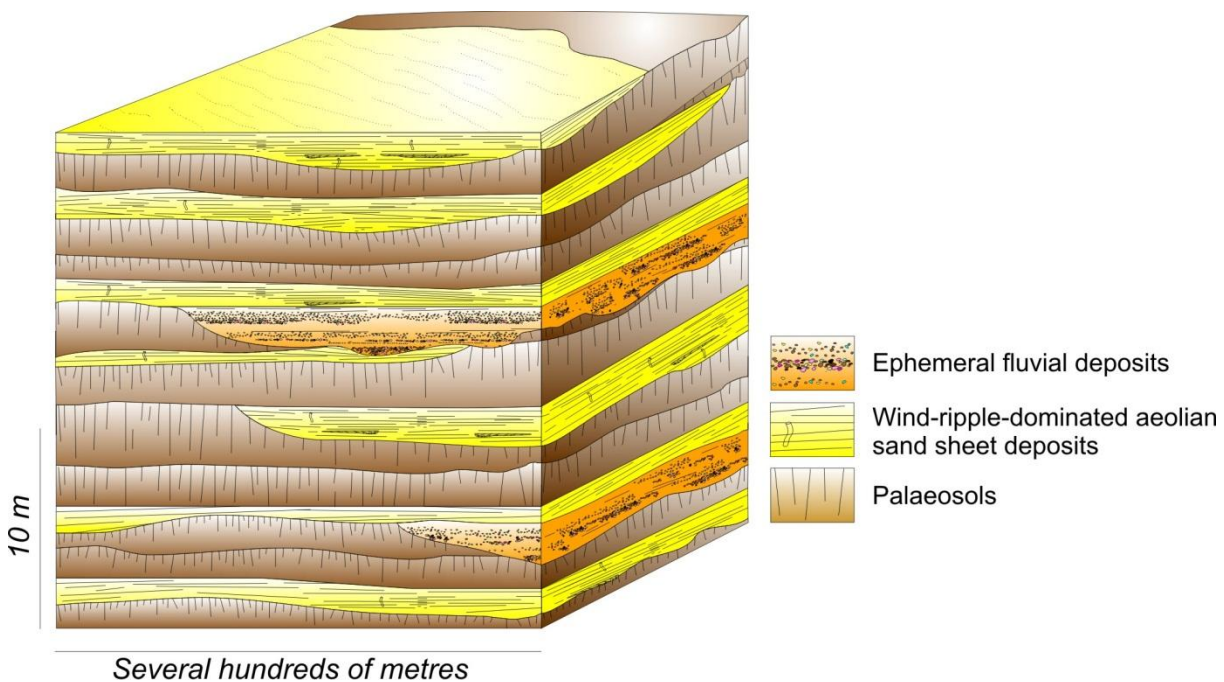


**Figure 17.** Synthetic sketch of the geometrical distribution of the architectural element that constitute the Adamantina and Marília formations in the study area.

Six types of erosional bounding surfaces are recognised within the Adamantina and Marília formations from their geometrical features (lateral extension and shape), the characteristics of the lithofacies that they divide, and their genetic interpretation (Fig. 18). A five-order hierarchy was established; the higher orders correspond to those surfaces representing greater spatial extension and passage of time. A synthesis of the characteristics of the bounding surfaces is described in Table 2. The orders used here, however, have no relationship with the hierarchical order of the surfaces developed by Brookfield (1977).

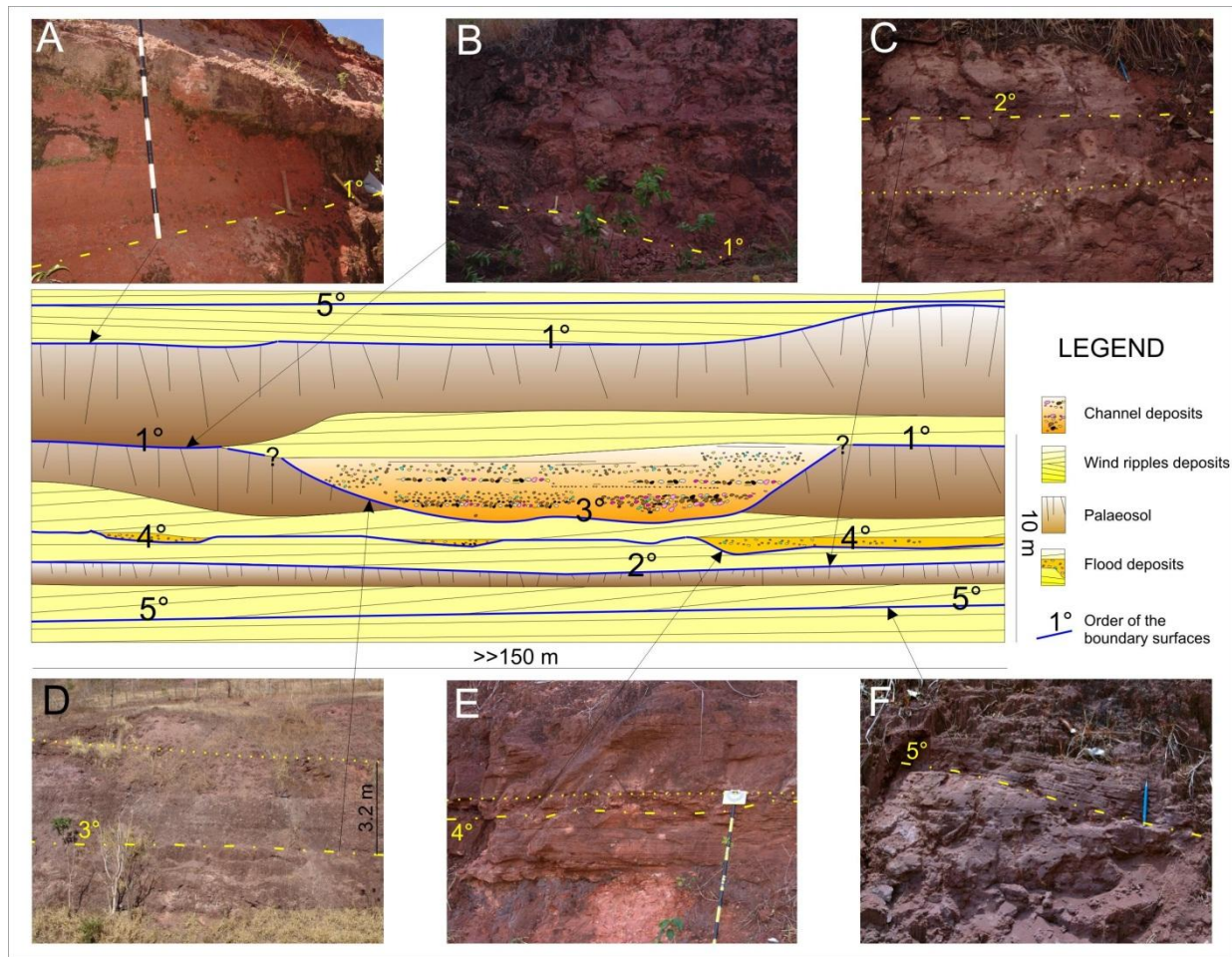


**Figure 18.** Sketch and photos of the orders of the erosional bounding surfaces. (A) The first type of first order outlines the contact between an underlying mature palaeosol profile and wind-ripple deposits. The Jacob's staff subdivisions are 0.1 m. (B) The second type of the first order is constituted by the transition between two palaeosols profiles. Hammer: 0.28 m. (C) The second order marks the boundary between the top of an immature palaeosol (Entisol) and wind-ripple deposits. The dotted line delineates the bottom of the Entisol. Pencil: 0.14 m. (D) The third order corresponds to the erosional bottom of the ephemeral channels. The dotted line represents the top of the channel fill. The question marks in the central sketch mean a not clear relationship between first and third order boundary surfaces. (E) The fourth order consists of the erosional bottom of flood deposits. The dotted line indicates the top of the flood deposits. The Jacob's staff subdivisions are 0.1 m. (F) The fifth order corresponds to the erosional division between cosets of translatent wind-ripple strata. Pencil: 0.14 m.

The first order bounding surfaces marks the upper limit of palaeosols exhibiting a high degree of development (Fig. 18A and B): Aridisols, Alfisols, and probably Vertisols. Two types of first order surfaces are observed. The first constitutes the contact between underlying palaeosols and overlying translatent wind-ripple strata. These surfaces are always clearly

recognisable because of the sharp variation lithofacies (Fig. 18A). The second type constitutes the vertical contact between two different palaeosol profiles (Fig. 18B). Both of these types of bounding surface mark an abrupt genetic change in the depositional system: from stable to unstable topographic conditions of the aeolian sand sheet. This environmental variation is quite apparent for the first type, where the palaeosols, which represent the phase of stability of the sand sheet, are eroded and covered by wind-rippled deposits, representing the phase of instability. The well-developed palaeosol profiles underlying this surface suggest a long period of stability of the sand sheet, more than  $10^3$  y. Moreover, since climate changes can be related to global conditions (Kocurek, 1988), which would involve large areas, such boundary surfaces may have great spatial-temporal importance in interpretation. The second type indicates a similar genetic transition, suggesting a similar stratigraphic interpretation. However, the boundary surface is less clearly visible, because the aeolian sediment structures were completely destroyed by subsequent pedogenesis, and the surface is marked only by the superposition of two palaeosol profiles.

The second order of bounding surfaces is represented by the contact between underlying Entisols and overlying wind-rippled deposits (Fig. 18C). The Entisols suggest a short interruption of the aeolian sedimentary processes, and a relative stability of the surface. The poor exposure of the sedimentary succession, however, does not allow the evaluation of the lateral continuity of this surface. Since the development time of Entisols was likely to have been of relatively short duration, and other factors such as a high water-table or areas of sediment bypassing, may generate local conditions for their formation on an unstable sand sheet, Entisols do not necessarily cover large areas. Therefore, since this surface should have limited extension and time of development, it has been ranked lower than have the other palaeosols.

The third order of boundary surfaces corresponds to the erosional bottom of an ephemeral river deposit (Fig. 18D). This surface is genetically interpreted as the erosional base of an ephemeral fluvial system, which was active during more humid climatic conditions of aeolian sand sheet development. However, although this surface may represent an important environmental change, its limited lateral extent of less than 2 km has led to its lower ranking in the hierarchy.

The fourth order bounding surface divides wind-rippled sediments from overlying flood sediments (Fig. 18E). Such surfaces are very clear, because they correspond to a lithofacies change, although laterally they seldom exceed 20 m.

The fifth order corresponds to the boundary between different sets of translatent wind-ripple strata (Fig. 18F), representing phases of abrupt migration of wind ripples or alternating phases of aeolian sedimentation and erosion (Hunter, 1977). Their lateral continuity is commonly less than 10 m.

**Table 2.** Summary of the characteristics and interpretations of bounding surfaces observed in Adamantina and Marília formations.

<i>Order of bounding surfaces</i>	<i>Characteristic</i>	<i>Genetic interpretation</i>
1° first type	Flat or irregularly undulated surface, that consists in the contact between underlying mature palaeosols (Aridisols, Alfisols, and probably Vertisols) and overlying translatent wind-ripple strata. The A horizon of the palaeosol profile is commonly absent. Gravel lags of granules or pebbles may be occurred on this surface. This surface probably extends for many kilometres.	Transition from stable (pedogenic) to instable (erosional or depositional) conditions of the topographic surface, which corresponds to the transition from semi-arid to arid palaeoenvironmental climatic conditions. This surface probably indicates a long period of absence of sedimentation and erosion. The contact with wind ripples, the geometry, and the gravel lags testify the erosional nature of this surface.
1° second type	Flat or weakly undulated surface, that divides two different mature palaeosol profiles (Aridisols, Alfisols, and probably Vertisols). The C or B horizon of the overlaying palaeosol profile superposes on the A or B horizon of the underlying. Gravel lags may be observed. This surface probably extends for many kilometres.	Transition from stable (pedogenic) to instable (erosional or depositional) conditions of the topographic surface, which corresponds to the transition from semi-arid to arid palaeoenvironmental climatic conditions. This surface probably indicates a long period of absence of sedimentation and erosion. The erosional nature is recognised by the absence of A horizon and by the presence of gravel lags.
2°	Flat or weakly undulated surface of contact between underlying immature palaeosols (Entisols) and overlying translatent wind-ripple strata. This surface probably has a limited extension.	Transition from relatively stable (pedogenic) to instable (erosional or depositional) conditions of the topographic surface. This surface suggests restricted areas temporarily isolated from depositional or erosional processes. It suggests a short period of topographic stability.
3°	Concave-up surface at the bottom of ephemeral river deposits. This surface overlies palaeosols and/or translatent wind-ripple strata, and it is overlain by fluvial deposits. Lateral extension, perpendicular to the channel axis, is up to 2 km; longitudinal extension may be several kilometres.	This surface corresponds to the erosional bottom of an ephemeral river channel.
4°	Weakly concave-up surface, that corresponds to the contact between underlying translatent wind-ripple strata and overlying flood deposits.	This surface represents the erosional effect of a flood in aeolian sand sheet area.

Lateral extension rarely exceeds 20 m.

- |    |  |  |
|----|--|--|
| 5° | Planar or weakly dipping surface that divides the sets of translatent wind-ripple strata. Lateral extension is not more than 10 m. | This surface is due to abrupt migration of wind ripples or alternating phases of erosion and deposition of wind ripples. |
|----|--|--|

Erosional bounding surfaces have been well described in dry depositional systems dominated by ergs, aeolian sand sheets, and the interaction between fluvial and erg systems (Kocurek, 1988; Langford and Chan, 1989; Fryberger, 1993; Kocurek and Havholm, 1993; Lancaster, 1993; Sweet, 1999; Newell, 2001). The most prominent of these, the super bounding surfaces or super surfaces, are surfaces that define the hiatus between different periods of erg deposition (Kocurek, 1988). Erosional bounding surfaces that delimit ergs can be compared to analogous surfaces within aeolian sand sheets, because the two systems are often developed close to each other, and are interdependent. Since these super surfaces represent a change in the factors that control the accumulation of aeolian sediment (Kocurek and Havholm, 1993; Carr-Crabaugh and Kocurek, 1998), they may be conceptually comparable to the first order surfaces established for the Marília and Adamantina formations.

Super bounding surfaces can be classified according to the sediment budget, the dry or damp aeolian environment, and the stability of the substrate (Kocurek and Havholm, 1993). However, the first order boundary surface described here does not represent any of the specific cases described by these authors, rather it represents a complex super surface resulting from the superposition of a planar deflationary super surface on a stabilised relict one (Kocurek and Havholm, 1993). The existence of pedogenesis of the underlying deposits of the aeolian sand sheet suggests stability of the substrate and a neutral sediment budget ( $Q_i=Q_o$ , where  $Q_i$  is the sediment entering into and  $Q_o$  is the sediment exiting from the depositional system), related to a generally humid climate (Fig. 19A). Resumption of a drier climate, accompanied by a reduction in the vegetation cover, favoured the unstabilisation of the substrate. Initially, restored erosional conditions ( $Q_i < Q_o$ , negative sediment budget) led to the deflation of the substrate, with the partial remotion of the palaeosol profile (Fig. 19B), later this was followed by renewed sedimentation by wind-ripple sediments ( $Q_i > Q_o$ , positive sediment budget) (Fig. 19C). The development of this first order bounding surface occurred in a dry environment with a water table

level that lay well beneath the accumulation surface such that its capillarity fringe did not extend to the surface, as suggested by the drained palaeosol profiles and by the absence of sabkha-like sediments or wet sedimentary structures in the overlying wind-rippled strata.

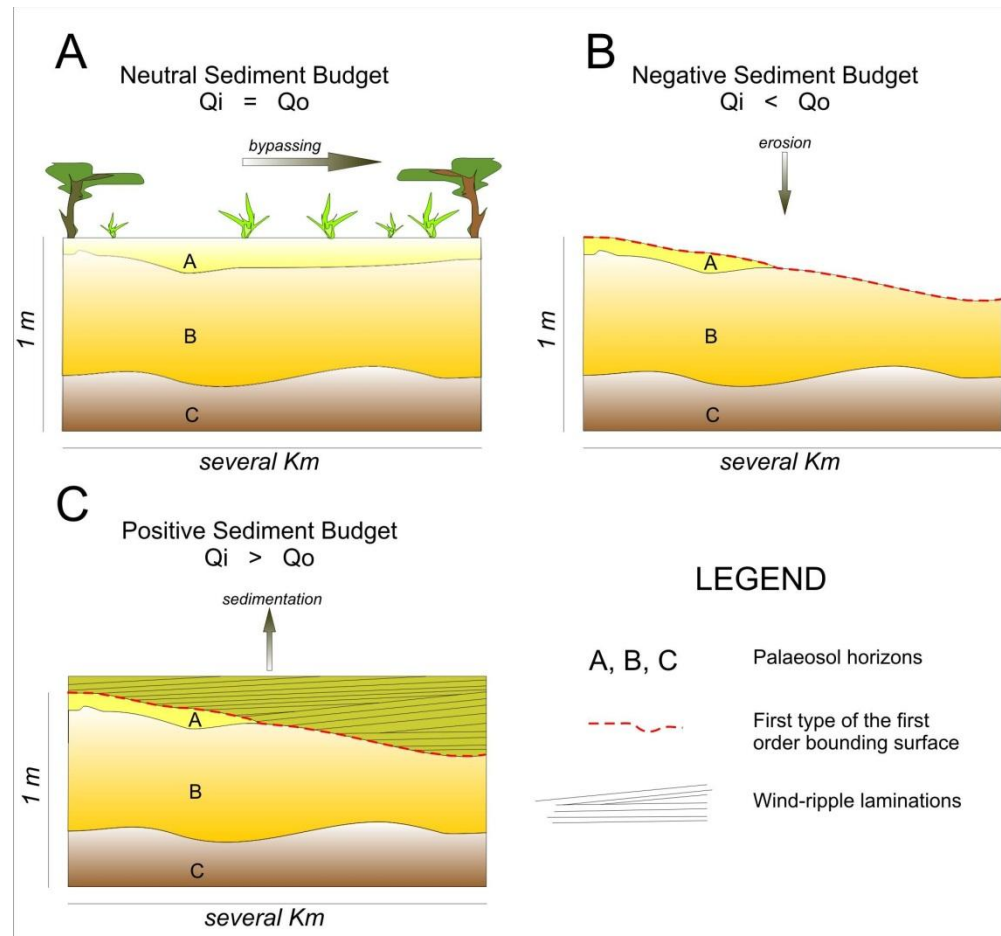


**Figure 19.** Phases of formation of the first type of erosional bounding surfaces.  $Q_i$  = sediment entering into the basin;  $Q_o$  = sediment exiting from the basin. (A) Soil formation in stable condition of the topographic surface ( $Q_i=Q_o$ ). (B) Erosion to the soils ( $Q_i<Q_o$ ), when a drier climate phase brings about the disappearance or rarefaction of the vegetation. (C) Sedimentation of wind-ripple sandstone ( $Q_i>Q_o$ ).

The regional boundary surface described by Talbot (1985) does not correspond physically and genetically to the first order erosional surface of this paper. Actually, the Talbot's surface cuts a degraded dune field, over which a thin crust of silty sand bound by filamentous algae and fungi and some sort of palaeosol developed. It formed during the transition from a dry to a humid climate and it is overlain by aeolian deposits, without any erosional surface developing above the incrusted surface. The first order erosional surface described here consists in a surface on the top

of a partially eroded palaeosol profile, which is covered by aeolian deposits. It marks the transition from humid to drier climatic conditions.

The third order boundary surfaces identified here can be compared with the incised bounding surfaces described by Newell (2001). This author described concave-up erosional surfaces of up to 7 m in depth and more than 30 m wide, overlain by sandy conglomerate fluvial deposits representing the cutting down of fluvial systems through an existing aeolian sand sheet, testifying to a more humid environment. The incision was related to a greater discharge, which increased the stream power available for bed erosion, rather than to base level variation due to tectonic tilting, which would also have caused slope increase and consequent enhancement of the river flow velocity (Quirk, 1996; Sweet, 1999).

Langford (1989) and Langford and Chan (1989) also described extensive erosional surfaces (called flood surfaces) at the bottom of river channel deposits which resemble the third order surfaces described here. However, it is improbable that these third order erosional bounding surfaces correspond to flood surfaces such as those described by Langford and Chan (1989). Actually, the third order erosional surfaces are limited to the channel bottom and disappear laterally; moreover, no overbank deposits were observed, nor was there any interbedding between fluvial and aeolian deposits. Figure 20 compares the third order bounding surfaces with the flood surfaces of Langford and Chan (1989).

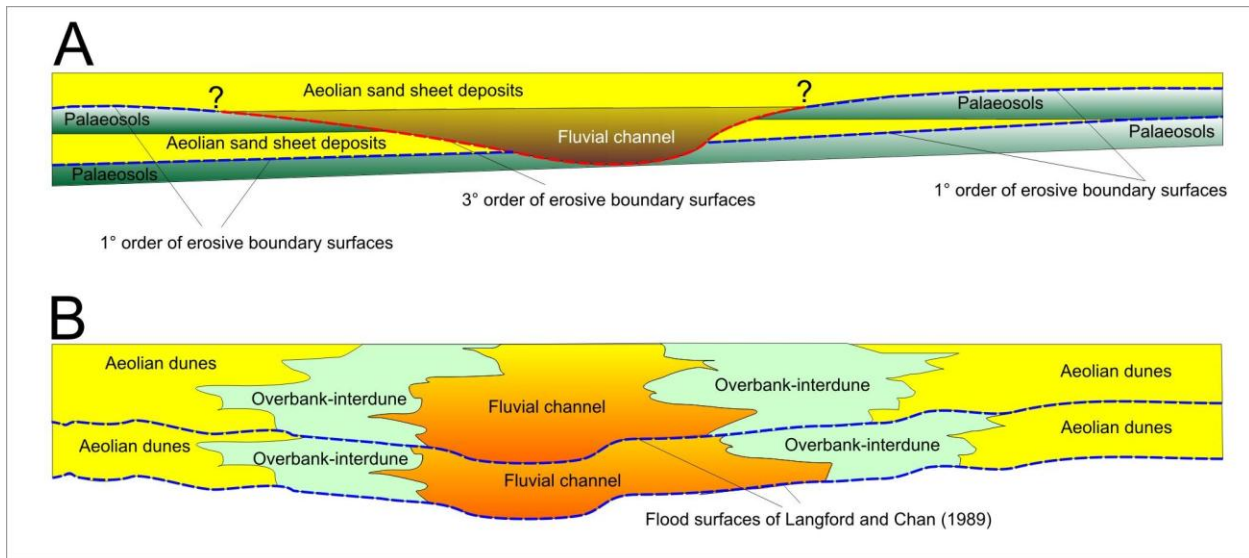


**Figure 20.** The third order boundary surfaces (A) are compared with the flood surfaces of Langford and Chan (1989) (B). For description see text. Figure B is modified after Langford and Chan (1989).

## 5. Palaeoenvironmental interpretation

The Adamantina and Marília formations formed on a widespread aeolian sand sheet, within which the three architectural elements represent different portions and/or different phases of development of the depositional system. Wind-ripple-dominated aeolian sand sheet deposits represent the phase of instability and construction of the aeolian sand sheet; these consist mainly of translatent climbing wind-ripple strata. The wind ripples were probably organised in flat sand sheets or small dunes without slipface, similar to the coppice dunes observed in recent aeolian sand sheets. This sand sheet area was, however, periodically invaded by floods that eroded the aeolian bed forms, depositing thin, lenticular strata of coarse-grained sand, overlain by mud. Petrographical data (Fig. 4) suggest that this sand was reworked by the wind-rippled deposits suggesting that the sand transport was localised. The formation of this sand sheet, rather than a dune field, was probably controlled by factors such as the presence of medium to coarse grained clastic material, cemented or protected surfaces (Bk or Bkm palaeosol horizons), periodic flooding, vegetation covering (even though sparse), and the limited availability of sandy material (Kocurek and Nielson, 1986).

Palaeosols represent the stable phase in the formation of the aeolian sand sheet, when the unavailability or bypassing of sediments, allied with the development of a covering vegetation,

led to the absence of sedimentation and erosional processes. Aridisols and Alfisols represent long interruptions in sedimentation, whereas Entisols represent shorter periods of interruption of the sedimentation. Vertisols, however, do not provide information about the time involved in development. The kind and the organisation of the paleosol profiles found here do not suggest contemporaneous aeolian sand input. High sedimentary input during pedogenesis would have been suggested by, for example, very frequent Entisols, exceptionally thick Entisols or over-thickened A horizons for the other palaeosol types (Catt, 1990; Wright, 1992). In the area of study, however, Entisols are rare (2.1% of the entire sedimentary succession) and very thin (0.3 to 0.5 m thick); moreover, no over-thickened A horizons have been observed for the other paleosols.

The ephemeral river deposits observed here involve up to ten depositional episodes of conglomerate or gravelly sandstone grading to sandstone, representing the sedimentation of gravelly or sandy sheet fluvial bars. These sedimentary structures and the geometry of the channel fill lead to the interpretation of the channel as an ephemeral braided or single-thread river (Tooth, 2000). Palaeocurrent data from imbricated pebbles of three channel deposits (Fig. 16) suggest palaeoflows towards the north, whereas a mapping of a channel deposit near the town of Itajá (cf. Basilici et al., 2009, their figure 6B) revealed a channel with a long N20 axis. The palaeocurrent data are in agreement with the analyses proposed by Andreis et al. (1999), although discordant with that of other authors (for instance, Fernandes and Coimbra, 1999), who interpreted the channels of the Marília Formation as being part of a drainage system of alluvial megafans developed on the eastern margin of the Bauru Basin and prograding towards the west. We disagree with this hypothesis, since (1) the palaeocurrent is parallel to the basin margins, (2) there are no debris flow deposits, that are common in alluvial fans, (3) the interchannel areas do not appear to be affected by non-channelised deposits, which would be typical of an alluvial fan, but rather are characterised by the stability of the morphological surface and the occurrence of pedogenesis, as explained below. The absence of debrite deposits suggest that water transport was relatively frequent within the channel. Moreover, aeolian reworking during the deposition of the fluvial deposits was uncommon. Only a few, thin sandstone beds with translatent climbing wind-rippled strata overlie the river channel episodes, and the sandstone strata are lacking in the gravel lags, which would have been formed by aeolian deflation, as is typical of a fluvial system in aeolian-dominated areas (Bullard and Livingstone, 2001; Krapf et al., 2005). Neither

pedogenesis, nor traces of bioturbation were observed in the river channel deposits, suggesting that long interruptions of the sedimentary processes during the channel fill did not occurred.

The depositional system of the Adamantina and Marília formations represents a dryland area with a flat morphology with a few isolated channels of wide, shallow rivers. Two alternating phases, controlled by variation in the climate, characterised the development of the two units: an arid phase, marked by prevalent aeolian deposition, responsible for the construction of the aeolian sand sheet, and a semi-arid phase, characterised by intense and prolonged pedogenesis of the previous aeolian deposits, as well as and by reactivation of fluvial transport and deposition.

No clear definition of geometrical and genetic relationships between ephemeral river deposits and other architectural elements were observed in outcrop. However, in dryland systems the processes of fluvial deposition are more intense during a more humid climate (when in the interchannel areas pedogenesis prevails), whereas they are reduced or absent during a drier phase (when mainly aeolian depositional processes develop in interchannel areas) (Kocurek, 1999; Tchakerian and Lancaster, 2002; Kocurek, 2003; Jain et al., 2005). Therefore, it is suggested that ephemeral river deposits formed when in interchannel areas prevailed the pedogenesis.

## **6. Construction, accumulation and preservation of the aeolian sand sheet**

To identify the factors which controlled the development of the Adamantina and Marília formations the model of genesis and evolution of an aeolian system suggested by Kocurek (1999), Kocurek and Lancaster (1999), and Kocurek (2003) was applied. According to this model three different phases allow the incorporation of a morpho-depositional aeolian system into the geological record: the construction of the aeolian system, the accumulation of a geological body, and the preservation within the rock record.

### **6.1. Construction**

Three factors are necessary to the construction of an aeolian system: sediment supply, sediment availability and wind transport capacity (Kocurek, 1999).

Most of the sediment is supplied by systems external to the aeolian-dominated environment, such as those involving rivers, alluvial fans, lakes or coastal systems. Within the

depositional system of the Adamantina and Marília formations, rivers supplied the primary sediment. In fact, the compositional distribution of the sandstone of the three architectural elements shows that ephemeral river deposits are composed of high percentage of lithic fragments (mainly basaltic clasts) that decreases drastically into wind-ripple-dominated aeolian sand sheet deposits and once more into palaeosols (Fig. 4E). Less resistant lithic fragments often break down to dust during aeolian transport and are easily weathered away in soils, whereas more resistant grains such as quartz become progressively concentrated (Fig. 4E). Therefore, sandstone in aeolian deposits, especially that found in palaeosols, is believed to have originated from various cycles of erosion and sedimentation of original fluvial deposits.

The supply of sediments by rivers, which occurs during the more humid climate phases, is widely described in recent and ancient examples of aeolian-dominated depositional systems (Langford, 1989; Langford and Chan, 1989; Tooth, 2000; Bullard and Livingstone, 2002). This kind of sediment supply originated as external to the basin. However, during the drier phase the disappearance of the vegetation brought about the erosion of the upper portion of the soil, originating an internal source of sediment. Clay cutans on the surfaces of quartz grains and fragments of calcareous nodules, both contained in the aeolian ripple strata, testify to an origin from previous soils. Soil erosion extended downwards to the cemented horizons of the soils (Bk or Bkm), or until the formation of a gravel lag, which sheltered the surface.

In the aeolian sand sheet described here, the availability of sediment was mainly controlled by the climate. During the formation of the mature soils, the vegetation covering protected the fine-grained sand from wind erosion; moreover, within the fluvial belt, where loose sediment might have been available for entrainment by the wind, the high water table inhibited its availability. Indeed, wind-reworked strata in fluvial deposits are very rare, and the aeolian gravel lags, common in wind-dominated fluvial deposits (Bullard and Livingstone, 2002; Krapf et al., 2005), were not observed here. Sediment availability increased during the drier period, however, because the lowering of the water table favoured the removal of the loose sand from the fluvial belt, and the retraction of the vegetation covering the interfluvial areas also permitted the deflation of the soils.

Transport capacity depends on the wind's power to carry sediment. Data on transport capacity during the two climatic phases of the aeolian sand sheet are unavailable. However,

considering the subtropical geographical position of the Bauru Basin during the Late Cretaceous, one might think that stronger wind activity occurred during the drier phase.

Basilici et al. (2009) plotted these three factors as separated curves on a diagram showing them as a function of time along a cycle of drier and more humid climatic phases (Fig. 21). The more humid phase is characterised by very low or non-existent value of sediment availability, despite the high fluvial sediment supply, which peak is just after the transition from drier to a more humid phase (Langhein and Schumm, 1958).

During the more humid phase, the sediment supplied is not transported by the wind, but remains stored within the fluvial belt (sediment availability limited -  $S_{AL}$ ). At the onset of the drier phase, the sediment availability increases, due to the disappearance of the vegetation and the lowering of the water table in the fluvial belt. Some of the sediment stored in the fluvial system is entrained by the wind as lagged influx, and, at the same time, soil deflation also produces sediment. The drier phase is characterised by a contemporaneous and lagged influx of sediment. At the beginning of the deflation the availability of sediment is limited (contemporaneous and lagged influx, availability limited -  $CLI_{AL}$ ), but increases with the aeolian deflation passing to be limited by the wind transport (contemporaneous and lagged influx, transported limited -  $CLI_{TL}$ ). When the lagged sediment in fluvial belt is exhausted and the soil erosion deepens up to the cemented horizons, the sediment availability comes back to be limited (contemporaneous and lagged influx, availability limited -  $CLI_{AL}$ ).

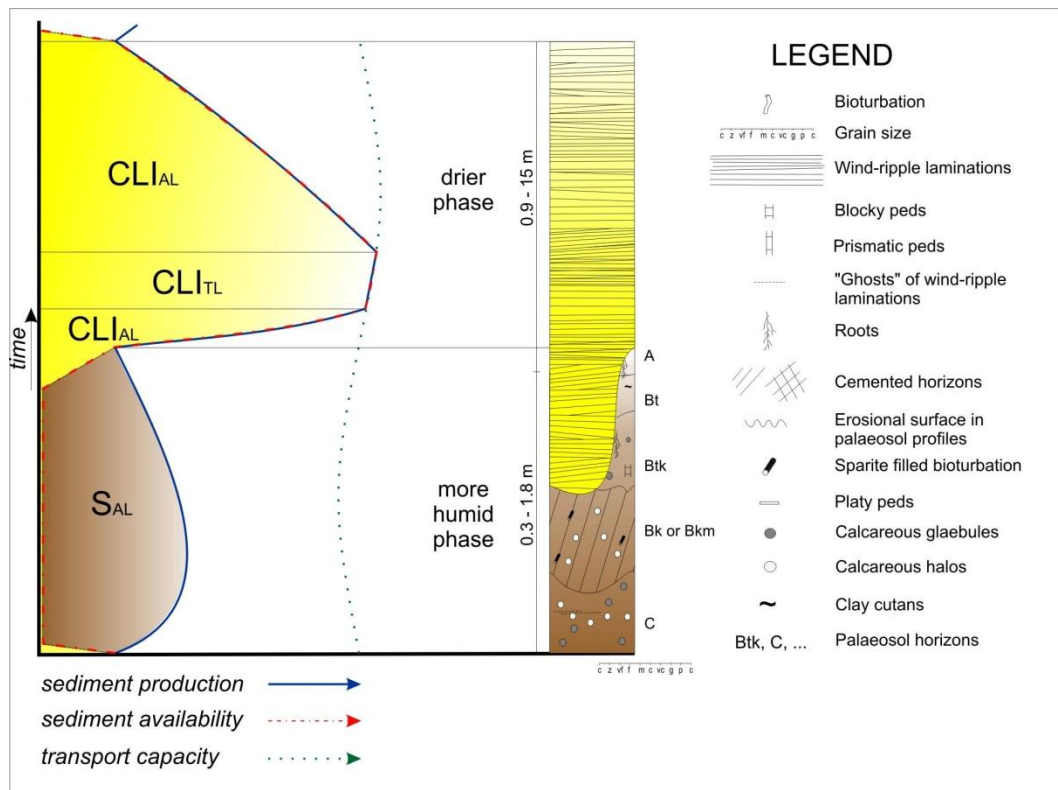


**Figure 21.** Idealised sediment state diagram for Adamantina and Marília formations. See the text for a complete explanation. Sediment states: S<sub>AL</sub> (sediment availability limited); CLI<sub>AL</sub> (contemporaneous and lagged influx, availability limited); CLI<sub>TL</sub> (contemporaneous and lagged influx, transported limited) (modified after Basilici et al., 2009).

## 6.2. Accumulation

Accumulation is the transition of sediment from the top of an accumulation surface to below it (Kocurek and Havholm, 1993; Kocurek, 1999). During the stable phase of the humid climate (the stabilised aeolian system - Kocurek and Havholm, 1993) the accumulation surface was controlled by the formation of soil and the consequent growth of a vegetation that protected it from deflation. During the drier unstable phase (the dry aeolian system - Kocurek and Havholm, 1993) this surface was determined by cemented horizons (Bk or Bkm) over the areas covered by Aridisols or controlled by the wind itself in areas covered by Vertisols, Entisols, and Alfisols, and where fluvial or aeolian deposits were found. Water table did not control the accumulation surface. Actually, adhesion structures (Kocurek and Fielder, 1982) and contorted laminations, suggesting high water table level, are absent in aeolian deposits; moreover,

palaeosols, developed during the more humid phase, indicate well drained conditions (Dal' Bó et al., 2009).

The accumulation of sediments in aeolian sediment transport system can be determined by applying the sediment conservation equation (Middleton and Southard, 1984):

$$\frac{\partial h}{\partial t} = \left( \frac{\partial q}{\partial x} + \frac{\partial c}{\partial t} \right),$$

where  $h$  is the height of the accumulation surface,  $t$  the time,  $q$  the rate of transport,  $x$  the distance, and  $c$  the sediment concentration in the wind transport. The solution provides a graphic which can represent the two phases in the development of an aeolian sand sheet (Fig. 22). The phase of stability is represented only by the conditions of the sediment bypassing (Fig. 22, Byp). The phase of instability includes erosion of the upper portion of the palaeosol profile, corresponding to a first order bounding surface (Fig. 22, Ep); deposition of strata of climbing translatent ripples (Fig. 22, D); erosion of these climbing translatent ripple strata and the generation of fifth order bounding surfaces (Fig. 22, Ed); and bypassing of sediment during wind ripple migration (Fig. 22, Byd).

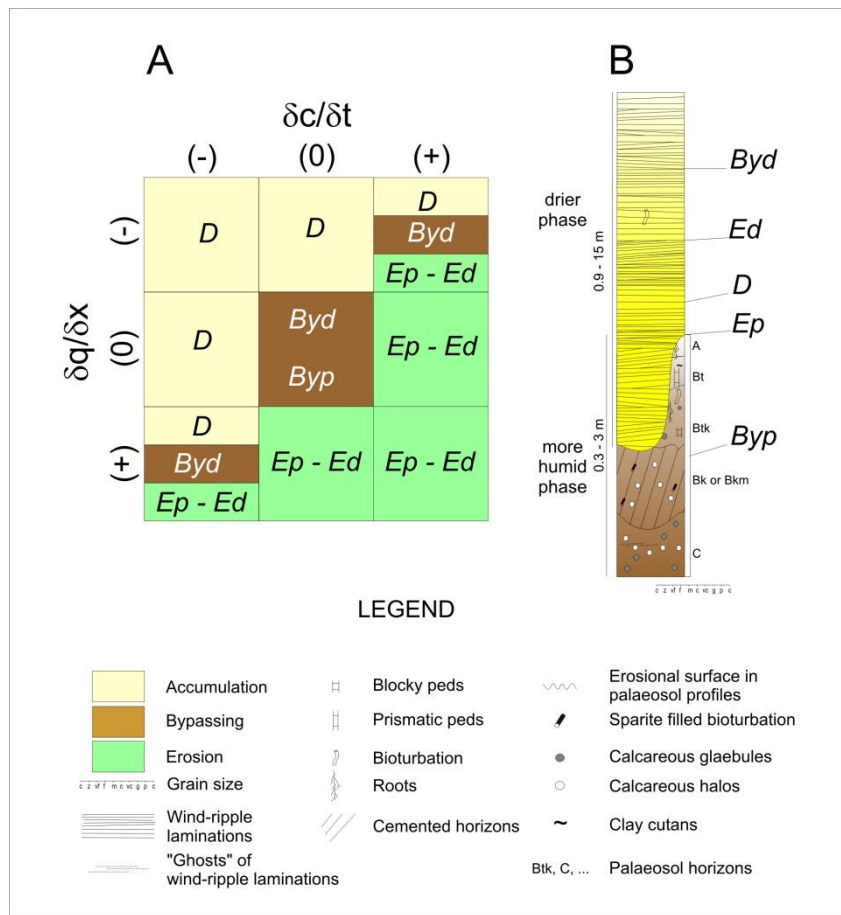


**Figure 22.** Application of the sediment conservation equation of Middleton and Southard (1984) to aeolian sand sheet system. (A) Solution to the sediment conservation equation by sign alone, defining the fields of erosion, bypassing and deposition (modified after Kocurek, 1999). (B) Sequential cycle of palaeosol and aeolian deposits interbedding tied to alternating more humid to drier climate phases. Byp: bypassing during pedogenesis; Byd: bypassing during deposition; D: deposition; Ep: erosion of soils; Ed: erosion of deposits.

### 6.3. Preservation

In the case of the Adamantina and Marília formations, and in the whole Bauru Basin, an absolute or relative rise in water table can be excluded as a cause of preservation, as no regional data suggest such a high water table. No internal playa-lake has been identified from the facies analysis. No did the more humid climate generate in the area high water table within the soil profiles. Thus, the most probable cause of the preservation of the Adamantina and Marília formations was tectonically induced subsidence and burial. The regional subsidence was accompanied by various climate-controlled, phases of construction, destruction, and stability of

the aeolian sand sheet. Figure 23 uses a modified Wheeler diagram to illustrate the preservation of three climate controlled cycles within the Adamantina and Marília formations. The construction of this diagram required the acknowledgement of various, not necessarily demonstrable, hypotheses. (1) Subsidence was constant, and calculated semi-quantitatively on the basis of geochronological and palaeontological data (Turner et al., 1994; Dias-Brito et al., 2001; Carvalho et al., 2005): an elapsed time between the Santonian and Maastrichtian of 20 My for the deposition of 220 m of sediments. (2) Climate cycles of an identical duration. (3) Only two architectural elements were considered: palaeosols and wind-ripple-dominated aeolian sand sheet deposits. The drier climate was assumed to be characterised by alternating moments of primarily construction, but also destruction of the aeolian sand sheet with erosional moments marking the formation of fifth order bounding surfaces. The more humid phase was assumed to be characterised by topographic stability, with each immediately successive drier phase marking the erosion to develop the first order bounding surface.

The low rate of subsidence negatively controlled the preservation of the aeolian deposits, since it fostered intense pedogenesis during periods of topographic stability and the consequently greater palaeosol profiles recorded in the sedimentary succession. However, this subsidence apparently did not influence the sequential organisation of the Adamantina and Marília formations, as this appear to have been controlled only by climate variation.

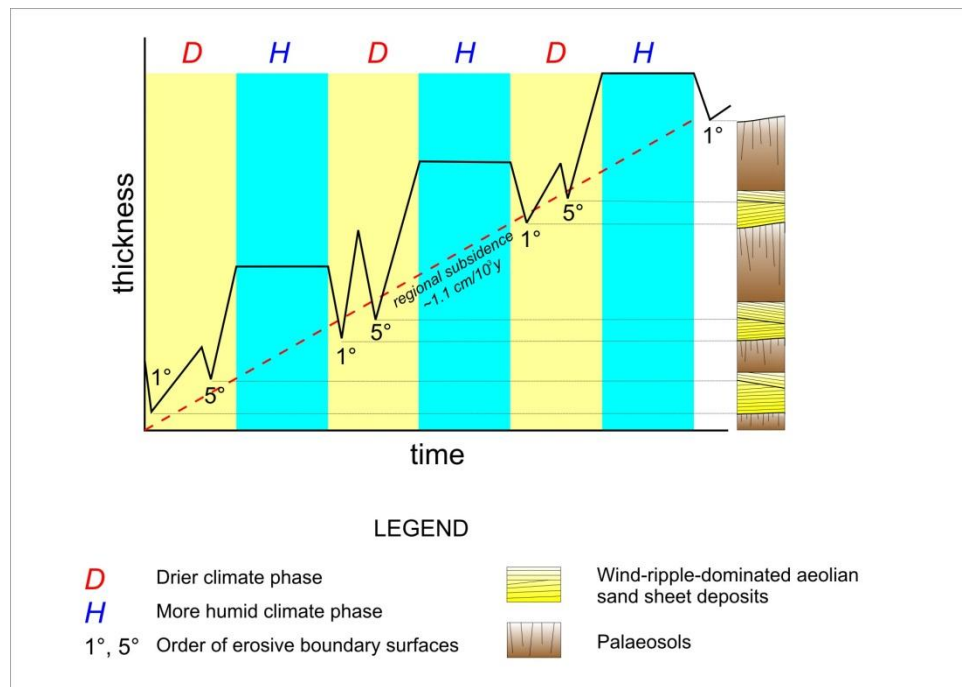


**Figure 23.** Modified Wheeler diagram to illustrate a model of building of the Adamantina and Marília formations during three climate-controlled drier to more humid cycles. The preservation is controlled by regional subsidence and burial of tectonic origin. The climate controls the construction of the aeolian sand sheet and the formation of the erosional boundary surfaces. Bounding surfaces of second, third and fourth order are not considered in this diagram.

## 7. Conclusions

Although most of the Adamantina and Marília formations are composed of palaeosols, previous studies considering detailed analyses of these palaeosols and their interrelations with sediments are few.

These two units were formed on a widespread aeolian sand sheet area crossed by wide, shallow ephemeral rivers. Three architectural elements were recognised and described: palaeosols, wind-ripple-dominated aeolian sand sheet deposits, and ephemeral river deposits. Palaeosols and wind-ripple-dominated aeolian sand sheet deposits alternate cyclically in vertical succession, although, at times, these cyclical sequences are substituted by alternating successions of palaeosol profiles separated by erosional surfaces. The ephemeral river channels are located randomly in the architectural structure. The analysis of the palaeosols was determinant in identifying climatic cycles within the sedimentary succession, as well revealing differential orders of the bounding surfaces.

The palaeosols and fluvial deposits formed during a more humid (semi-arid) climate, (fluvial-dominated dryland environment - Bullard and Livingstone, 2002), whereas the aeolian deposits represent a drier (arid) climate (aeolian-dominated dryland environment - Bullard and Livingstone, 2002). The more humid phase coincided with the stability of the topographic surface characterised by prolonged pedogenesis in previously deposited aeolian sediments, and transport and deposition of sediment limited within the fluvial channels. The drier phase corresponded to an unstable topographic surface suffering widespread aeolian erosion and deposition on a sand sheet characterised by an absence of dunes.

This study has identified five orders of bounding surfaces for this aeolian sand sheet. The first order bounding surface, developed above mature palaeosol profiles, is comparable to the super bounding surface of Kocurek (1988) and Kocurek and Havholm (1993). A second order bounding surface is located above immature palaeosols. A third order surface corresponds to the erosional bottom of the ephemeral river channels. A fourth and fifth order erosional surfaces result from infrequent floods or aeolian activity on the wind-ripple-dominated aeolian sand sheet surface.

The principles of construction, accumulation, and preservation of an aeolian system (Kocurek, 1999; Kocurek and Lancaster, 1999; Kocurek, 2003) were tentatively applied to this ancient sand sheet. However, some differences from the principles described were found: (1) Although it is commonly believed that the supply of sediment is exclusive to the more humid climate (Kocurek and Lancaster, 1999; Tooth, 2000; Tchakerian and Lancaster, 2002), this study has provided evidence of an internal sediment supply, even during the drier period, resulting from the erosion of the upper part of the soil. (2) The model of an aeolian sand sheet proposed here demonstrates that the kind of accumulation surface varies with the climate and the nature of the topographic surface. During more humid phases, the accumulation surface is a stabilising surface (Kocurek and Havholm, 1993), represented by the soil, where bypassing or the simple absence of erosion and sedimentation prevail. During drier phases, however, the accumulation surface is represented by the cemented surface over the Aridisols (Bk or Bkm horizons), or by the force of the wind flowing over the Alfisols, Entisols, Vertisols and aeolian deposits. (3) Preservation is controlled exclusively by tectonics, because variations in the internal base level or phreatic water table are not clearly registered during the evolution of the two formations. The low rate of subsidence seems to agree with the geotectonic configuration of the Bauru Basin. The rare

preservation of aeolian deposits, in contrast to the rich palaeosol record, would be a direct consequence of the low rate of subsidence.

### Acknowledgements

The authors would like to thank to Fapesp for the financing of this study (Projects 07/00140-6 and 07/02079-2). We are grateful to Clayton Scherer and Nigel Mountney for their very detailed revisions that contributed to the improvement of the manuscript. Thanks also to Francisco Ladeira for the glad fellowship in the field.

### 8. References

- Ahmad, N., 1983. Vertisols. In: Wilding, L.P., Smeck, N.E., Hall, G.F. (Eds.), Pedogenesis and soil taxonomy II. The soil orders. Developments in soil science 11B. Elsevier, Amsterdam, pp. 91-123.
- Andreis, R.R., Capilla, R., Reis, C.C., 1999. Considerações estratigráficas e composição dos arenitos da Formação Marília (Cretáceo superior) na região de Uberaba (MG). In: Boletim do 5º Simpósio sobre o Cretáceo do Brasil, Unesp - Campus de Rio Claro, pp. 449-455.
- Basilici, G., Dal' Bó, P.F.F., Ladeira, F.S.B., 2009. Climate-induced sediment-palaeosol cycles in a Late Cretaceous dry aeolian sand sheet: Marília Formation (North-West Bauru Basin, Brazil). *Sedimentology* 56, 1876-1904.
- Birkeland, P.W., 1999. Soils and geomorphology, 3rd ed. Oxford University Press, New York. 448 p.
- Blair, T.C., 1999. Sedimentary processes and facies of the waterlaid Anvil Spring Canyon alluvial fan, Death Valley, California. *Sedimentology* 46, 913-940.
- Blair, T.C., 2003. Features and origin of the giant Cucomungo Canyon alluvial fan, Eureka Valley, California. *Geological Society of America Special Paper* 370, 105-125.
- Breed, C.S., McCauley, J.F., Davis, P.A., 1987. Sand sheet of the eastern Sahara and ripples blankets on Mars. In: Frostick, L., Reid, I. (Eds.), *Desert sediments: ancient and modern*. Geological Society of America Special Publication 35, 337-359.
- Brookfield, M.E., 1977. The origin of bounding surfaces in ancient aeolian sandstone. *Sedimentology* 24, 303-332.
- Bullard, J.E., Livingstone, I., 2002. Interactions between aeolian and fluvial systems in dryland environments. *Area* 34 (1), 8-16.

Cain, S.A., Mountney, N., P., 2009. Spatial and temporal evolution of a terminal fan system: the Permian Organ Rock Formation, South-east Utah, USA. *Sedimentology* 56, 1774-1800.

Carr-Craubagh, M., Kocurek, G., 1998. Continental sequence stratigraphy of a wet eolian system: a key to relative sea-level change. In: Shanley, K.W., McCabe, P.J. (Eds.), *Relative role of eustasy, climate, and tectonism in continental rocks*. Society for Sedimentary Geology Special Publication 59, 213-228.

Carvalho, I.S., Campos, A.C.A., Nobre, P.H., 2005. *Baurusuchus salgadoensis*, a new Crocodylomorpha from the Bauru Basin (Cretaceous), Brazil. *Gondwana Research* 8, 11-30.

Catt, J.A., 1990. Paleopedology manual. *Quaternary International* 6, 1-95.

Chakraborty, T., Chakraborty, C., 2001. Eolian-aqueous interaction in the development of a Proterozoic sand sheet: Shikaoda Formation, Hosangabad, India. *Journal of Sedimentary Research* 71, 107-117.

CPRM – Serviço Geológico do Brasil, 2004. Carta Geológica do Brasil ao Milionésimo, Folha SE22, Goiânia, Secretaria de Minas e Metalurgia e Ministério de Minas e Energia, Brasília.

Dal' Bó, P.F.F., Basilici, G., Angelica, R.S., Ladeira, F.S.B., 2009. Paleoclimatic interpretations from pedogenic calcretes in a Maastrichtian semi-arid eolian sand-sheet palaeoenvironment: Marília Formation (Bauru Basin, southeastern Brazil). *Cretaceous Research* 30, 659-675.

Dias-Brito, D., Musacchio, E.A., Castro, J.C. de., Maranhão, M.da.S., Suarez, J.M., Rodrigues, R., 2001. Grupo Bauru: uma unidade continental do Cretáceo no Brasil – concepções baseadas em dados micropaleontológicos, isotópicos e estratigráficos. *Revue de Paléobiologie* 20 (1), 245-304.

El-Baz, F., Maingue, M., Robinson, C., 2000. Fluvio-aeolian dynamics in the north-eastern Sahara: the relationship between fluvial/aeolian systems and ground-water concentration. *Journal of Arid Environments* 44, 173-183.

Fernandes, L.A., Coimbra, A.M., 1996. A Bacia Bauru (Cretáceo Superior, Brasil). *Anais da Academia Brasileira de Ciências* 68, 195-205.

Fernandes, L.A., Coimbra, A.M., 1999. Paleocorrentes da parte oriental da Bacia Bauru (Ks, Brasil). In: *Boletim do 5º Simpósio sobre o Cretáceo do Brasil*, Unesp - Campus de Rio Claro, pp. 51-57.

Fernandes, L.A., Coimbra, A.M., 2000. Revisão estratigráfica da parte oriental da Bacia Bauru (Neocretáceo). *Revista Brasileira de Geociências* 30, 717-728.

Fisher, J.A., Nichols, G.J., Waltham, D.A., 2007. Unconfined flow deposits in distal sectors of fluvial distributary systems: Examples from the Miocene Luna and Huesca Systems, northern Spain. *Sedimentary Geology* 195, 55-73.

Fryberger, S.G., 1993. A review of aeolian bounding surfaces, with examples from the Permian Minnelusa Formation, USA. In: North, C.P., Prosser, D.J. (Eds.), Characterization of fluvial and aeolian reservoirs. Geological Society of America Special Publication 73, 167-197.

Fryberger, S.G., Ahlbrandt, T.S., Andrews, S., 1979. Origin, sedimentary features and significance of low-angle aeolian ‘sand sheet’ deposits, Great Sand Dunes National Monument and vicinity, Colorado. *Journal of Sedimentary Petrology* 49, 733-746.

Fúlfaro, V.J., Perinotto, J.A.J., 1996. A Bacia Bauru: estado da arte. In: Dias-Brito, D., Rohn, R., Perinotto, J.A.J., Boletim do 4º Simpósio sobre o Cretáceo do Brasil, Unesp - Campus de Rio Claro, pp. 297-303.

Gile, L.H., Peterson, F.F., Grossman, R.B., 1966. Morphological and genetic sequences of carbonate accumulation in desert soils. *Soil Science* 101, 347-360.

Goldberg, K., Garcia, A.J.V., 2000. Palaeobiogeography of the Bauru Group, a dinosaur-bearing Cretaceous unit, northeastern Paraná Basin, Brazil. *Cretaceous Research* 21, 241-254.

Grossman, R.B., 1983. Entisols. In: Wilding, L.P., Smeck, N.E., Hall, G.F. (Eds.), Pedogenesis and soil taxonomy II. The soil orders. *Developments in soil science* 11B. Elsevier, Amsterdam, pp. 55-90.

Gustavson, T.C., Holliday, V.T., 1999. Eolian sedimentation and soil development on a semi-arid to subhumid grassland, Tertiary Ogallala and Quaternary Blackwater Draw formations, Texas and New Mexico High Plains. *Journal of Sedimentary Research* 69, 622-634.

Gustavson, T.C., Wrinkler, D.A., 1988. Depositional facies of the Miocene-Pliocene Ogallala Formation, northwestern Texas and eastern New Mexico. *Geology* 16, 203-206.

Heidari, A., Mahmoodi, Sh., Roozitala, M.H., Mermut, A.R., 2008. Diversity of clay minerals in the Vertisols of three different climatic regions in Western Iran. *J. Agric. Sci. Technol.* 10, 269-284.

Hunter, R.E., 1977. Basic types of stratification in small eolian dunes. *Sedimentology* 24, 361-387.

Jain, M., Tandon, S.K., Singhvi, A.K., Mishra, S., Bhatt, S.C., 2005. Quaternary alluvial stratigraphic development in a desert setting: a case study from the Luni river basin, Thar Desert of western India. In: Blum, M.D., Marriot, S.B., Leclair, S.F. (Eds.), Fluvial sedimentology VII. International Association of Sedimentologists Special Publication 35, pp. 349-371.

- Kocurek, G., 1988. First-order and super bounding surfaces in eolian sequences - bounding surfaces revisited. In: Kocurek, G. (Ed.), Late Paleozoic and Mesozoic eolian systems of the western interior of the United States. *Sedimentary Geology* 56, pp. 193-206.
- Kocurek, G., 1999. The aeolian rock record (Yes, Virginia, it exists, but it really is rather special to create one). In: Goudie, A.S., Livingstone, I. (Eds.), *Aeolian environments, sediments and landforms*. John Wiley & Sons, London, pp. 239-259.
- Kocurek, G., 2003. Limits on extreme eolian systems: Sahara of Mauritania and Jurassic Navajo Sandstone examples. In: Chan, M.A., Archer, A.W. (Eds.), *Extreme depositional environments: mega end members in geological time*. Geological Society of America Special Paper 370, pp. 43-52.
- Kocurek, G., Fielder, G., 1982. Adhesion structures. *Journal of Sedimentary Petrology* 52 (4): 1229-1241.
- Kocurek, G., Havholm, K.G., 1993. Eolian sequence stratigraphy - a conceptual framework. In: Weimer, P., Posamentier, H. (Eds.), *Siliciclastic sequence stratigraphy. Recent developments and applications*. American Association of Petroleum Geologists Memoir 58, pp. 393-409.
- Kocurek, G., Lancaster, N., 1999. Aeolian system sediment state: theory and Mojave Desert Kelso dune field example. *Sedimentology* 46, 505-515.
- Kocurek, G., Nielson, J., 1986. Conditions favourable to the formation of warm-climate aeolian sand sheets. *Sedimentology* 33, 795-816.
- Krapf, C.B.E., Stanistreet, I.G., Stollhofen, H., 2005. Morphology and fluvio-aeolian interaction of the tropical latitude, ephemeral braided-river dominated Koigab Fan, north-west Namibia. In: Blum, M.D., Marriot, S.B., Leclair, S.F. (Eds.), *Fluvial sedimentology VII*. International Association of Sedimentologists Special Publication 35, pp. 99-120.
- Lancaster, N., 1993. Origins and sedimentary features of supersurfaces in the northwestern Gran Desierto sand sea. In: Pye, K., Lancaster, N. (Eds.), *Aeolian sedimentation, ancient and modern*. International Association of Sedimentologists Special Publication 16, pp. 71-83.
- Lancaster, N., 1994. Dune morphology and dynamics. In: Abrahams, A.D., Parson, A.J. (Eds.), *Geomorphology of desert environments*. Chapman & Hall, London, pp. 474-505.
- Lancaster, N., Greeley, R., Christensen, P.R., 1987. Dunes of the Gran Desierto sand sea, Sonora, Mexico. *Earth Surface Processes and Landforms* 12, 277-288.
- Langford, R.P., 1989. Fluvial-aeolian interactions: part I, modern systems. *Sedimentology* 36, 1023-1035.
- Langford, R.P., Chan, M.A., 1989. Fluvial-aeolian interactions: part II, ancient systems. *Sedimentology* 36, 1037-1051.

- Langbein, W.B., Schumm, S.A., 1958. Yield of sediment in relation to mean annual precipitation. *Eos, Transactions, American Geophysical Union* 39, 1076-1084.
- Machette, M.N., 1985. Calcic soils of the southwestern United States. In: Weide, D.L. (Ed.), *Soils and quaternary geology of the southwestern United States*. Geological Society of America Special Paper 203, pp. 1-21.
- Mack, G.H., James, W.C., 1992. Paleosols for sedimentologists. *Geological Society of America Short Course Notes*, 127 p.
- Mack, G.H., James, W.C., Monger, H.C., 1993. Classification of paleosols. *Geological Society of American Bulletin* 105, 129-136.
- Mermut, A.R., Dasog, G.S., Dowuona, G.N., 1996. Soil morphology. In: Ahmad, N., Mermut, A. (Eds.), *Vertisols and technologies for their management. Development in soil science* 24. Elsevier, Amsterdam, pp. 89-114.
- Miall, A.D., 1985. Architectural-element analysis: a new method of facies analysis applied to fluvial deposits. *Earth Science Reviews* 22, 261-308.
- Miall, A.D., 1990. Principles of sedimentary basin analysis, 2nd ed. Springer-Verlag, Berlin, 668 p.
- Miall, A.D., 1996. The geology of fluvial deposits. Springer-Verlag, Berlin, 582 p.
- Middleton, G.V., Southard, J.B., 1984. Mechanisms of sediment movement. *Society for Sedimentary Geology Short Course* 3, 401 p.
- Monger, H. C., Daughert, A., Gile, L.H., 1991. A microscopic examination of pedogenic calcite in an Aridisol of southern New Mexico. In: Nettleton, W.D. (Ed.), *Occurrence, characteristics, and genesis of carbonate, gypsum, and silica accumulations in soils*. Soil Science Society of America Special Publication 26, 37-60.
- Mountney, N.P., 2006. Eolian facies models. In: Posamentier, H.W., Walker, R.G. (Eds.), *Facies models revisited*. Society for Sedimentary Geology Special Publication 84, pp. 19-83.
- Mountney, N.P., Russell, A.J., 2004. Sedimentology of aeolian sand sheet deposits in the Askja region of northeast Iceland. *Sedimentary Geology* 166, 223-244.
- Nettleton, W.D., Peterson, P.F., 1983. Aridisols. In: Wilding, L.P., Smeck, N.E., Hall, G.F. (Eds.), *Pedogenesis and soil taxonomy II. The soil orders. Developments in soil science* 11B. Elsevier, Amsterdam, pp. 165-215.
- Newell, A.J., 2001. Bounding surfaces in a mixed aeolian-fluvial system (Rotliegend, Wessex Basin, SW UK). *Marine and Petroleum Geology* 18, 339-347.

- North, C., 1996. The prediction and modeling of subsurface fluvial stratigraphy. In: Carling, P.A., Dawson, M.R. (Eds.), *Advances in fluvial dynamics and stratigraphy*. John Wiley & Sons, Chichester, pp. 395-519.
- Pettijohn, F.J., Potter, P.E., Siever, R., 1987. *Sand and sandstone*. Springer-Verlag, New York, 553 p.
- Quirk, D.G., 1996. ‘Base profile’: a unifying concept in alluvial sequence stratigraphy. In: Howell, J.A., Aitken, J.F. (Eds.), *High resolution sequence stratigraphy: innovations and applications*. Geological Society of America Special Publication 104, pp. 37-49.
- Rees, A.I., 1968. The production of preferred orientation in a concentrated dispersion of elongated and flattened grains. *Journal of Geology* 76, 457-465.
- Renne, P.R., Ernesto, M., Pacca, I.G., Coe, R.S., Glen, J., Prévot, M., Perrin, M., 1992. Rapid eruption of the Paraná flood volcanism, rifting of southern Gondwanaland and the Jurassic-Cretaceous boundary. *Science* 258, 975-979.
- Retallack, G.J., 1988. Field recognition of paleosols. In: Reinhardt, J., Sigleo, W.R. (Eds.), *Paleosols and weathering through geologic time: principles and applications*. Geological Society of America Special Paper 216, pp. 1-20.
- Retallack, G.J., 1991. *Miocene Paleosols and Ape Habitats of Pakistan and Kenya*. Oxford University Press, New York, 346 p.
- Retallack, G.J., 2001. *Soils of the past: an introduction to paleopedology*, 2nd ed. Blackwell, Oxford, 404 p.
- Retallack, G.J., 2005. Pedogenic carbonate proxies for amount and seasonality of precipitation in paleosols. *Geology* 33 (4), 333-336.
- Riccomini, C., 1997. Arcabouço estrutural e aspectos do tectonismo gerador e deformador da Bacia Bauru no Estado de São Paulo. *Revista Brasileira de Geociências* 27 (2), 153-162.
- Rust, R.H., 1983. Alfisols. In: Wilding, L.P., Smeck, N.E., Hall, G.F. (Eds.), *Pedogenesis and soil taxonomy II. The soil orders. Developments in soil science* 11B. Elsevier, Amsterdam, pp. 253-281.
- Schaetzl, R., Anderson, S., 2005. *Soil: genesis and geomorphology*. Cambridge University Press, Cambridge, 832 p.
- Scherer, C.M.S., Lavinia, E.L.C., 2005. Sedimentary cycles and facies architecture of aeolian–fluvial strata of the Upper Jurassic Guará Formation, southern Brazil. *Sedimentology* 52, 1323-1341.
- Soil Survey Staff, 1993. *Soil Survey Manual. Handbook*. U.S Department of Agriculture, Natural Resource Conservation Service 18, Washington, D.C.

Soil Survey Staff, 1999. Soil taxonomy, 2nd edn. A basic system of soil classification for making and interpreting soil surveys. U.S Department of Agriculture, Natural Resource Conservation Service 436, Washington, D.C., 871 p.

Soil Survey Staff, 2006. Keys to soil taxonomy, 10th edn. U.S. Department of Agriculture, Natural Resource Conservation Service, Washington, D.C., 332 p.

Sweet, M.L., 1999. Interaction between aeolian, fluvial and playa environments in the Permian Upper Rotliegend Group, UK southern North Sea. *Sedimentology* 46, 171-187.

Talbot, M.R., 1985. Major bounding surfaces in aeolian sandstones – a climatic model. *Sedimentology* 32, 257-265.

Tchakerian, V.P., Lancaster, N., 2002. Late Quaternary arid/humid cycles in the Mojave Desert and western Great Basin of North America. *Quaternary Science Reviews* 21, 799-810.

Tooth, S., 2000. Process, form and change in dryland rivers: a review of recent research. *Earth-Science Reviews* 51, 67-107.

Trewin, N.H., 1993. Mixed aeolian sand sheet and fluvial deposits in the Tumblagooda Sandstone, western Australia. In: North, C.P., Prosser, D.J. (Eds.), Characterization of fluvial and aeolian reservoirs. Geological Society of America Special Publication 73, pp. 219-230.

Turner, S., Regelous, M., Kelley, S., Hawkesworth, C., Mantovani, M., 1994. Magmatism and continental break-up in the South Atlantic: high precision  $^{40}\text{Ar}$ - $^{39}\text{Ar}$  geochronology. *Earth and Planetary Science Letters* 121 (3-4): 333-348.

Walker, R.G., 1975. Conglomerate: Sedimentary structures and facies models. In: Harms, J.C., Southard, J.B., Spearing, D.R., Walker, R.G. (Eds.), Depositional Environments as Interpreted from Primary Sedimentary Structures and Stratification Sequences. Soc. Econ. Paleont. Miner. Short Course Notes 2, pp. 133-161.

Watson, A., 1992. Desert soils. In: Martini, I.P., Chesworth, W. (Eds.), *Weathering, Soils & Paleosols*. Elsevier, Amsterdam, pp. 225-260.

Watts, N.L., 1980. Quaternary pedogenetic calcretes from Kalahari (southern Africa): mineralogy, genesis and diagenesis. *Sedimentology* 27, 661-686.

Wright, V.P., 1989. Paleosol recognition. In: Allen J.R.N., Wright, V.P. (Eds.), *Paleosols in siliciclastic sequences*. Postgraduate Research Institute for Sedimentology, University of Reading, Reading, pp.1-25.

Wright, V. P., 1992. Paleosols recognition: A guide to early diagenesis in terrestrial settings. In: Wolf, K. and Chilingarian, G. (Eds.), *Diagenesis, III, Developments in Sedimentology*, 47, Elsevier, 591-619.

Wright, V.P., Tucker, M.E., 1991. Calcretes: an introduction. In: Wright, V.P., Tucker, M.E. (Eds.), *Calcretes*. Blackwell, Oxford, pp. 1-22.

Zaher, H., Pol, D., Carvalho, A.B., Riccomini, C., Campos, D., Navas, W., 2006. Re-description of the cranial morphology of *Mariliasuchus amarali*, and its phylogenetic affinities (Crocodyliformes, Notosuchia). American Museum Novitates 3512, 1-40.

Zalán, O.V., Wolff, S., Conceição, J.C.J., Marques, A., Astolfi, M.A.M., Vieira, I.S., Appi, V.T., Zanotto, O.A., 1991. Bacia do Paraná. In: Gabaglia, G.P.R., Milani, E.J. (Eds.), *Origem e evolução de Bacias Sedimentares*. Petrobras, Rio de Janeiro, pp. 135-168.



## ANEXO VI

“Dal’ Bo, P.F.F. & Basilici, G., 2011. *Interactions of eolian and subaqueous processes in the development of the La Salina eolian sand sheet, central-western Argentina. Sedimentary Geology, em submissão.*”



*"The most satisfying genetic explanations of ancient phenomena were by analogy with modern geological processes."*

*Johannes Walther*



# **INTERACTIONS OF EOLIAN AND SUBAQUEOUS PROCESSES IN THE DEVELOPMENT OF THE LA SALINA EOLIAN SAND SHEET, CENTRAL-WESTERN ARGENTINA**

Patrick Francisco Führ Dal' Bó<sup>1</sup>, Giorgio Basilici

DGRN/IG – Universidade Estadual de Campinas, Cidade Universitária, 13083-870, Campinas  
(SP), Brazil

<sup>1</sup> Corresponding author. (Tel.: 55 19 35215944; fax: 55 19 32891562)

E-mail addresses: patrickdalbo@gmail.com; basilici@ige.unicamp.br

## **Abstract**

The La Salina eolian sand sheet is a small morphodepositional area located in the province of San Juan (central-western Argentina), in the tectonic intermontane Tulum depression. The La Salina eolian sand sheet is a currently aggrading system which is characterized by eolian sand cover in excess of 4 m of thickness, upon which dry and damp eolian and subaqueous features are developed. Detailed field studies carried out in several natural sections and in trenches excavated in the sand sheet surface have revealed that cyclic alternations between eolian and subaqueous processes are frequent in the stratigraphic record. Dynamic interactions between those processes have been ongoing for at least ~3.6 ka with an average sedimentation rate of 86.1 cm/ka. The sand sheet construction is maintained by a conjunction of factors which includes an available amount of sand-grade sediment sourced by the deflation of conglomeratic hills and by southerly winds which periodically exceed the threshold velocity required for sand transport. Accumulation of geological bodies is enhanced by stabilizing influence of surface elements, mainly vegetation, and the long-term preservation of the sand sheet accumulations is attributed to tectonically induced subsidence and burial.

Keywords: Eolian and subaqueous processes; eolian sand sheet; Tulum Basin; La Salina.



## 1. Introduction

Eolian sand sheets are extensive, flat to gently undulating sandy surfaces covered predominantly with wind ripples and marked by the absence of dunes with slip faces (Fryberger et al., 1979; Kocurek and Nielson, 1986). Modern eolian sand sheets form significant part of desertic systems worldwide and although the well known examples are in trailing and advancing margins of ergs (Fryberger et al., 1979), there are a number of examples from coastal, alluvial fan, ephemeral river, and periglacial settings (Hummel and Kocurek, 1984; Kocurek and Nielson, 1986; Langford, 1989; Mountney and Russell, 2004). Observations from these modern areas suggest that a number of factors operate single or in conjunction to withhold dune development including a high water table, surface cementation or binding, periodic flooding, significant population of coarse-grained sediment, and vegetation (Kocurek and Nielson, 1986). Interactions of eolian and subaqueous processes are an important component of eolian sand sheets (Glennie, 1970; Mountney, 2006), and have been described from modern settings to try to understand the spatial and temporal variability of sedimentary facies (Ahlbrandt and Fryberger, 1981; Kocurek, 1981; Langford, 1989; Kocurek et al., 1992), surface morphology (Saqqa and Atallah, 2004), and landscape development of arid areas (Maxwell and Haynes Jr., 2001; Bullard and McTainsh, 2003; Al Farraj and Harvey, 2004). Although such studies have become more frequent in recent years (Bullard and McTainsh, 2003), great part of these studies tend to separate the processes in different phases, where eolian processes are dominant in arid phases (eolian-dominated system *sensu* Bullard and Livingstone, 2002) and subaqueous activity is restricted to more humid phases (fluvial-dominated system *sensu* Bullard and Livingstone, 2002). Far less studies have tried to investigate the interactions of eolian and subaqueous-derived sediments as a consequence of short-term autogenic processes which often results in the vertical interbedding of eolian and subaqueous facies (Lancaster, 1997).

The aim of this paper is to document the sedimentology, internal architecture and geomorphology of a currently active, warm-climate eolian sand sheet in central-western Argentina, and to explain its morphology and resulting facies architecture in terms of dynamic interactions between eolian and subaqueous processes from Late Quaternary to recent. Furthermore, understanding such interactions between both processes in an actively aggrading system can provide recent analogues that can help elucidate eolian-subeaqueous interactions found in the stratigraphic and paleoenvironmental record of other successions.

## **2. Geological setting**

The study area is situated in the intermontane Tulum depression (Fig. 1). The Tulum depression, which extension is about 4,000 km<sup>2</sup>, is a tectonic depression filled with Quaternary alluvial and eolian sediments several hundreds of meters thick (Lloret and Suvires, 2006). This depression is bounded by the Eastern Precordillera to the north and west and by the Pie de Palo range to the east. The area is a rain shadow desert created by a 4,000-m tall Andean Cordillera, which acts as a topographic barrier for the cyclonic circulation from the west.

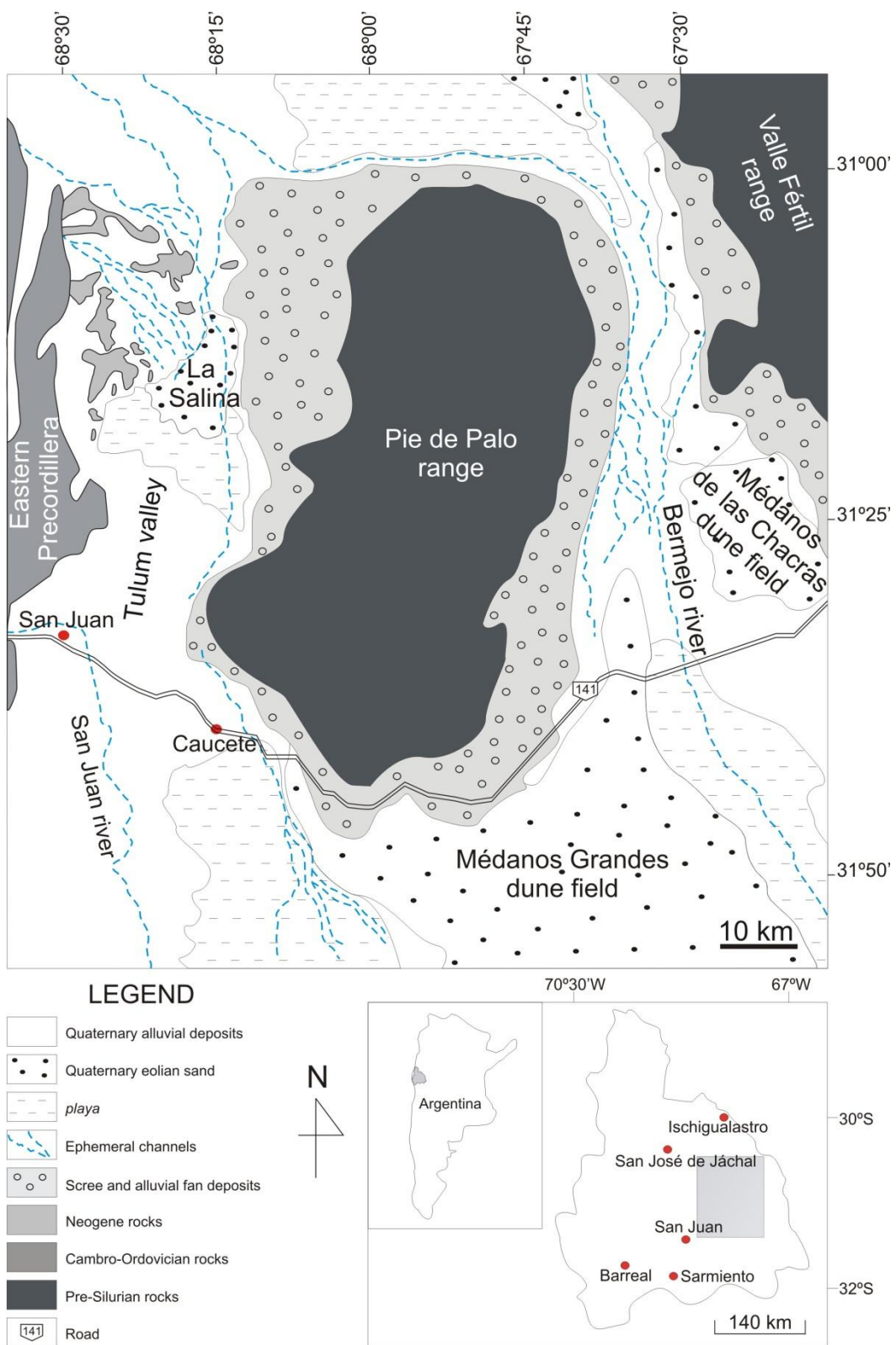


**Figure 1.** Geologic and geomorphologic map of the study area showing the extent of the La Salina sand sheet and the distribution of the main geologic units and geomorphologic elements.

Fluvial deposits intercalated with windblown sand and loess make up the great part of the Quaternary sedimentary fill of the Tulum depression (Lloret and Suvires, 2006). The regime of the rivers that transport these sediments is variable during the years and can be subjected to pluriannual cycles of droughts and floods (Lloret and Suvires, 2006), being greatly fed by groundwater springs (Milana et al., 2003). Eolian cover is most important at north of the depression and to the south there is interbedding between eolian and *playa* deposits (Suvires, 2004).

The source of sediments for eolian transport and deposition is mainly derived from erosion of the Neogene rocks composed by conglomerates, sandstones, and siltstones with abundant volcanic and plutonic clasts. The Neogene exposures are of Lomas de Las Tapias and Mogna formations (SEGEMAR, 2000).

The tectonic configuration of the area is dominated by a series of thrust sheets comprising the Eastern Precordillera structural province to the west and the thick-skinned Pie de Palo range to the east (Meigs et al., 2006). The principal tectonic structure is a southeast dipping thrust sheet beneath Precordillera, which is limited at the base on the northwest by the Villicum reverse fault along the range front and on the southeast by the Tulum valley syncline (Meigs et al., 2006). Cambro-Ordovician carbonates of the Eastern Precordillera are unconformably overlain by Neogene rocks that comprise the bedrock of the thrust sheet (Fig. 2).

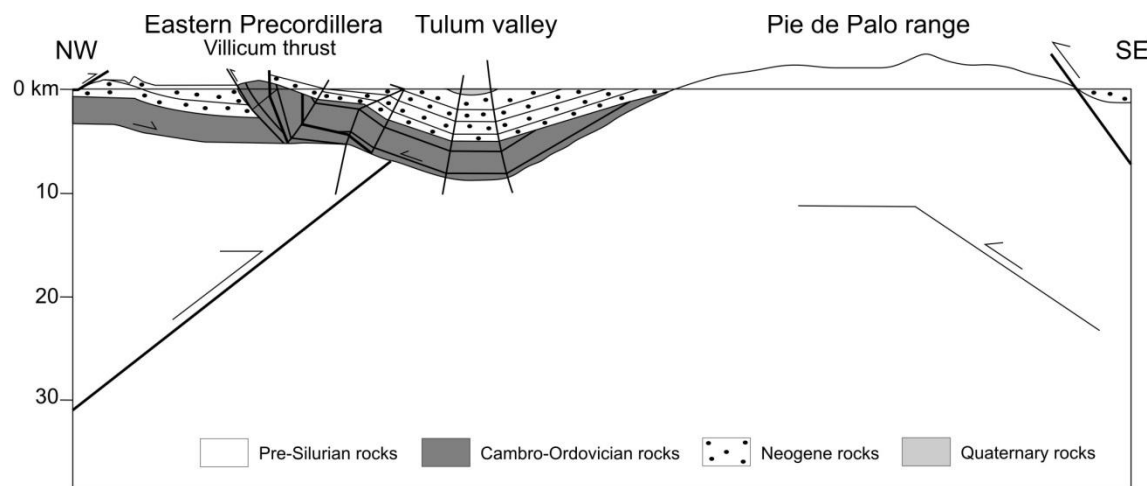


**Figure 2.** Schematic SE-NW crustal-scale regional profile from Pie de Palo range (southeast) through intermontane Tulum depression to Eastern Precordillera (northwest). Modified from Meigs et al. (2006).

## 2.1. Climate data

The Argentine Meteorological Office (Servicio Meteorológico Nacional) records annual weather data from this region since 1973 (SMA, 2010). The historical climatic data presented here (Fig. 3) is from San Juan aerodrome weather station located approximately 35 km to the south of La Salina. Based on data from 1973 to 2010, the mean annual temperature is 17°C, with mean annual maximum and minimum temperatures being 26.5°C and 13.5°C, respectively (Fig. 3A). The mean annual precipitation over the period 1973 to 2010 is 160 mm, and the climate of the area can be classed as arid (Köppen, 1948) (Fig. 3C). The monthly analysis of the last 5-year available climatic data shows a strong concentration of the precipitations during the summer months (Fig. 3B), and reveals that more than 40% of the annual precipitation can fall during heavy rains in just a day. The hydric balance is negative, where evaporation greatly exceeds precipitation rates. The volume of annual precipitation only accounts for 5% of the total amount of evaporated water (Pereyra, 2000). From 1973 to 2010, the mean annual wind speed registered a steadily increase from 2.6 to 4 m s<sup>-1</sup>, with the increase being greatest during summer months, in which the average wind speed can reach 6 m s<sup>-1</sup>, with daily peaks by a maximum of 40.7 m s<sup>-1</sup> (Fig. 3E). In effect, the maximum registered monthly wind speeds are concentrated during the late spring (October-November) and summer months (December-January) (Fig. 3D). Wind is not a limiting factor for sand movement in considering that the threshold velocity (>3.76 m s<sup>-1</sup>) is attained periodically, principally during summer months when more than 60% of the days are characterized by wind velocities above the threshold (Fig. 3F).

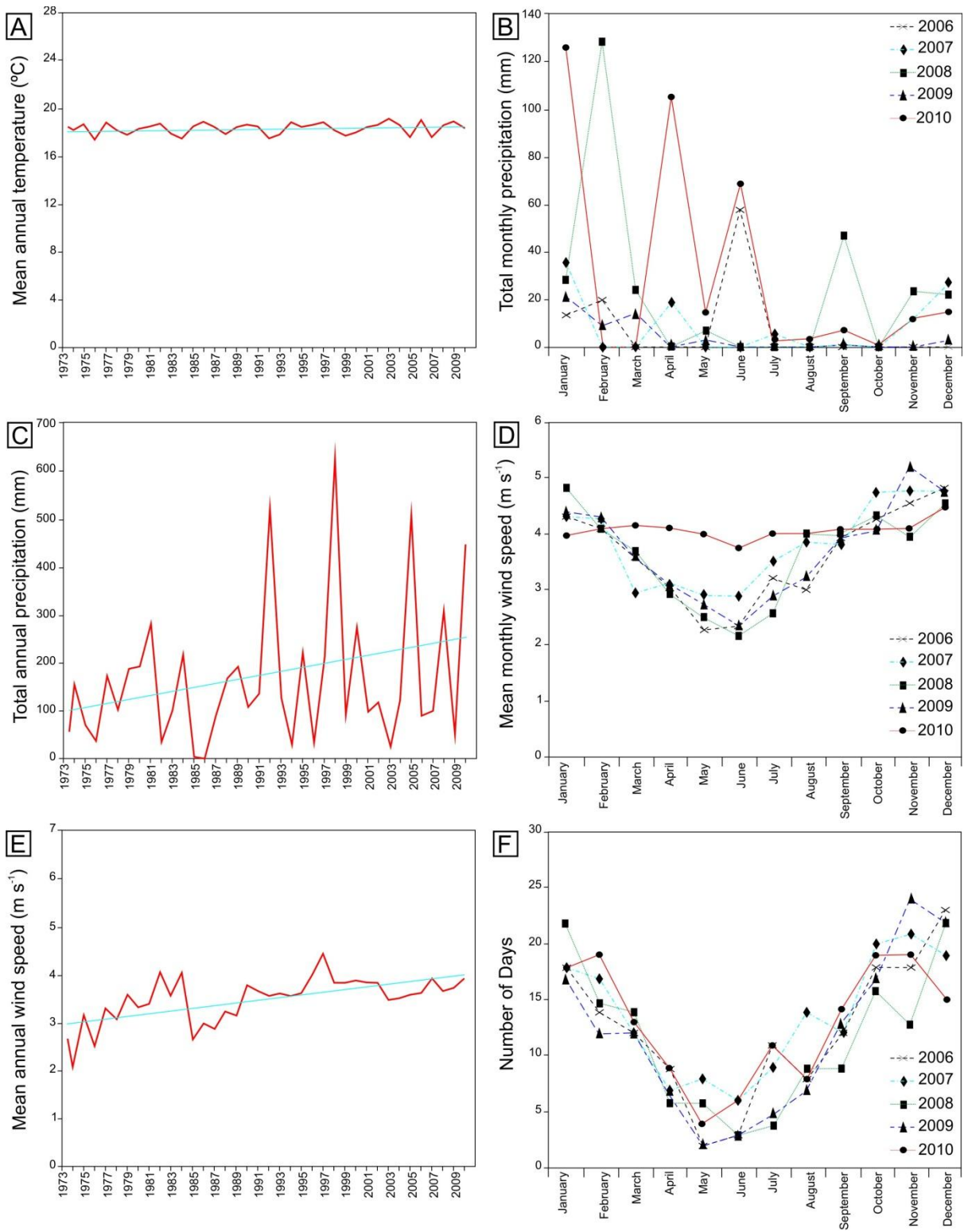


**Figure 3.** Summary climatic data for the San Juan region (data from weather station San Juan Aero:  $31^{\circ}34'\text{S}$ ;  $68^{\circ}41'\text{W}$ ).

No data regarding wind direction were available from the meteorological station, although Tripaldi and Forman (2007) working at Médanos Grandes Dune Field, a small erg located approximately 60 km southeast of the study area, recorded a strongly south to southwesterly component, and indicated a resultant drift potential (RDP) to N352, which is in agreement with data recorded from sedimentary structures that indicate sediment transport towards north (Fig. 4).

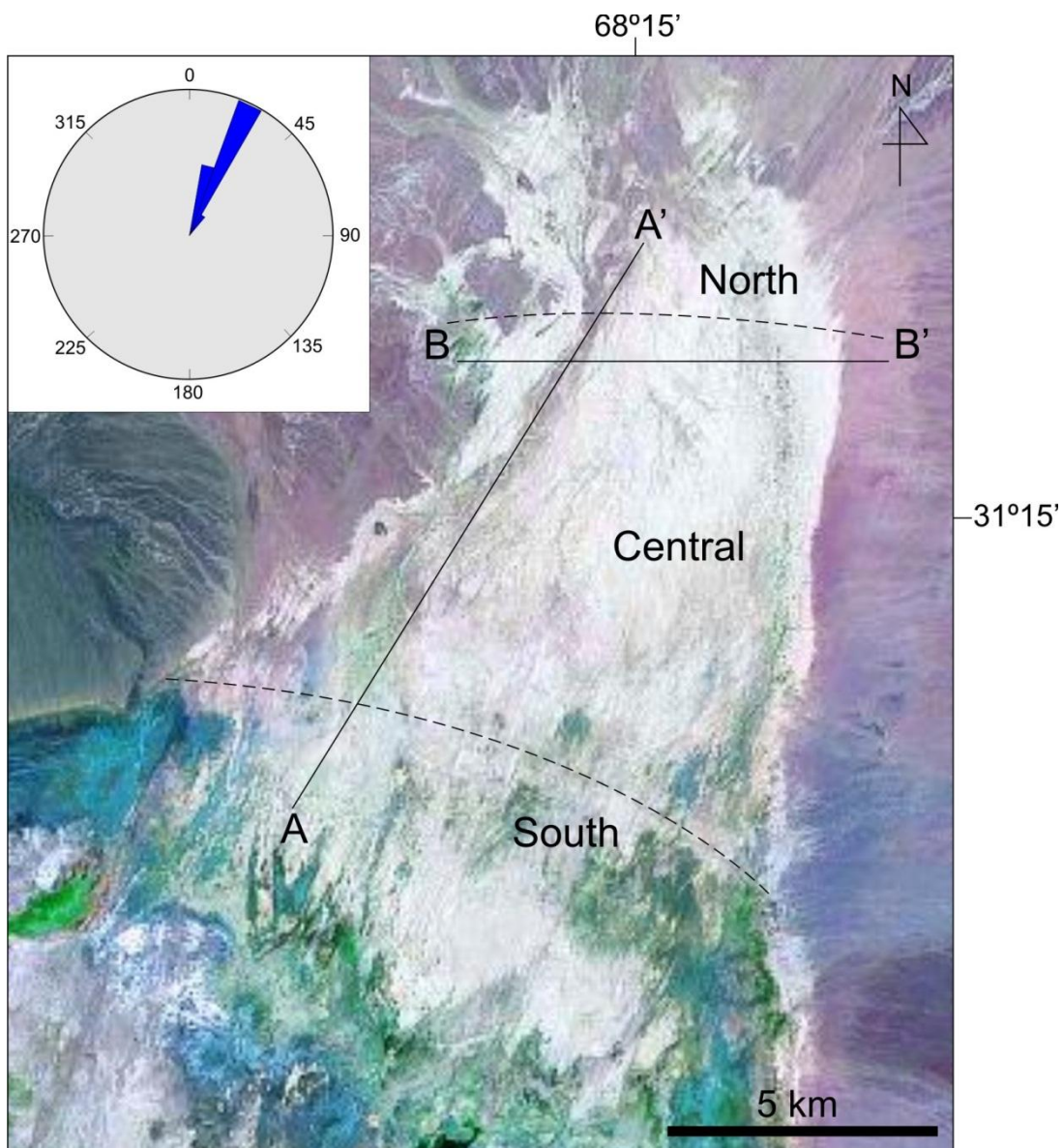


**Figure 4.** Landsat ETM+ image (bands 7, 4 and 2) of the La Salina sand sheet. The transect A-A' follows the main dry channel of the study area and transect B-B' cuts transversally the dry channel section. The sand sheet compartmentalization into south, central, and north regions follows A-A' transect. Wind rose diagram (on the upper left corner) was constructed from measured sedimentary structures and indicates sediment transport towards northeast.

### **3. Methods**

Eolian sand sheet deposits cover ~125 km<sup>2</sup> of the La Salina surface (Fig. 4). Sand sheet form, distribution, and relationship to the other geomorphologic elements were mapped from Landsat ETM+ satellite images (NASA, 2000). Surface observations were conducted along two single transects (Fig. 4). The transect A-A' is parallel oriented to the main dry channel that crosses the area, and follows the dominant wind direction. This transect allowed the measurement of 5 stratigraphic sections, each of 3 m to 4 m thick, exposed in the river banks. The compartmentalization of the sand sheet into three regions (Fig. 4), each of which is characterized by distinctive set of bedforms and landforms, follows this transect. The transect B-B' is transversal oriented to the channel section, and allowed to verify the lateral extend and distribution of the sedimentary features in relation to bedforms and facies developed inside the channel section.

On the ground, the morphological characteristics of bedforms were evaluated by measuring the length, width, height, crestline orientation, vegetation type and present state of covering, and relationship with adjoining bedforms or other surface features. To quantify the morphometric parameters of the nebkhas, 50 randomly chosen nebkhas were measured in the vicinities and inside of the dry channel transect. In addition to the surface observations, 16 trenches were dug at 10 sites to ascertain the nature of the internal structure of the bedforms and the preserved stratigraphic record. Trenches attained depths of 0.5 to 1.5 m and extended for up to 5 m in directions parallel to wind directions and up to 2 m in directions perpendicular to wind directions. The observation into these trenches was used for the confection of scaled architectural drawings. Sediment samples representative of the main bedform types and deposits were collected from 70 sites across the study area for grain-size analysis.

In the 4-m-high bank river section, 1 sample from the base of the section was taken to optically stimulated luminescence (OSL) dating. OSL analysis was carried out at the Laboratory of Glasses and Dating of the Faculdade de Tecnologia de São Paulo, Brazil, using an OSL Automated System, model 1100-series of Daybreak Nuclear Instruments. The 100-160 µm quartz fractions were extracted by wet sieving after chemical treatments with HCl (10%), H<sub>2</sub>O<sub>2</sub> (20%) and HF (20%), in order to remove carbonates, organic carbon and feldspars, respectively. The

gamma irradiation was performed using a  $^{60}\text{Co}$  source, and the natural radioactive isotope contents were determined by gamma spectroscopy using a portable inspector spectroscopy workstation, equipped with a NaI(Tl) detector model 802 of the Canberra. The optical filter used for OSL dating was Hoya U-340. The equivalent dose ( $D_{\text{e}}$ ) was measured using the single-aliquot regenerative (SAR) dose protocol (Murray and Wintle, 2000). Dose rates were obtained from the concentrations of U, Th, and K determined by gamma spectroscopy. The OSL age was obtained by the standardized growth curve (SGC) method. The natural luminescence signal and the laboratory test dose were measured for the SGC (Table 1).

**Table 1.** OSL age for La Salina sand sheet

Sample	Th (ppm)	U (ppm)	K (%)	Annual dose rate ( $\mu\text{Gy/yr}$ )	Accumulated dose (Gy)	Age (years)
LSA	10.493	2.266	0.133	$1650 \pm 60$	6.0	$3,600 \pm 310$

#### 4. Components of the sand sheet environment

##### 4.1. Dry eolian features

Wind ripples represent the most widespread dry eolian feature developed in the three regions of the sand sheet. They are present over all the sandy flat surfaces, superimposed on granule megaripples and on upwind side and lateral flanks of nebkha dunes. Wind ripples are characterized by well sorted to sorted, well rounded fine-grained sand on ripple stoss and troughs and by sorted to moderately sorted, well rounded to rounded, fine- to medium-grained sand on ripple crests (Fig. 5A and B). The ripple heights vary from 10 to 30 mm and wavelengths are 30–100 mm. In plain view, they show straight to few sinuous crest lines. Trenches excavated around low-relief mounds (incipient nebkhas) that are dominated by wind ripples showed the dominance of planar horizontal or low-angle laminae ( $<10^\circ$ ) organized in sets not more than a decimeter thick. Laminae vary in thickness from less than a millimeter to less than a centimeter and laterally may extent for several decimeters. Thinner laminae are enhanced by finer sand covered with hematite coatings. Inverse-graded strata are observed in thicker laminae, whereas thinner laminae

composed of only two or three grains thick show pin stripe laminations. Gently inclined foreset laminae can not be distinguished maybe because of well sorted nature of sand grains.

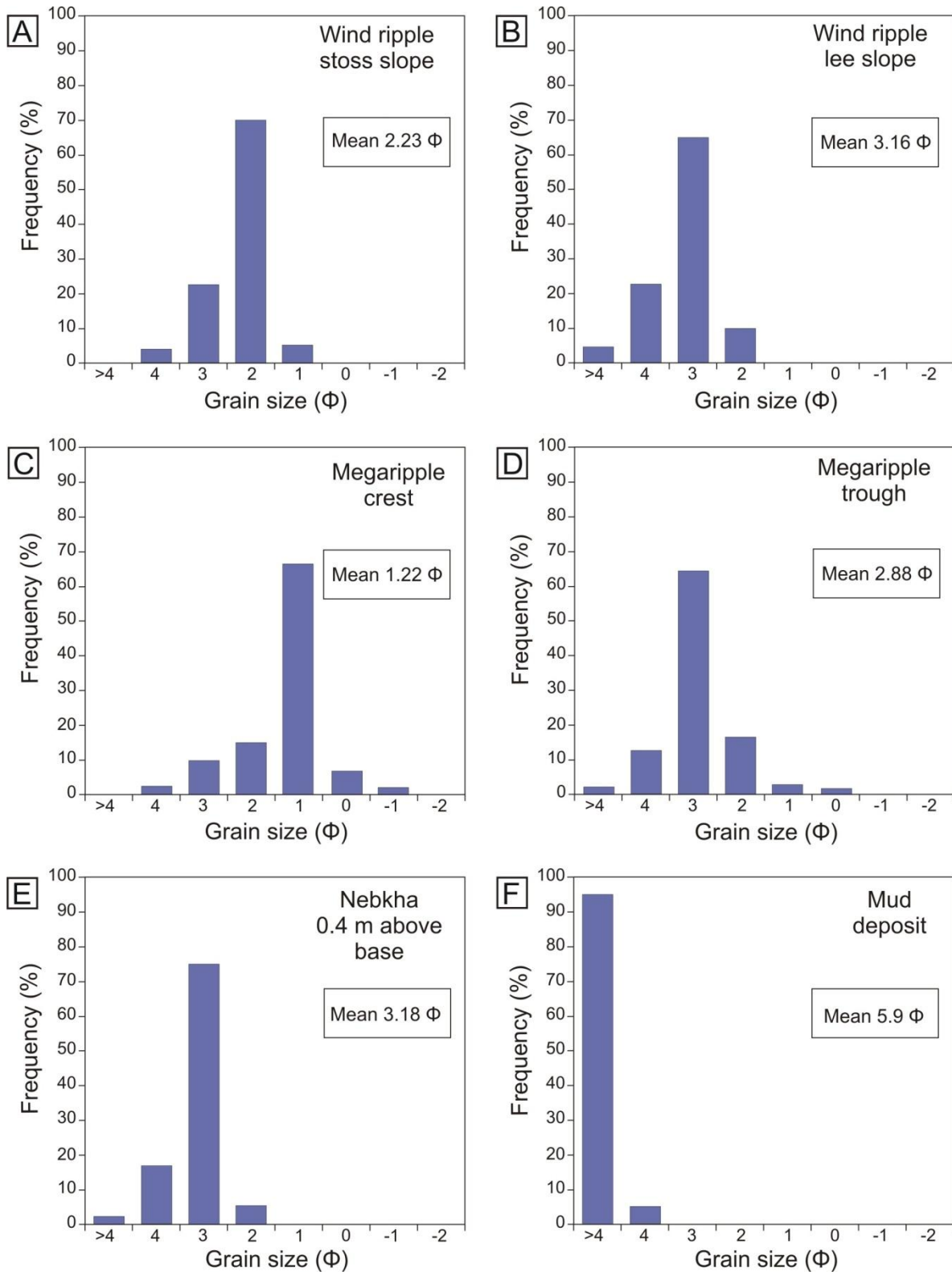


**Figure 5.** Grain size data.

Laterally, these small bedforms can be replaced by sinuous-crested granule megaripples (Fig. 6). Granule megaripples are restricted to unvegetated portions of the along channel section, and are characterized by moderately sorted fine- to medium-grained sand on ripple troughs and by poorly sorted coarse- to very coarse-grained sand and granules on stoss side and megaripple crests (Fig. 5C and D). The higher forms attain 50 mm of height, whereas the average height is 30 mm. Upwind slopes are 10° inclined and capped by a variety of volcanic, plutonic, metamorphic, and mud clasts with predominant (~70%) mode at 1 phi. Bimodal sediment distribution is clearly evident in the megaripples where the coarsest and poorly sorted grain fractions are concentrated on upper ripple stoss slope and crest, whilst ripple lee slopes and troughs are populated by finer and better sorted sediments. Wavelengths are 0.7-1.2 m and the crest lines are oriented N40. The maximum length of the crest line measured in an orientation perpendicular to wind direction is 3 m. Positive correlations between wavelength and coarser grain sizes and wavelength and along-crest line length exist. These forms have an average ripple index ( $RI =$  bedform wavelength/bedform height) of 35 and an asymmetry index (stoss slope length/lee slope length) of 2.3. The absence of surface cementation did not enable the complete resolution of the internal structures of the megaripples. Small trenches that were excavated around megaripples without disrupt the surface arrangement of grains exposed a non-layered arrangement of fine- and coarse-grained sand and granules without a clear distinction of the foresets.



**Figure 6.** Oblique view showing wind ripples in the foreground and megaripples in the background. Arrow shows a thin layer of mud deposits.

Nebkha is the only dune form identified in the field. All the dunes are colonized to various extents by shrubs (*Larrea cuneifolia*, *Larrea divaricata*, *Prosopis flexuosa*) and small herbs (*Salicornia perennis*). Vegetation cover occurs on the upwind side of the bedforms, whereas lateral flanks and downwind termination tend to lack vegetation cover. Nebkhas have the long axes oriented N25-40, which is a direction parallel to the prevailing wind direction. They can attain heights of up to 1 m, lengths of up to 13.5 m, and widths of up to 4.5 m. The highest and largest structures are strictly associated with the tallest and denser vegetation.

The nebkhlas in the region are typically elongate forms with average width to length ratio of 0.40. Fig. 7A shows a strong positive correlation between dune length and width ( $r = 0.86$ ); the solid line shows a linear trend between these two measured parameters at a high significance ( $R^2 = 0.71$ ). The data scattered in this plot principally reflects local variation in vegetation cover, as plant morphology, distribution and density. The dunes are not large forms, only one dune attains 1 m of height, and the average height is 0.34. A direct relationship between dune length and height is shown in Fig. 7B, it has a strong positive correlation ( $r = 0.85$ ) and a determination coefficient ( $R^2$ ) estimated to be 0.72 attesting that a linear trend between the variants fits the data very well.

Horizontal component ( $L$ ) of the dune is the mean of length ( $l$ ) and width ( $w$ ) of the dune, thus  $L = (l + w)/2$ . For the 50 measured nebkhlas, the height increases with the increase in the

horizontal component (Fig. 7C). Different orders of polynomials were tested, and it was found that order-two best fit the data as follows:

$$H = A \cdot L^2 + B \cdot L + C,$$

where  $H$  is the dune height,  $L$  is the horizontal component, and  $A$ ,  $B$ , and  $C$  are constants. Although the linear function fit is also significant, the polynomial function shows a relative better fit (1.3%,  $R^2 = 0.74$ ), with a positive correlation of 0.86. The ratio between the height and horizontal component of 1/8 indicates flattened forms.

The most developed nebkhlas occur along the transect A-A', in the central sand sheet part, where two or three nebkhlas have grown together to form amalgamated dunes by lateral linking and merging. Lateral and lower dune flanks are entirely populated by wind ripples, and the resulting grain size characteristics are very similar to the wind ripples (Fig. 5E).

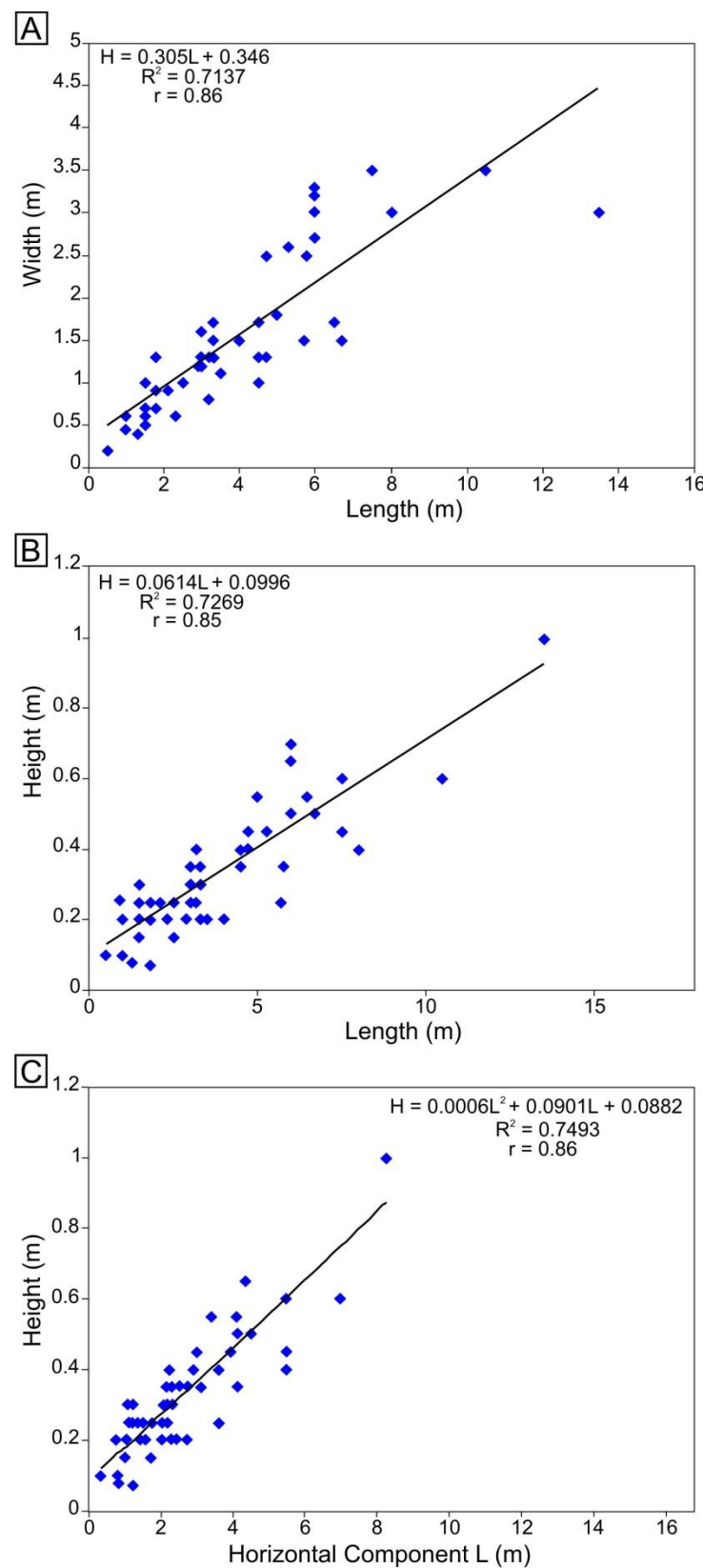


**Figure 7.** Morphometric parameters of the nebkhlas.

Erosional features such as yardangs only occur in the north part of the sand sheet. These linear wind-abraded erosional forms are developed on sand-cemented wind ripple deposits (Fig. 8), and attain a maximum height of 0.8 m. The morphometric parameters of these forms have revealed a ratio of length, width, height of 5.4: 2.2: 1. They have long axes oriented ~N20, parallel to the prevailing southerly winds.



**Figure 8.** Yardang. A) Wind sculptured micro-yardang form developed on wind ripple deposits. B) Detail of the deposits showing very fine- to fine-grained sandstone with inversely graded wind ripple laminae. Hammer is 0.34 m long.

#### 4.1.1. Interpretation

Wind ripples and megaripples are the most common dry eolian features described in the La Salina eolian sand sheet and in another eolian sand sheet environments elsewhere (Kocurek and Nielson, 1986; Fryberger et al., 1992; Mountney, 2006).

The basic difference between ripples and megaripples lies in the relative magnitudes of the wind strength and the size of the crest grains (Bagnold, 1941). In the case of ripples, the wind is strong enough to remove the topmost crest grains whenever the crest height reaches a certain limiting height. In the megaripples, the coarsest grains which accumulate at the crest are too large to be removed by average winds, except by occasional strong winds. Bagnold also suggested that the conditions necessary for the growth of megaripples are (1) availability of sufficient coarse grains which have a diameter 3-7 times larger than the mean diameter of grains in saltation, (2) a constant supply of fine sand in saltation to sustain forward movement of the coarse grains by creep, and (3) wind velocity below the threshold to remove coarse grains from the megaripple

crest. The positive correlation between wavelength and grain size suggests that the formation of these bedforms are connected to saltation or reptation path length, where minor surface perturbations act as the catalyst required to initiate ripple development (Anderson, 1987). Several studies suggest that granule megaripples form like common wind ripples (Fryberger et al., 1992 and references therein). The larger size and spacing of these forms are related to higher wind speeds that enhances the saltation and reptation path length and probably are associated with topographic depressions, which promotes wind deceleration and expansion, thus enhancing accumulation. On daily wind peaks during the study, sediment grain transport over the megaripples was active and comprised a combination of grain creep, saltation and reptation. Milana (2009) called these small megaripple forms described herein of small-scale gravel ripples, where the term large-scale gravel ripples was used to describe bedforms reaching 43 m in wavelength and 2.3 m in height.

Deposits of coarse-grained or granule megaripples are characterized commonly by inverse grading with or without development of coarse-grained foresets (Clemmensen and Abrahamsen, 1983). In the studied megaripples there was not a clear distinction of coarse-grained foresets, and the deposits show a non-layered, irregular distribution of fine- and coarse-grained sand, resulting in deposits with a poorly sorted texture, similar to those described by Fryberger et al. (1992) around megaripple fields of central-west Namibia. This texture results from an admixture of fine sand that fall among the spaces between the coarse sand and granule during deposition, and from the fine sand collected in the ripple troughs at the surface.

The internal architecture of incipient nebkhlas (embryonic state) dominated by wind ripples revealed planar or low angle parallel strata which have formed by wind ripple migration on a flat or gently undulatory sandy surface and have been preserved by subcritical climbing (Hunter, 1977). The pin stripe lamination is also characteristic of wind ripple deposits (Fryberger and Schenk, 1986). According to Sharp (1963) the active short-lived ripples tend to develop on sandy surfaces that are in a state of relative equilibrium or slow deposition, while surfaces experiencing marked erosion or vigorous deposition generally do not display ripples.

The internal stratigraphic architecture of 5 nebkhlas (mature state) was examined by digging 0.5 to 1 m deep and 1 to 3 m wide trenches oriented at a variety of angles around the bedforms. The distribution of lithofacies types, their orientation to the prevailing wind direction,

their bounding surfaces, and other biological features are recorded in architectural drawings (Fig. 9).

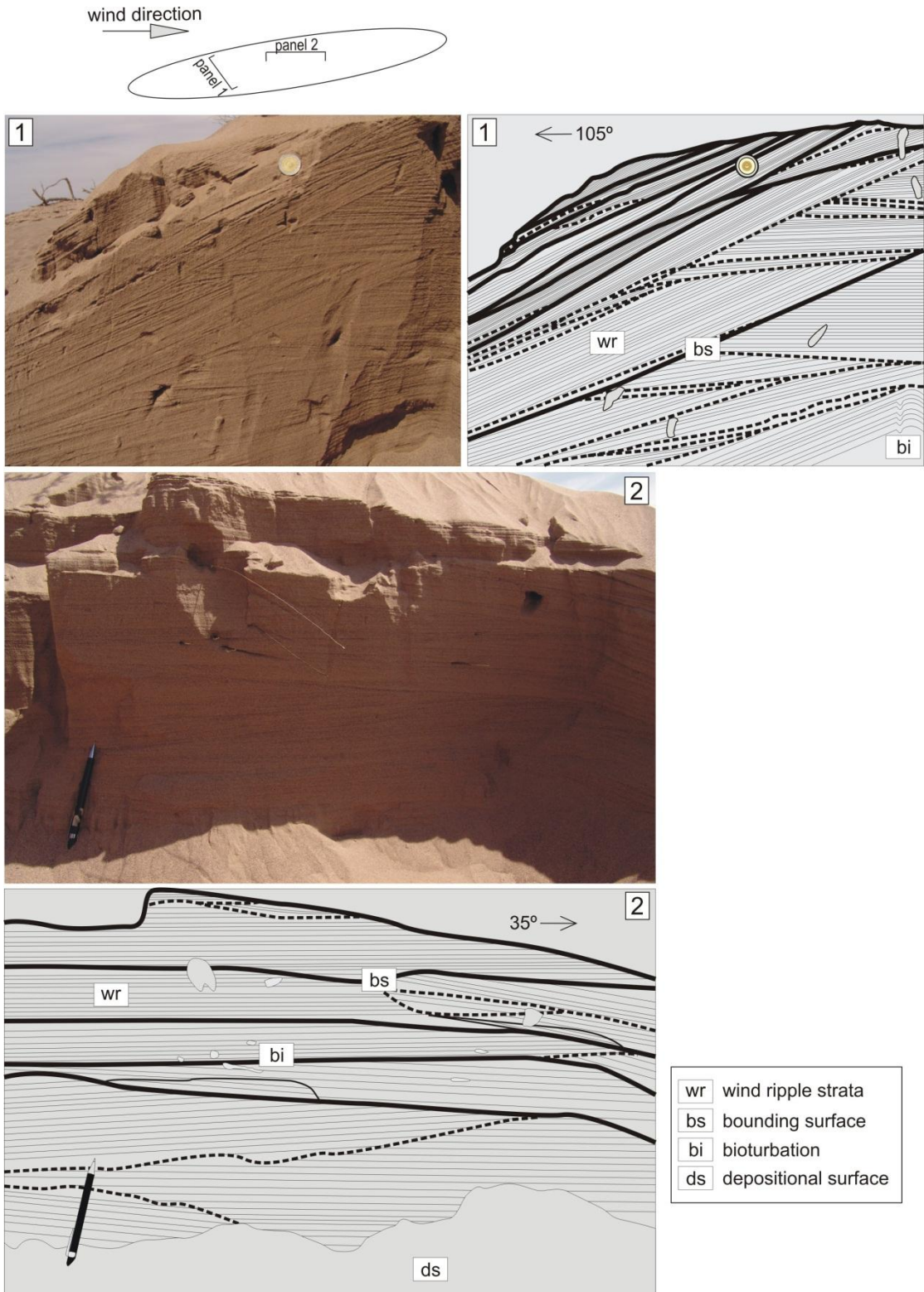


**Figure 9.** Internal sedimentary architecture of a nebkha. Panel 1 is oriented perpendicular to the wind direction and panel 2 is oriented parallel to the wind direction. Solid lines represent major bounding surfaces and dashed lines minor bounding surfaces. Coin for scale is 20 mm in diameter, and pencil is 0.14 m long.

The low angle of much of the strata and bounding surfaces in the lower parts of dune cores indicate that these bedforms initiated as low-relief mounds. The broad spread of low angle strata azimuths reflects the dome-shaped form of the dunes and signifies bedform growth on east, north and west facing flanks, probably in response to a prevailing southerly wind. Planar or low angle laminae are the depositional product of wind ripple migration and have been preserved by subcritical climbing (Hunter, 1977).

Major bounding surfaces represent episodes of dune stabilization and their convex-up geometries oriented parallel to the wind direction reflect the dome-shaped form of the dunes at various stages in their development. The minor bounding surfaces are reactivation surfaces, generated by local scouring of the dune flanks, probably in response to storm events and short-lived changes in wind direction (Rubin, 1987).

We did not identify grainfall strata as described by Mountney and Russell (2009) in nebkhlas of the same structure. Kocurek et al. (1992) pointed out that the transition from “protodunes” dominated by wind ripples to “protodunes” with a grainfall strata involves necessarily an upwind slope inclined of at least 10° and a lee slope with an angle of about 22°, which promotes the change from a flow expansion to a complete flow separation, and once separation occurred, wind speed at the base of the lee slope fell to near zero, promoting the deposition of thin fine-grained grainfall strata. In the sectioned dunes, the angle of upwind slope was about 3-5° and the downwind angle never surpassed 10°.

The presence of vegetation is essential to the initiation, growth, and stabilization of nebkhlas (Tengberg and Chen, 1998). Even in settings characterized by airflows that are undersaturated with respect to their potential sediment carrying capacity, nebkhlas are able to grow, as long as the surface of the dune remains colonized by vegetation (Mountney and Russell, 2006). In particular, the effectiveness of various species of *Larrea* and *Prosopis* as an agent to reduce near surface wind velocity is crucial to the sand trapping and their root mats are essential to the sand stabilization that enables long-term nebkhla growth (Tengberg and Chen, 1998; Langford, 2000). The preferential development of larger nebkhlas within the dry channel results exclusively from the localized disruption of airflow induced by vegetation (Mountney and Russell, 2006) because wind contraction and acceleration is intensified as the airflow is funneled between channel banks (Mountney and Russell, 2004). The increased frequency of small nebkhlas

along the base of terrace slopes probably reflects the development of a separation cell as the airflow rises up the channel banks and over the terrace slope (Mountney and Russell, 2006). Progressively away from the base of terrace (following transect B-B'), dunes show a reduction in size and frequency as the airflow reattach and the transport capacity of the wind is locally increased.

Yardangs found in the north part of the sand sheet were classified as micro-yardangs (Goudie, 2007), and their occurrence suggest local deflationary conditions where the wind is undersaturated with respect to sediment load (Kocurek and Havholm, 1993). The well developed wind-abraded lateral surfaces of yardangs oriented parallel to the prevailing wind direction indicate that sediment transport towards the northeast has been ongoing for a considerable time. Although the rates of yardang formation and development are still poorly known, some quantifications have shown that small yardangs may form in less than 2000 years (Laity, 1994).

## 4.2. Damp eolian features

In the area close to the south extremity of the sand sheet (transitional area from sand sheet to *playa* environment) where the surface is periodically damp, a variety of adhesion features are found, including adhesion ripples, adhesion warts, and evaporitic-adhesion structures (Kocurek and Fielder, 1982; Olsen et al., 1989; Goodall et al., 2000). Adhesion ripples and warts are small structures, 0.3-2 mm high, less than 5 mm in wavelength, characterized by very-fine- to fine-grained sand adhered to the damp surface. These structures form small undulations randomly distributed on the depositional surface, with discontinuous crest lines crudely oriented transversal to the wind direction. Evaporitic-adhesion structure forms irregular surface reliefs of <30 mm high, in which high proportion of sand and silty mud grains are adhered to the hygroscopic damp surface of salts (Fig. 10A). This structure exhibits a characteristic wrinkled morphology and a bicolored pattern, formed by differentiations between dark adhering sand and silty mud grains and white salt crusts.

Soft sediment deformational structures are more common in sediments at the south margin of the sand sheet, but can also occur in sections located in the central part. Sets composed of deformed laminae, 0.1-0.3 m thick, are common in the middle and upper portions of the wind ripple deposits. The lower surface of the deformed sets may have sharp to gradational contacts

and are underlain by undeformed low angle wind ripple deposits. The deformed sets may extend laterally for up to 1 m. In cross section, the deformational structures are characterized by small contortions, convex-up and isolated concave-up forms due to folding and disruption of the horizontal wind ripple laminae (Fig. 10B). Despite the magnitude of deformation, the parallel horizontal strata remain unbroken in some parts of the sections and the primary sedimentary structures are still evident.

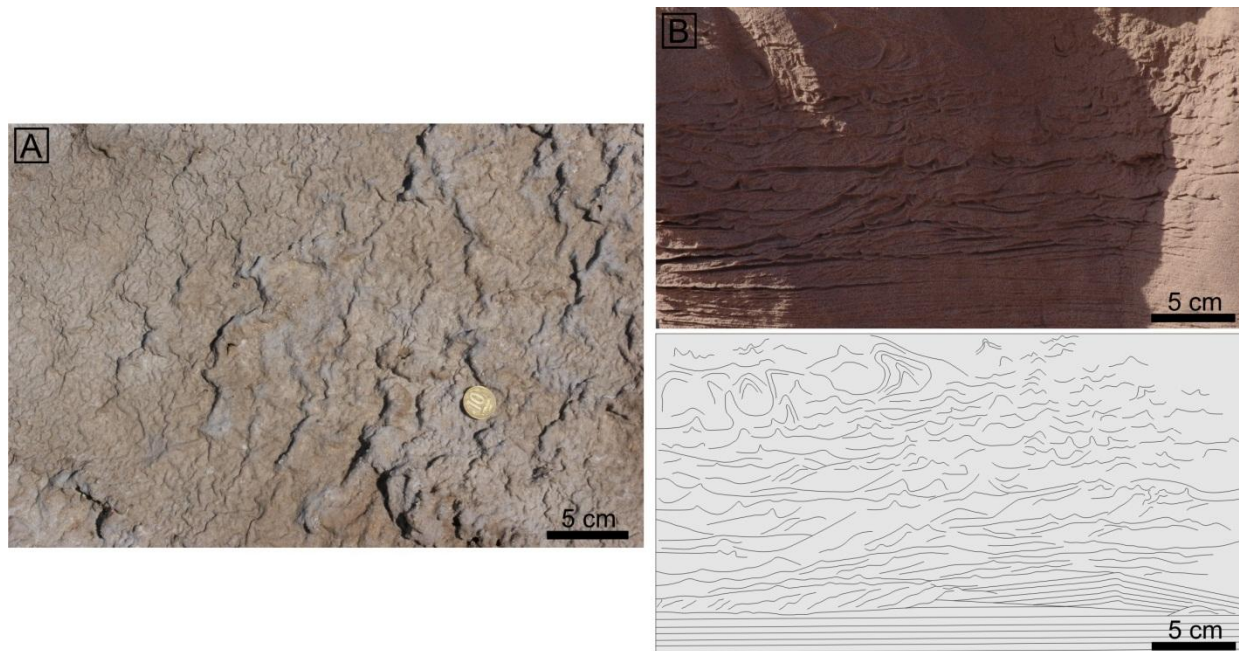


**Figure 10.** Damp eolian features. A) Evaporitic-adhesion structure in plain view. The topographic surface is wrinkled and shows the bicolored pattern typical of this structure. B) Small-scale deformation on wind ripple deposits. Contortion and disruption of the laminae evidence liquefaction at or close to the depositional surface.

#### 4.2.1. Interpretation

The adhesion of grains transported by the wind to damp surfaces results in the generation of adhesion structures (Kocurek and Fielder, 1982; Olsen et al., 1989). Formation of adhesion structures requires high substrate moisture (>80%) and growth can only take place as long as moisture is drawn to the surface by capillary action (Kocurek and Fielder, 1982). These structures are characterized by low-relief ridges and the accretion of saltating grains to the upwind side of the ripples generates a slightly convex inclination of the crests to the upwind direction. Adhesion warts have a more random distribution than adhesion ripples and probably are associated to the

roughly nature of the substrate and frequent changes in wind direction (Kocurek and Fielder, 1982; Olsen et al., 1989).

Evaporitic-adhesion structure is the larger adhesion structure observed, and its formation is associated to the presence of evaporites. The conspicuous occurrence of this structure on the depositional surface at the south extremity of the sand sheet suggests a high water table in this region. Evaporite formation may follow two main processes, efflorescence and precipitation. Efflorescence of salt crystals occurs where salt accumulates by direct crystallization onto sediment grains as a result of the evaporation of saline ground water adhering to those grains, and precipitation forms by the evaporation to dryness of ephemeral ponds of rainwater (Goodall et al., 2000). The adhesion of sand and silty mud to salt crystals is by the hygroscopic action of evaporites (Kocurek and Fielder, 1982), and the bicolored pattern seen on the surface of this structure is given by the high proportion of adhering dark windblown dust on white salt crystals. The ground water in the Tulum depression is enriched in saline compounds such as sodium chloride and calcium sulphate (Lloret and Suvires, 2006).

The limited extent of the small-scale deformation and its occurrence in the middle to upper parts of the wind ripple strata indicate that folding and disruption of the horizontal laminae developed by liquefaction near the depositional surface. Liquefaction results from an elevation of pore-water pressure as the wetting front infiltrates into highly porous eolian sands (Mountney, 2006). The tightly packed wind ripple laminae are susceptible to liquefaction by collapse of grain packing due to mechanical loading (Mountney and Thompson, 2002).

The vertical transition between dry to damp eolian features reflects changes in the substrate wetness possibly associated to minor fluctuations in the ground water level resulting from seasonal weather variations (Mountney and Thompson, 2002), small-scale climatic variations (Kocurek and Havholm, 1993), or episodic interdune flooding (Lancaster and Teller, 1988; Langford, 1989).

#### **4.3. Subaqueous features**

Two types of subaqueous sedimentary features are noted in the sand sheet area: current ripples and mud layers. The both features are developed in the three regions of the sand sheet.

Current ripples are the most conspicuous subaqueous feature observed. They occur on depositional surface and in trenches excavated in the areas affected by flood deposition. They are characterized by well sorted to sorted, rounded fine-grained sand, organized in sets 10 to 50 mm thick, which have a lateral continuity of more than 1 m. Ripples are asymmetrical, have straight crest lines, and show foreset azimuths oriented N210-250. The heights vary from 10 to 20 mm and wavelengths are 90-180 mm. The ripple cross laminae are formed by inclined foresets with dip angles typically around 20°, which in some cases show climbing laminae with preserved form sets. Current ripples abruptly overlie wind ripple strata and are overlain by thin silty mud deposits (Fig. 11).

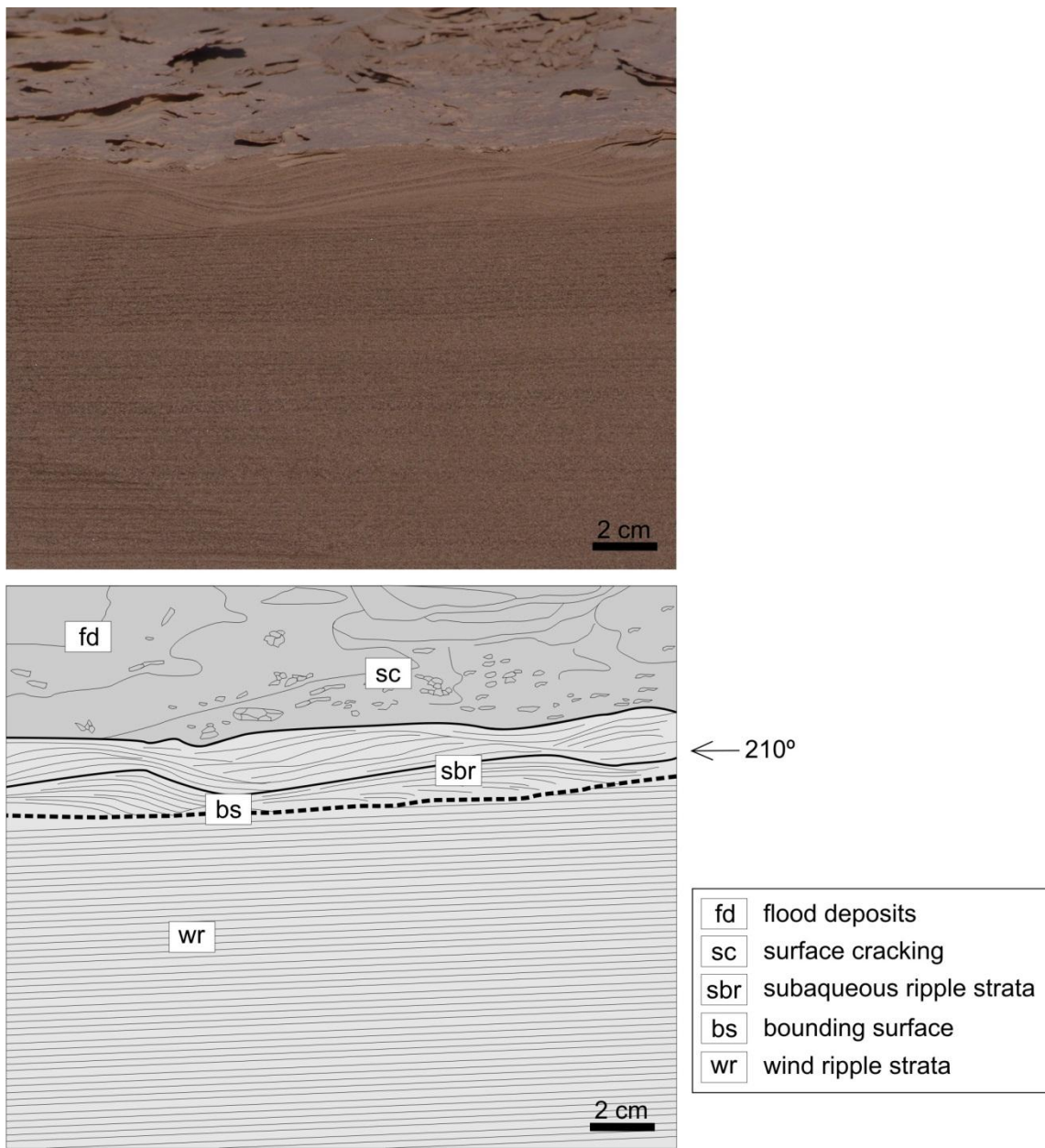


**Figure 11.** Subaqueous sedimentary features showing the vertical transition from wind ripple strata to subaqueous ripple strata which are overlain by silty mud deposits.

Mud deposits are composed by more than 90% of the grain size distribution >4 phi (Fig. 5F). They cover almost the entire sand sheet surface and show differentiations between thicker and continuous layers and thinner and reworked portions that are associated with wind deposits (Fig. 12A). The deposits are 10 to 150 mm thick, and exhibit an irregular and cracking pattern on surface and an undulatory to roughly lenticular shape in cross section. The surface cracking is marked by polygonal fractures, 20 to 100 mm in diameter, filled with fine-grained eolian sand,

and shows rain drop impressions (Fig. 12B). These muddy deposits also constitute an important source of low-density clasts that are transported by the wind and forms a significant part of the granule mode of the megaripples. In natural sections, 0.6 m thick, is possible to observe the occurrence of several mud layers interbedded with wind ripple strata (Fig. 12C), and mud flakes within wind ripple strata.

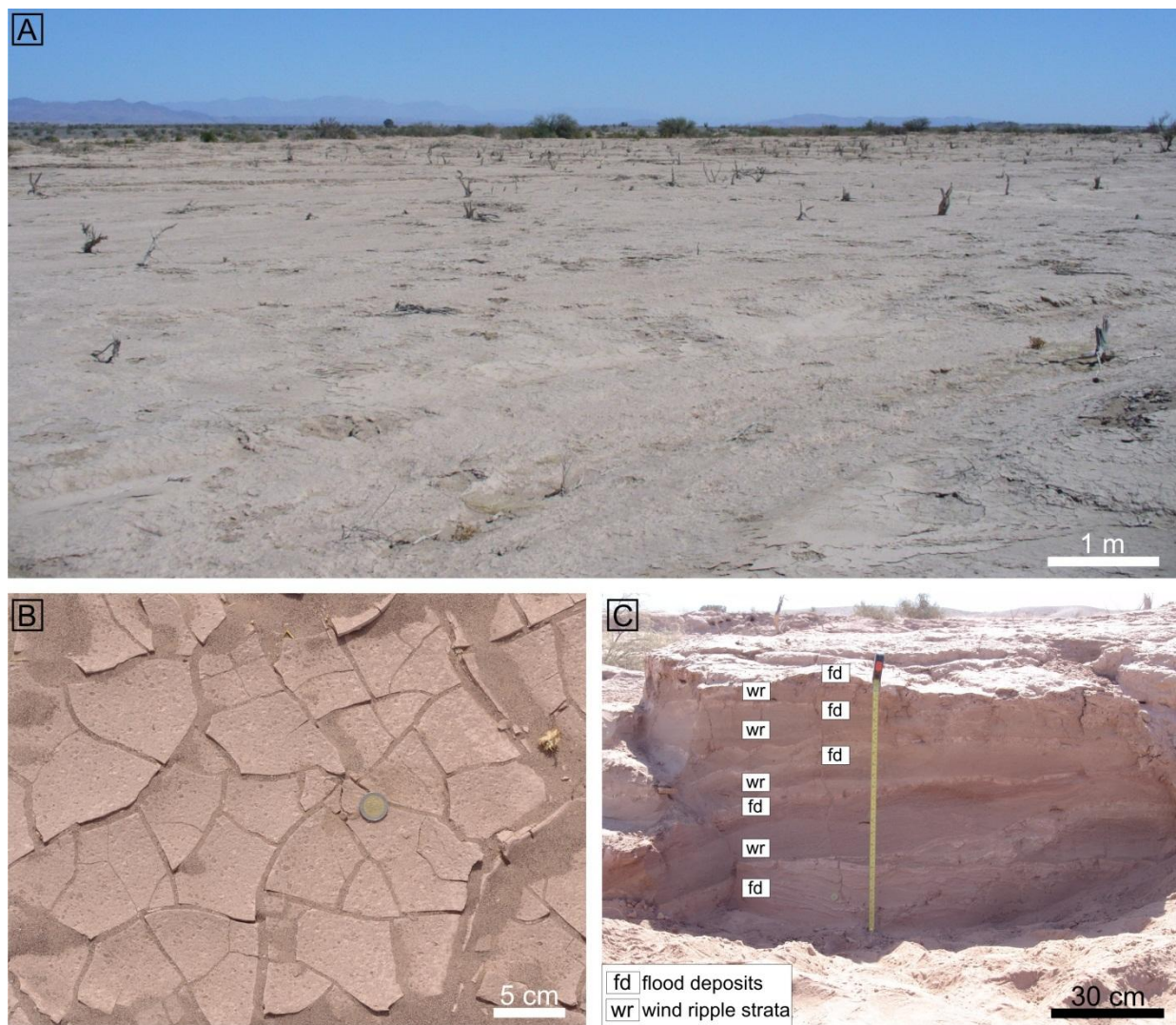


**Figure 12.** Flood deposits. A) Irregular and newly formed depositional surface after rainwater flooding. B) Desiccation cracks filled with eolian sand. C) Natural exposure showing the vertical interbedding of flood deposits and wind ripple strata.

#### **4.3.1. Interpretation**

The presence of current ripples and mud deposits in an eolian setting suggests water-driven processes (Ahlbrandt and Fryberger, 1981; Kocurek, 1981; Kocurek and Nielson, 1986; Lancaster and Teller, 1988; Langford, 1989; Langford and Chan, 1989). Current ripples characterized by straight crest lines indicate water flow conditions at low velocities and were primarily associated with upper sequences of wadi deposits (Glennie, 1970) whereas mud deposits suggest stagnant waters in interdune settings (Glennie, 1970; Ahlbrandt and Fryberger, 1981; Mountney and Russell, 2006).

The La Salina sand sheet is crossed by a dry river channel crudely oriented in the north-south direction (transect A-A'). The morphological characterization and sedimentological analysis of 5 stratigraphic sections insight the river channel have revealed that most of the sedimentary facies are the product of wind deposition, and there was not observed other sedimentary facies or subaqueous structures that support a fluvial origin for the described deposits.

Kocurek (1981) working in the Jurassic Entrada Sandstone Formation, Utah, described an array of subaqueous sedimentary features in interdune deposits characterized by the absence of channel systems. Based on observations carried out in a modern sand sheet adjacent to the dune field of Padre Island, Texas, Kocurek (1981) found an analogous situation and interpreted those water-laid deposits as a depositional product of ephemeral shallow floods associated to heavy rains. Similarly, Langford (1989) described several layers formed by couplets of subaqueous climbing ripples overlaid by mud deposits in the Mojave River Wash area, California, and interpreted those features as shallow water rework of eolian sands produced by floodwaters, where climbing structures indicate rapid deposition followed by short periods of stagnant water.

A flash flood can be generated in a desert environment during or shortly following a rainfall event, especially when the rain is of high intensity (Lancaster and Teller, 1988). The analysis of historical climatic data available for the La Salina region showed that precipitations are concentrated in the summer months, and that extreme rain storms are prone to occur in this area. Probably, the high concentrated precipitation events enhanced the surface runoff around the

sand sheet area and the sediment has been carried through the depositional surface in unconfined flows to very shallow channels unable to generate large sedimentary structures.

Rainwater flooding is also an important agent in the formation of depositional surfaces. Following a rainy period during January, the authors' visited the area and observed that most of the eolian bedforms were covered by subaqueous deposits and that much of the substrate was characterized by straight-crested current ripples and thin mud deposits.

## **5. Discussion and conclusions**

The La Salina eolian sand sheet is a currently aggrading system which is characterized by eolian sand cover in excess of 4 m of thickness, upon which dry and damp eolian and subaqueous features are developed. The stratigraphic record displays a set of dynamic interactions between eolian and subaqueous processes which have been ongoing for at least ~3.6 ka with an average sedimentation rate of 86.1 cm/ka (Fig. 13).

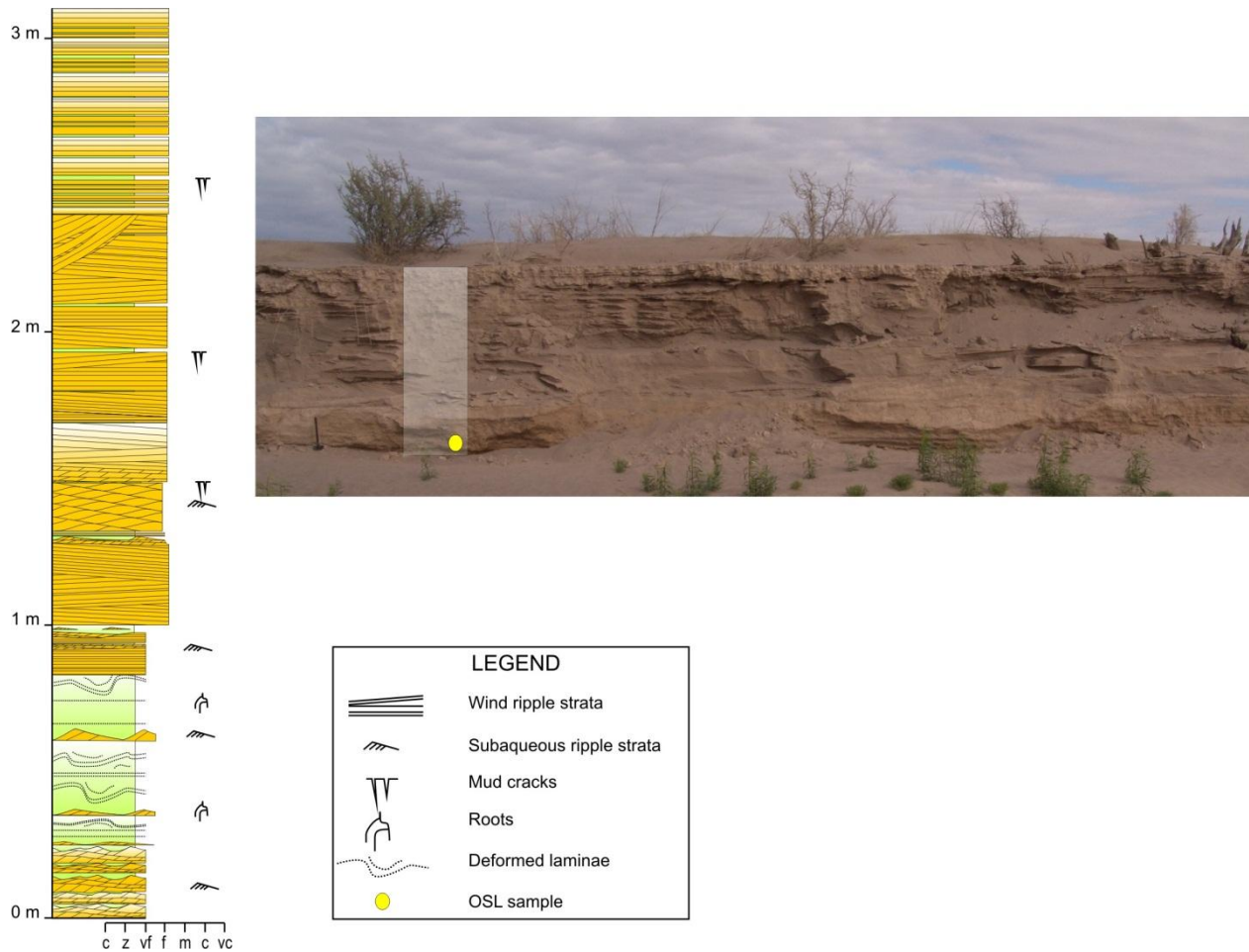


**Figure 13.** Stratigraphic section measured in the central part of the sand sheet showing the vertical interbedding of eolian and subaqueous deposits.

Water fluxes driven by heavy rains generated subaqueous deposits which have been frequently modified by wind action. The subaqueous deposition formed subaqueous current ripple strata and is accompanied by a thin layer of mud sediments. The mud sediments act to blanket the surface, thus protecting underlying eolian sand from deflation, and also sources mud clasts to megaripples formation, when the surface is completely dry.

The periodic changes in available water content are also responsible for the modification in the configuration of the morpho-depositional surface. During the dry season (July-October), the surface is little affected by water fluxes, and the near flat-lying depositional surface is covered by deposits of loose sand-grade wind ripples and granule-grade megaripples. Although just after a rainy day the surface can exhibit a different aspect and the sedimentary structures that were forming as a consequence of sand-free movement can change to subaqueous deposits at the

north and central and small adhesion structures controlled by the temporally rise of the water table at the south of the sand sheet.

According to Kocurek and Lancaster (1999), eolian bedform construction occurs as a consequence of bedform growth upon a depositional surface. Construction demands the generation of a suitable upwind amount of sediment supply, the availability of that supply for wind transport and a spatial reduction in sediment carrying capacity of the wind.

Ongoing sand sheet construction is possible because neogenic conglomeratic hills sources sand-grade sediment to the south and central parts of the sand sheet surface. This sediment is entrained and transported across the sand sheet by south and southwesterly winds which periodically exceed the threshold velocity required for sand transport. From morphological observations, it was evident that the surface roughness plays an essential role for the potential sand deposition. All initial depositional sites are related to elements of surface roughness, from small grasses to shrubs. Deposition of sand has occurred close to roughness elements possibly because of a conjunction of two factors that include local lowering of the wind transport capacity caused by deceleration of the wind and formation of secondary airflow patterns around obstacles (i.e., shadow effect), and as a consequence of an impediment to grain movement itself caused by direct collisions to obstacles. The larger plants are the most effective sand traps, and following construction is enhanced by root mats which act as a binding agent on upwind dune slopes. The availability of this sediment is controlled in the source area by wind itself, contemporaneous input - transport limited ( $CI_{TL}$ ), in the terminology of Kocurek and Lancaster (1999), and by elements of surface stabilization, such as vegetation, surface cementation, and thin veneer of mud in the south and central parts of the sand sheet. The presence of stabilizing agents on sand sheet surface accounts for the contemporaneous input – availability limited ( $CI_{AL}$ ) in the model of Kocurek and Lancaster (1999), and enhances accumulation of sedimentary strata in a stabilizing eolian setting (Kocurek and Havholm, 1993).

The stabilizing influence of surface elements has been responsible for accumulation to taken place. The airflow is undersaturated with respect to its potential sand carrying capacity in much of the year and across the sand sheet surface. The ubiquitous presence of bounding surfaces within cores of nebkhas and the development of yardangs attest the undersaturated flow conditions. The main region of eolian accumulation is the central part of the sand sheet where sand has accumulated to in excess of 4 m of thickness and is largely stabilized by vegetation. The

nebkhas that are almost fully stabilized by vegetation in this region have accumulated vertically as non-migratory bedforms as sediment is trapped by the stabilizing influence of vegetation. Surface cementation and thin mud veneers have enabled accumulation of sedimentary strata in the south whereas in the north the minor eolian accumulation has been formed by mud deposition and aerodynamic deceleration of the wind as it enters into small topographic depressions.

The long-term preservation of sand sheet accumulations is attributed to tectonically induced subsidence and burial. The high rates of sedimentation has enabled the continuous burial of the geological bodies, and the progressive creation of the preservation space in the tectonic active subsiding Tulum depression has enabled the accumulations be gradually placed beneath the level of deflation, thereby protecting them from future erosion and reworking (Kocurek, 1999).

## 6. References

- Ahlbrandt, T.S., Fryberger, S.G., 1981. Sedimentary features and significance of interdune deposits. In: Etheridge, F.G., Flore, R.M. (Eds.), Recent and Ancient Nonmarine Depositional Environments: Models for Exploration. SEPM Special Publication 31, pp. 293-314.
- Al Farraj, A., Harvey, A.M., 2004. Late Quaternary interactions between aeolian and fluvial processes: a case study in the northern UAE. Journal of Arid Environments 56, 235-248.
- Anderson, R.S., 1987. A theoretical model for aeolian impact ripples. Sedimentology 34, 943-956.
- Bagnold, R.A., 1941. The Physics of Blown Sand and Desert Dunes. Methuen and Company, London.
- Bullard, J.E., Livingstone, I., 2002. Interactions between aeolian and fluvial systems in dryland environments. Area 34, 8-16.
- Bullard, J.E., McTainsh, G.H., 2003. Aeolian fluvial interactions in dryland environments: examples, concepts and Australia case study. Progress in Physical Geography 27, 471-501.
- Clemmensen, L.B., Abrahamsen, K., 1983. Aeolian stratification and facies association in desert sediments, Arran Basin (Permian), Scotland. Sedimentology 30, 311-339.
- Fryberger, S.G., Schenk, C.J., 1988. Pin stripe lamination: a distinctive feature of modern and ancient eolian sediments. Sedimentary Geology 55, 1-15.

- Fryberger, S.G., Ahlbrandt, T.S., Andrews, S., 1979. Origin, sedimentary features and significance of low-angle aeolian 'sand sheet' deposits, Great Sand Dunes National Monument and vicinity, Colorado. *Journal of Sedimentary Petrology* 49, 733-746.
- Fryberger, S.G., Hesp, P., Hastings, K., 1992. Aeolian granule ripple deposits, Namibia. *Sedimentology* 39, 319-331.
- Glennie, K.W., 1970. Desert Sedimentary Environments. *Developments in Sedimentology* 14. Elsevier, New York.
- Goodall, T.M., North, C.P., Glennie, K.W., 2000. Surface and subsurface sedimentary structures produced by salt crusts. *Sedimentology* 47, 99-118.
- Goudie, A.S., 2007. Mega-yardangs: a global analysis. *Geography Compass* 1, 65-81.
- Hummel, G., Kocurek, G., 1984. Interdune areas of the Back-Island dune field, North Padre-Island, Texas. *Sedimentary Geology* 39, 1-26.
- Hunter, R.E., 1977. Basic types of stratification in small eolian dunes. *Sedimentology* 24, 361-387.
- Kocurek, G., 1981. Significance of interdune deposits and bounding surfaces in aeolian dune sands. *Sedimentology* 28, 753-780.
- Kocurek, G., 1999. The Aeolian rock record (Yes, Virginia, it exists, but it really is rather special to create one). In: Goudie, A.S., Livingstone, I. (Eds.), *Aeolian Environments, Sediments and Landforms*. John Wiley and Sons, Chichester, pp. 239-259.
- Kocurek, G., Fielder, G., 1982. Adhesion structures. *Journal of Sedimentary Petrology* 52, 1229-1241.
- Kocurek, G., Havholm, K.G., 1993. Eolian sequence stratigraphy - a conceptual framework. In: Weimer, P., Posamentier, H. (Eds.), *Siliciclastic Sequence Stratigraphy. Recent Developments and Applications*. AAPG Memoir 58, pp. 393-409.
- Kocurek, G., Lancaster, N., 1999. Aeolian system sediment state: theory and Mojave Desert Kelso dune field example. *Sedimentology* 46, 505-515.
- Kocurek, G., Nielson, J., 1986. Conditions favourable to the formation of warm-climate aeolian sand sheets. *Sedimentology* 33, 795-816.
- Kocurek, G., Townsley, M., Yeh, E., Havholm, K., Sweet, M.L., 1992. Dune and dune field development on Padre Island, Texas, with implications for interdune deposition and water-table-controlled accumulation. *Journal of Sedimentary Petrology* 62, 622-635.

- Köppen, W., 1948. Climatología: con un estudio de los climas de la tierra. Fondo de Cultura Económica, Panuco.
- Koster, E.A., 1988. Ancient and modern cold-climate aeolian sand deposition: a review. *Journal of Quaternary Science* 3, 69-83.
- Laity, J.E., 1994. Landforms of aeolian erosion. In: Abrahams, A.D., Parsons, A.J. (Eds.), *Geomorphology of Desert Environments*. Chapman and Hall, London, pp. 506-535.
- Lancaster, N., 1997. Response of eolian geomorphic systems to minor climate change: examples from the southern Californian deserts. *Geomorphology* 19, 333-347.
- Lancaster, N., Teller, J.T., 1988. Interdune deposits of the Namib Sand Sea. *Sedimentary Geology* 55, 91-107.
- Langford, R.P., 1989. Fluvial-aeolian interactions: part I, modern systems. *Sedimentology* 36, 1023-1035.
- Langford, R.P., 2000. Nabkha (coppice dune) fields of south-central New Mexico, USA. *Journal of Arid Environments* 46, 25-41.
- Langford, R.P., Chan, M.A., 1989. Fluvial-aeolian interactions: part II, ancient systems. *Sedimentology* 36, 1037-1051.
- Lloret, G., Suvires, G.M., 2006. Groundwater basin of the Tulum Valley, San Juan, Argentina: a morphohydrogeologic analysis of its central sector. *Journal of South American Earth Sciences* 21, 267-275.
- Maxwell, T.A., Haynes Jr., C.V., 2001. Sand sheet dynamics and Quaternary landscape evolution of the Selima Sand Sheet, southern Egypt. *Quaternary Science Reviews* 20, 1623-1647.
- Meigs, A., Krugh, W.C., Schiffman, C., Vergés, J., Ramos, V.A., 2006. Refolding of thin-skinned thrust sheets by active basement-involved thrust faults in the Eastern Precordillera of western Argentina. *Revista de la Asociación Geológica Argentina* 61, 589-603.
- Milana, J.P., 2009. Largest wind ripples on Earth? *Geology* 37, 343-346.
- Milana, J.P., Bercowski, F., Jordan, T., 2003. Paleoambientes y magnetoestratigrafía del Neógeno de la Sierra de Mogna, y su relación con la Cuenca de Antepaís Andina. *Revista de la Asociación Geológica Argentina* 58, 447-473.
- Mountney, N.P., 2006. Eolian facies models. In: Posamentier, H.W., Walker, R.G. (Eds.), *Facies models revisited*. SEPM Special Publication 84, pp. 19-83.
- Mountney, N.P., Russell, A.J., 2004. Sedimentology of aeolian sand sheet deposits in the Askja region of northeast Iceland. *Sedimentary Geology* 166, 223-244.

- Mountney, N.P., Russell, A.J., 2006. Coastal aeolian dunefield development and response to periodic fluvial inundation, Sólheimasandur, southern Iceland. *Sedimentary Geology* 192, 167-181.
- Mountney, N.P., Russell, A.J., 2009. Aeolian dune-field development in a water table-controlled system: Skeidararsandur, southern Iceland. *Sedimentology* 56, 2107-2131.
- Mountney, N.P., Thompson, D.B., 2002. Stratigraphic evolution and preservation of aeolian dune and damp/wet interdune strata: an example from Triassic Helsby Sandstone Formation, Cheshire Basin, UK. *Sedimentology* 49, 805-833.
- Murray, A.S., Wintle, A.G., 2000. Luminescence dating of quartz using an improved single-aliquot regenerative-dose protocol. *Radiation Measurements* 32, 57-73.
- NASA - National Aeronautics and Space Administration, 2000. Landsat Program. Landsat ETM+ images, S-19-30\_2000. Available on <http://zulu.ssc.nasa.gov/mrsid/>. Access date 6 December 2010.
- Olsen, H., Due, P.H., Clemmensen, L.B., 1989. Morphology and genesis of asymmetric adhesion warts - a new adhesion surface structure. *Sedimentary Geology* 61, 277-285.
- Pereyra, B.R., 2000. Clima de la provincia de San Juan, Argentina. Recursos y problemas ambientales de la zona árida. Programa Cooperativo Junta Gobierno Andalucía, Andalucía, pp. 71-78.
- Rubin, D.M., 1987. Cross-bedding, bedform and paleocurrents. SEPM Concepts in Sedimentology and Paleontology 1, Tulsa.
- Saqqa, W., Atallah, M., 2004. Characterization of the aeolian terrain facies in Wadi Araba Desert, southwestern Jordan. *Geomorphology* 62, 63-87.
- SEGEMAR – Servicio Geológico Mineiro Argentino, 2000. Hoja Geológica 3169-IV (1:250 000). Povincia de San Juan, Buenos Aires.
- Sharp, R.P., 1963. Wind ripples. *Journal of Geology* 71, 617-636.
- SMA – Servicio Meteorológico Nacional, 2010. Estadísticas Climatológicas 1973-2010. Available on [http://www.tutiempo.net/clima/San\\_Juan\\_Aerodrome/873110.htm](http://www.tutiempo.net/clima/San_Juan_Aerodrome/873110.htm). Access date 25 February 2011.
- Suvires, G.M., 2004. Distribución de los suelos en función del relieve y de la neotectónica en la región sureste de la provincia de San Juan. *Revista de la Asociación Geológica Argentina* 59, 376-384.
- Tengberg, A., Chen, D., 1998. A comparative analysis of nebkhlas in central Tunisia and northern Burkina Faso. *Geomorphology* 22, 180-192.

Tripaldi, A., Forman, S.L., 2007. Geomorphology and chronology of Late Quaternary dune fields of western Argentina. *Palaeogeography, Palaeoclimatology, Palaeoecology* 251, 300-320.



## **ANEXO VII**

### **GLOSSÁRIO**



## GLOSSÁRIO

Cerosidade – Concentração de material inorgânico, que ocorre sob a forma de preenchimento de porosidade, revestimento de unidades estruturais ou de superfícies de grãos. Apresenta aspecto lustroso e brilho graxo, resultantes da iluminação de material coloidal.

Cristalária – Termo usado em micromorfologia para definir a ocorrência de cristal unitário ou arranjo de cristais de frações puras do plasma, que não fecham o fundo matricial, mas formam massas coerentes.

Crotovina – Escavação animal, de diâmetro milimétrico a métrico, preenchida por sedimentos provenientes de camadas diferentes das quais a escavação foi formada. Geralmente é distinguida em campo pelo preenchimento possuir cor e granulação diferente da matriz.

Cutã – Termo designativo usado para indicar revestimentos muito tênues e pouco nítidos, geralmente de aspecto embaçado ou fosco, que ocorre sobre as estruturas pedogênicas ou superfície de grãos. Em micromorfologia, é utilizado para indicar as modificações de textura, estrutura ou trama nas superfícies do material pedológico causadas pela concentração de certos constituintes (concentrações plásticas), ou a modificações *in situ* do plasma (separações plásticas).

Gilgai – Microrrelevo típico de solos compostos por argilas expansivas, que variam consideravelmente de volume em consequência do regime hídrico do solo. Consiste em saliências convexas e depressões côncavas que formam relevos de pouca expressão morfológica.

Mosqueado – Um horizonte de solo pode apresentar cor única ou multiplicidade de cores. No caso de haver predominância de uma cor sobre as demais têm-se os mosqueados, que formam manchas de cores diferenciadas da cor predominante na matriz do horizonte. O mosqueado ocorre em muitos horizontes do solo, especialmente em horizontes de transição com o material de formação do solo. Pode também ser decorrente de drenagem imperfeita.

*Mukkara* – Expressão morfológica em subsuperfície das saliências convexas que compõem o microrrelevo gilgai. O modo de formação é atribuído aos processos de argilituração, principalmente relacionados a modificações sazonais no volume do material pedológico em solos ricos em argilas expansivas.

Órico – Característica de horizonte mineral A do solo, que apresenta cores muito claras, ou altos valores de croma, ou pouco conteúdo de matéria orgânica, ou pouca espessura para ser classificado em outro tipo de epipedon diagnóstico. Comumente utilizado para designar epipedons pouco desenvolvidos.

Ped – Agregação das partículas primárias do solo em unidades estruturais. Indica a constituição física do material pedológico, expressa pelo tamanho, forma, e arranjo dos agregados elementares, podendo ser avaliada segundo seus graus de desenvolvimento e acomodação. Para volumes de solo que não apresentam estruturação (maciça ou grão simples), emprega-se o termo apedal.

Pedoturbação – Qualquer forma, atividade ou processo físico, químico ou biológico que resulte na ciclagem e homogeneidade do material pedológico, culminando por último, com a destruição dos horizontes do solo.

Perfil poligenético – Perfil de solo que apresenta sobreposição de horizontes pedogênicos caracterizados por possuírem propriedades pedogênicas distintas entre si e não geneticamente relacionadas aos mesmos processos de formação.

Petrocálcico – Horizonte de solo cimentado e endurecido por carbonato de cálcio, apresentando lâminas contínuas de carbonato de cálcio. Representa os estágios IV, V e VI de evolução morfológica de horizontes cimentados por carbonato de cálcio em solos.

Plasma – Porção do material pedológico composto por partículas menores que 2  $\mu\text{m}$ . O plasma pode conter argilominerais, matéria orgânica, sais, óxidos e hidróxidos.

*Slickenside* – Superfícies alisadas e lustrosas, apresentando estiramentos na massa do solo, consequentes do deslizamento e atrito entre o material pedológico que foi sujeito a modificações de volume.